Magnetostratigraphy and Tectonic Rotation in South Wales

Thesis submitted in accordance with the requirements of the University of Liverpool for the degree of Doctor in Philosophy by

Dedi Setiabudidaya

May 1991

Abstract

Magnetostratigraphy and Tectonic Rotation in South Wales

by Dedi Setiabudidaya

This project has two facets. Firstly, it has aimed to establish the lower boundary of the Permo-Carboniferous reversed superchron by studying the magnetostratigraphy of Westphalian A sediments in the Coal Measures of South Wales. Secondly, an attempt has been made to detect rotations in this zone at the junction of the Caledonian (Acadian) and Variscan orogenic belts by studying both the palaeomagnetism of Westphalian A and the Old Red Sandstone sediments in the area. For this purpose, rocks were sampled from each major block separated by major Variscan structures.

The Natural Remanent Magnetisations (NRMs) of 332 specimens from the Westphalian A rocks were measured and 239 specimens were subjected to stepwise thermal demagnetisation. The NRM intensities of these specimens were so low that the first objective of this project could not be fulfilled satisfactorily. Hence, interpretation of the results is limited to contributing to and/or refining the present polarity time scale for this age from the British Isles and northwestern Europe as proposed by Palmer and others (1985). From this study it can be concluded that the Westphalian A sediments from South Wales were magnetised in a field of reversed polarity. The remanence is carried by magnetite and acquired during diagenesis at a time later than deposition of these rocks but is Carboniferous in age.

Since the magnetisation of the Old Red Sandstones is syn-deformational, a technique has been developed for presenting the result of grouping palaeomagnetic directions from fold limbs at all stages of unfolding. This method requires predicted palaeomagnetic directions which can be derived either from adjoining horizontal and undeformed strata or from an established Apparent Polar Wander Path (APWP) for the area being investigated. The mean palaeomagnetic direction with the highest k-value within a certain band of the expected values is considered as the acceptable one. The mean palaeomagnetic direction can enable the fold geometry to be recovered at the time of magnetisation when the time of remanence acquisition can be inferred from other evidence.

Four hundreds and fifty three specimens from the Old Red Sandstones were subjected to stepwise thermal demagnetisation up to 700°C. All specimens proved to be partially or completely remagnetised during Permo-Carboniferous times and the remanence is carried by haematite. This secondary component was acquired at different stages of folding at different localities. This indicates that either the remagnetisation or the deformation took place over a time interval. Small populations of high blocking temperature components which are not Permo-Carboniferous in origin were resolved. These higher temperature components were found to be preserved mostly in the northeastern area. No confirmation was obtained for the supposed Devonian components reported by earlier workers in the southwest where it is inferred that Permo-Carboniferous overprinting has been comprehensive.

It was also observed that the more westerly localities have progressively more westerly-directed palaeomagnetic directions. This phenomenon is explained in terms of regional tectonic rotation since acquisition of the overprinted remanence. Studies of Anisotropy of Magnetic Susceptibility (AMS) in these sediments identify a rotation in the same sense and show that the magnitude of this parameter is too small to appreciably influence the magnetic remanence direction.

Declaration

I declare that the work submitted is entirely the results of my own investigations and that the work has not already been accepted in substance for any degree, and is not concurrently submitted in candidature for any degree.

Dedi Setiabudidaya ..... (candidate)

Acknowledgements

Firstly, I would like to thank my supervisor Dr. J. Shaw for supervising this research and for everything he has done for me. My success is partly due to his encouragement and support.

Secondly, I would like to thank everyone in the Geomagnetism Laboratory, Department of Earth Sciences and in the Magnetic Laboratory, Department of Geography who helped me during my three and half years in Liverpool. The following are those who I cannot forget. Dr. J.D.A. Piper helped me in the field to collect some core samples from the Westphalian A strata and all core samples from the ORS. He also gave me some geological advice and corrected my English in all chapters of this thesis. The rest of the core samples from the Westphalian A strata were due to invaluable assistance from Dr. G.J. Sherwood. I thank Dr. T.C. Rolph for suggesting methods for distinguishing magnetite from haematite using thermal demagnetisation of the IRMs. Mr. R. Jude and Dr. D.J. Robertson of the Magnetic Laboratory helped me with the IRM experiments. Dr. Robertson is also the first person who taught me palaeomagnetism when I was a student at Leeds. I thank Prof. N. Kusznir of the Department of Earth Sciences, University of Liverpool, for accepting me as his student. Although it lasted only for one year, my knowledge of computer programming was gained mostly under his supervision. For this, I also thank Mr. A.G. McCormack.

Thirdly, I would like to thank Drs. R. Gayer and A. Hartley of the University of Wales College Cardiff. All sampling sites were suggested by Dr. Gayer. He also included me as a member of his Cardiff Coalfield Research Team (CCRT). Due to involvement in the team, I picked up and learned geological jargon. I thank Dr. Hartley for helping me in the field to collect all block samples.

Finally, I would like to thank the University of Sriwijaya (Indonesia) for the financial support. Without their support, I could not have met the people I have mentioned above.

To all these people, and the many others I have forgotten, I am extremely grateful.

List of Abbreviations

A	: Ampere
a95	: alpha-95, the cone of 95 percent confidence
AMS	: Anisotropy of Magnetic Susceptibility
APWP	: Apparent Polar Wander Path
CDec	: tilt-Corrected Declination
CInc	: tilt-Corrected Inclination
CRM	: Chemical Remanent Magnetisation
D-CRM	: Depositional-Chemical Remanent Magnetisation
D,Dec	: Declination
deg	: degrees
°C	: degrees Celsius
Dir	: Direction
DRM	: Detrital (Depositional) Remanent Magnetisation
F	: Intensity
I,Inc	: Inclination
IRM	: Isothermal Remanent Magnetisation
k	: Fisher precision parameter or susceptibility or kilo-
	kg = kilograms
	km = kilometres
Lat	: Latitude
Loc	: Locality
Lon	: Longitude
M,m	: metres or million
	My = million years
NRM	: Natural Remanent Magnetisation
ORS	: Old Red Sandstone
PDDRM	: Post-Depositional Detrital Remanent Magnetisation
R	: Resultant
SI	: Systéme International

SQUID	: Superconducting Quantum Interference Detector
T	: Tesla or Temperature
	mT = milli-Tesla
	uT = micro-Tesla
Temp	: Temperature
TRM	: Thermo-Remanent Magnetisation
VGP	: Virtual Geomagnetic Pole

Table of Contents

List of Figures and Tables

CHAPTER 1 INTRODUCTION

1.1 The Aim of the Research

The initial aim of this research was to detect rotations resulting from the Variscan orogeny within the South Wales main coalfield using palaeomagnetic techniques. It subsequently evolved into three projects which developed from one project into another as the research progressed.

The first project was undertaken as part of a comprehensive investigation of the South Wales coalfield initiated by the University of Cardiff and deals with the magnetostratigraphy of the Westphalian A sediments from South Wales. Normal and mixed polarities within the Westphalian A interval recorded within from British Upper Carboniferous rocks were reported by some earlier workers (Belshé, 1957 and Titman, 1971). By studying the magnetostratigraphy of these sediments from South Wales, it was hoped that :

1. the results would refine the present polarity time scale for this age (see, for example, Palmer and others, 1985).

2. the directional results from these rocks would detect any block rotations within the South Wales main coalfield.

Preliminary results showed that the NRMs (Natural Remanent Magnetisations) in these sediments were very weak. However, a combination of palaeomagnetic and rock magnetic studies of these rocks has shown that they have a diagenetic remanence originating later in Carboniferous times.

The dispersion of the palaeomagnetic directions in these rocks made it almost impossible to detect any kind of rotation accurately. Also, the difficulty of finding suitable outcrops in the western area of the basin led on to the second project, the palaeomagnetic study of the Old Red Sandstone (ORS) sediments. There are three basic reasons why these red beds were chosen for investigation.

1. Their NRM intensities are usually well-above the noise level of the spinner magnetometers employed routinely in this study.

2. Red beds are known to be good recorders of the ancient magnetic field.

3. The composition of the remanence and the tectonic significance of the results are in dispute and recognised to require further investigation. In addition, since these rocks are older than the Westphalian A, they should record the integrated effect of the rotations influencing the Carboniferous rocks.

The palaeomagnetism of the ORS has been studied by several workers (Creer, 1957; Chamalaun and Creer, 1964; McClelland-Brown, 1983; Channell and others, 1991). It is generally agreed that the ORS sediments were largely remagnetised during Permo-Carboniferous times. In other words, although the age of the rock is Devonian, the palaeomagnetic direction records a palaeofield mostly representative of Permo-Carboniferous

times. By studying these rocks palaeomagnetically, it was hoped that any movement/rotation within the main basin at least since the acquisition of this secondary magnetisation could be detected. The above references also report variable recovery of a Lower Devonian component of magnetisation and if this component could be recovered throughout South Wales, it would be an indicator of rotations across this region since Devonian times. It is known from the earlier studies that these red beds are stable palaeomagnetically with a resolvable component structure and that their NRMs are mostly well-above the noise level of the Molspin spinner magnetometers. Hence, any rotation of more than a few degrees can be detected palaeomagnetically. A systematic sampling was therefore carried out in which each major block, separated by major Variscan structures, was sampled.

In the event, some samples from the Brecon/Abergavenny area showed two components: a lower and higher blocking temperature component. The directions of the higher temperature components proved to be different to those reported by McClelland-Brown (1983) and Chamalaun and Creer (1964). It was therefore considered necessary to re-sample the rocks from southern Pembrokeshire both to evaluate the cause of the differences and to endeavour to resolve rotations across the full outcrop in South Wales. Other magnetic properties like the IRM (Isothermal Remanent Magnetisation) and the AMS (Anisotropy of Magnetic Susceptibility) could then be compared from both areas.

Since some of the magnetisation in the ORS may be syn-folding (McClelland-Brown, 1983, also called "syn-deformational magnetisation"),

the application of the classic fold test based on two geometries (in situ and fully unfolded, e.g. McElhinny, 1964; McFadden and Jones, 1981) is not entirely appropriate to the analysis. Van der Pluijm (1987) suggested that a stepwise unfolding (e.g. 10% intervals) should be employed routinely rather than one-step (100%) unfolding in palaeomagnetic studies since it would enable the possibility that secondary magnetisations were acquired during the straining and pore fluid migration occurring during the folding to be identified. However, it has been reported by some workers (e.g. Hudson and others, 1989) that the palaeomagnetic direction derived from the highest k-value during unfolding (partial tilt correction) does not conform to the predicted ancient field value. Hence techniques of progressive unfolding should not be used to the exclusion of the application of the classical fold test. As a third facet of this project, a simple visual display (two dimensional) of the application of progressive unfolding has been developed and it is applied to the palaeomagnetic studies in parallel with the conventional (one dimensional) palaeomagnetic fold test.

In summary, there were three major aims of this investigation. The first attempted to refine the present magnetostratigraphy of Westphalian A times for the British Isles and north-western Europe and compare it with that proposed by Palmer and others (1985), but it led on to a more general rock magnetic/palaeomagnetic study of these rocks. The second was to detect any block movement/rotation in South Wales based on palaeomagnetic studies of the secondary and possible primary magnetisations and magnetic fabrics of the Old Red Sandstones. The third was to develop a simple visual (two dimensional) method for displaying the results of progressively un-

folding palaeomagnetic directions and comparing the results with the conventional (one dimensional) fold test.

1.2 The Outline of the Thesis

- The basic palaeomagnetic techniques used in the experimental work are described in Chapter 2. The (two dimensional) visual method for presenting the results of progressive unfolding is given in section 2.7.1.

- Chapter 3 describes the palaeomagnetism of the ORS and section 3.4.2 describes the results of fold tests on specimens from Locality 1 (Llanthony, Group 1), Locality 9 (Llanstephan, Group 2), Locality 10 (Freshwater East, Group 3) and Locality 11 (Freshwater West, Group 3). The mean palaeomagnetic directions for Group 1 (the Brecon/Abergavenny area), Group 2 (the Carmarthen area) and Group 3 (the southern Pembrokeshire) are presented in section 3.5.

- The magnetostratigraphy of the Westphalian A rocks is discussed in Chapter 4. Previous results and their reliability are discussed in section 4.1.2.

- Chapter 5 is a brief summary of previous chapters and provides some suggestions for future work.

CHAPTER 2 BASIC PALAEOMAGNETISM

2.1 Introduction

Although magnetism is a very old science, palaeomagnetism, the study of the magnetism in rocks, became a science on its own only during the early 1950's. Due to the development of a sensitive magnetometer by Lord Blackett, the direction and intensity of the magnetisations in very weak rock samples could be measured. At that time the continental drift hypothesis was still a controversial topic and Earth scientists were divided into "drifters", the supporter of the hypothesis, and "non-drifters" who were against it; the latter dominated the Earth Science community at that time. However, research around the world conducted using this new science during the 1960's and 1970's produced findings which were in the drifters' side. Since then palaeomagnetism has developed in sophistication and its application in Earth Sciences is now enormous.

Palaeomagnetism is the study of the fossil magnetism in naturally-produced materials. It is a means of investigating the history of the geomagnetic field over the geological time-scale (McElhinny, 1973). Press and Siever (1986) define palaeomagnetism as the science of the reconstruction of the Earth's ancient magnetic field and the positioning of the continent from the evidence of the remanent magnetisation in rocks. From the definitions above ,

there are two common things that are essential in palaeomagnetism; the existence of Earth's magnetic field and the ability of rocks to acquire remanent magnetisation. Although it has only been widely accepted in the present century that the origin of the Earth's magnetic field resides in the liquid outer core and probably originates in a self-sustaining dynamo, the effect of the field itself has been studied scientifically since the sixteenth century.

2.2 Earth's Magnetic Field

The Earth's magnetic field is a vector quantity and has a magnitude and direction. The field is commonly represented in terms of a Declination (Dec), Inclination (Inc) and the magnitude; the latter quantity is the Intensity (F). Declination is the angle between the field, on the horizontal plane, and the geographic north. Inclination is the angle of dip of the field from the horizontal plane measured positive down and negative up. A cartesian coordinate system can also be used to describe the field. The field is resolved into the North (X), East (Y) and Down (Z) components (see Figure 2.1). Both representations are extensively used by palaeomagnetists and geomagnetists in presenting and analysing the Earth's magnetic field. The transformation from the cartesian coordinate to polar coordinate is given below.

$$X = F \cos(Dec) \cos(Inc)$$

$$Y = F \sin(Dec) \cos(Inc)$$

$$Z = F \sin(Inc)$$

or

$$F^2 = X^2 + Y^2 + Z^2$$

$$\tan(Dec) = Y / X$$

Figure 2.1 Relationship of the geomagnetic elements. The geomagnetic field at any point on the Earth's surface can be described by three parameters either in orthogonal or polar coordinates.

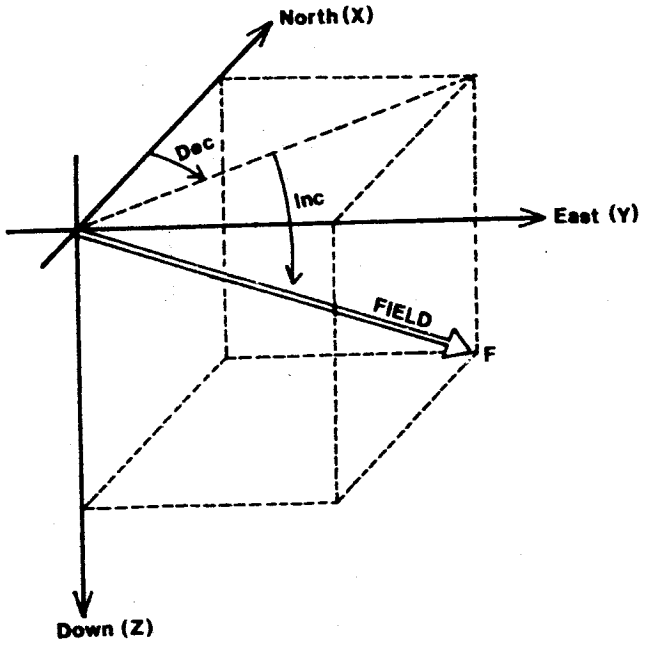

$$\sin (Inc) = Z / F$$

About 90% of the magnetic field on the Earth's surface can be described in term of a dipole field source. The remaining part of the field is referred as the "non-dipole field" (Merrill and McElhinny, 1983). Both the dipole and non-dipole parts of the Earth's magnetic field change with time. If the dipole is placed at the centre of the Earth and aligned to the axis of rotation, the model is called an axial geocentric dipole model. The magnetic pattern on the surface of the Earth associated with the dipole has three characteristics (in SI units) :

1. Intensity (F) = $(\mu_o M / 4\pi R^3) \sqrt{(1 + 3 \sin^2 \lambda)}$ in Tesla (T)
2. Inclination (Inc) = $\tan^{-1} (2 \tan \lambda)$
3. Declination (Dec) = 0° (by definition)

where

μ_o = permeability of free space (henry/m)

λ = latitude (°)

R = radius of the Earth (m), and

M = magnetic moment of the dipole ($A.m^2$)

The axial geocentric dipole assumption for ancient Earth's magnetic field is widely used in interpreting palaeomagnetic data. For example, shallow inclinations found in Upper Carboniferous rocks from Britain have been interpreted to mean that during Late Carboniferous times Britain was located near to the equator. The abundance of coal seams in the Upper Carboniferous rocks of the kind linked to tropical swamp environments seems to support the view.

The validity of the axial geocentric dipole assumption can be tested in several ways. For example, the inclinations observed in sediments deposited during the last few million years are very close to those expected for an axial geocentric dipole. In addition, palaeomagnetic poles from igneous rocks for the last 25 million years, when plate movements were too small to have caused major dispersion, are grouped around the Earth's rotational axis (Tarling, 1983). For older times, the consistency of palaeomagnetic poles from magnetisations of the same age for rocks sampled from different locations within a rigid continental block provides evidence that the dipole assumption used in calculating the poles (see section 2.7.2) is correct. The simple relationship between inclination and latitude in the axial geocentric dipole model (see above) has also been tested. Extensive Mesozoic palaeomagnetic studies in northwest Africa and in southern Africa showed that the palaeolatitude difference between both regions is close to their angular great circle distance (Merrill and McElhinny, 1983; Piper, 1987). Evans (1976) showed that the distribution of magnetic inclinations in the Phanerozoic palaeomagnetic data is close to that predicted by a dipole source and is less compatible with more complex source models.

More recently, Piper and Grant (1989) reexamined the distribution of the magnetic inclinations in the global palaeomagnetic data from Cenozoic to Archean times compiled up to mid 1987. The amount of the data they analysed was ten times more than the amount of data analysed by Evans in 1976 and they were able to evaluate the data through time windows. These authors concluded that the axial dipole assumption is reliably valid for most of the geological times except during Palaeozoic times. They referred the

anomalous Palaeozoic inclination distribution to the effects of remagnetisation during Late Palaeozoic times.

It has been mentioned earlier that the dipole and the non-dipole parts of the Earth's magnetic field change with time. Variations in the field have a time scale ranging from milliseconds to millions of years. Medium scale variations with periods of 10^2 - 10^4 years are called geomagnetic secular variations. These are likely to be recorded by geological events such as volcanic eruptions and rapid sedimentation. In order that the Earth's magnetic field approximates to the axial geocentric dipole assumption used to derive a long term representation of the ancient field, the secular variations have to be averaged out over 10^4 years or more.

From palaeomagnetic studies, it has been found that the polarity of the Earth's magnetic field has changed from a normal to reversed polarity or vice versa frequently over most of geological times. These inversions of polarity usually reckoned tc take place over an interval of 5000 - 10,000 years while intervals of constant polarity have lasted for periods of 100,000 years to 70 million years or more. This phenomenon is known as the geomagnetic field reversal. By convention, the polarity of the present Earth's magnetic field is normal. At the present time, the N-seeking of a compass needle points towards geographical north. If the Earth's magnetic field is in a reversed polarity state, the N-seeking of the compass would point south. It is generally believed that the assumption of a geocentric dipole source is not valid during polarity transitions.

2.3 Magnetisation in Rocks

The other property which is essential in palaeomagnetism is the magnetisation in rocks. The permanent magnetisation is termed the Natural Remanent Magnetisation (NRM). Since the natural process by which this magnetisation is acquired in rocks may vary, other specific terms are also used to accommodate the ways in which NRM is acquired. The NRM of igneous rocks is commonly a TRM (Thermo Remanent Magnetisation). In these cases, the rocks acquire magnetism when their constituent magnetic minerals are cooled through their Curie temperature in the ambient geomagnetic field. The magnetisation acquired by the magnetic mineral then become "frozen" and the thermal energies at lower temperatures are not strong enough to destroy the magnetisation. In other words, the magnetisation has become "blocked" as the temperature falls. A TRM is generally acquired over the whole temperature range from the Curie temperature down to ambient temperatures and is the sum of each partial TRM (pTRM) acquired over a temperature interval.

The NRM of sedimentary rocks may be a DRM (Detrital/Depositional Remanent Magnetisation) and/or CRM (Chemical Remanent Magnetisation). DRM is acquired during deposition of magnetic particles as a sediment. Due to the ambient magnetic field, these particles align themselves to the direction of the field during their passage through the fluid medium. Hence, smaller particles for which the counteracting gravitational force is least are then most likely to have their magnetic directions parallel to the field. The DRM usually represents the primary magnetisation since it reflects the palaeofield at the time when the rock was formed. However,

grain alignment is likely to be modified during subsequent dewatering and lithification of the sediment. This produces a Post-Depositional Detrital Remanent Magnetisation (PDDRM). The inclination error (shallowing the palaeomagnetic direction of sediments towards the horizontal plane) only occur with DRM (Piper, 1987) and it is rare in natural sediments (Tarling, 1983). In contrast, the CRM is acquired sometime after the rock formation by growth of magnetic minerals in the ambient field well below their Curie temperatures. A new magnetic mineral in rocks is either a product of precipitation from solutions, or of interaction between fluids and solids to produce alteration of existing minerals. The magnetisation of the new mineral is aligned with the ambient magnetic field when the grains have grown to a certain critical volume and the rock acquires a CRM. Changes in the ambient magnetic fields may not be strong enough to deflect or to destroy the magnetisation. It is not uncommon for rocks to have two kinds of remanence. For example, the NRM of red beds often consists of a DRM, which is primary, and a CRM which is secondary. The DRM is carried by detrital specularite and the CRM by pigments or authigenic grains (Dunlop, 1972 ; Collinson, 1983). Specularites ($> 1\ \mu m$) and pigments ($< 1\ \mu m$) are haematite with different forms. However, Walker and others (1981) suggest that red beds may have a more complex classification (at least six forms of haematite) based on petrographic studies.

Whatever the process by which rocks acquire magnetism (TRM, DRM/PDDRM or CRM), the time required by the magnetic grains in the rocks to achieve equilibrium with the ambient field (the relaxation time) is usually very long. This is the reason why the remanence is very stable and may not change for millions or even billions of years.

The response of material to magnetic fields is classified as diamagnetic, paramagnetic and ferromagnetic. The term magnetic mineral is usually applied to ferromagnetic phases, the only ones which can retain a remanence after the causative field is removed. The effect of external fields on diamagnetic and paramagnetic substances is reversible and the magnetisation is lost when the external field is removed. In contrast, ferromagnetic materials will retain the magnetisation when the external field is removed and the effect of the external field on the materials is irreversible. Ferromagnetic substances are divided further into ferromagnetic, antiferromagnetic, ferrimagnetic and canted antiferromagnetic substances. This classification is based on the arrangement of the magnetic moments of the ions (see Figure 2.2). Domain theory is used to explain magnetism in ferromagnetic materials. A magnetic grain is normally divided into smaller volumes called domains so that within a domain, the magnetisation is uniform. If the magnetic grain is exposed to an external magnetic field, the domain with magnetisation parallel to the external field will grow at the expense of the other domains. This movement of the domain wall is usually not reversible and the magnetic grain will retain the remanence with or without the presence of an external field. If the volume of the magnetic grain is so small that it is incapable of subdivision, it is single domained. Since a single domain grain does not have a domain wall, the response of the grain to the external field will be determined by the orientation of the grain with respect to this field.

Most magnetic minerals in rocks can be classified into iron oxides, iron sulphides and iron hydroxides. The most important of these three groups is the iron oxides. Magnetite (Fe_3O_4) and haematite (αFe_2O_3) are common

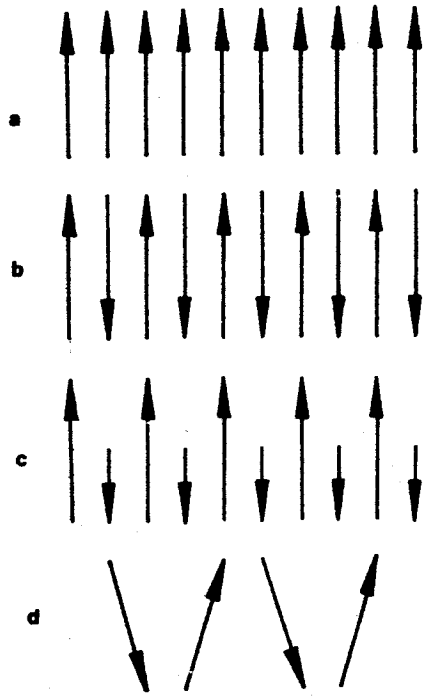

Figure 2.2 Arrangement of magnetic moments in ferromagnetic (a), antiferromagnetic (b), ferrimagnetic (c) and canted antiferromagnetic (d) materials. Only antiferromagnetic material (b) exhibits zero spontaneous magnetisation.

examples of iron oxides. Magnetite is a very common magnetic mineral and has strong magnetic properties. Magnetite is ferrimagnetic and its saturation magnetisation (single domain magnetite) is ~480 k A/m. The saturation is achieved in fields below 1 T (Tesla). In nature, magnetite can be found in single or multi domain forms whereas haematite has a much larger domain size and usually occurs in single domains. Haematite is canted antiferromagnetic with a saturation magnetisation of ~2.5 k A/m and needs higher fields (> 1 T) to saturate. Also the coercivity of haematite is generally much higher than the coercivity of magnetite. The coercivity is the applied magnetic field required to reduce the remanence to zero. Owing to its high coercivity, AF (Alternating Field) demagnetisations are not very successful in dealing with haematite-bearing sediments. However, thermal demagnetisation usually works very well for both minerals. The decay curves (intensity versus temperature) are different and identify the unblocking temperature spectrum of the minerals holding the remanence. The unblocking temperature is the temperature at which the relaxation time of particles carrying the NRM is reduced to a period of time comparable to the experiment (say the hold time at an elevated temperature) and their contribution to the NRM of the rocks is subtracted. The unblocking temperature is mostly above 600° for haematite and the remanence of this mineral may not be fully unblocked to 680° - 720°C. It is below 580° for magnetite. Above these temperatures ferromagnetic materials become paramagnetic. Although it is commonly assumed that the magnetisation with the highest unblocking temperature is the primary magnetisation, this is not always the case. The term "primary" and "secondary" should not be used to assign the

time of the remanence acquisition to the time of formation unless this can be established by an unambiguous test.

2.4 Sampling

There are two basic methods of sampling consolidated rocks for palaeomagnetic study: block sampling and core sampling. In block sampling, a piece of rock is removed from an outcrop. The volume of the sample is about the same as a thick pocket book and a surface is chosen as flat as possible. Before removal, a strike line and a dip direction are marked on the flat surface. The bearing of the strike line is recorded as well as the name of the sample, the dip, the bedding correction (the tilt and direction of tilt of the bed where the sample comes from, in the case of sedimentary rocks) together with the location. Using a chisel and a hammer, the sample is removed from the outcrop. Sample collection is rapid and can be done by one person. The equipment used is quite simple, a magnetic/sun compass, a chisel, a hammer, a note book, a pen (or pencil) and a waterproof marker.

There are some disadvantages to block sampling. More work and time will be spent in the laboratory for sample preparation including re-orientation and drilling. Before drilling, the sample is set up using plaster of Paris. The flat surface is placed horizontal. A few lines parallel to the strike line are drawn and also the dip marked on each new line. Usually, 5 cores were drilled from each sample in this study. Then, a line representing the north is drawn along each core using a diamond scriber. Each core is given a laboratory number and the top and bottom of the core are distinguished. This re-orientation is one of several drawbacks of using the block sampling tech-

nique because it adds to the orientation errors. Another disadvantage is the large weight and volume of the samples taken from the field to the laboratory. Finally, there is a restriction on a piece of rocks which can be sampled. The piece must be loose or easy to remove using a chisel and a hammer from the rest of the outcrop. The possibility that the sample comes from the weathered part of the rock is therefore very high.

In core sampling, cores of 1 inch in diameter (and usually about 5 cm long) are drilled in the field. During the drilling, coolant water is pumped through the drill in order to keep the temperature low and wash out the rock dust. The drilling usually takes a few minutes depending on the hardness of the rocks. The core is oriented in situ using a sun/magnetic compass and clinometer before it is taken out. Some disadvantages of using the core sampling technique are that the operation needs two people and the equipment is bulky; a coolant water tank, a petrol tank, several drills and two or three drilling machines besides the standard equipments used in block sampling; also various extraction tools are needed to recover the core (or bits) from the hole. More time is therefore spent in the field work. However, the advantages make this technique more preferable to block sampling. There is less restriction on the material that can be sampled. Cores can be drilled from the interior of joint blocks remote from weathering. The weight and the volume of the rocks taken from the exposure are very small. Less time is needed in sample preparation in the laboratory. There is no re-orientation of the sample which makes the orientation of core sampling more reliable than block sampling.

The terms Locality, Site, Sample and Specimen are mostly adapted from Tarling (1983). A specimen refers to a core which has been trimmed into a standard size (usually 1 inch in diameter and in length). Specimens are derived from samples. A sample is a piece of rock which is individually oriented in the field. In core sampling, most specimens are identical to samples. In block sampling it was common to have five specimens from one block sample in this study. A collection of samples is termed a site. At the same site (for example, samples taken from the same bed or stratigraphic level in sedimentary rocks) it is usually assumed that the samples have been magnetised at the same time. In block sampling, samples are usually identical to sites although more than one block may be collected. Sites are grouped into localities. A locality typically covers a few kilometre squares.

2.5 Magnetometer

2.5.1 The Spinner Magnetometer

As in a generator, an alternating voltage will be generated if a magnetised sample rotates continuously within or near a coil or fluxgate system (the sensor). The amplitude of the output voltage is proportional to the component of magnetic moment of the sample which is perpendicular to the rotation axis. The phase of the voltage is used to relate the direction of the component to a reference direction in the sample. This is the basic principle of a spinner magnetometer.

In a "Molspin" spinner magnetometer, a circular fluxgate sensor surrounds the rotating sample and a computer is used to manipulate the output. The alternating output from the sensor for each cycle is fed to an ADC (Analog

to Digital Converter) and is defined by 128 twelve-bit numbers proportional to the amplitude of the output waveform at approximately 3° intervals. Each number related to each interval is added for each complete revolution. This number proportional to the mean amplitude of each interval is then analysed by the computer using Fourier analysis. The results are printed out on the screen and/or the printer and the data are saved in a diskette. In the Geomagnetism Laboratory, Department of Earth Sciences, University of Liverpool, the data from the diskette are sent to a database in the University mainframe computer. The lowest NRM that can be measured by this magnetometer is within the region of ~10E-8 A.m^2/kg. When measuring samples with intensities close to this region, the average of several measurements for each sample must be made to improve the signal÷noise ratio for a greater accuracy. This takes a longer time for the measurement of each sample than the normal procedure which is usually done with single measurements.

2.5.2 The SQUID Magnetometer

In contrast, the SQUID (Superconducting Quantum Interference Detector) magnetometer is a more sophisticated and complex instrument and it is also much more expensive. The magnetometer is also known as a cryogenic magnetometer since the sensor (the SQUID detectors and pick-up coils) works in a very low temperature environment created by liquid helium. The basic principle of the magnetometer is to detect extremely small current changes in a superconducting ring due to changes in its external field. When the ring is in the superconductive state, the ring inhibits any magnetic flux within the ring by creating an opposed magnetic field. This phenomenon is

known as the Meissner effect. A typical noise level of a SQUID magnetometer is about 10E-11 A.m^2/kg. However, the fluctuation of the external field (e.g. the Earth's magnetic field) also affects the sensitivity of the magnetometer (Collinson, 1983). A low field cage housing the magnetometer will possibly improve the sensitivity. One of four SQUID magnetometers in the Geomagnetism Laboratory is located inside a low field cage. The sensitivity of the magnetometer is about 10 times more than that of a MOLSPIN spinner magnetometer. Some very weak samples which could not be measured with the spinner were able to be measured with the SQUID magnetometer with a certain accuracy.

2.6 Thermal Demagnetisation

AF (Alternating Field) and thermal demagnetisations are the two basic magnetic cleanings which are routinely used in palaeomagnetic analysis. The principle of the magnetic cleaning is to recover the component structure of the NRM. Since thermal demagnetisation is commonly applied to sediments which comprise the material of this study, the technique will be discussed in this section. It has often been reported that thermal demagnetisation is able to isolate the high blocking temperature component from red beds samples including the study areas relevant to this investigation. Chamalaun (1963,1964) was one of the first workers to use thermal demagnetisation on red beds. He suggested that the technique was able to successfully isolate the primary from the secondary component in these rocks. McClelland-Brown (1983) reported the recovery of a primary Devonian component from South Wales Old Red Sandstones. She employed thermal demagnetisation techniques and claimed to have isolated the pri-

mary from an overprint overwhelmingly of Permo-Carboniferous age. Quite recently, Channell and others (1991) found that their Old Red Sandstone samples from central South Wales showed two resolvable magnetisation components when they were subjected to stepwise thermal demagnetisation. Probably one of the best examples of the effective application of thermal demagnetisation is concerned with the controversial topic of the base of the Permo-Carboniferous superchron which was solved by thermal demagnetisation studies (Miller and Opdyke, 1985). McMahon and Strangway (1968) reported normal polarities within Colorado red beds and proposed the youngest normal horizon as the base of the superchron. However, the re-examination by Miller and Opdyke using thermal demagnetisation techniques failed to find the normal zones. They suggested that the AF demagnetisation carried out by previous workers had been unable to subtract a secondary component from a primary component of reversed polarity.

There are two major reasons for applying stepwise thermal demagnetisation to palaeomagnetic samples :

1. to test for the stability of the remanence.
2. to recover the components comprising the NRM.

However, exposing a specimen to a higher temperature will increase the probability of chemical changes and/or the acquisition a TRM (Thermo Remanent Magnetisation) during cooling. This will obscure the existing NRM, if the purpose of the experiment is to measure the remaining NRM after heating to that temperature. In order to eliminate this unwanted magnetisation, it is necessary to cancel any external magnetic field affecting the specimen. For example, a combination of a low field cage and a good

thermal demagnetiser like those used in the Geomagnetism Laboratory is required to suppress the external magnetic field (e.g. Earth's magnetic field which is of the order of tens of micro T (Tesla)). This system reduces the ambient field to a few hundred nano T within the cage and down to < 10 nano T inside the oven. Using this system, the specimen is exposed to a very low magnetic field throughout the thermal treatment.

2.7 Data Analysis

There are two standard ways of representing progressive demagnetisation data : directions may be plotted on a circular equal area or stereographic plot and the total vector may be plotted on an orthogonal plot (Zijderveld plot). At specimen level, the orthogonal plot gives information about the directional changes as well as the changes in intensity during the demagnetisation treatment. From the plot each component of the NRM can be revealed if their spectra are not similar. In contrast, the circular plot which shows the changes in direction only, is more difficult to interpret especially if two components with similar directions are present. If the NRM of the specimen consists of one component only both plots are simple to interpret. In the circular plot, the data will gather closely around the NRM direction, and in the orthogonal plot the data will fall in a straight line converging from the NRM value to the origin of the plot (usually the noise level of the magnetometer). If the NRM is resistant to change or close to the noise level, the orthogonal plot is more difficult to interpret since no linear segments can be defined. In this case use can be made of the circular plot with a lower level of confidence on the assumption that the NRM consists of one component only.

To determine a mean from a collection of palaeomagnetic directions the Fisher statistics are applied (named after Sir Ronald Fisher who published the theory of these statistics in 1953). Actually, the method can be used for any kind of data representing points on a sphere. Two parameters in this statistical system are widely used in palaeomagnetism : the precision parameter k and the alpha-95. The precision parameter k is a measure of how well grouped the directions are. It measures from 0 for a random distribution to infinity for perfect grouping (no dispersion). The alpha-95 is the radius of 95 percent confidence of the cone with its origin at the centre of the sphere. In other words, there is a 95% probability that the mean lies within $\alpha°$ of the calculated mean.

In Fisher statistics, the probability distribution for points on a sphere can be described by

$$P \sim e^{(k \cos\varphi)}$$

where φ is the angle between a point and the true mean and k is the precision parameter.

To calculate the mean of N magnetisation directions, one should

-transform declination (D) and inclination (I) of each direction into its cosine direction.

$$x_i = \cos D_i \cos I_i$$

$$y_i = \sin D_i \cos I_i$$

$$z_i = \sin I_i$$

-find the resultant, R, where

$$R^2 = (\sum x_i)^2 + (\sum y_i)^2 + (\sum z_i)^2$$

-For $k > 3$, the precision parameter is of the form

$$k = (N - 1)/(N - R)$$

-The mean declination (D_m) and inclination (I_m) are given by

$$\tan D_m = \sum y_i / \sum x_i$$

$$\sin I_m = \sum z_i / R$$

-The estimate of the confidence in this direction can be found by calculating alpha-95.

$$\cos \alpha_{95} = 1 - [(N - R)/R] [(20)^{1/(N - 1)} - 1]$$

It is not appropriate to use Fisher statistics to find a mean at specimen level if the NRM of the specimen consists of two components or more. The components must first be isolated and the statistics applied to each component in turn. In this study, component directions were determined by picking (by eye and/or by comparing the alpha-95 values) the straight line segments from the orthogonal plots of the thermal demagnetisation data and using principal component analysis (Kirschvink, 1980; Sherwood, 1989) to compute the component directions. These features can be found in the PLOTCORE program.

The PLOTCORE program available in the library disk of the Department of Earth Sciences, University of Liverpool, is a sophisticated program and easy to run. The program analyses demagnetisation data of a specimen taken directly from the database in a mainframe.

There are three basic calculations which can be made and visually displayed by the PLOTCORE program; The intensity plot, circular plot and orthogonal plot. The demagnetisation data are shown on a screen of a terminal (usually graphic) and by pressing the return key on the keyboard the

data from each demagnetisation step will be placed in rejected or accepted status. Then the plots will appear on the screen based on the accepted data. Although only one plot appears on the screen each time, four plots (e.g. the intensity, circular and two orthogonal plots) can be drawn out on the plotter for a hard copy. Examples of these are illustrated in Chapters 3 and 4. This enables each specimen to be studied comprehensively and the consistency of specimen behaviour within a site to be fully evaluated.

2.7.1 Fold Test

A number of palaeomagnetic field tests can be applied to evaluate the age of a remanence with respect to geological events. They comprise the fold, contact, conglomerate and unconformity tests (Piper, 1987). Of these only the fold test could be routinely applied in this study. A fold can be used for the study of the age of a remanence which can then be dated relative to the time of deformation (Graham,1949). The ideal fold for application of this test should have a horizontal axis and be as orthogonal to (and therefore sensitive to) the bearing of the palaeomagnetic direction as possible. If the axis is not horizontal (i.e. the fold plunges) the in situ palaeomagnetic direction must be corrected for the plunge before applying the fold/tilt-test. Actually both corrections are commutative. The plunge correction is a rotation about a horizontal axis and therefore only affects the declinations. MacDonald (1980) pointed out that tilt/fold correction may be incorrect if the plunge is the resultant of more than one deformation or if small scale block rotations have taken place between sites. Sometimes the optimum grouping of magnetisations is obtained when tilt is only partially adjusted

for and it may then be possible to link the remanence directly to the deformation event (e.g. McClelland-Brown, 1983).

McElhinny (1964) proposed a statistical test in employing the Graham's fold test. The null hypothesis of the McElhinny test is that the value k_1 and k_2 are drawn from the same population; where k_1 and k_2 are the estimates of the precision parameter before and after adjusting for the tilt. The ratio of k_2/k_1 has the F distribution with 2(N-1) degrees of freedom and N is the number of directions of magnetisation involved in the test. If the null hypothesis has only 5 percent significance (or less), the hypothesis can reasonably be rejected at 95 percent (or more) level of confidence. For a simple application of the fold test, McElhinny tabulated values of k_2/k_1 at which the fold test is significant for various N values. To use the test one can simply compare their ratio of k_2/k_1 with the value in the table. If the ratio k_2/k_1 is greater than this value, then the improvement of the grouping with tilt adjustment is significant at the 95 percent confidence level. The 99 percent confidence level can also be tested for using McElhinny's test. In this study, the F distribution values can be generated by calling a statistical function in the NAG FORTRAN Library in the university mainframe (the function is called G01CBF).

McFadden and Jones (1981) pointed out that the McElhinny test is invalid in statistical terms because it assumes implicitly that the overall population of the magnetisations involved in the test has a Fisherian distribution which is not always the case; in particular, if it is the case before tilt adjustment, it will not generally be the case after adjustment. McFadden and Jones argued that even if the overall population is Fisherian, k_1 and k_2 derived from

the population are not independent as they should be. They gave an alternative formulation of the test accommodating this problem. Their revised test shows that the McElhinny test is actually too stringent. In other words, the absence of a significant fold test after applying the simple McElhinny test does not necessarily mean that the remanence is not pre-folding. Facer (1983) also showed that a simple tilt test applied by rotating the palaeomagnetic direction about the present strike of beds is often insufficient because the beds will often undergo internal straining during deformation. More information about the style of the fold is necessary, especially when the result of the fold test is negative. It was also acknowledged that the remanence carried by CRMs (secondary) may not be affected in the same way as DRMs.

In applying a fold (or tilt) test, palaeomagnetic directions are corrected for plunging first if all the plunging is reckoned to postdate the tilting. The plunge correction is a rotation about a horizontal axis orthogonal to the fold axis. The bedding correction is also a rotation about a horizontal axis which in this case is parallel to the strike of the bed. MacDonald (1980) suggested that the tilt correction may be incorrect even when all rotations have taken place about horizontal axes. This can happen since they may be the resultants of several separate motions and because corrections may not be applied in the order which they actually occurred. The result is to produce an increased scatter in declination relative to inclination.

Successive tectonic events, such as a folding and faulting, reorient rock masses repeatedly during orogeny. These reorientations are equivalent to sequential rotations and can be combined into a single equivalent rotation,

which is called a net tectonic rotation (MacDonald, 1980). The net tectonic rotation is defined as the single equivalent rotation which rotates a rock mass from its initial depositional orientation to its present deformed orientation. The apparent tectonic rotation is a net tectonic rotation followed by a tilt/bedding correction. This apparent tectonic rotation results in a declination anomaly. However, it may be difficult to demonstrate that a fold test in palaeomagnetism always produces a declination anomaly. The plunge correction usually affects the declination and if the scatter is increased then it can be concluded that the plunge was already there when the rock acquired its magnetism. If the plunge correction does not have an effect on the k precision parameter and the discrepancy of the declinations is significant, some explanation for the discrepancy must be sought (e.g. localised rotations). In this situation the bedding correction will always give a declination anomaly since it only averages the scatter of declinations.

If rocks acquire a remanence during folding (i.e. a syn-folding magnetisation), the fold test can be presented by a graph showing the relationship between the k values and the stages of unfolding (partial tilt correction; see Figure 2.3a). This stepwise unfolding has been applied to document syn-folding magnetisation (e.g. McClelland-Brown, 1983; Schwartz and Van der Voo, 1984). Van der Pluijm (1987) suggested that in palaeomagnetic studies a stepwise unfolding (e.g. 10% steps) should be performed routinely rather than one-step (100%) unfolding. Since it is possible that secondary magnetisation may be acquired during the first few percent of folding, a pre-folding origin may be erroneously concluded. Nowadays it is common to carry out a stepwise unfolding in palaeomagnetic

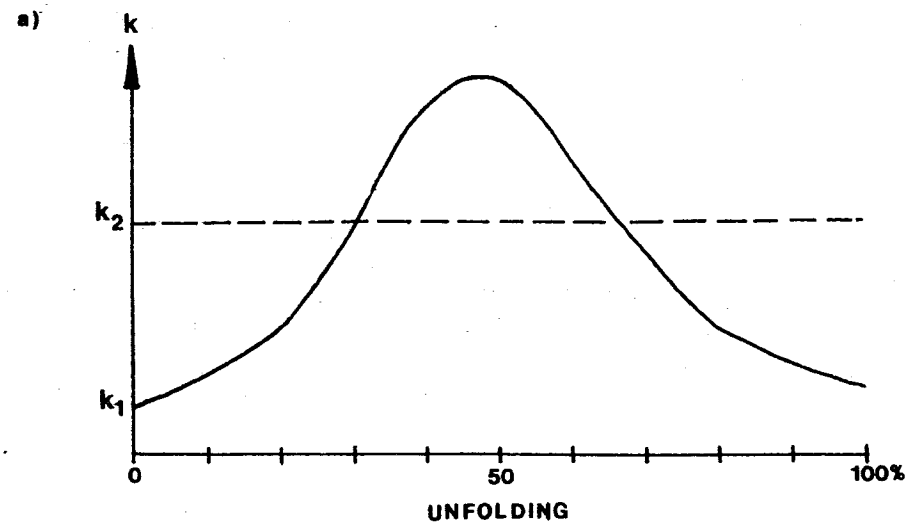

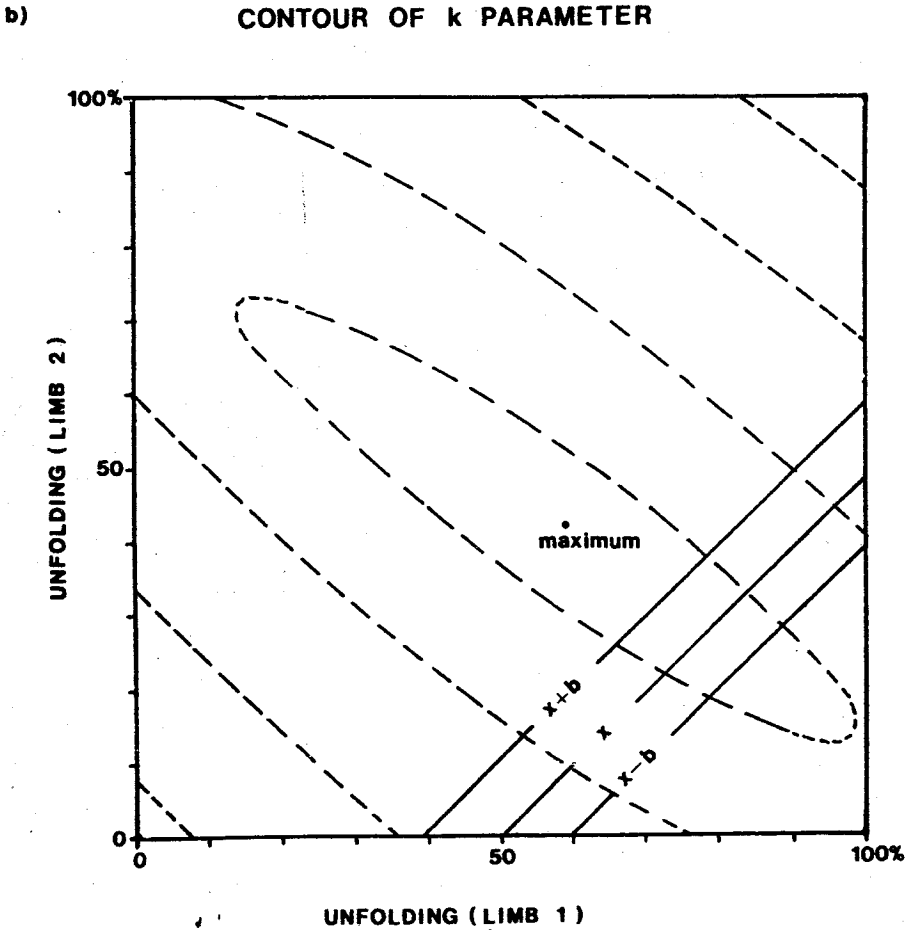

Figure 2.3 Partial tilt correction in a fold test (c f Figure 2.4 and 2.5).
(a) One dimensional fold test (usual fold test) where both limbs of a fold are unfolded simultaneously. The k-values above the broken line (k2) pass the McElhinny test (k2/k1) at 95% confidence level.
(b) Two dimensional fold test (this study) where both limbs of a fold are unfolded separately. (x + b) and (x-b) are the upper and lower limit of the expected inclination (x).

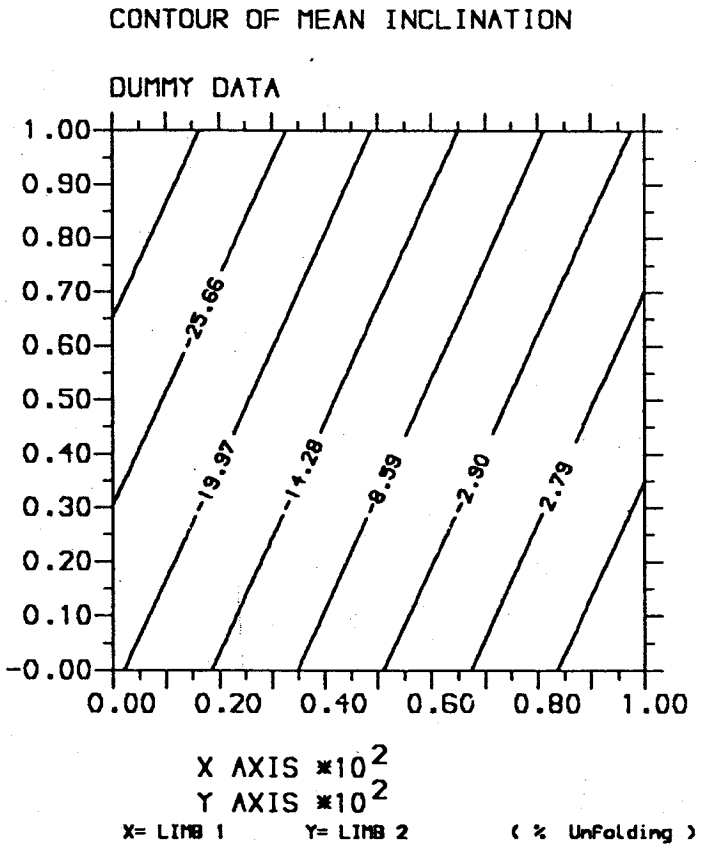

Figure 2.4 Contour of the mean inclinations for the dummy data in responding to unfolding of each limb. Since the inclination contour exhibits a simple distribution (usually straight lines but not always), only the expected, upper limit and lower limit of the mean inclinations will be shown in the two dimensional fold test.

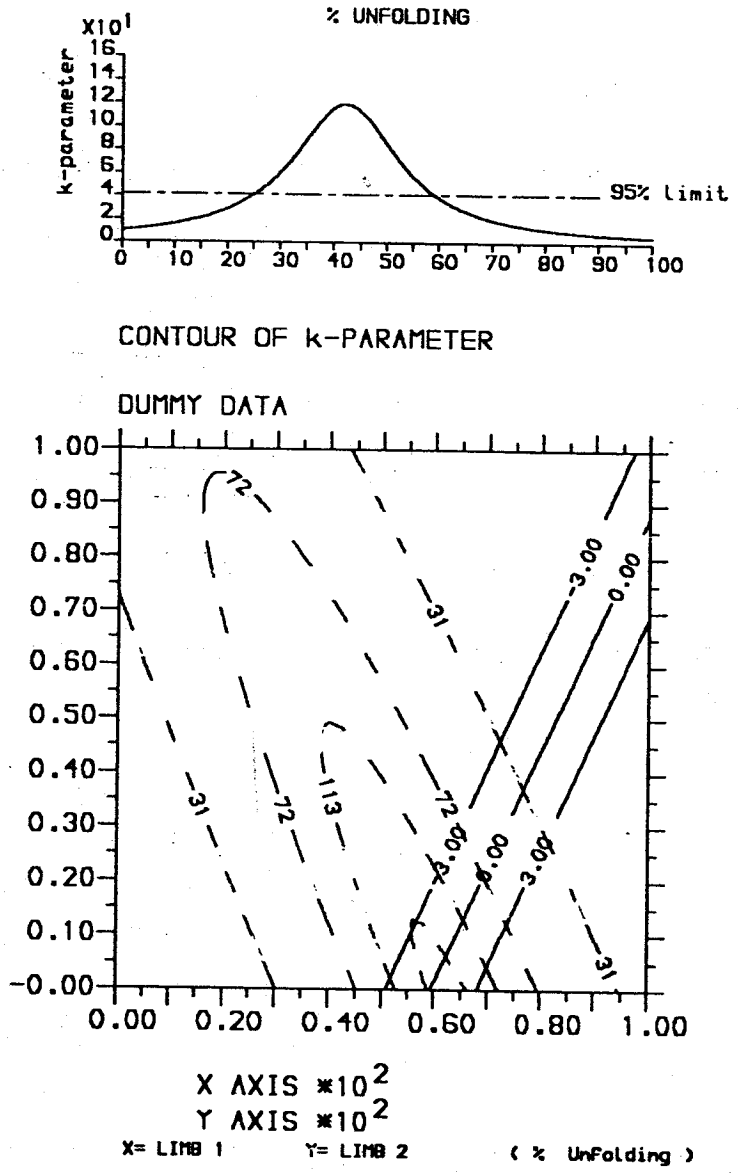

Figure 2.5 Fold test results from the dummy data (see also, Table C-1). The top picture is the usual fold test and the broken line represents the 95% limit of the McElhinny test. The bottom picture is the two dimensional fold test; the X axis is horizontal and the Y axis is vertical. The k-parameter and the mean inclination values are given by the dashed and solid contour lines respectively. The usual fold test is exactly similar to the cross section of the two dimensional fold test along the diagonal line from (0,0) to (100,100) % unfolding.

investigations (e.g. Torsvik and others, 1989; Storetvedt and others, 1990; Burmester and others, 1990).

In a stepwise unfolding a peak may be found where the value of k attains a maximum value. Some authors (e.g. Miller and Kent, 1986; Burmester and others, 1990) have introduced statistics which are equivalent to the McElhinny test. They compare the k values relative to the k maximum and use the logarithmic scale of k in order that the 95% level of confidence can be drawn. Any k values falling within the k maximum and the k at 95% level of confidence can be used to determine the mean palaeomagnetic directions from both limbs of a fold. It is implicit in this method that the k maximum has passed the McElhinny test. This is not always the case. If the k maximum does not pass the McElhinny test (i.e. the test is negative), this method may give an unrealistic level of confidence in which all stages of unfolding (including the in situ) may fall within the interval. Since this k maximum may also be altered after plunge correction (if the fold is plunging), it is appropriate to compare the k values in incremental untilting to a fixed k value. In present study, the k values are being compared to the k value at the in situ configuration (the only one which is unchanged after plunge correction) as in the original McElhinny test instead of the k maximum. The k values above k_{limit} (or k_2, see Figure 2.3a) at which the null hypothesis of the McElhinny test cannot be rejected at 95% level of confidence are considered to be statistically justifiable for deriving the palaeomagnetic directions. It can be shown in this study (see CHAPTER 3) that k_2 is sometimes higher than the maximum k. It may then be possible that either the test is too stringent as in the pre-folding case (cf. McFadden and Jones, 1981) or the remanence is post-folding (or acquired before the

folding was fully completed). In this case, the k will be plotted automatically on a logarithmic scale so that the k curve can still be seen clearly although the value of k_2 is much higher than the k maximum. The value of k_2 could be lowered by application the statistics suggested by McFadden and Jones (1981). This is not considered in this thesis (cf Li and others, 1989) because the author has a strong feeling that a more important problem arising in a such fold test is that the derived palaeomagnetic direction sometimes deviates from the expected palaeofield direction. In this study, although the k maximum is lower than k_2 (the McElhinny test is negative), the derivation of the palaeomagnetic direction based on this maximum k-value is assumed to be justifiable.

It is not always clear that the palaeomagnetic direction derived from this maximum k refers to a true palaeomagnetic field. For example, Hudson and others (1989) reported a palaeomagnetic direction derived from the highest k value which did not coincide with the expected palaeomagnetic direction for the area they were investigating. They suggested that derivation of the palaeomagnetic direction from the highest k value was incorrect in this case. In the present study this one dimensional fold test where both limbs of a fold are unfolded simultaneously has been expanded into a two dimensional fold test where each limb is unfolded separately (see Figure 2.3b). The maximum k value derived from this new method is usually different to, and higher than, that derived from the one-dimensional method. The aim of this analysis is to evaluate whether the highest k obtained by this new method also gives 'unexpected' palaeomagnetic directions and to try to solve the problem by introducing the predicted palaeofield into the fold test as a constraint. In other words, the geometry of the fold at the time of

remanence acquisition is being determined not only by the highest k value but also by the assumed palaeofield direction.

In the one-dimensional fold test it is possible to have 50 stages of unfolding (2% steps) in the present analysis. There are 51 values of the k parameter which correspond with 51 configurations of both limbs of the fold from the in situ position to the horizontal. At each stage of unfolding (except the horizontal) the ratio of the dip of one limb to the other is kept constant. In the new method, where each limb is unfolded independently, there are 2601 values of the k parameter for the same stages of unfolding (2% steps). Since this involves a large amount of dimensional data , contouring techniques are used to present them. The contour usually has one maximum although sometimes two maxima result. Since the palaeomagnetic direction derived from the maximum k value does not necessarily reflect the palaeofield, the expected palaeomagnetic direction must be determined from an independent source; for example, the palaeomagnetic direction from adjoining horizontal and undeformed strata or from the established APWP (Apparent Polar Wander Path, see section 2.7.2) for the area being investigated. For the sake of simplicity, only the expected inclination (x) with the upper (x+b) and lower (x-b) limits (these values usually form straight lines on the contour plot; Figure 2.3b) will be shown and will guide the program in finding the highest k value within the range of the expected palaeomagnetic directions. A listing of the program, called the FOLDCONT program, with a brief explanation is given in APPENDIX C. Three mean palaeomagnetic directions are calculated by this method. The first is derived from the two-dimensional maximum k value, the second is from the highest k value within the range of the expected palaeomagnetic direction and the third is from the usual one-

dimensional maximum k value. Also, the F distribution value (the ratio of k_2/k_1), k_1, k_2 and k_3 are presented for the McElhinny test where k_1, k_2 and k_3 represent k-parameters before the tilt adjustment (in situ), at 95 percent limit and after fully unfolded respectively. One of the advantages of using this new method is that no restrictions are placed on the orientation of each limb during the acquisition of the secondary magnetisation. This means that it is possible to relate stages of unfolding to the geometry of a fold at the time of remagnetisation.

The FOLDCONT program is tested using a set of dummy data. Let a palaeofield direction Dec/Inc = 190°/0° be taken as the predicted palaeomagnetic direction; this is typical of the field direction in the study area of this thesis during Permo-Carboniferous times. Rocks on both limbs of a fold in an area located somewhere in South Wales recorded this palaeofield during folding. At that time (~ 290 My, see Table 3.2), the limb 1 and limb 2 were between a quarter and fully folded. The field and the laboratory measurement data are shown in Table C-1, APPENDIX C. For the sake of clarity, the magnetic directions were dispersed slightly so that the maximum k value was lowered to a value typically found in real data. These data imply that the fold was more symmetric when the remagnetisation occurred. Figure 2.4 shows the relationship between the mean inclinations and unfolding stages of each limb. It can be seen clearly that each possible inclination value is represented by a unique straight line. Hence, the position of the expected palaeofield inclination (0°, located between contour lines -2.90 and 2.79) on the contour is fixed. If both limbs of the fold are unfolded simultaneously, the mean inclinations will have a profile which is similar to the cross section of Figure 2.4 along the diagonal line from points (0,0) to

(100,100) % unfolding. Whatever the distribution of k-parameter is, the mean inclination derived from the usual fold test will fall within a range of -2° and -20°. In other words, the result may deviate from the predicted palaeofield direction. The nearest value (-2°) is achieved if the maximum k-parameter lies near to the intersection point between the diagonal line and the inclination line of -2°. In this case, the maximum k should be near the (100,100) % unfolding point which means that both limbs should be unfolded fully (i.e. the beds restored to horizontal) in order to achieve the mean inclination as close as possible to the palaeofield direction at the times of remagnetisation. However, it has been mentioned earlier that in this model the strata were remagnetised when the limb 1 and limb 2 were a quarter and fully folded, and not horizontal as the usual (one dimensional) fold test assumed. This shows that the one dimensional fold test has failed to relate the palaeomagnetic directions derived from the test to a geomagnetic field and has not been able to document the unfolding stage when the remagnetisation occurred.

The results of the new fold test are shown by Figure 2.5 (see also Table C-1, APPENDIX C). The result from the usual fold test (Inc=-13°) is steeper than the result from the two dimensional fold test (Inc=0.9°) and deviates from the expected palaeofield direction. This means that the usual fold test misplaces the dummy area about 6° further north (~ 600 km or about twice the distance between Liverpool and Cardiff). There are two possible explanations for the discrepancy in this study. Firstly, the diagonal line from (0,0) to (100,100) % unfolding does not intersect the straight line representing the assumed inclination (0°). Secondly, the position of the maximum k lies far off the intersection point. These problems related to the

Mechanisms to Produce Cross-over Geometry of Magnetization

Mechanism	Reference
Class 1. Acquisition of magnetization during folding	
CRM	McClelland-Brown, 1983 McCabe et al., 1983 Schwartz and Van der Voo, 1984 Kent and Opdyke, 1985 Miller and Kent, 1986a Benthien and Elmore, 1987 Bachtadse et al., 1987
TCRM	Granier et al., 1986
VpTRM	Kent, 1985
PRM	this study
Class 2. Combinations of different magnetization components	
Prefolding + postfolding	Schwartz and Van der Voo, 1984 Miller and Kent, 1988b
Prefolding + synfolding	this study
Prefolding + synfolding + postfolding	this study
Synfolding + postfolding	this study
Class 3. Structural modification of rocks with prefolding magnetization	
Indirect effect - oversteepened fold limbs	
1. Shear-slip folding 2. Discontinuous strain (e.g., pressure solution)	Tarling, 1983 Kodama, 1988
Direct effect - deflection of magnetization	
1. Magnetization as passive marker	Kligfield et al., 1983 Cogne' and Perroud, 1985 Hirt et al., 1986 Kodama, 1988
2. Rotation of magnetic minerals a. March model b. Layer-parallel shear & particle rotation	Cogne' et al., 1986 van der Pluijm, 1987 Kodama, 1988

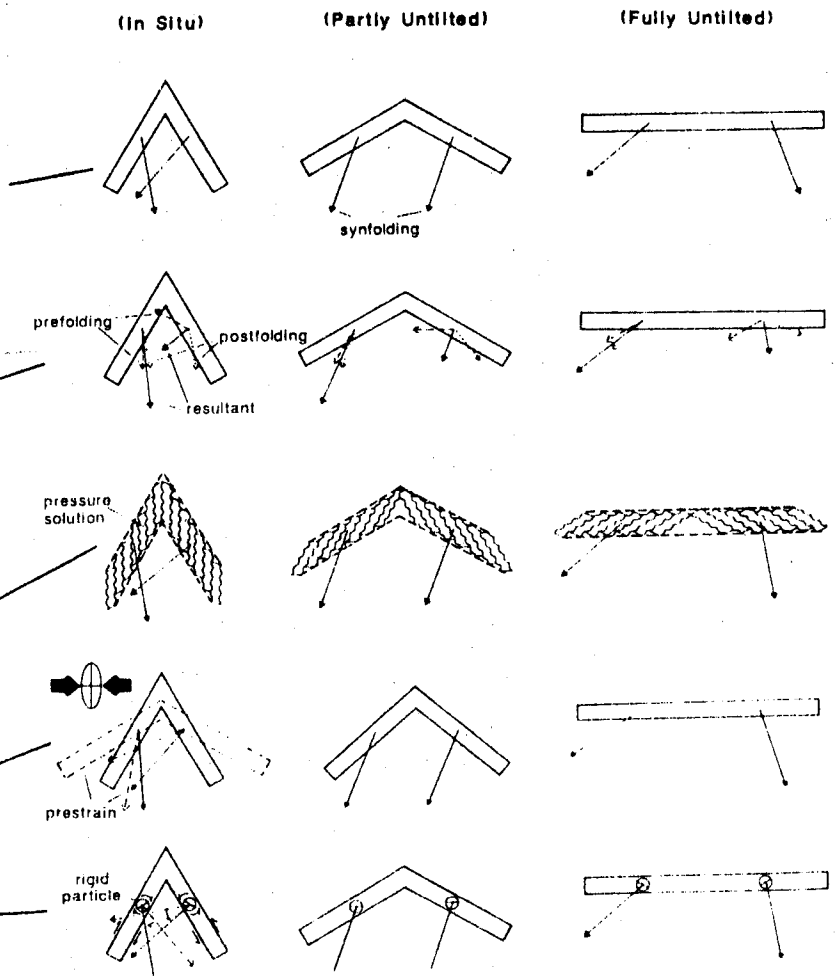

Figure 2.6 Mechanisms that could produce a cross-over geometry magnetisation. Only the mechanism of Class 1 (which is relevant to this thesis), the mean palaeomagnetic direction derived from the one dimensional fold test should be parallel to the geomagnetic field at the time of its acquisition. The references cited in this figure are given in the original paper (Hudson and others, 1989).

one-dimensional fold test could be solved by placing the assumed inclination line near the maximum k as done by the two-dimensional fold test.

Other explanations for the deviation of the palaeomagnetic direction derived from one-dimensional fold tests from the expected direction (assuming implicitly that the results from the one dimensional fold test are correct) are possible. They include COMPOSITE MAGNETISATIONS and STRUCTURAL MODIFICATIONS and are discussed by Hudson and others (1989). These authors propose a general term ("cross-over geometry") to describe directions of magnetisation which are most closely grouped at an intermediate stage of untilting (previously known as "syn-folding" magnetisation). They note further that the acquisition of magnetisation during folding is not the only mechanism producing a cross-over geometry of magnetisation (Figure 2.6). There are three major classes of mechanisms which can produce a cross-over geometry of magnetisation; (1) acquisition of magnetisation during folding ("true" synfolding), (2) combinations of pre-folding, "syn-folding" and (or) post-folding components magnetisation and (3) structural modifications of rocks that contain pre-folding magnetisation. Both mechanism of Class 2 and Class 3 will not record the the orientation of the geomagnetic field during its acquisition. It may then be possible that the result of the fold test (one dimensional) from these classes will not be parallel to the expected palaeofield direction for the area being investigated.

In summary, the usual (one-dimensional) fold test will be valid when magnetisation predates or postdates all folding. For general cases, the two dimensional fold test presented in this study provides a more complete

analysis especially when remanences are "true" syn-folding (Class 1, see above). An example of "true" syn-folding is the remanence of the South Wales red beds which is incorporated in this study (see also McClelland-Brown, 1983; Hudson and others, 1989). Since the geology of the area is complex, especially in southern Pembrokeshire, the author prefers to use the term "syn-deformational" rather than "syn-folding" magnetisation. Hudson and others (1989) propose that in the mechanism of Class 1 (syn-deformational magnetisation) the direction of the remanence should then be parallel to the orientation of the geomagnetic field at the stage of folding during which remagnetisation occurred. Generally, this cannot be done by application of the usual (one dimensional) fold test (see the dummy data case) since the palaeomagnetic direction derived from the test is determined by the k values only. In this case, the assumed palaeomagnetic field has to be given a major role in a fold test as in this presentation of the fold test. The FOLDCONT program has also been tested on various real data (e.g. see Table C-2) and other computer programs (e.g. the PLUNGE program which runs on a BBC micro). The results show that the program works well but does not necessarily mean that it is error-free.

2.7.2 Palaeomagnetic Pole

Since palaeomagnetic directions reflect the ambient field at the time the rocks acquired their magnetisations, the palaeopole position in the present geographical reference axes can be calculated if a model for the geomagnetic field configuration is assumed. If the paleomagnetic directions have not sampled and averaged out secular variations (for example, the results from a single lava flow) the derived palaeopole is a geologically-instantaneous

position of the pole called the Virtual Geomagnetic Pole (VGP). However, the palaeopole derived from sediments, where the processes of magnetisation will generally have taken a long time and averaged out the secular variations, yields a time-average of the field called the palaeomagnetic pole. Hence, there are two methods for estimating the position of the palaeomagnetic pole. Firstly, it can be derived from a collection of palaeomagnetic directions (declinations and inclinations). By averaging the declinations and the inclinations, the secular variations are averaged out. Secondly, it can be calculated from a number of VGPs (latitudes and longitudes). In practice the results obtained by either method differ only slightly (Collinson, 1983). Averaging VGPs has a minor computational advantage since the result is automatically corrected for site latitudes and longitudes although this is significant only for a wide spread of sites.

The formula for calculating the palaeopole position in the present geographical reference axes is given by

$$\sin\lambda_p = \sin\lambda_s \cos p + \cos\lambda_s \sin p \cos D$$

$$\varphi_p = \varphi_s + \beta \text{ (for } \cos p > \sin\lambda_s \sin\lambda_p)$$

or

$$\varphi_p = \varphi_s + (180° - \beta) \text{ (for } \cos p < \sin\lambda_s \sin\lambda_p)$$

where

$\sin\beta = \sin p \sin D / \cos\lambda_p$

$\cot p = 1/2 \tan I$ (for the axial geocentric dipole)

p = ancient colatitude

λ_s, φ_s = the latitude and longitude of the site

λ_p, φ_p = the latitude and longitude of the palaeopole

D,I = the declination and inclination of the palaeomagnetic direction

The error associated with the pole position is given by an oval of semiaxes :

$$dp = \tfrac{1}{2}\, \alpha_{95} (1 + 3 \cos^2 p)$$

$$dm = \alpha_{95} \sin p / \cos I$$

where

α_{95} = the cone of 95% confidence

The error dp lies along a great circle passing through the sampling site and the palaeomagnetic pole and the error dm is in the direction perpendicular to this great circle (see Figure 2.7).

Successive positions of palaeomagnetic poles in a time sequence from a region in the present geographical coordinate system trace out a path called the APWP for that region. The positions of the palaeomagnetic poles are usually different to the position of the present geomagnetic pole. Hence, the APWP will imply that the region has moved relative to the Earth's rotational axis. An established APWP for a tectonic unit can also be used as a dating tool to determine whether a magnetisation residing within a rock is a younger overprint (i.e. yields a pole position plotting on a part of the APWP younger than the rock age).

2.7.3 Rock Magnetic Studies

Knowing the magnetic minerals in palaeomagnetic samples before and after a thermal treatment will give valuable information on the chemical changes which may occur during the treatment. This is important in palaeomagnetism, since the purpose of thermal demagnetisation is to isolate the components making up the NRM. The aim will not be achieved suc-

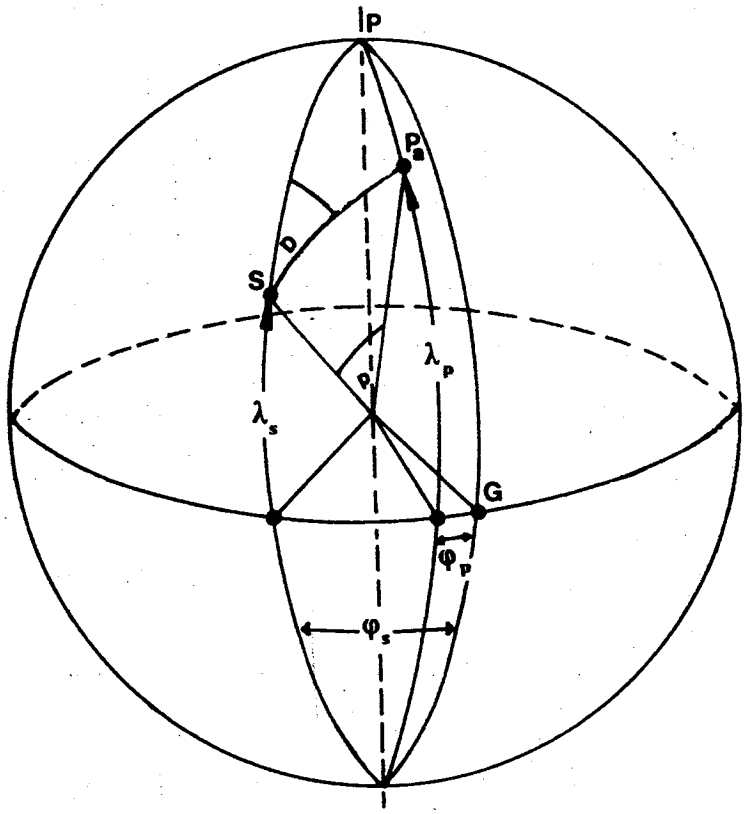

Figure 2.7 Relationship to calculate the palaeomagnetic pole (P_a) from the coordinates of the sampling site and the remanence vector. P is the present geographic pole and S is the sampling site. PG is the Greenwich meridian. See section 2.7.2.

cessfully if the constituents of the specimen being investigated change chemically. Since red beds contain haematite, they are often considered to be stable when heated in air. However, it has been reported by several workers (Dunlop, 1972; Collinson, 1983) that there is sometimes a production of magnetite during the heating process of red sediments. Different magnetic properties of magnetite and haematite (see section 2.3) provide a method for distinguishing these minerals in palaeomagnetic samples. For example, Dunlop's coercivity spectrum technique reveals that heating above 620° causes increase in magnetite content without reducing the haematite. The basic principle of Dunlop's technique is a comparison of the different coercivities of magnetite and haematite. A specimen is given an IRM (Isothermal Remanent Magnetisation) in progressively increasing fields to produce an IRM acquisition curve. From this curve, the magnetisation increment is calculated using a 0.1 T interval and is plotted against the external field. The curve illustrates the coercivity spectrum. It is generally believed that the magnetite production is due to the breakdown of some clay minerals and not due to reduction of haematite; the haematite itself may become hardened due to annealing (Dunlop, 1972 and Collinson, 1983).

IRM is acquired by magnetic particles when they are exposed to a strong steady magnetic field for few seconds. The acquisition curves for specimens containing haematite is different from those containing magnetite, since haematite and magnetite saturate at different fields. Magnetite saturates at lower fields than haematite although haematite has a saturation magnetisation (J_s) only about 0.5% of that of magnetite. However, the IRM acquisition curve is not very discriminating for some cases when the quantity of magnetite within red beds is very small compared with the haematite.

The blocking temperatures of magnetite and haematite are also markedly different. If a specimen is given two IRMs (lower and higher fields) at orthogonal directions to each other, thermal demagnetisation of the IRMs will be able to detect the presence of magnetite and haematite in the specimen (T. Rolph, personal communication). It can clearly be seen that the components carried by magnetite and by haematite should be orthogonal to each other on orthogonal plots. The combination of the IRM acquisition curves and thermal demagnetisation of the IRMs may provide a better method for identifying the magnetic minerals in rocks qualitatively and possibly quantitatively (by calculating the intensity of each component on the orthogonal plots).

2.7.4 Anisotropy of Magnetic Susceptibility (AMS)

A study of anisotropy of magnetic susceptibility (AMS) determines the relationship between the orientation of the sample and the ability to acquire magnetisation in different directions. The susceptibility axes are defined below. For an anisotropic medium the relationship between the acquired magnetisation and the external magnetic field is given by

$$J_i = \sum k_{ij} H_j$$

where

J_i = the magnetisation component in i direction

H_j = the applied field component in j direction

k_{ij} = the susceptibility tensor

For a given reference frame and with some assumptions (e.g. $k_{ij} = k_{ji}$), the susceptibility tensor can be transformed into an ellipsoid with maximum (k_1), intermediate (k_2) and the minimum (k_3) susceptibility axes ($k_1 > k_2$

$> k_3$). The axes of reference are called the principal axes. An anisotropy susceptibility meter determines the orientation of these three principal susceptibilities.

The shape of susceptibility ellipsoid is defined by the magnitude of the principal susceptibilities and a number of terms are used to describe the ellipsoid and the causative magnetic fabric (see Tarling, 1983). However, only three combinations are generally agreed to be most useful in AMS studies. They are

A = anisotropy factor = k_1/k_3

L = lineation factor = k_1/k_2

and F = foliation factor = k_2/k_3

The eccentricity E of the ellipsoid is given by

$$E = F/L = (k_2)^2 / k_1 k_3$$

If $E > 1$ the ellipsoid is oblate and for $L \sim 1$ it is disc-shaped.

If $E < 1$ the ellipsoid is prolate and for $F \sim 1$ it is cigar-shaped.

McElhinny (1973) reported that anisotropies of 10%, 20% and 50% ($A = 1.1$, 1.2 and 1.5) are able to deflect a magnetisation direction by 2.7°, 5.2° and 11.6° respectively. However the relationship between the susceptibility axes and the NRM is often not clear. The two parameters may be unrelated if the AMS is dominated by the paramagnetic constituents in the rock. Van den Ende (1977) studied the relationship between the NRM and the susceptibility axes in Permian red beds from South France. It was found that the cause of the NRM and the alignment of the susceptibility axes are independent although in some places both are of primary origin. Turner and others (1985) studied the relationship between the magnetic fabric of the red

beds from the Coal Measures of Central England and the direction of magnetisation. It is believed that these red beds were formed in a humid environment. These authors found that the angular difference between the remanence and the k_1 (k_{max}) axis was quite small. They suggest that depositional processes probably played an important role in the magnetisation of the red beds they investigated. This implies that the process of magnetisation in red beds under humid is less complex than under arid environments. Hrouda and Janak (1971) studied Devonian red beds from Central Moravia (Czechoslovakia). They did not relate the susceptibility axes with the NRM directions but were able to show that susceptibility ellipsoids are rotational which means that the intermediate and maximum susceptibility axes cannot be distinguished and the minimum susceptibility axis concentrates around the poles to the bedding. One facet of this study has been to find out whether there is any relationship between the NRM directions and the susceptibility axes in Devonian red beds from South Wales. The Devonian outcrop in South Wales has been rotated by 40° clockwise according to McClelland-Brown (1983). However, this argument depends critically on the age of the NRM and it may also be tested by determining whether or not the AMS is rotated in the same way as the remanence. The relationship between the NRM and the susceptibility axes may be found by applying bedding corrections to the susceptibility axes and by comparing these axes from the un-rotated and rotated areas.

CHAPTER 3 PALAEOMAGNETISM OF OLD RED SANDSTONES, SOUTH WALES

3.1 Introduction

3.1.1 Previous Results

The palaeomagnetism of the Old Red Sandstone (ORS) of the Anglo-Welsh Cuvette (basin) has been studied since the earliest palaeomagnetic investigations in the 1950s. It was found that the inclinations of the palaeomagnetic directions varied according to the attitude of the bedding (Creer, 1957) and were evidently neither entirely pre- or post-folding in origin. For some time, this was a puzzle to palaeomagnetists. Thermal demagnetisation studies of these rocks, however, subsequently revealed that a variable but often strong component of secondary magnetisation was superimposed on a magnetisation of possible primary Devonian age. This secondary magnetisation appeared to have been acquired during the Variscan (also referred to as the Hercynian or Armorican) orogeny (Chamalaun, 1964). The variations in inclination could be reduced to a minimum if the magnetisation acquired when both limbs of the fold structures being investigated were partially unfolded to make an angle of 30° with the horizontal. Chamalaun and Creer (1964) therefore proposed that the pole position derived from this component within the ORS of the

Anglo-Welsh cuvette was applicable to a palaeomagnetic field post-dating their deposition. It was concluded that remagnetisation had occurred in both dipping and horizontal beds. It is now generally agreed that the ORS was remagnetised during the Variscan orogeny although the mechanism of remagnetisation is not well understood.

Chamalaun and Creer (1964) found that the directions of magnetisation isolated in some of their specimens at higher temperature (Mean Dec. = 66° and Inc. = -37°). were in agreement with the direction of remanence in Lower Devonian lavas from the Midland Valley of Scotland. However, they did not consider that calculation of a pole position from these specimens from the Anglo-Welsh cuvette was justified. One of the reasons given was that the specimens became capable of acquiring isothermal remanence during storage when a temperature of 500°C was reached. Although the specimens were kept in zero field, they had to be transported over a distance of 24 km to a magnetometer.

In a later study of the ORS, McClelland-Brown (1983) used sophisticated vector analysis to resolve the component of Permo-Carboniferous overprinting and isolate directions inferred to be of primary Devonian origin. The higher temperature components were considered to be representative of the Lower Devonian palaeofield direction. The mean direction for this higher temperature components is as follows :

in situ	Dec. = 121.5° Inc. = -26.8°
tilt-corrected	Dec. = 98.1° Inc. = -19.4°

By comparison with Lower Devonian field directions elsewhere in Britain, she interpreted this result as indicative of a 40° clockwise block rotation. The clockwise rotation of the Devonian palaeomagnetic directions is supported by the observation that the Permo-Carboniferous components have also been rotated by the same amount. McClelland-Brown concluded that the area she investigated in southern Pembrokeshire had been rotated since the acquisition of the secondary magnetisation. She also noted that the westernmost site (Mill Haven) gave a more westerly declination and she suggested that the Mill Haven Permo-Carboniferous directions may have been rotated more than the sites to the east.

More recently Stearns and Van der Voo (1987) reported a palaeomagnetic study of the Llandstadwell Formation in Pembrokeshire also of Lower Devonian age. Their sampling locality is on the same thrust sheet as the Mill Haven fold of McClelland-Brown and within Zone 1b of Hancock's classification (see Hancock and others, 1983). They argued that their results did not support McClelland-Brown's observation of either a 40° clockwise rotation or a syn-deformational (or syn-folding) magnetisation residing in the Lower Devonian red beds from this area. However, McClelland (1987) defended her previous conclusion and maintained that rotation had occurred in southern Pembrokeshire. She also rejected the idea of a rotation on a very localised scale which was suggested by Stearns and Van der Voo.

It is difficult to judge which observation is more reliable. However, Stearns and Van der Voo did not give any detail on their stepwise unfolding method. The author has used the FOLDCONT program (described in CHAPTER 2 also see Table C-2) to analyse their data and it was found

that the age of magnetisation is more likely to be syn-deformational not pre-folding as they concluded. In the author's opinion, Stearns and Van der Voo's conclusion is more difficult to accept since it is based on the results from one location only.

One aspect of this project was originally to detect any rotations within the South Wales main coalfield using palaeomagnetic techniques. The sampling localities were distributed around the basin and across major Variscan structures. The study has been extended to the Lower ORS of southern Pembrokeshire to determine the integrated effect of post-Devonian rotations and to attempt to resolve the dispute concerning the scale of rotation recorded here. The sampling localities are the same as McClelland-Brown's and are located within Zone 1a of Hancock. This zone is dominated by a few large amplitude (2 - 3 km) macrofolds (i.e. folds with an axial plane separation of more than 150 m). These macrofolds are relatively uncomplicated by parasitic mesofolds (an axial plane separation of less than 150 m) as are other zones within Zone 1. The plunges are sub-horizontal (0 - 10°) or gentle (10 - 30°). The dominant sense of plunging is to the east although west-plunging folds are not uncommon. One west-plunging fold which is important in this context is the Castlemartin Corse anticline and the results from this area are relevant to the interpretations discussed in this chapter.

3.1.2 Remagnetisation in Red Beds

Research conducted during the 1980s has confirmed earlier evidence indicating that sedimentary rocks over a large portion of North America and Europe were remagnetised during Permo-Carboniferous times (e.g.

McCabe and Elmore, 1989). However, the widespread remagnetisation of British Palaeozoic rocks has been known since 1960s (Belshé and Everitt (1960), Chamalaun and Creer (1964)). Belshé and Everitt (1960) found different palaeomagnetic results from sedimentary and non-sedimentary rocks of Carboniferous age. The results from the sedimentary rocks were close to the Triassic palaeofield direction. These authors suggested that the magnetisation in these rocks was acquired by ancient weathering. Tneir view was supported by geological evidence that the rocks had sometimes been reddened to depths of as much as 300 metres. However, remagnetisation in red beds due to near surface weathering has few supporters in the palaeomagnetic community nowadays. It seems that the hypothesis of fluid migration during orogenic loading (e.g. Oliver, 1986) as a cause for remagnetisation is, in general, more acceptable.

Acquisition of magnetism in red beds is a very complex phenomenon. Roy and Morris (1983) suggest a simple three phase model of acquisition. The model consists of a first phase DRM (Detrital Remanent Magnetisation) closely associated with deposition, a second phase D-CRM (Depositional-Chemical Remanent Magnetisation) produced by chemical changes during formation and dewatering and a third phase CRM (Chemical Remanent Magnetisation) produced during compaction, cementation or later metamorphism. Although, the acquisition of each phase may overlap, this simple scheme can accommodate models to explain whether the magnetisation in red beds was acquired soon or long after deposition. For example, if the CRM phase is dominant, it may be inferred that the magnetisation was acquired long after the deposition of the rocks.

The palaeomagnetic fold test enables the remanence acquisition to be dated relative to the age of the folding. From this information, the terms primary and secondary remanence are often used. However, to use the term "primary" to denote the remanence which has higher blocking temperature without knowing the age of the remanence is inappropriate and a remanence may be younger than the rock age although it predates folding (Roy and Morris, 1983). The blocking temperature depends on grain size and shape as well as on mineralogy. High blocking temperature haematite may, for example, be in the form of detrital specularite grains or large authigenic grains deposited in the porosity.

Knowing the nature of the magnetic carrier in red beds will probably help to understand the process of the acquisition. It is known that haematite is the principal mineral responsible for remanence in these rocks. The haematite usually occurs as two principal phases: as large grains and as fine pigment coating silicate grains (Collinson, 1983). It is known that the large specularite grains may be of primary (detrital) or secondary (authigenic) origin (Turner, 1980). The anisotropy susceptibility measurements in this study show that the minimum susceptibility axis (after tilt correction) are parallel to the bedding pole. However, this does not necessarily mean that the remanence is of depositional origin (Piper,1987) and there is no unambiguous test to establish whether or not the remanence in a red bed is strictly primary (i.e. acquired at the time of deposition).

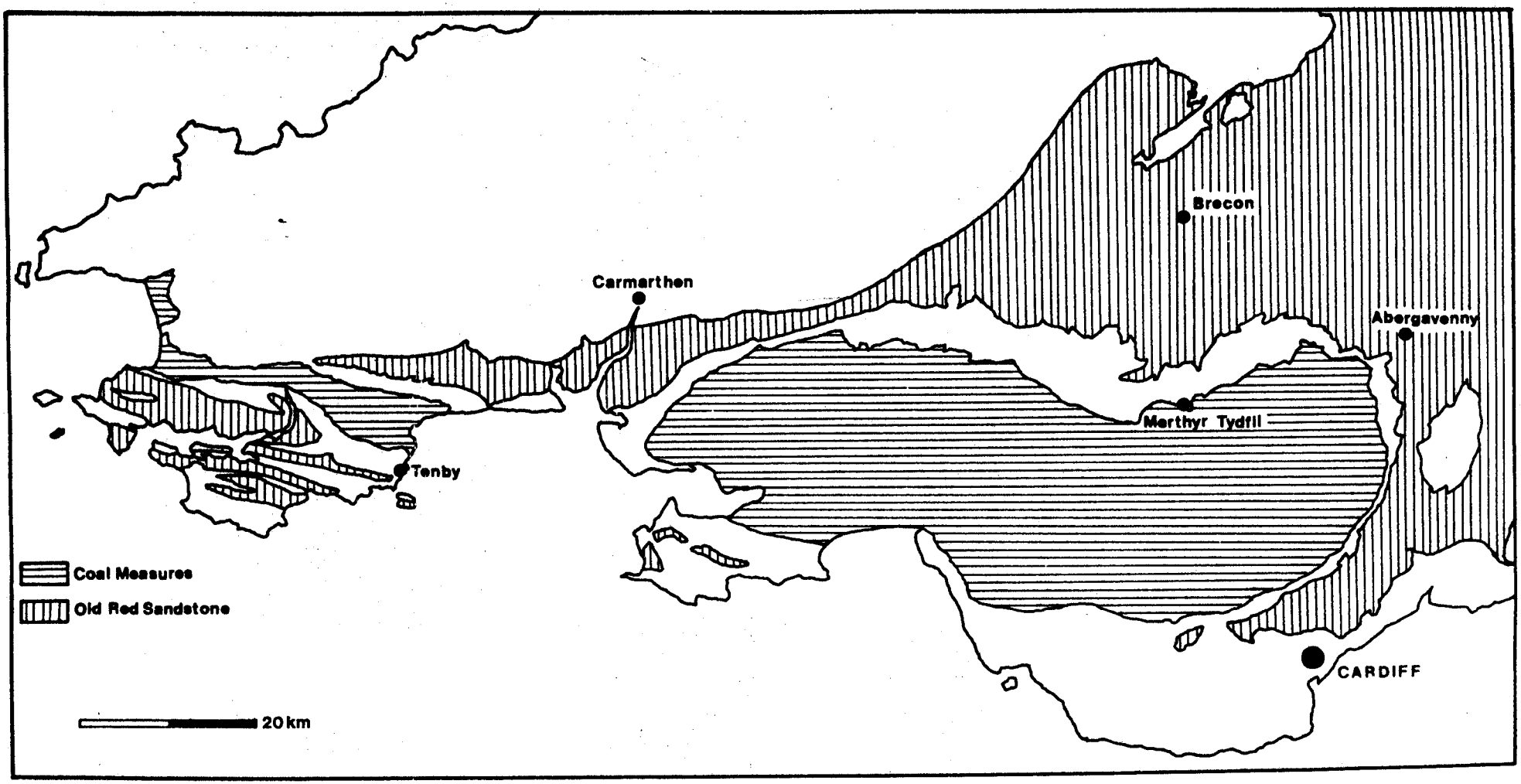

Figure 3.1 Outcrops of Old Red Sandstones (ORS) in South Wales (George, 1970).

3.2 Location and Sampling

3.2.1 Geological Outline

This section is based mainly on the papers of George (1970) and Owen (1974). Figure 3.1 is a generalised geological map of South Wales. The map shows the outcrops of the Old Red Sandstones (ORS). These are generally attributed to sedimentation in Devonian times although this style of deposition probably commenced in Upper Silurian (Downtonian) times and continued into early Carboniferous times in some areas. The basin of deposition of the ORS which covered southern England and the southeastern part of Wales bordering the paratectonic Caledonides is called the Anglo-Welsh cuvette (George, 1970). Before the close of Silurian times much of Britain was affected by strong earth-movements that caused deformation and uplift of the Lower Palaeozoic geosyncline. With the uplift, the sea retreated southward to the present vicinity of Devon and Cornwall and terrigenous sediments were laid down between the Devonian sea and the land in the north. These sediments were deposited under fluviatile and deltaic condition and are mostly unfossiliferous. The sedimentary rocks consist mostly of marls and sandstones. The rock sequence in this region falls into two stratigraphic divisions: the Lower Old Red Sandstone and the Upper Old Red Sandstone. The Middle Old Red Sandstone is unknown in South Wales and there is a strong unconformity between the Upper and the Lower divisions.

The Variscan (Armorican or Hercynian) orogeny spanned from at least late Devonian times to the middle Triassic (Owen, 1974). The orogenic climax,

as far as Western Europe is concerned, seems to have moved northward with time. In South Wales, there are three major belts of folded and fractured strata (so-called disturbances) - the Neath, the Swansea Valley and the Llandyfaelog-Careg Cennen disturbances. Their trends are NE - SW. The first two disturbances run across the main coal field (see Figure 3.2). In Pembrokeshire, where the (Siluro-Devonian) Acadian folding converges with the (Carboniferous-Permian) Variscan Front, the Variscan structures are more intense. The folds are sharp with steep limbs.

The Lower Palaeozoic rocks in Pembrokeshire swing into an east-and-west strike parallel to the Variscan folds. The swing has been interpreted as a remoulding of earlier structures of northeast-and-southwest trend by powerful south-north stresses during Variscan times. However, such a rotation has not been accepted by George (1970). Recently, Dunne(1983) presented a new model for the tectonic evolution of South West Wales during the Upper Palaeozoic. He suggested that during the late stages of Variscan deformation southern Pembrokeshire was rotated clockwise by displacements on the Johnston Thrust (see Figure 3.3a where the Johnston Thrust is indicated by letter J).

3.2.2 Sampling

Twenty block samples and 376 core samples were collected from various parts of the basin (Figure 3.2). All 11 localities are located within the grid area defined by latitudes 51.50°N to 52.00°N and longitudes of 355°E and 357°E. The samples were oriented using a magnetic compass and many orientation measurements on cores were checked using a sun compass. Also

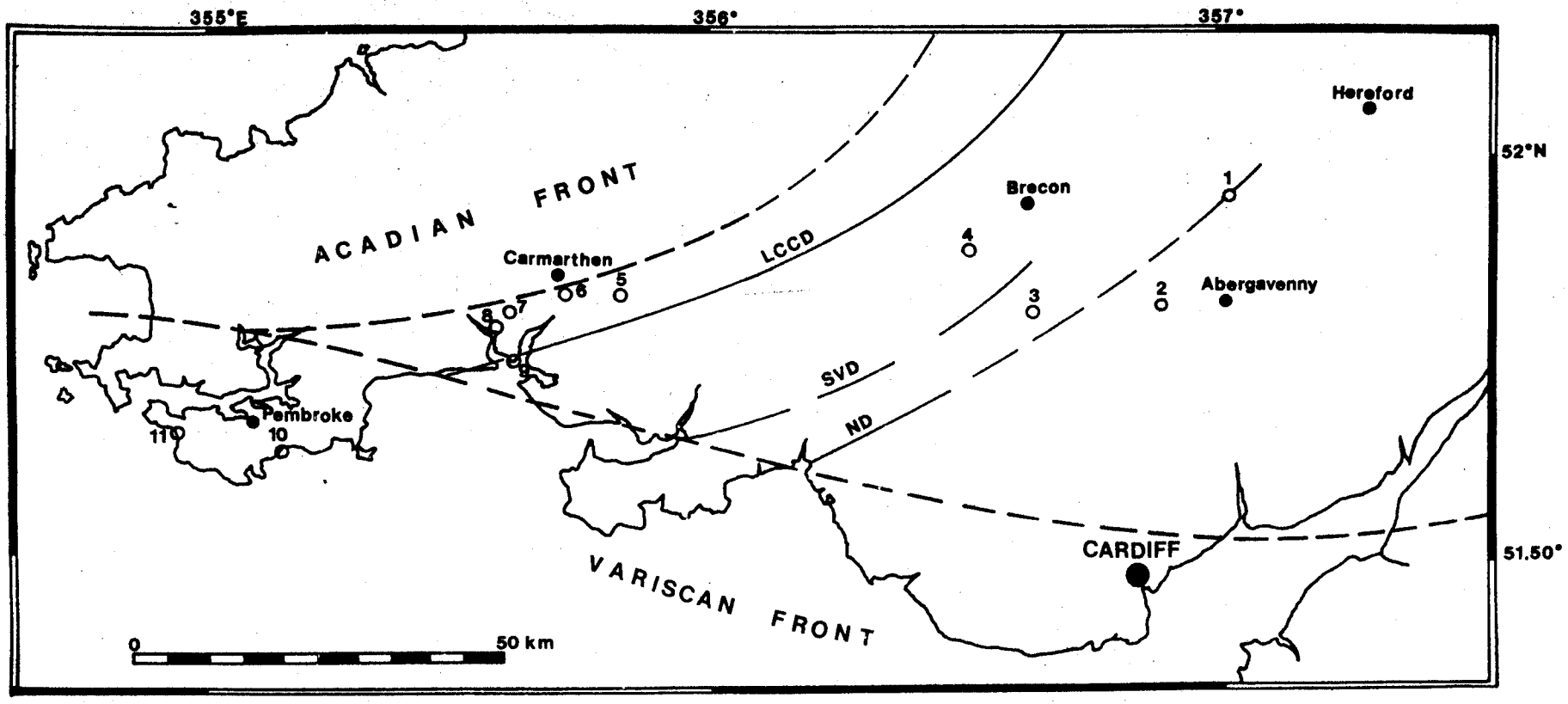

Figure 3.2 Location map and some major Variscan structures.
1-Llanthony, 2-Clydach, 3-Ponsticill, 4-Storey Arms, 5-Llanddarog, 6-Oaksland, 7-Pen y coed, 8-Pilgrim Rest, 9-Llanstephan, 10-Freshwater East (including Manorbier Bay), 11-Freshwater West, LCCD-Llandyfaelog Carreg Cennen Disturbances, SVD-Swansea Valley Disturbances, ND-Neath Disturbances.

the magnetic effect of the surroundings was monitored by sights on distant objects and it was found to have no effect on the magnetic readings.

The sampling localities can be grouped into three regions;

-Group 1 : localities around Brecon and Abergavenny.

-Group 2 : localities around Carmarthen.

-Group 3 : localities around southern Pembrokeshire

Group 1 consists of Locality 1, Locality 2, Locality 3 and Locality 4. The attitudes of the beds from this group are only mildly folded. There are three sites from Locality 1: GGB1DV37, GGB1DV38 and GGB1DV39. A fold test can be performed on these sites since the first two are moderately dipping southeast and the other is close to horizontal. These sites are separated by the Neath Disturbance which is unexposed. Core sampling was used at this locality. Locality 2 consists of 11 block samples; GGB1DV01, GGB1DV02, GGB1DV03, GGB1DV04, GGB1DV14, GGB1DV15, GGB1DV16, GGB1DV17, GGB1DV18, GGB1DV19 and GGB1DV20. Except for the last block (4 cores), 5 cores were drilled in the laboratory from each block. The beds are gently dipping to the south. GGB1DV35 and GGB1DV36 are from Locality 3 and GGB1DV40, GGB1DV41 and GGB1DV42 are from Locality 4. Core sampling is used in both localities. The beds are sub-horizontal (0 - 10°).

There are five (5) localities in Group 2. Most beds in this group are moderately dipping to the south (except Locality 9 south and north). The core sampling technique was used in this group except at Locality 9 where block and core sampling were both used. Locality 5 has only one site,

GGB1DV24. This site was divided further into three sub-sites according to the dip of the beds. Locality 6 consists of sites GGB1DV21, GGB1DV22 and GGB1DV23. Locality 7 has three sites, GGB1DV45, GGB1DV46 and GGB1DV47. Locality 8 has two sites, GGB1DV43 and GGB1DV44. Locality 9 is an open fold with the fold axis running E-W. The fold is an ideal structure on which to perform a fold test. There are 9 block sample sites (GGB1DV05 to GGB1DV13) and 9 core sample sites (GGB1DV26 to GGB1DV34). Five cores were drilled from each block except GGB1DV09 which comprises only 3 cores. Eight sites (5 from block samples) were taken from the southern limb and six sites (4 from block samples) from the northern limb. Four sites (all from core samples) were taken from the hinge zone area where the dip of the beds is horizontal.

Group 3 has two localities: Locality 10 and Locality 11. This group is located within the Variscan front (see also section 3.1). The beds from this groups are mostly steeply dipping south or north (see Figure 3.3b). Sites GGB1DV48, GGB1DV49 and GGB1DV50 belong to Locality 10 and sites GGB1DV51 and GGB1DV52 to Locality 11. Since the fold in Locality 10 (the Freshwater East anticline) is different to the fold in the Locality 11 (the Castlemartin Corse anticline), a fold test can be performed on each locality. However, McClelland-Brown (1983), in her analysis, considered these folds as a single major anticline (the Freshwater anticline; on the BGS geological map this is called the Orielton anticline). The Orielton anticline is a compound fold comprising the Freshwater East (Locality 10) and the Castlemartin Corse (Locality 11, Freshwater West) anticlines and the intervening the Orielton syncline (Hancock and others, 1983). In this study, a fold test is performed on each possible fold configuration. For example,

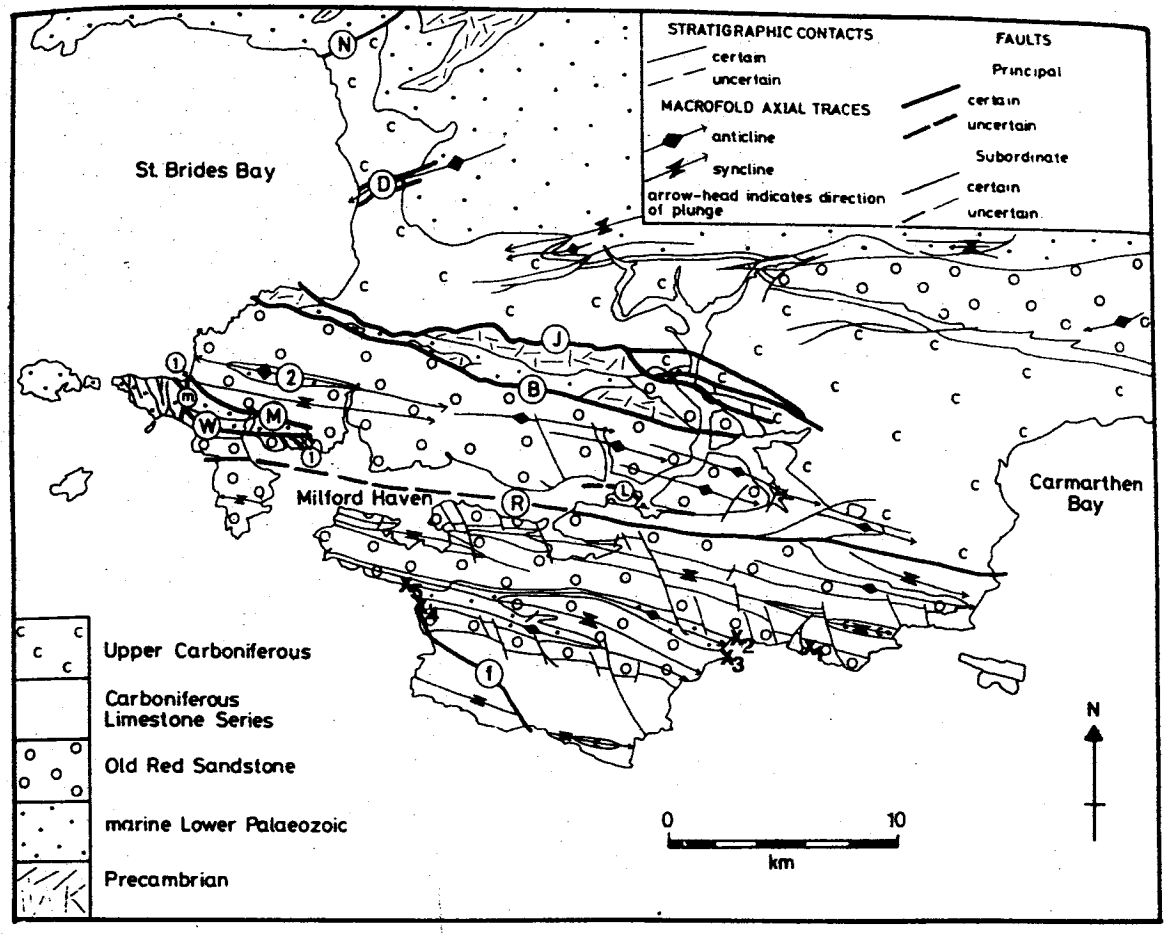

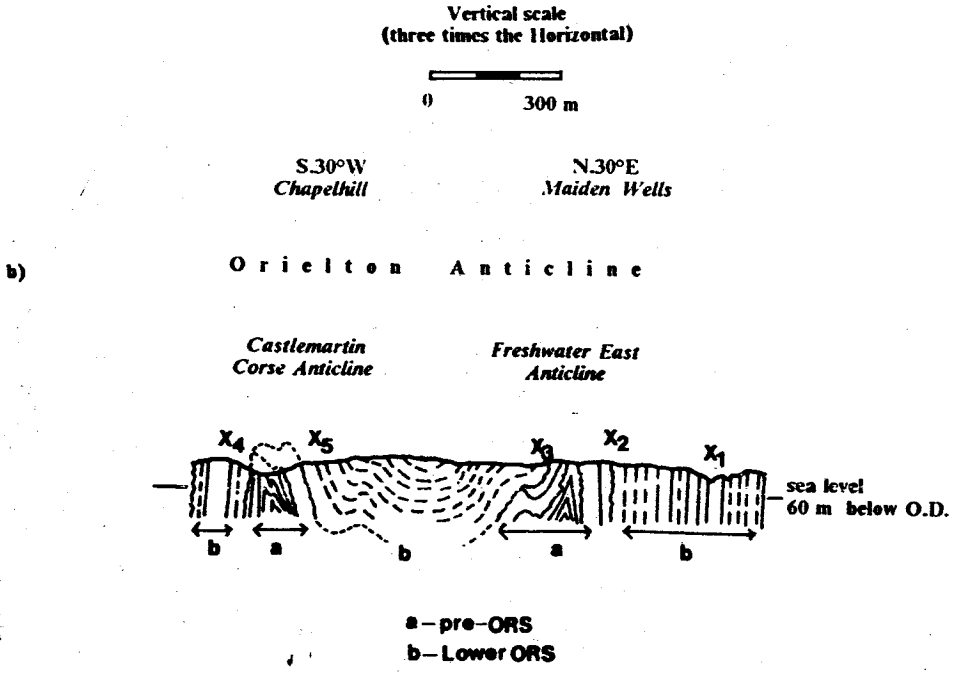

Figure 3.3 Position of sites GGB1DV48 (X1), GGB1DV49 (X2), GGB1DV50 (X3), GGB1DV51 (X4) and GGB1DV52 (X5)
a) on a geological map (from Dunne, 1983).
b) on a vertical section (redrawn from a 1:50,000 geological map, BGS, 1983).

the Orielton anticline comprises sites GGB1DV48 and GGB1DV49 sampled from the northern limb of the Freshwater East anticline and site GGB1DV51 from the southern limb of the Castlemartin Corse anticline; the rest of the sites are from the Orielton syncline.

Ten cores from block samples GGB1DV11 and GGB1DV13 (both from green beds) have very low intensities of magnetisation and they were excluded from any further treatments. Ten core samples were lost during the fieldwork. This left 453 specimens (87 from 18 block samples) of 1 inch diameter and 1 inch in length for thermal demagnetisation.

Table 3.1 is a summary of the location and sampling technique used in the field work.

Table 3.1 Locality and National Grid Reference.

Loc.	area	Nat.Grid	Lat(°N)/Lon(°E)	sampling
1	Llanthony	c.SO(2860,2530)	51.92/356.97	core
2	Clydach	c.SO(2320,1350)	51.81/356.85	block
3	Ponstiscill	c.SO(0630,1230)	51.80/356.64	core
4	Storey Arms	c.SN(9715,2080)	51.88/356.51	core
5	Llanddarog	c.SN(5150,1660)	51.82/355.84	core
6	Oaksland	c.SN(4245,1620)	51.82/355.72	core
7	Pen-y-coed	c.SN(3490,1465)	51.80/355.60	core
8	Pilgrim Rest	c.SN(3145,1245)	51.78/355.55	core
9	Llanstephan	c.SN(3450,0950)	51.76/355.59	block + core
10*	Freshwater E.	c.SS(0220,9780)	c.51.6/355.1	core
11	Freshwater W.	c.SR(8840,9950)	c.51.7/355.0	core

Note : * This locality includes Manorbier Bay c.SS(0550,9760)

3.3 Experimental Methods

All experiments were carried out in the Geomagnetism Laboratory of the Department of Earth Sciences with the exception of the isothermal remanence acquisition studies which were undertaken in the Department of Geography, the University of Liverpool. The instruments used throughout were a Molspin spinner, an MM demagnetiser and a computer plus printer all contained within a field-free space provided by a set of large Rubens coils monitored by a set of fluxgate detectors.

3.3.1 Thermal Demagnetisation

In general, 15 to 18 specimens were heated at the same time in a magnetic field-free oven. They were put on a tray and arranged systematically. They were faced in different directions between steps in order to minimise the effect of any stray magnetic field inside the oven. If possible, a space was retained between specimens. Most specimens were heated up to 700°C and some up to 720°C. Only three specimens disintegrated during heating to 350° and 400°C. The temperature increment applied was 50°C for temperatures less than 580°C and 25°C or 20°C for temperature higher than 575°C or 580°C. The parameters of the oven applied consistently to all specimens are as follows :

heating rate : 100°C/minute
hold time : 20 minutes
cooling rate : 500°C/minute
end temperature: 28°C

The directions and intensities of the specimens were measured using a Molspin spinner magnetometer with a sensitivity of ~10E-7 A.m^2/kg. The oven and the spinner were located inside the low field cage designed to cancel the Earth's magnetic field. In other words, the specimens were treated and measured in an almost magnetic field-free environment during the thermal treatment. Two hundreds and three out of 453 specimens had to be taken out of the cage for room temperature susceptibility checks after their directions and intensities had been measured. This was undertaken at every step to monitor any changes in magnetic mineralogy during heating. The susceptibility measurements of each batch of specimens took only a few minutes.

3.3.2 Isothermal Remanent Magnetisation (IRM)

Sixty four specimens (unheated and heated) were given a stepwise IRM up to 3 Tesla (T). The incremental magnetic field was chosen in such a way that it is about equally spaced in a logarithmic scale. The direction of the field was to the north (X direction). Three different pulse magnetisers were used to impart the magnetic field to the specimens. For magnetic fields less than 1 Tesla (T), small and medium pulse magnetisers were used. For higher fields, a Trilec pulse magnetiser was used. The intensities were measured using a Molspin spinner magnetometer connected to an IBM portable microcomputer. After the highest field was reached, the specimens were given a lower field (300 mT) in an orthogonal direction to the previous ones (Z direction). Both component directions might be recovered using a thermal demagnetisation technique (T.Rolph, personal communication). The specimens were thermally demagnetised up to 680°C or 700°C in a stepwise

manner. The values for the Y direction and the dip during the demagnetisation for all the specimens were chosen zero. This means that the horizontal component would point to the east instead of to the north and the inclination would be (90° - the applied field direction) in the orthogonal plots.

3.3.3 Anisotropy of Magnetic Susceptibility (AMS)

Seventy specimens were subjected to AMS measurements. They comprise 15 specimens from Locality 1 (Llanthony), 19 specimens from Locality 9 (Llanstephan), 18 specimens from Locality 10 (Freshwater East) and 18 specimens from Locality 11 (Freshwater West). These localities were chosen by their suitability for the fold test. The instrument used was a Molspin spinner-Anisotropy susceptibility meter. Since the susceptibility of the specimens was weak, the longer spinning time (~ 128 revolutions) was chosen during the measurements.

3.4 Data Analysis

3.4.1 Permo-Carboniferous Component

The NRM (Natural Remanent Magnetisation) intensities of the specimens are significantly above the noise level of the Molspin spinner. Figure 3.4a is a histogram of NRM intensities. The average value is 3.5 X 10E-6 $A.m^2/kg$. Generally, the intensity of coarse sandstones is lower than fine sandstones/siltstones. The directions of the NRMs generally reflect the directions of the specimens subsequently isolated on their orthogonal plots (described below). In other words, most specimens did not change their di-

rections during their thermal treatment from their NRM directions until they became unstable. This means that the majority of the specimens are carrying only one component of NRM. Figure 3.5 shows the NRM directions for each specimens (in situ and tilt corrected and see Figure 3.6 for comparison). The directions are clustered about the Upper Carboniferous palaeofield direction for southern Britain (i.e. shallow inclination toward the south-southwest). Few specimens deviate from this direction. It is likely that this deviation is due to human error during field works or measurements in the laboratory. For example, more than half of these specimens come from site GGB1DV26 (see Table A-1, APPENDIX A). Some markings on the samples from this site were uncertain because they were applied in a hurry due to the incoming tide and approaching night. These specimens, being supposed to have Permo-Carboniferous components (PC), are classified as having XX components and excluded, accordingly, from PC site mean calculations.

The PLOTCORE program (available from the department's library disk) was used to determine the mean direction of each component. The program mainly consists of drawing and analysing orthogonal plots, circular plots and intensity decay curves for selected components. Linear segments in the orthogonal plot are used to define the palaeomagnetic directions in this collection. Three data points were the minimum chosen to define a segment but generally more were used in stable samples. For single component samples, the directions derived from this technique (3-D least square method) are in agreement within the 95 percent confidence limits to those derived from their circular plots (based on Fisher statistics). Where the NRM of a specimen consists of two or more components, there will be large discrepancies

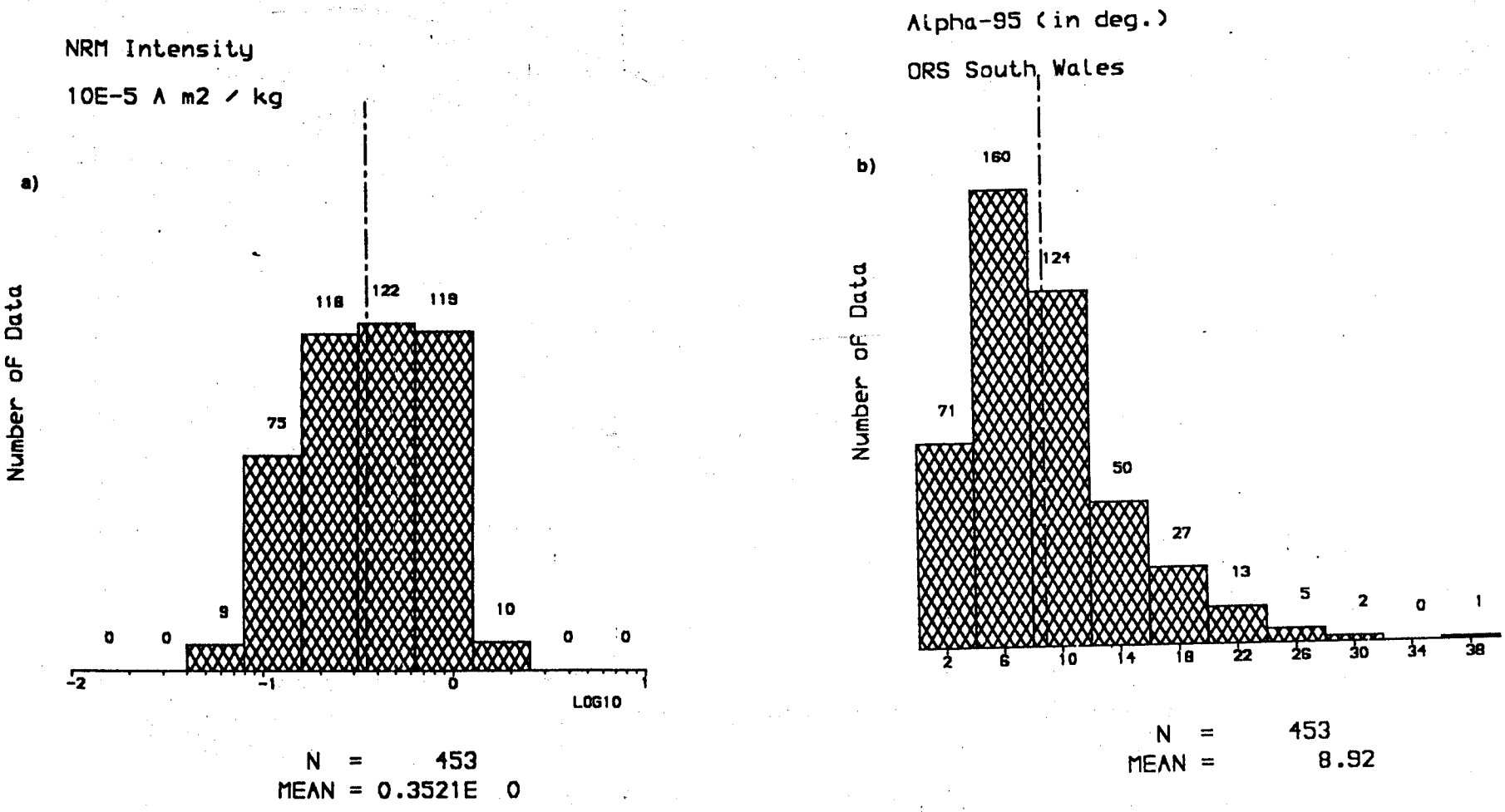

Figure 3.4 Histogram of NRM intensities (a) and of alpha-95 (b).

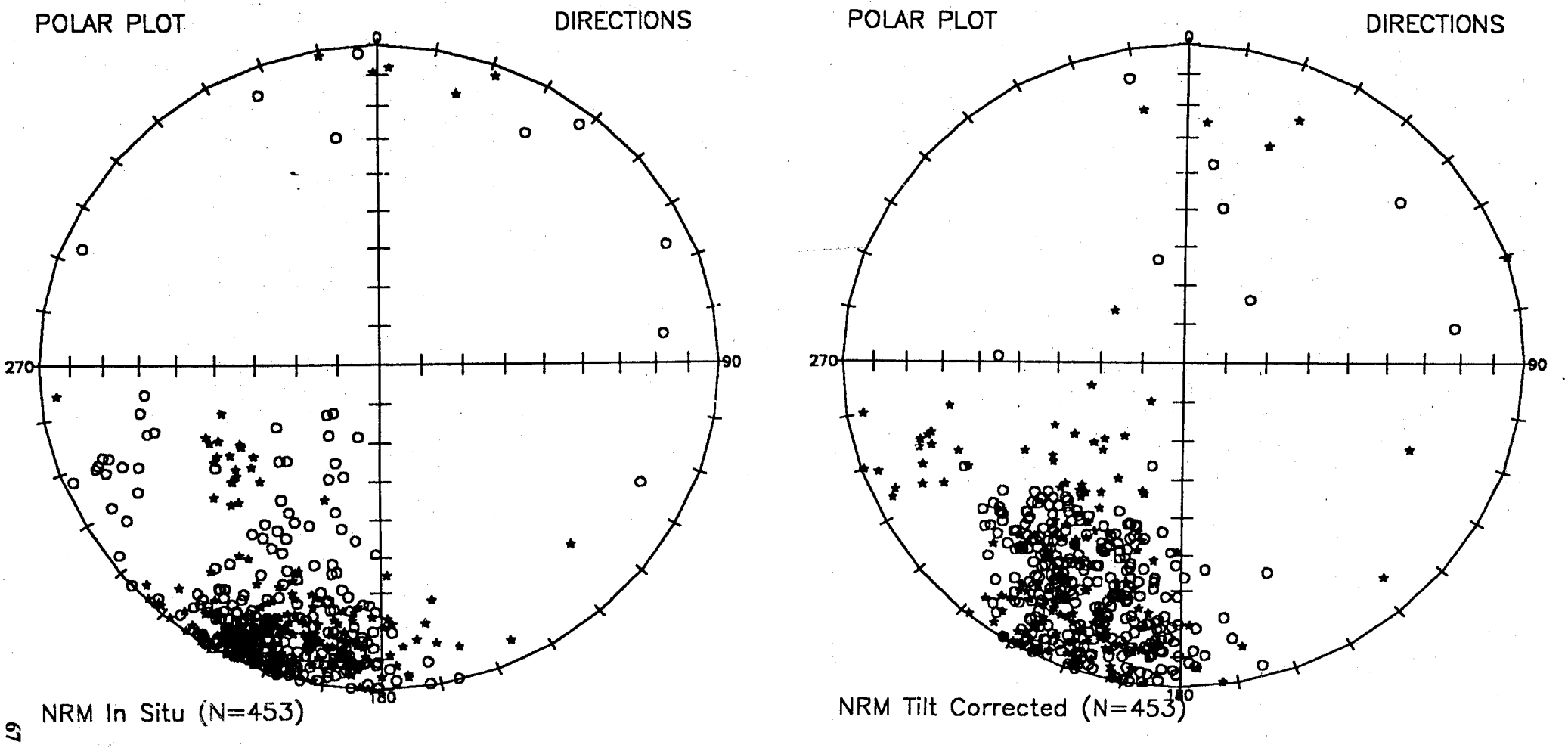

Figure 3.5a Equal area projection (polar) of NRM directions (in situ and tilt corrected). Star (circle) symbol = lower (upper) hemisphere.

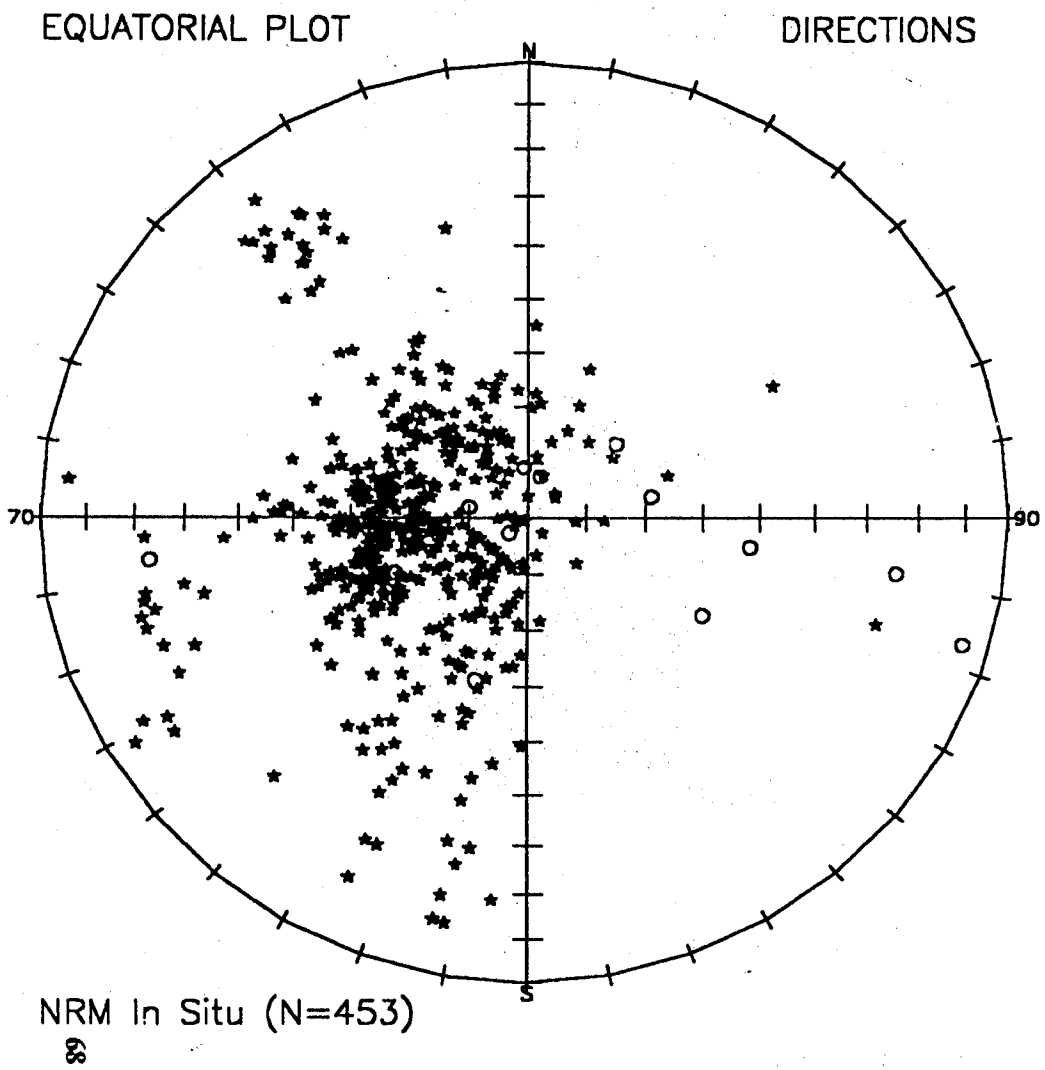

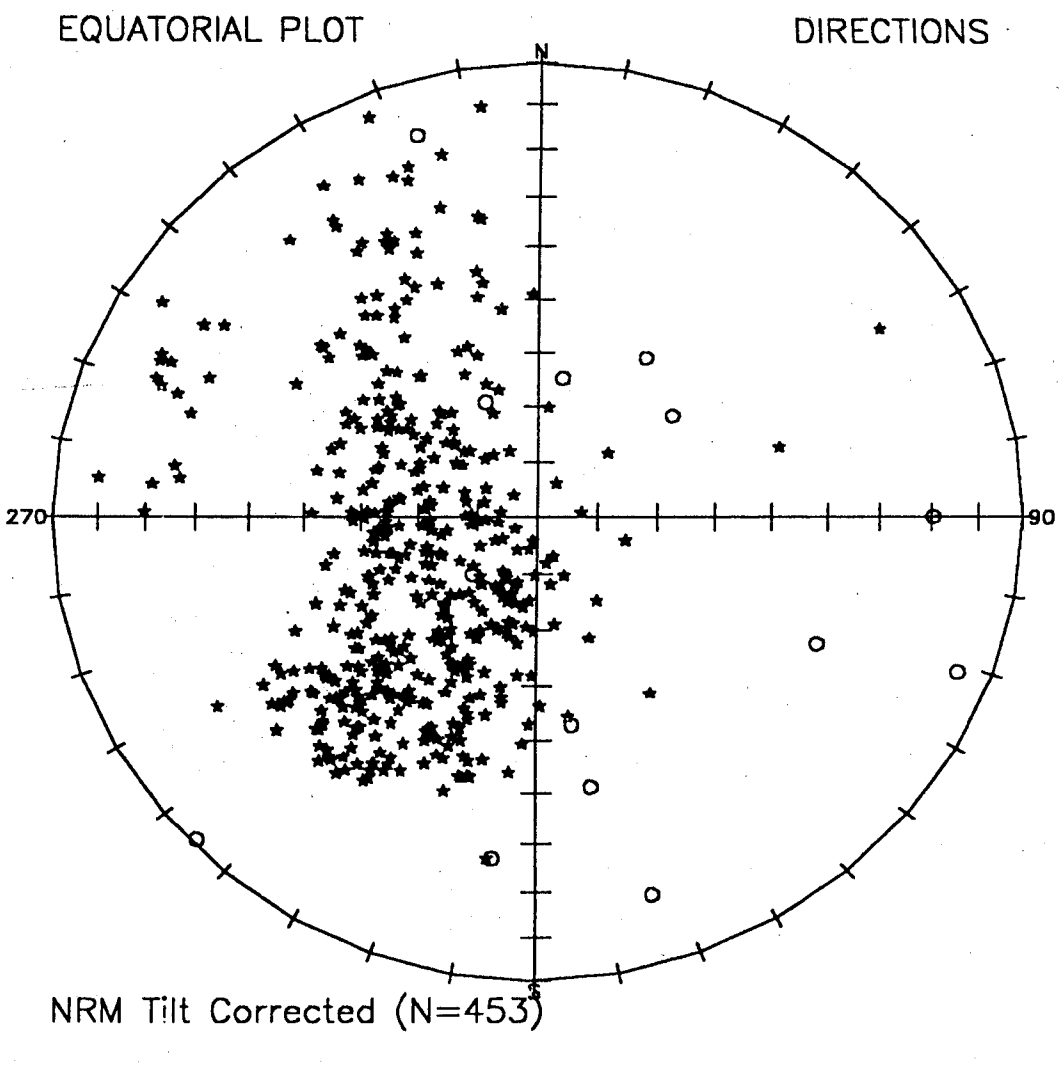

Figure 3.5b Equal area projection (equatorial) of NRM directions (in situ and tilt corrected). Star (circle) symbol = near (far) side.

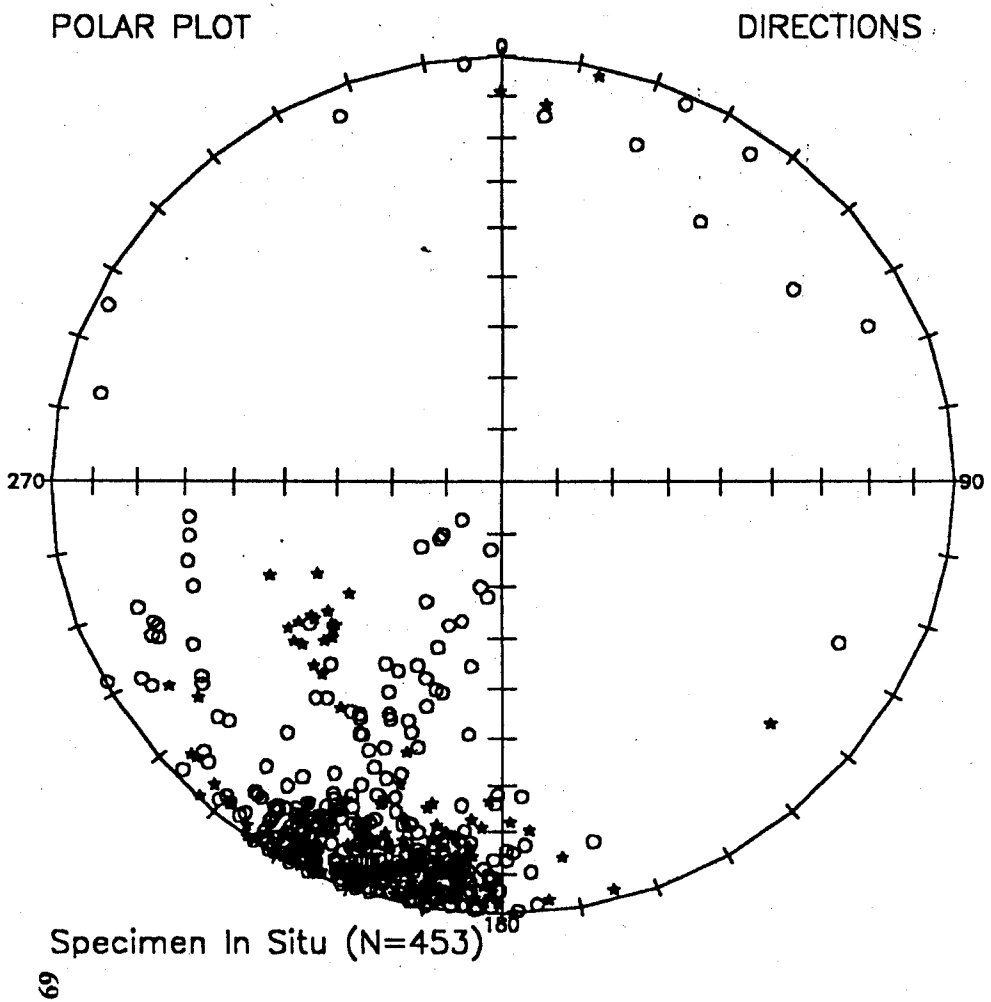

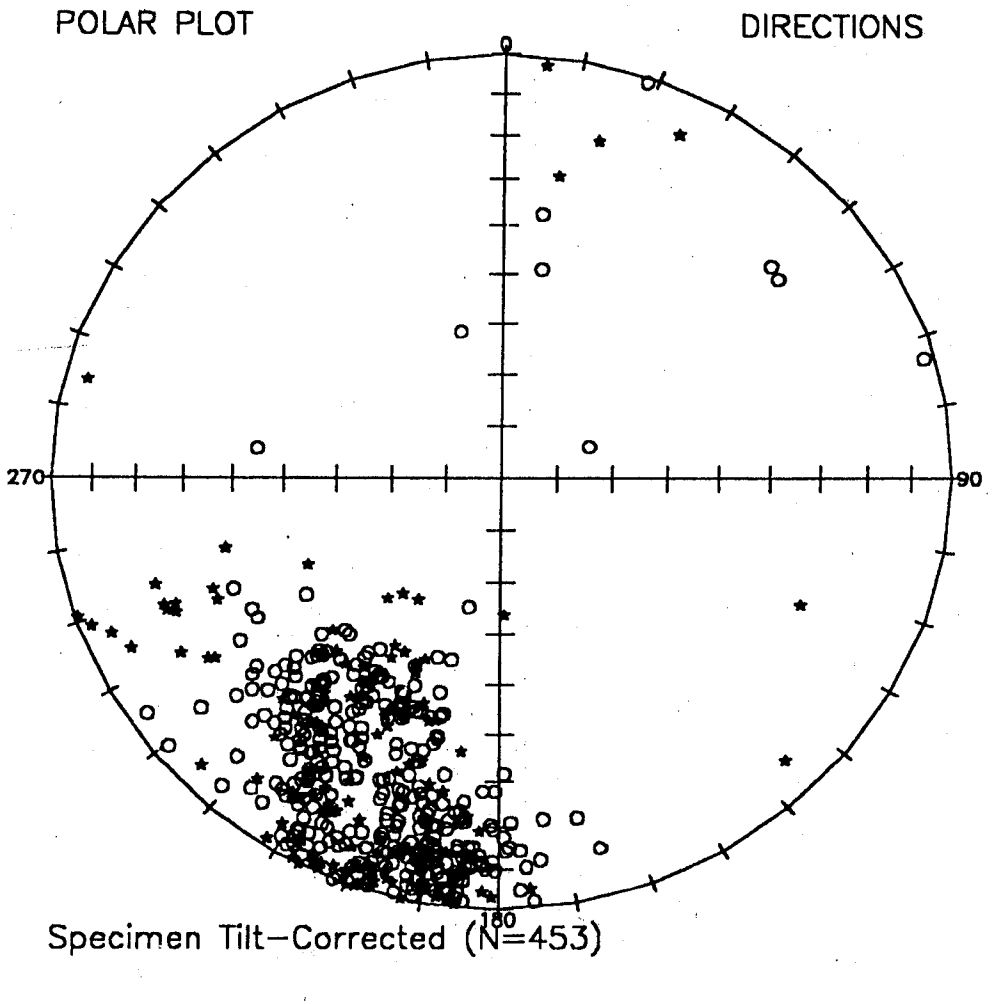

Figure 3.6a Equal area projection (polar) of mean directions for each specimen based on linear segment in its orthogonal plot (in situ and tilt corrected). Star (circle) symbol = lower (upper) hemisphere.

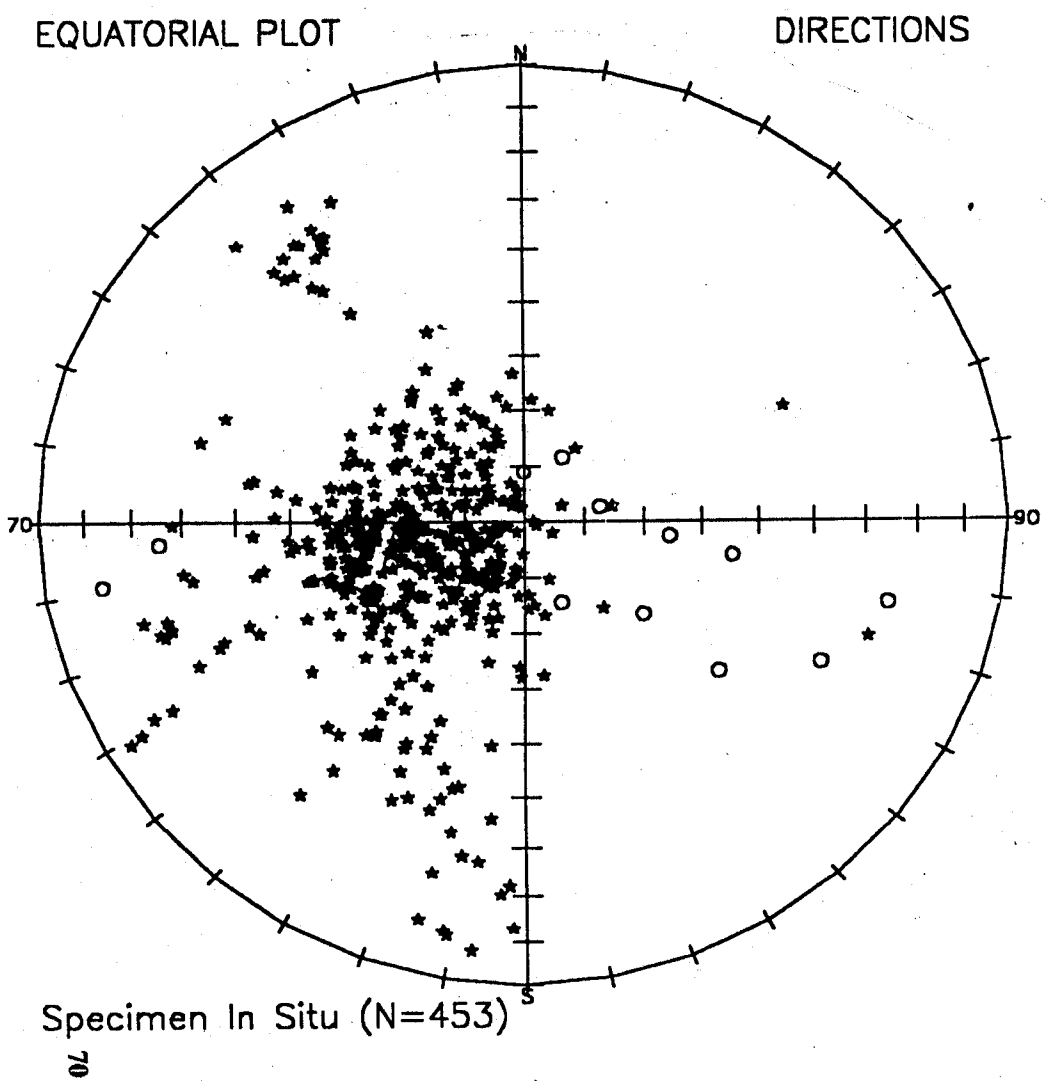

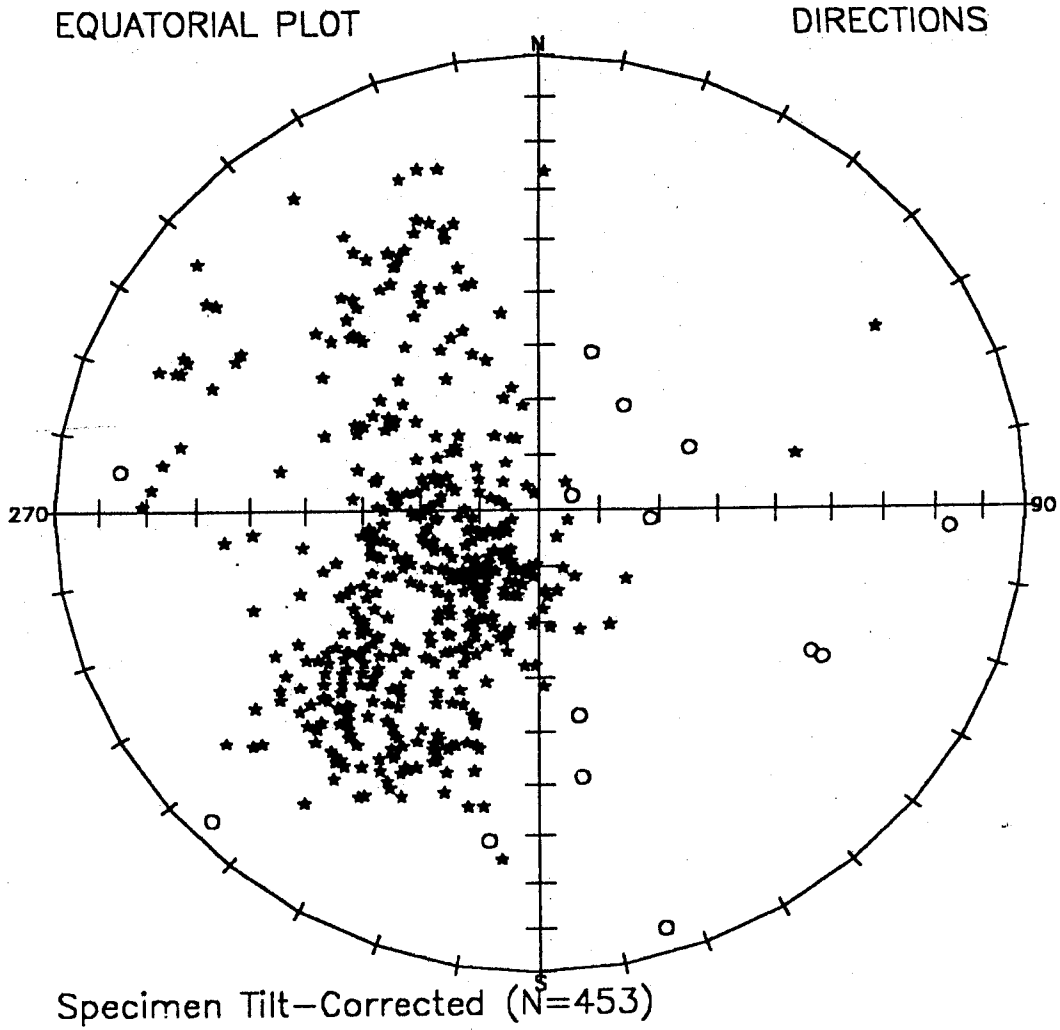

Figure 3.6b Equal area projection (equatorial) of mean directions for each specimen based on linear segment in its orthogonal plot. (in situ and tilt corrected). Star (circle) symbol = near (far) side.

between the results derived from both method and end point estimations from circular plots are not then reliable.

The majority of these specimens showed single component behaviour and hence exhibit only one linear segment on the orthogonal plot. By comparing the value of alpha-95 (more appropriate MAD = Maximum Angular Deviation), at least three data points were chosen as to determine the characteristic magnetisation of the specimen. Figure 3.4b is a histogram of the calculated alpha-95s for Permo-Carboniferous (PC) components. The average is less than 10° and no specimens have alpha-95 more than 40°.

Figure 3.6 shows the equal area projection of the direction derived from the linear segment on the orthogonal plot for each specimen. The directions are clustered round the Late Palaeozoic reversed palaeofield direction for southern Britain. It can be seen clearly that the in situ directions are more tightly grouped than the tilt-corrected directions. The expected reversed palaeomagnetic directions at the sampling area of Group 1, Group 2 and Group 3 from 310 My up to present times are shown in Table 3.2. The pole positions during these times are adapted from Piper (1987) and the DIRE program (in the department's library disk) was used to calculate the palaeomagnetic directions.

Figures 3.7, 3.8 and 3.9 show some palaeomagnetic results (fully tilt corrected) from Groups 1, 2 and 3 respectively. The inclinations depend on the attitude of the beddings. For example, if the bedding is dipping to the north (south), in general, the inclination is positive (negative). This observation

Figure 3.7a Some examples of palaeomagnetic results from Group 1 (Brecon/Abergavenny area). The intensity unit is 10E-5 A.m^2/kg. Four first letters are a sample code (G = Devonian, GB = Great Britain, 1 = South Wales); the next four letters are a site code and the last two letters are a specimen code).

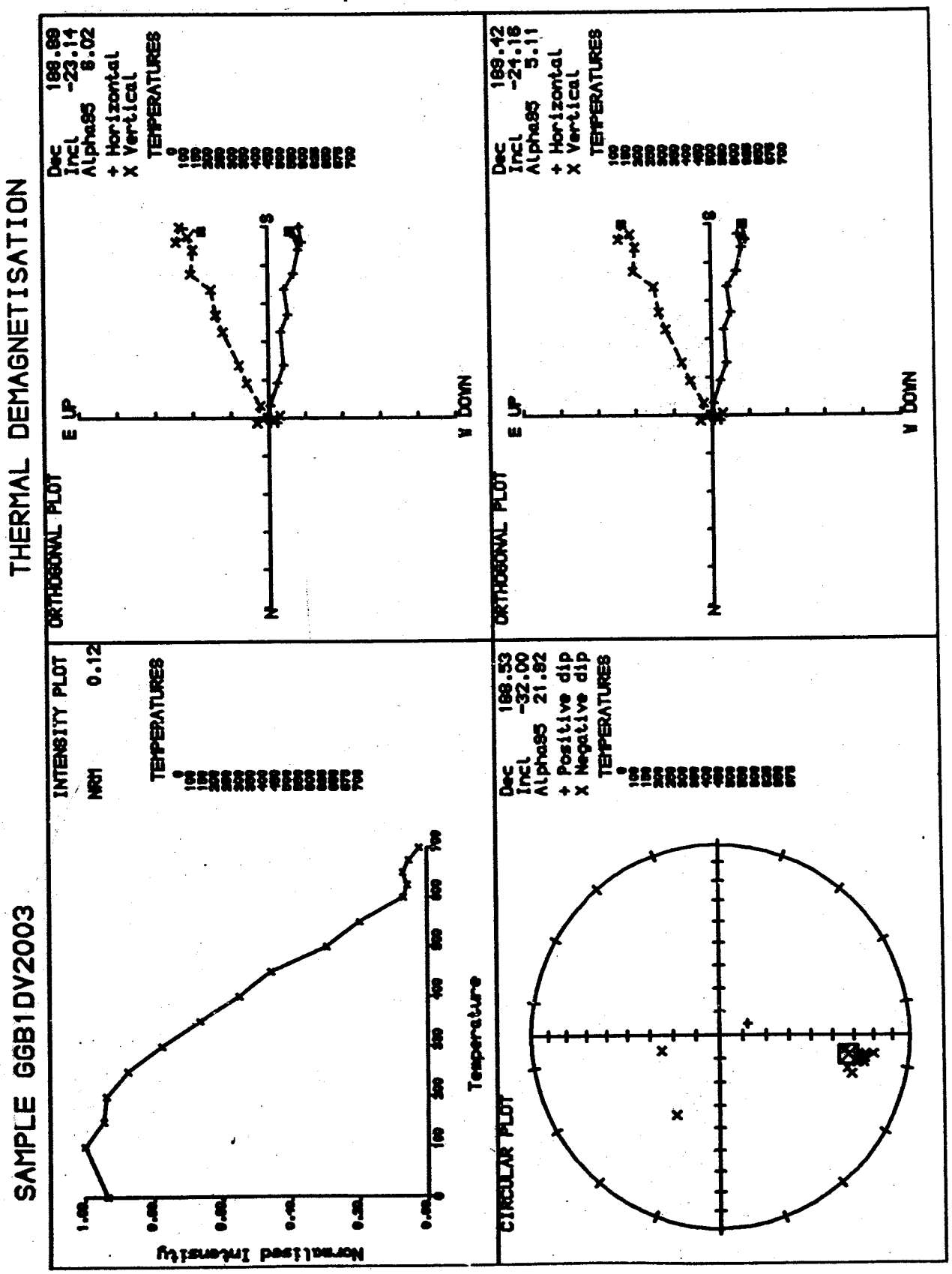

Figure 3.7b.

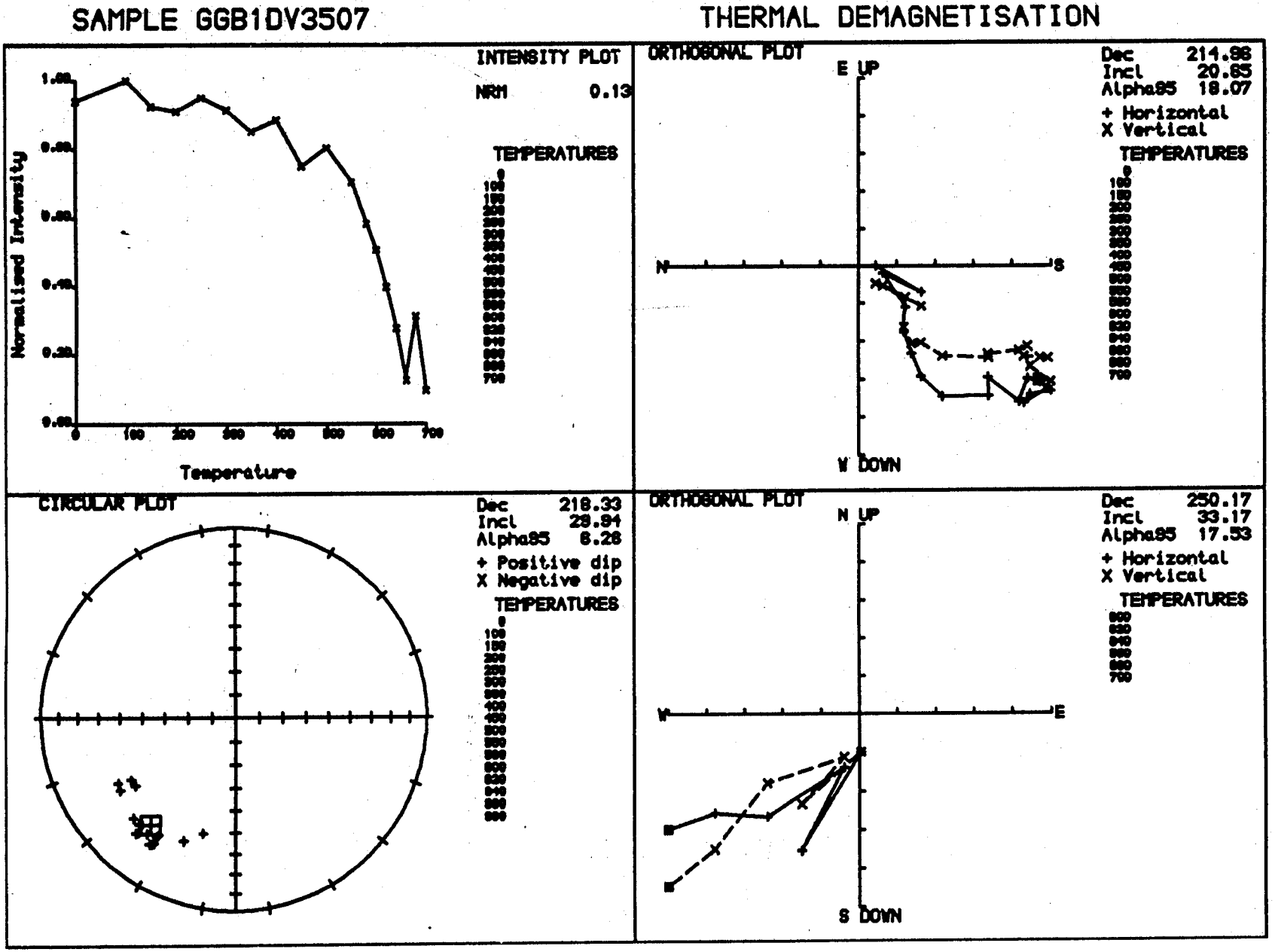
SAMPLE GGB1DV3507
THERMAL DEMAGNETISATION
INTENSITY PLOT
NRM 0.13
TEMPERATURES
Normalised Intensity
Temperature
ORTHOGONAL PLOT
E UP
N
S
W DOWN
Dec 214.86
Incl 20.65
Alpha95 18.07
+ Horizontal
X Vertical
TEMPERATURES
CIRCULAR PLOT
Dec 218.33
Incl 29.94
Alpha95 6.26
+ Positive dip
X Negative dip
TEMPERATURES
ORTHOGONAL PLOT
N UP
W
E
S DOWN
Dec 250.17
Incl 33.17
Alpha95 17.53
+ Horizontal
X Vertical
TEMPERATURES

Figure 3.7c.

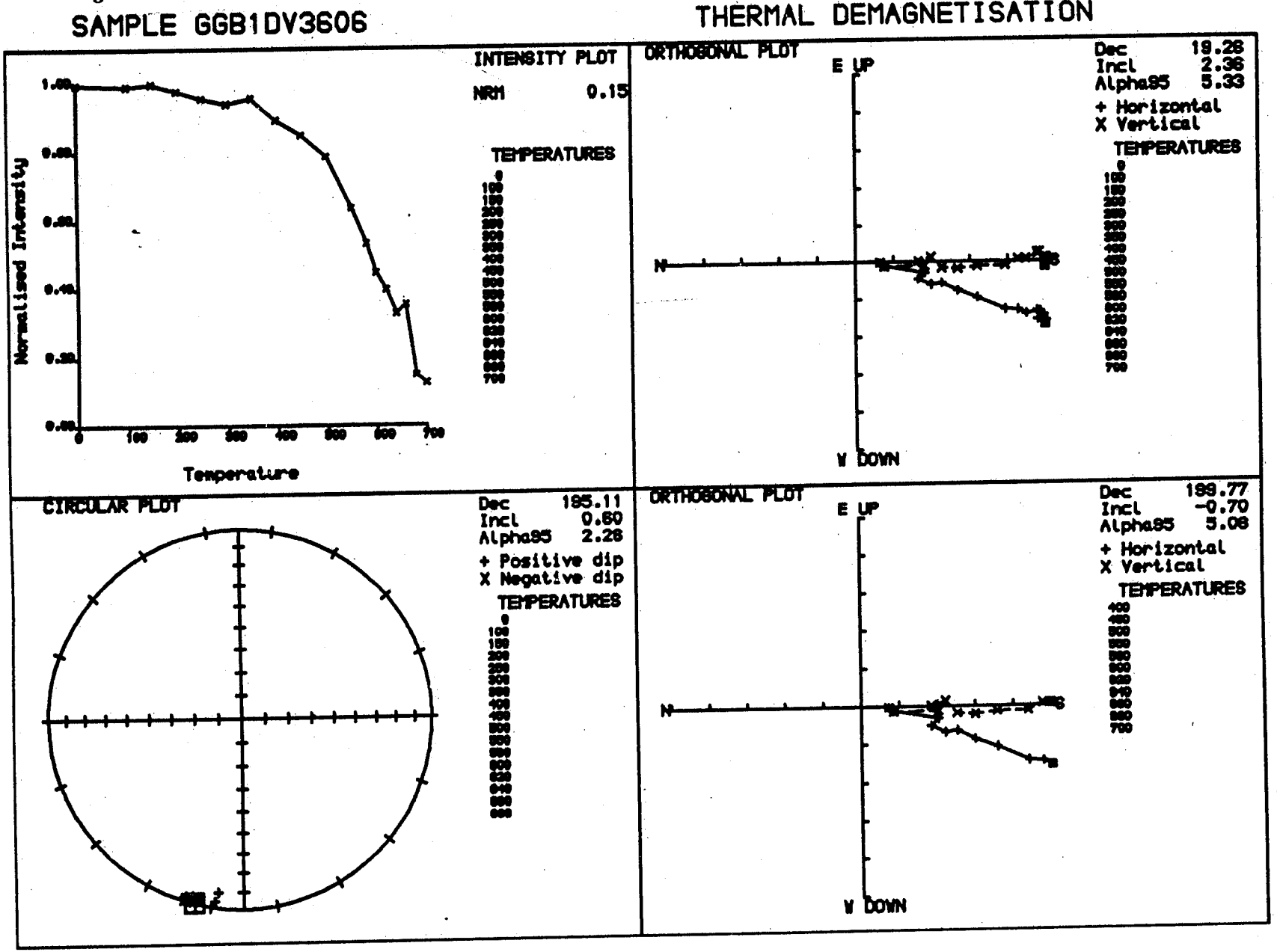
SAMPLE GGB1DV3606
THERMAL DEMAGNETISATION
INTENSITY PLOT
NRM 0.15
TEMPERATURES
Normalised Intensity
Temperature
ORTHOGONAL PLOT
E UP
N
W DOWN
Dec 19.26
Incl 2.36
Alpha95 5.33
+ Horizontal
X Vertical
TEMPERATURES
CIRCULAR PLOT
Dec 195.11
Incl 0.60
Alpha95 2.26
+ Positive dip
X Negative dip
TEMPERATURES
ORTHOGONAL PLOT
E UP
N
W DOWN
Dec 189.77
Incl -0.70
Alpha95 5.08
+ Horizontal
X Vertical
TEMPERATURES

Figure 3.7d.

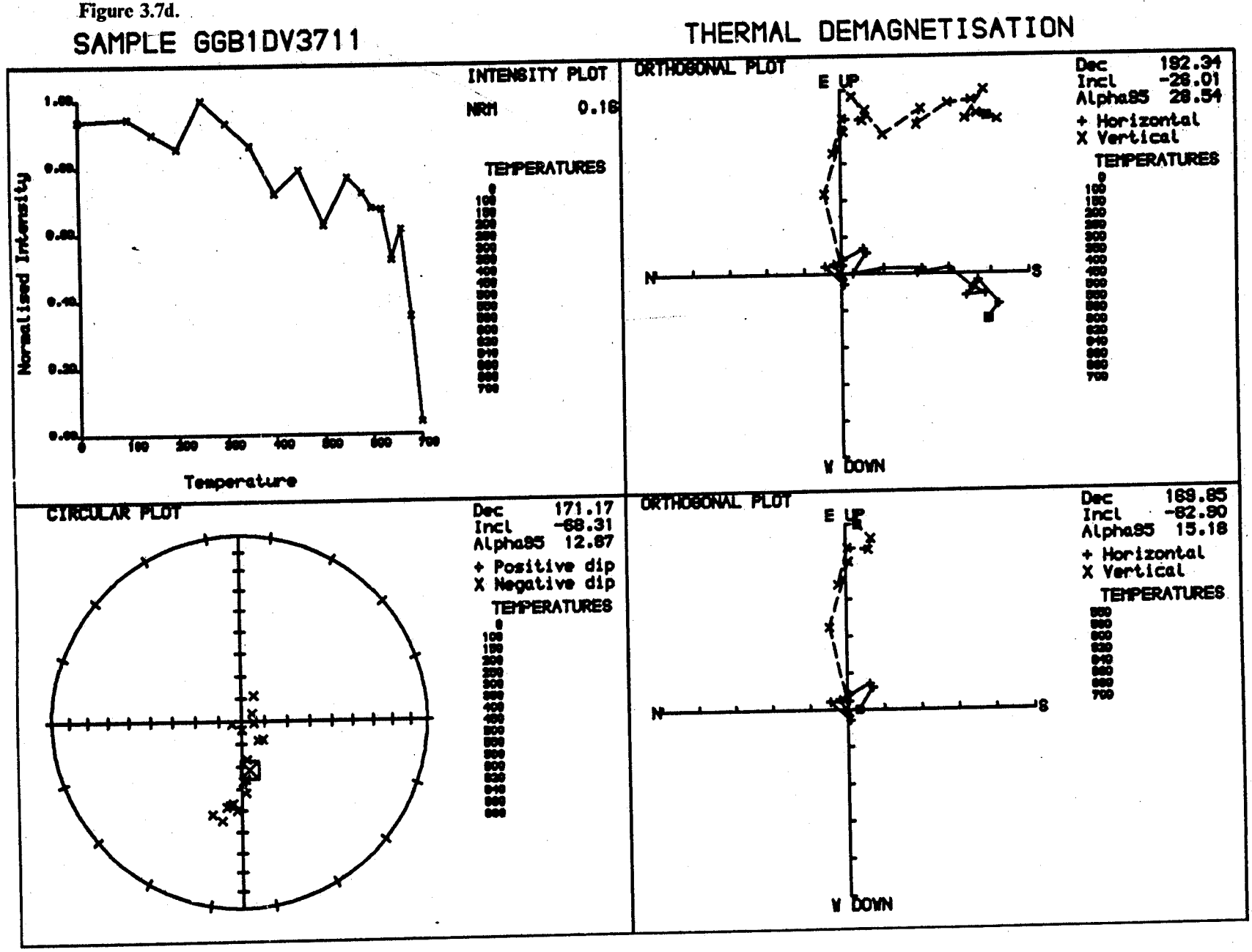
SAMPLE GGB1DV3711
THERMAL DEMAGNETISATION
INTENSITY PLOT
NRM 0.16
TEMPERATURES
Normalised Intensity
Temperature
ORTHOGONAL PLOT
E UP
N
S
W DOWN
Dec 192.34
Incl -26.01
Alpha95 28.54
+ Horizontal
X Vertical
TEMPERATURES
CIRCULAR PLOT
Dec 171.17
Incl -68.31
Alpha95 12.87
+ Positive dip
X Negative dip
TEMPERATURES
ORTHOGONAL PLOT
E UP
N
S
W DOWN
Dec 169.85
Incl -62.90
Alpha95 15.18
+ Horizontal
X Vertical
TEMPERATURES

Figure 3.7e.

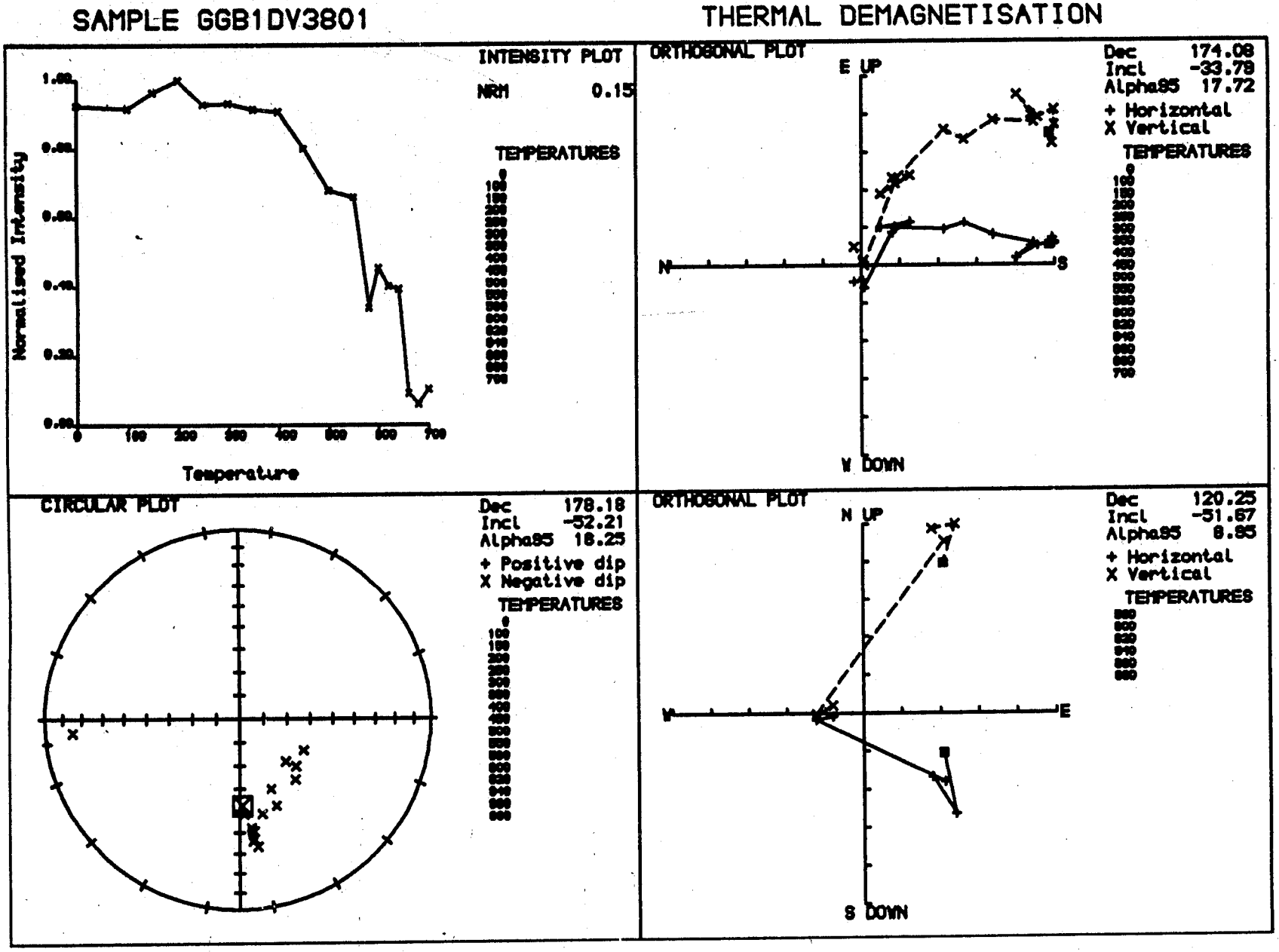
SAMPLE GGB1DV3801
THERMAL DEMAGNETISATION
INTENSITY PLOT
NRM 0.15
TEMPERATURES
Normalised Intensity
Temperature
ORTHOGONAL PLOT
E UP
N
S
W DOWN
Dec 174.08
Incl -33.79
Alpha95 17.72
+ Horizontal
X Vertical
TEMPERATURES
CIRCULAR PLOT
Dec 178.18
Incl -52.21
Alpha95 18.25
+ Positive dip
X Negative dip
TEMPERATURES
ORTHOGONAL PLOT
N UP
W
E
S DOWN
Dec 120.25
Incl -51.67
Alpha95 8.85
+ Horizontal
X Vertical
TEMPERATURES

Figure 3.7f.

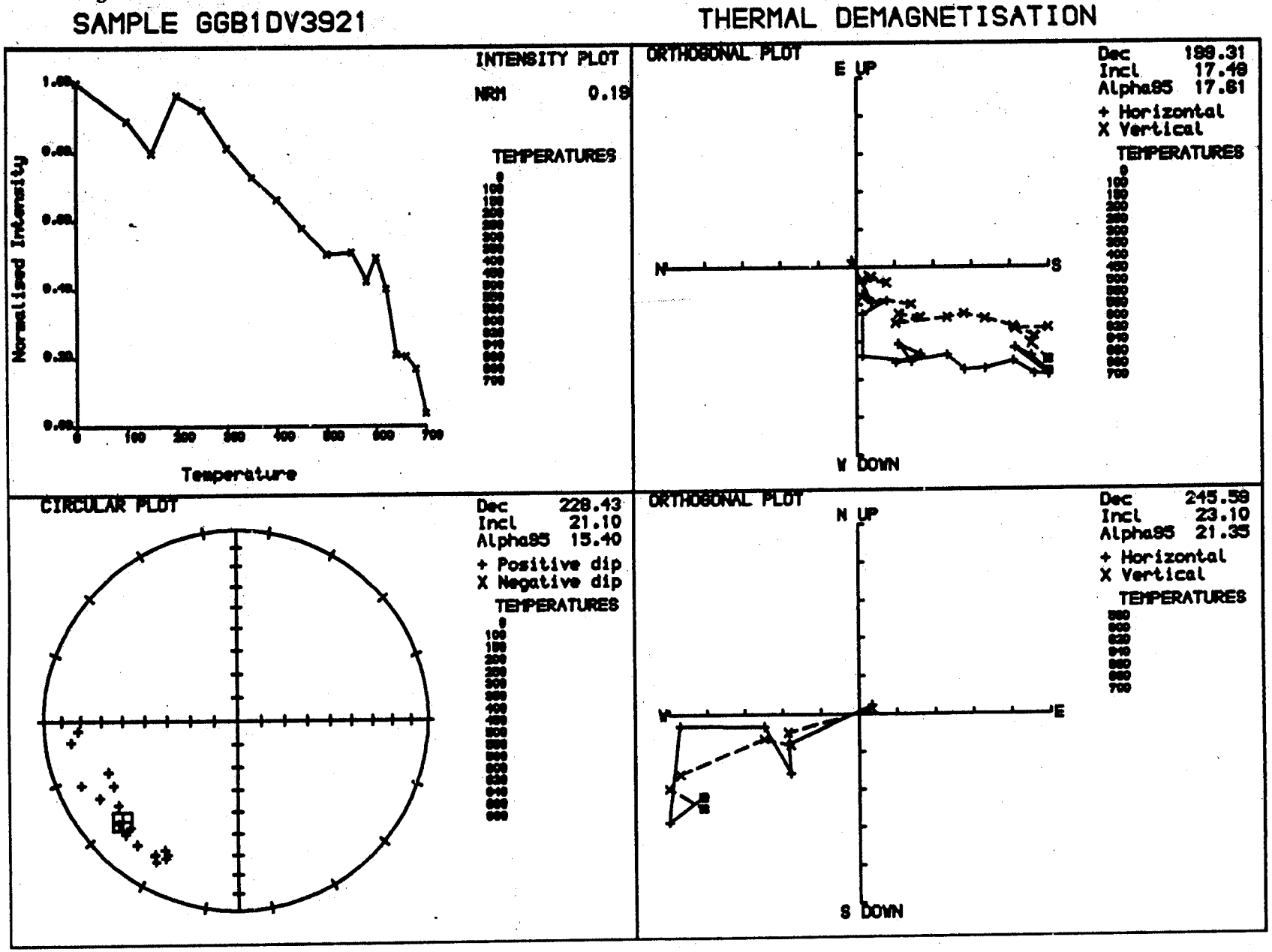
SAMPLE GGB1DV3921
THERMAL DEMAGNETISATION
INTENSITY PLOT
NRM 0.19
TEMPERATURES
Normalised Intensity
Temperature
ORTHOGONAL PLOT
E UP
N
S
W DOWN
Dec 189.31
Incl 17.48
Alpha95 17.81
+ Horizontal
X Vertical
TEMPERATURES
CIRCULAR PLOT
Dec 228.43
Incl 21.10
Alpha95 15.40
+ Positive dip
X Negative dip
TEMPERATURES
ORTHOGONAL PLOT
N UP
W
E
S DOWN
Dec 245.58
Incl 23.10
Alpha95 21.35
+ Horizontal
X Vertical
TEMPERATURES

Figure 3.7g.

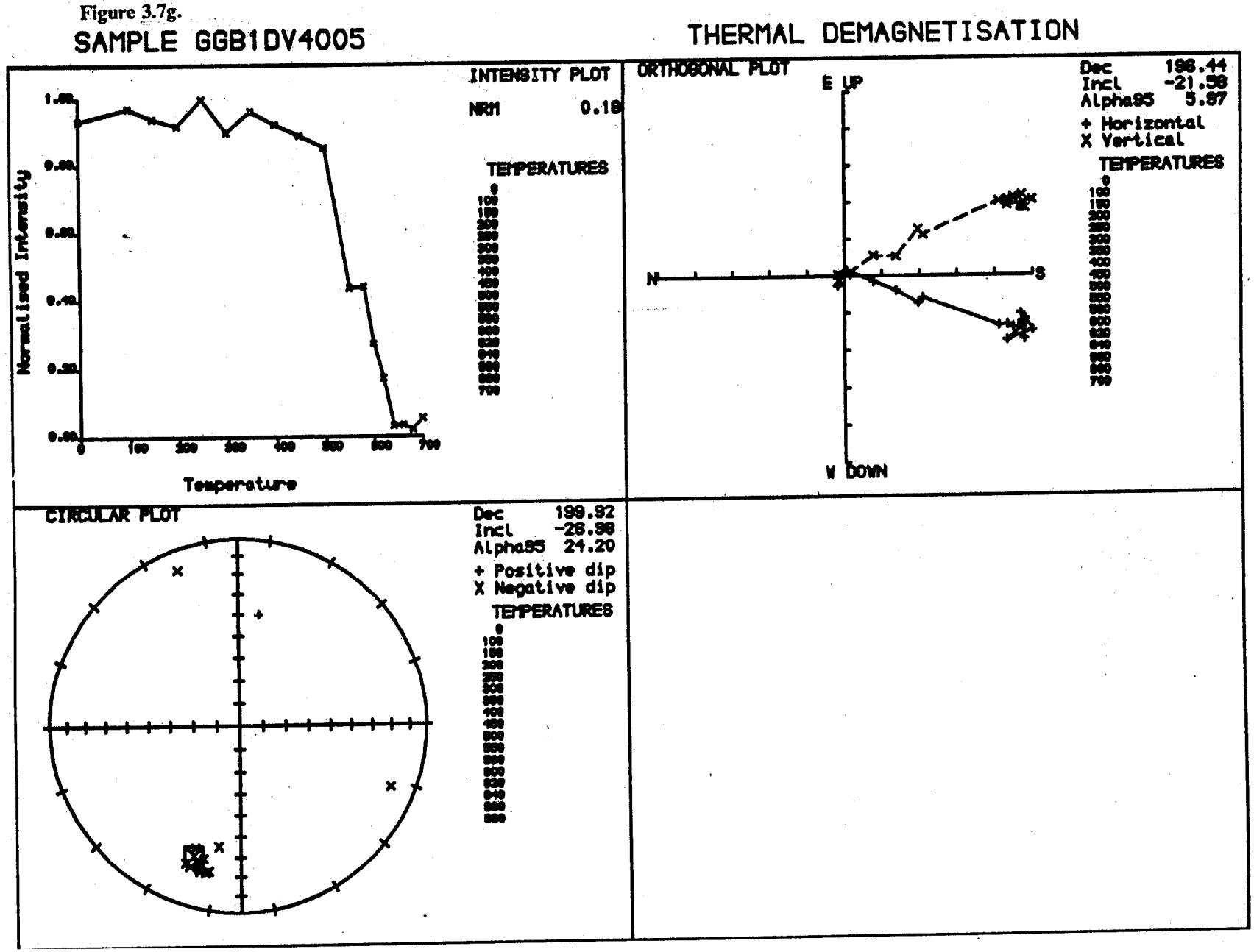
SAMPLE GGB1DV4005
THERMAL DEMAGNETISATION
INTENSITY PLOT
NRM 0.18
TEMPERATURES
Normalised Intensity
Temperature
ORTHOGONAL PLOT
E UP
N
S
W DOWN
Dec 196.44
Incl -21.59
Alpha95 5.87
+ Horizontal
X Vertical
TEMPERATURES
CIRCULAR PLOT
Dec 199.92
Incl -26.98
Alpha95 24.20
+ Positive dip
X Negative dip
TEMPERATURES

Figure 3.7h.

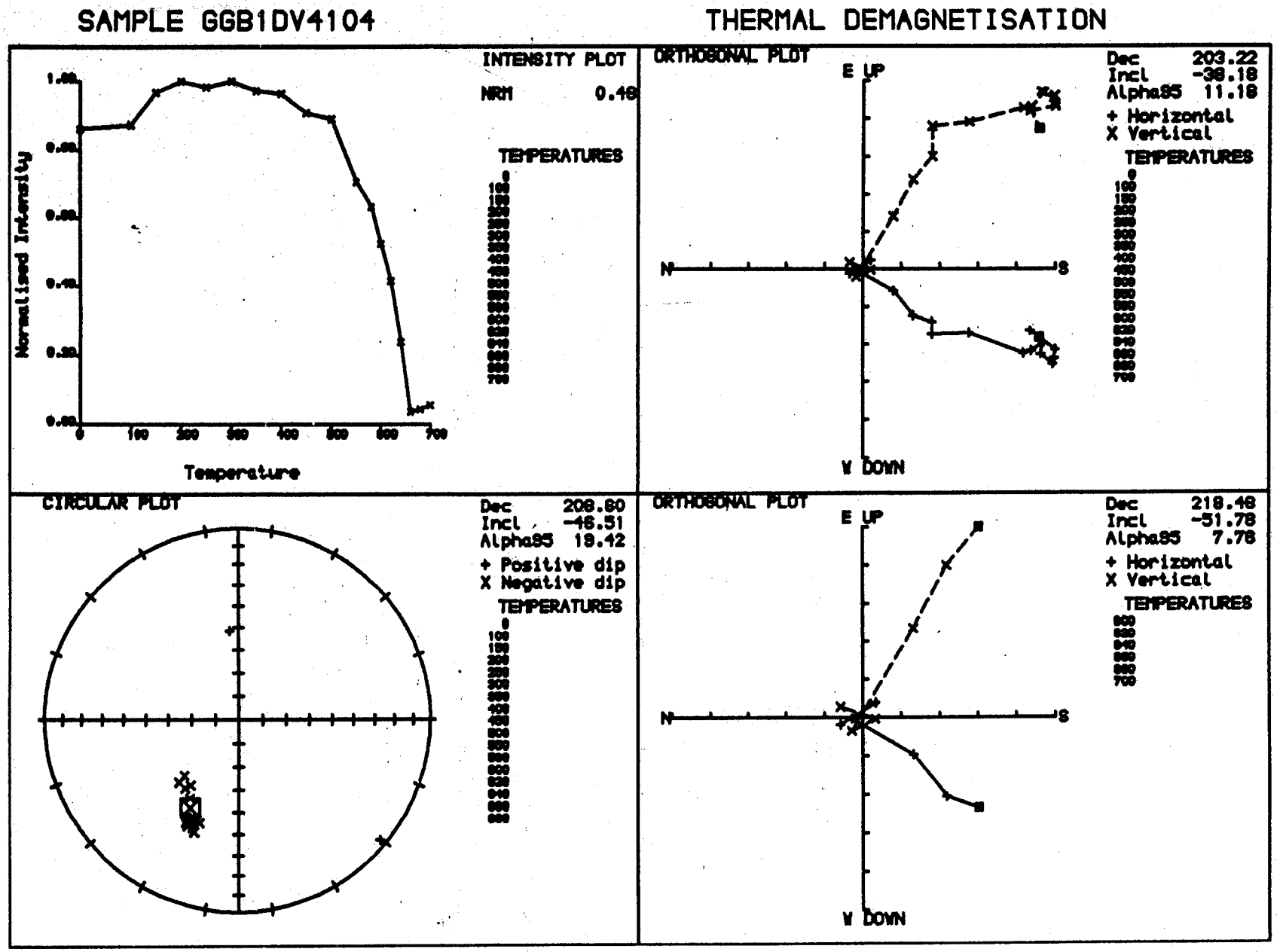
SAMPLE GGB1DV4104
THERMAL DEMAGNETISATION
INTENSITY PLOT
NRM 0.48
TEMPERATURES
Normalised Intensity
Temperature
ORTHOGONAL PLOT
E UP
N
S
W DOWN
Dec 203.22
Incl -38.18
Alpha95 11.18
+ Horizontal
X Vertical
TEMPERATURES
CIRCULAR PLOT
Dec 208.80
Incl -46.51
Alpha95 19.42
+ Positive dip
X Negative dip
TEMPERATURES
ORTHOGONAL PLOT
E UP
N
S
W DOWN
Dec 218.48
Incl -51.78
Alpha95 7.78
+ Horizontal
X Vertical
TEMPERATURES

Figure 3.7i.

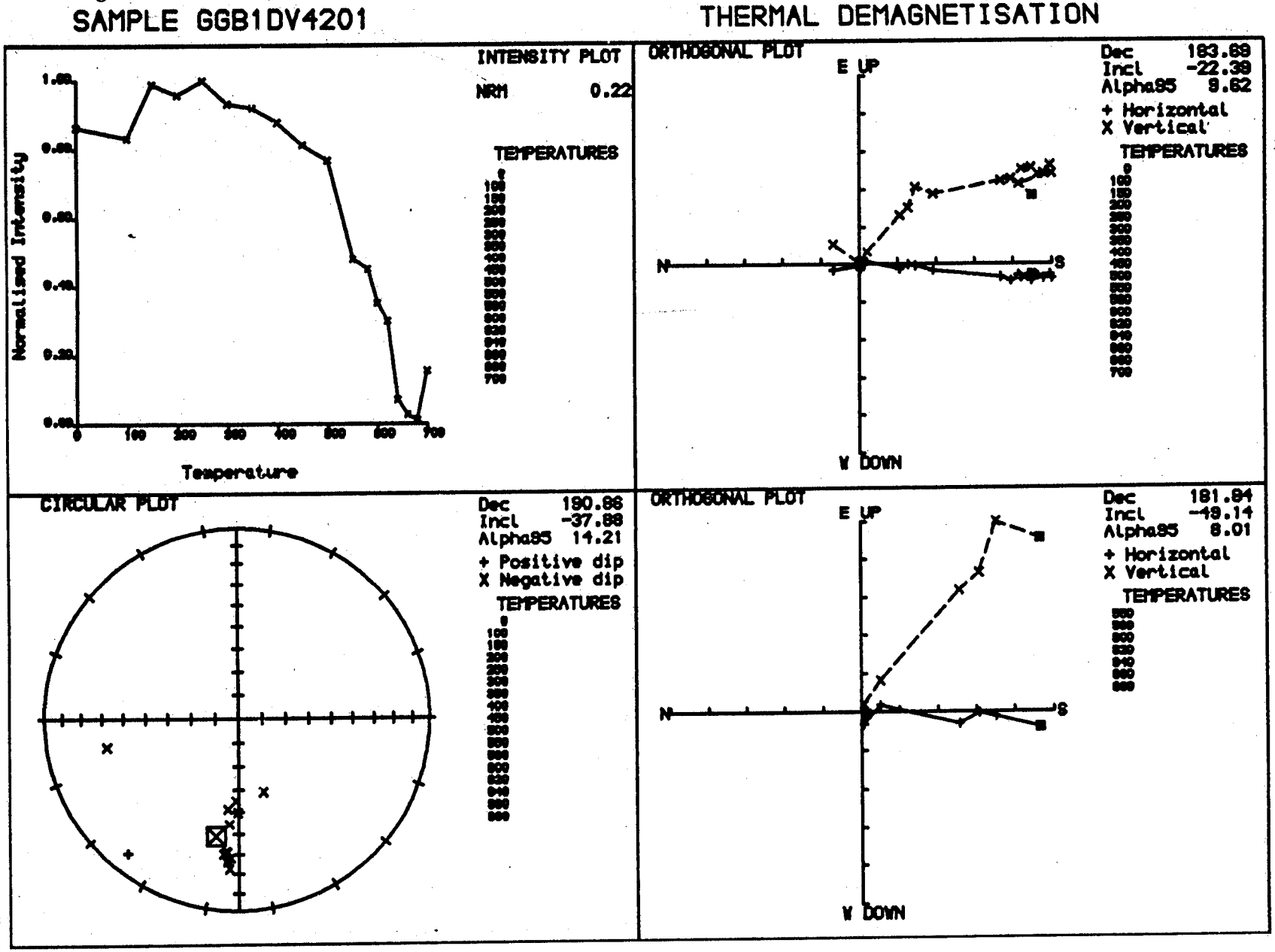
SAMPLE GGB1DV4201
THERMAL DEMAGNETISATION
INTENSITY PLOT
NRM 0.22
TEMPERATURES
Normalised Intensity
Temperature
ORTHOGONAL PLOT
E UP
N
S
W DOWN
Dec 183.69
Incl -22.39
Alpha95 9.62
+ Horizontal
X Vertical
TEMPERATURES
CIRCULAR PLOT
Dec 190.86
Incl -37.88
Alpha95 14.21
+ Positive dip
X Negative dip
TEMPERATURES
ORTHOGONAL PLOT
E UP
N
S
W DOWN
Dec 181.84
Incl -49.14
Alpha95 8.01
+ Horizontal
X Vertical
TEMPERATURES

Figure 3.8a Some examples of palaeomagnetic results from Group 2 (Carmarthen area) (see caption Figure 3.7a).

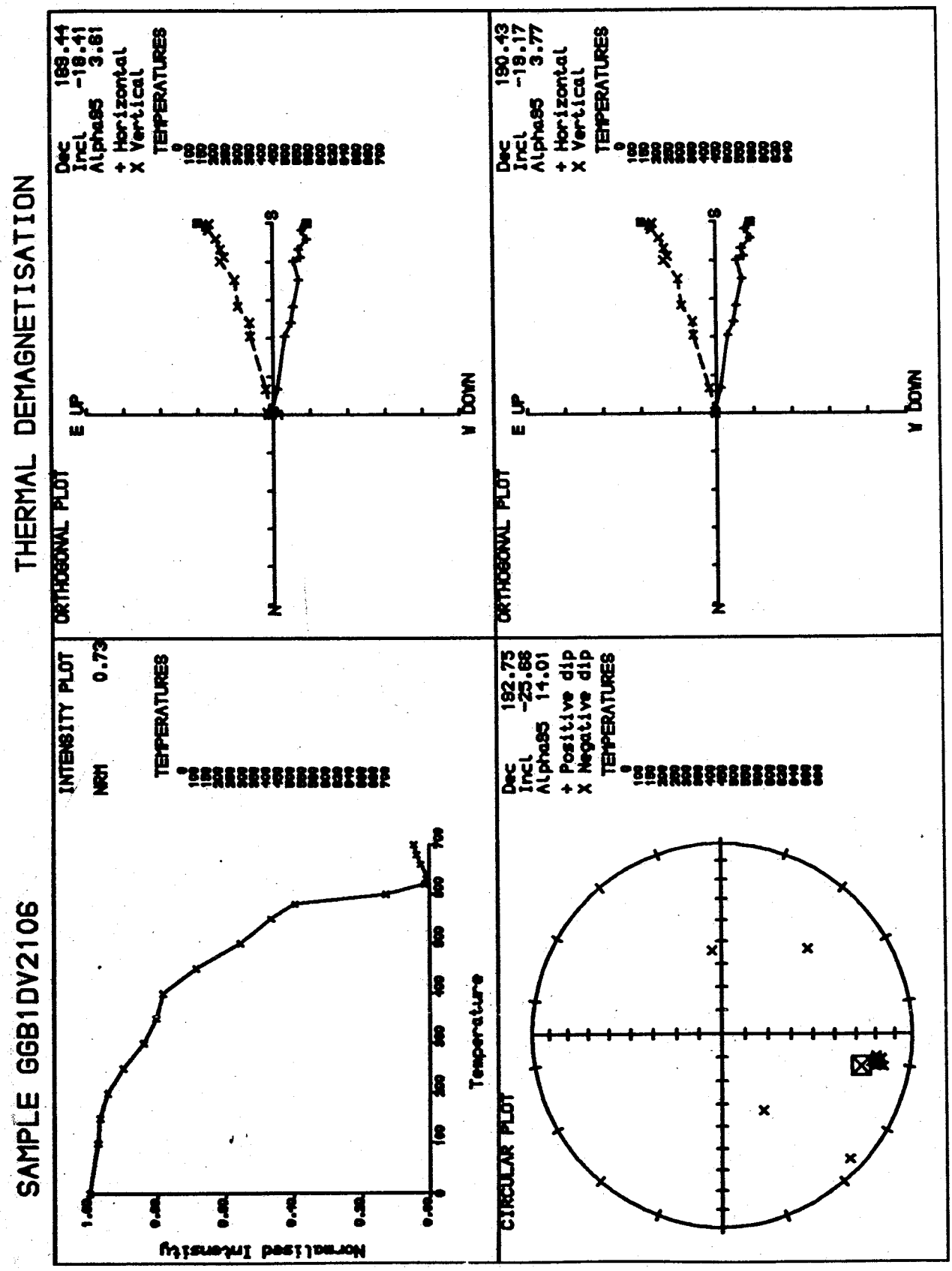

Figure 3.8b.

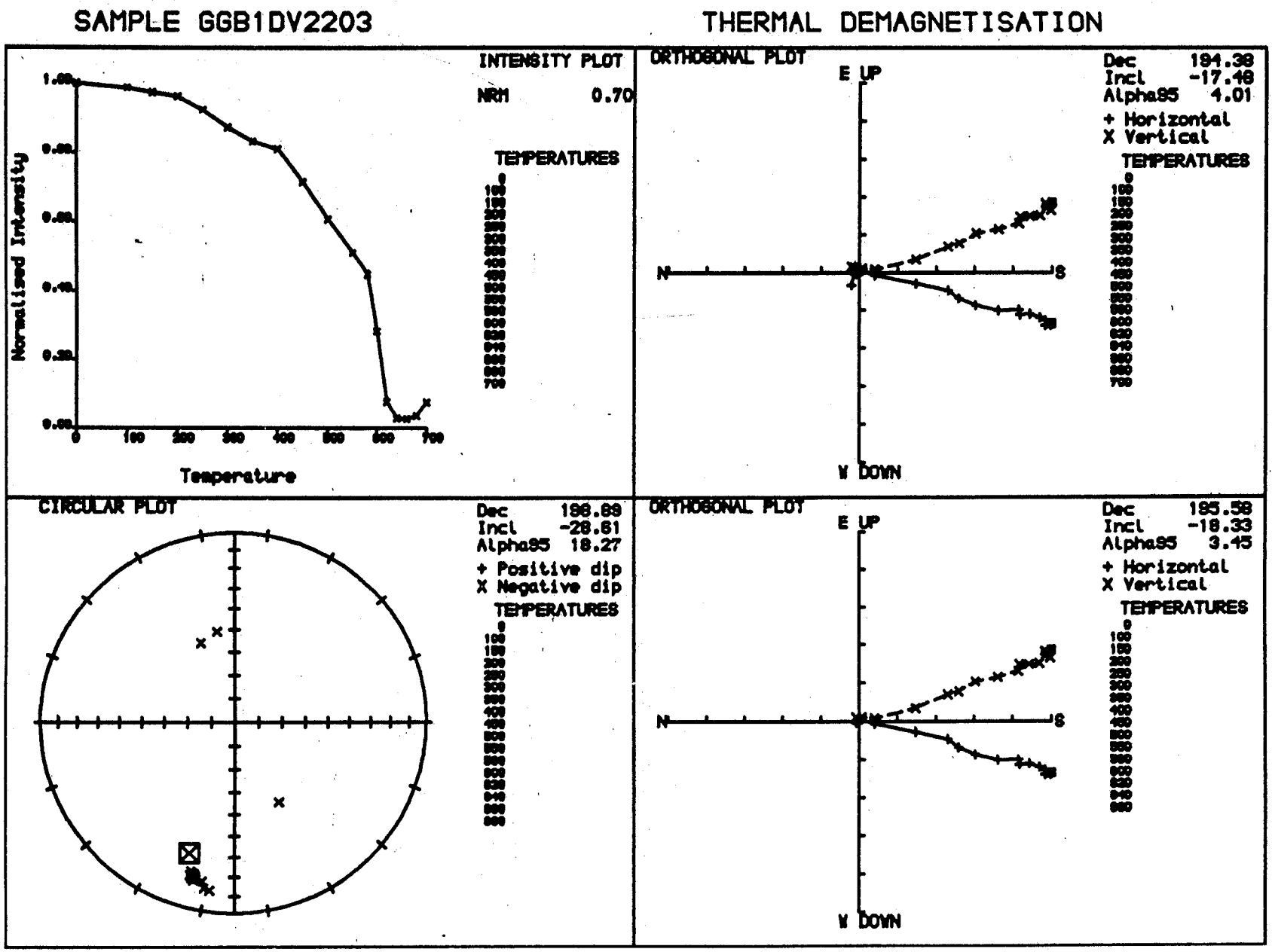
SAMPLE GGB1DV2203
THERMAL DEMAGNETISATION
INTENSITY PLOT
NRM 0.70
TEMPERATURES
Normalised Intensity
Temperature
ORTHOGONAL PLOT
E UP
N
S
W DOWN
Dec 194.38
Incl -17.48
Alpha95 4.01
+ Horizontal
X Vertical
TEMPERATURES
CIRCULAR PLOT
Dec 196.89
Incl -28.61
Alpha95 18.27
+ Positive dip
X Negative dip
TEMPERATURES
ORTHOGONAL PLOT
E UP
N
S
W DOWN
Dec 195.58
Incl -18.33
Alpha95 3.45
+ Horizontal
X Vertical
TEMPERATURES

Figure 3.8c.

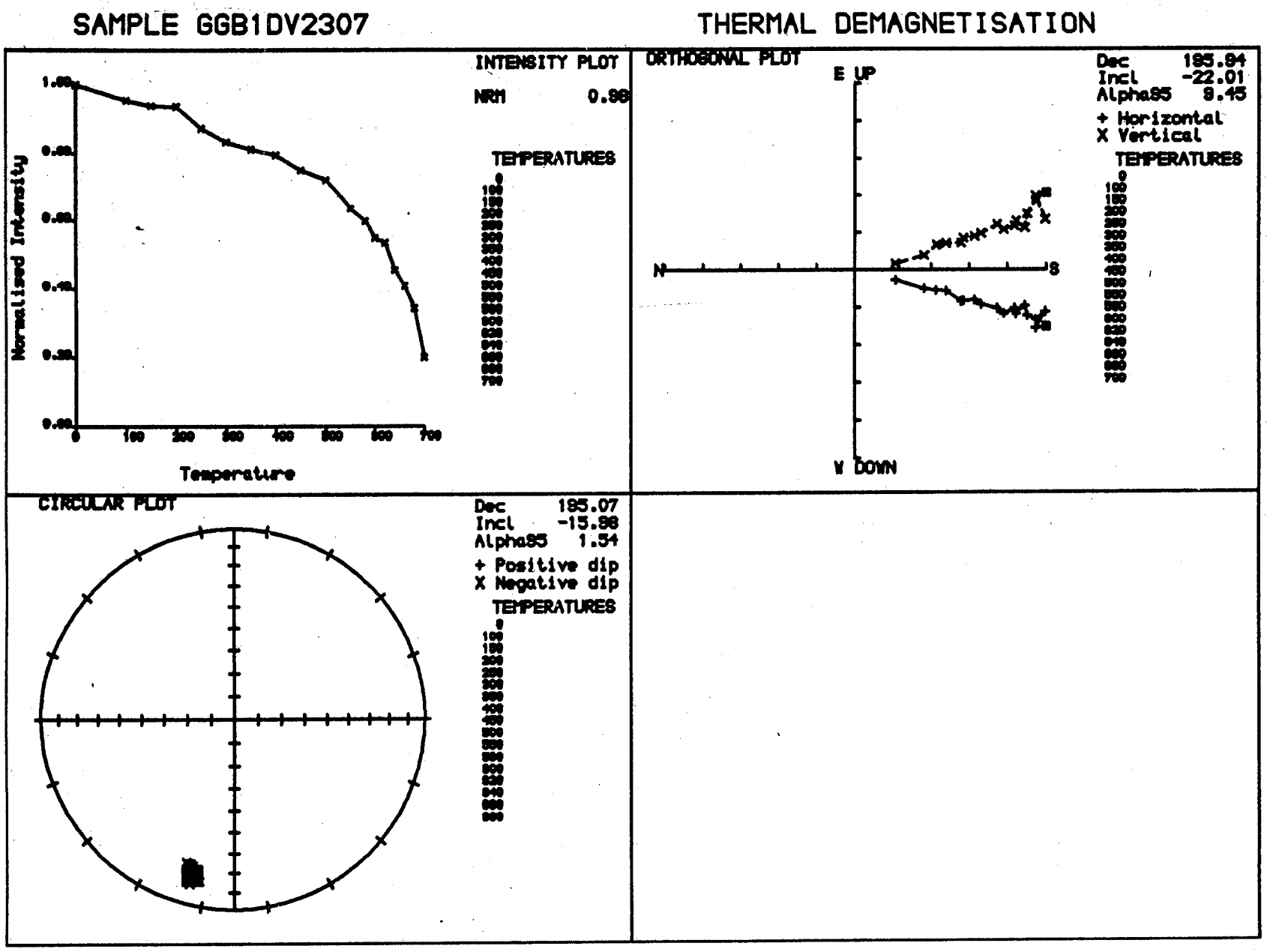
SAMPLE GGB1DV2307
THERMAL DEMAGNETISATION
INTENSITY PLOT
NRM 0.98
TEMPERATURES
Normalised Intensity
Temperature
ORTHOGONAL PLOT
E UP
N
S
W DOWN
Dec 185.94
Incl -22.01
Alpha95 8.45
+ Horizontal
X Vertical
TEMPERATURES
CIRCULAR PLOT
Dec 185.07
Incl -15.88
Alpha95 1.54
+ Positive dip
X Negative dip
TEMPERATURES

Figure 3.8d.

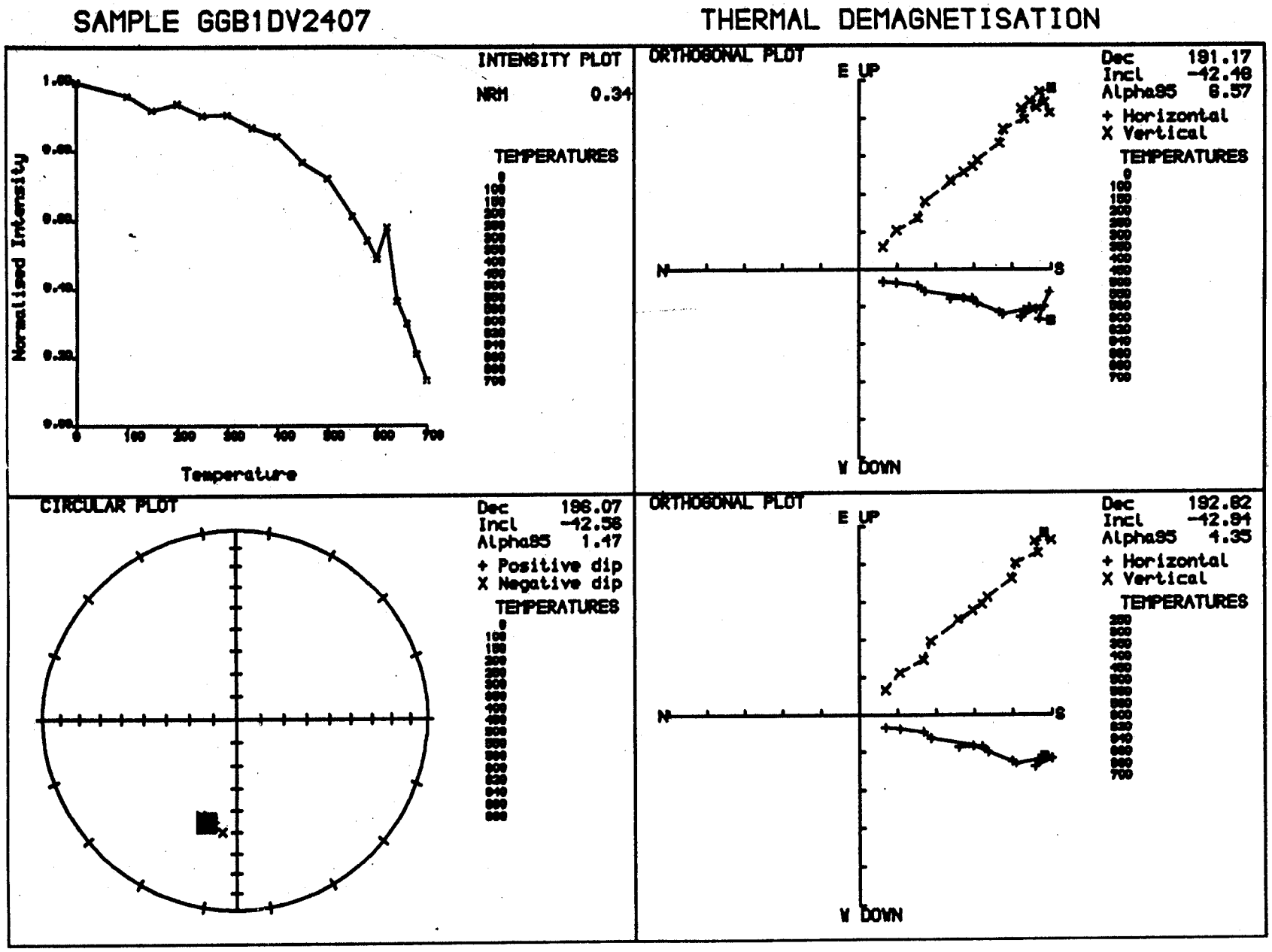
SAMPLE GGB1DV2407
THERMAL DEMAGNETISATION
INTENSITY PLOT
NRM 0.34
TEMPERATURES
Normalised Intensity
Temperature
ORTHOGONAL PLOT
E UP
N
S
W DOWN
Dec 191.17
Incl -42.48
Alpha95 6.57
+ Horizontal
X Vertical
TEMPERATURES
CIRCULAR PLOT
Dec 196.07
Incl -42.56
Alpha95 1.47
+ Positive dip
X Negative dip
TEMPERATURES
ORTHOGONAL PLOT
E UP
N
S
W DOWN
Dec 192.82
Incl -42.91
Alpha95 4.35
+ Horizontal
X Vertical
TEMPERATURES

Figure 3.8e.

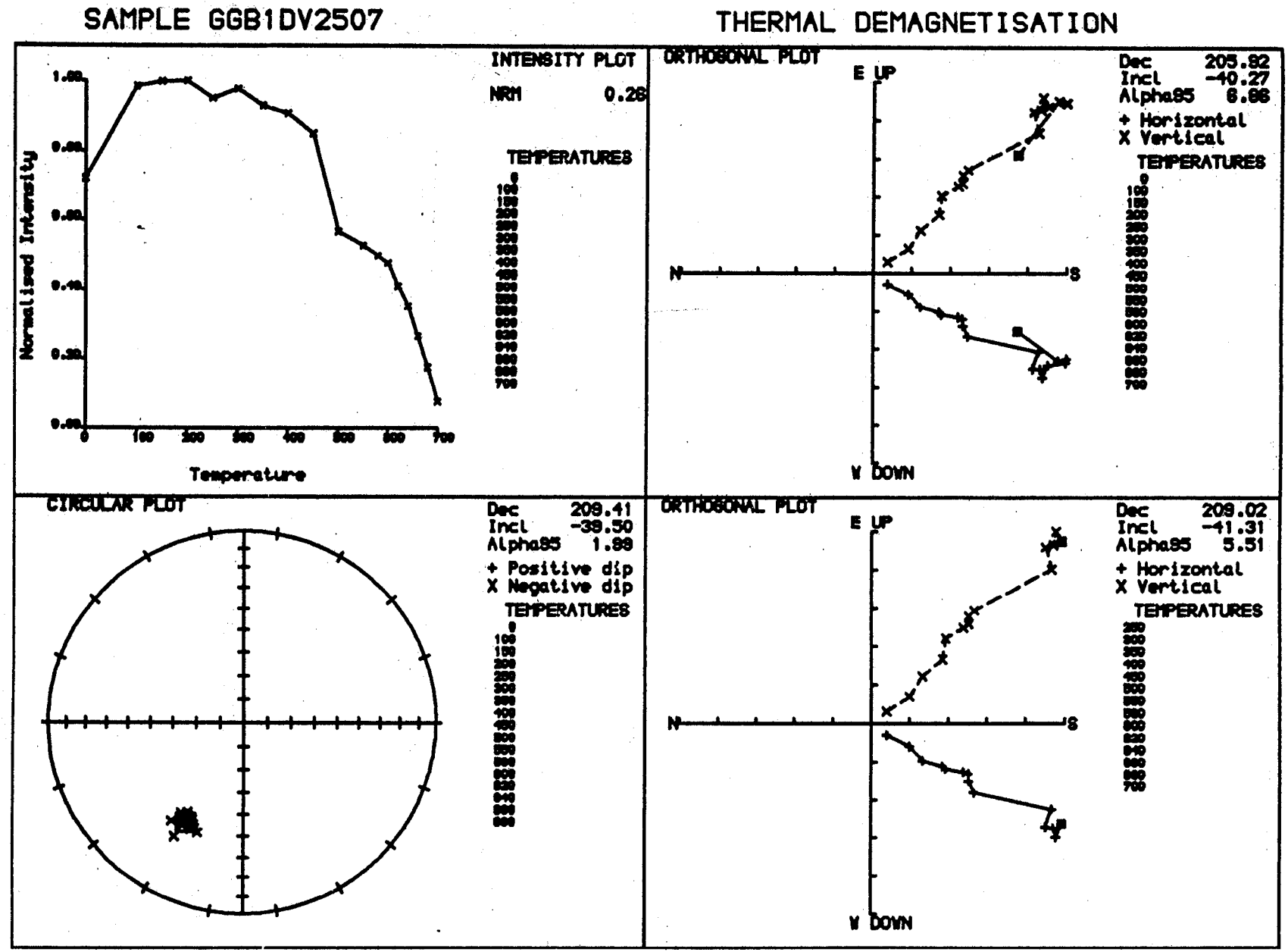
SAMPLE GGB1DV2507
THERMAL DEMAGNETISATION
INTENSITY PLOT
NRM 0.26
TEMPERATURES
Normalised Intensity
Temperature
ORTHOGONAL PLOT
E UP
N
S
W DOWN
Dec 205.82
Incl -40.27
Alpha95 6.66
+ Horizontal
X Vertical
TEMPERATURES
CIRCULAR PLOT
Dec 209.41
Incl -39.50
Alpha95 1.89
+ Positive dip
X Negative dip
TEMPERATURES
ORTHOGONAL PLOT
E UP
N
S
W DOWN
Dec 209.02
Incl -41.31
Alpha95 5.51
+ Horizontal
X Vertical
TEMPERATURES

Figure 3.8f.

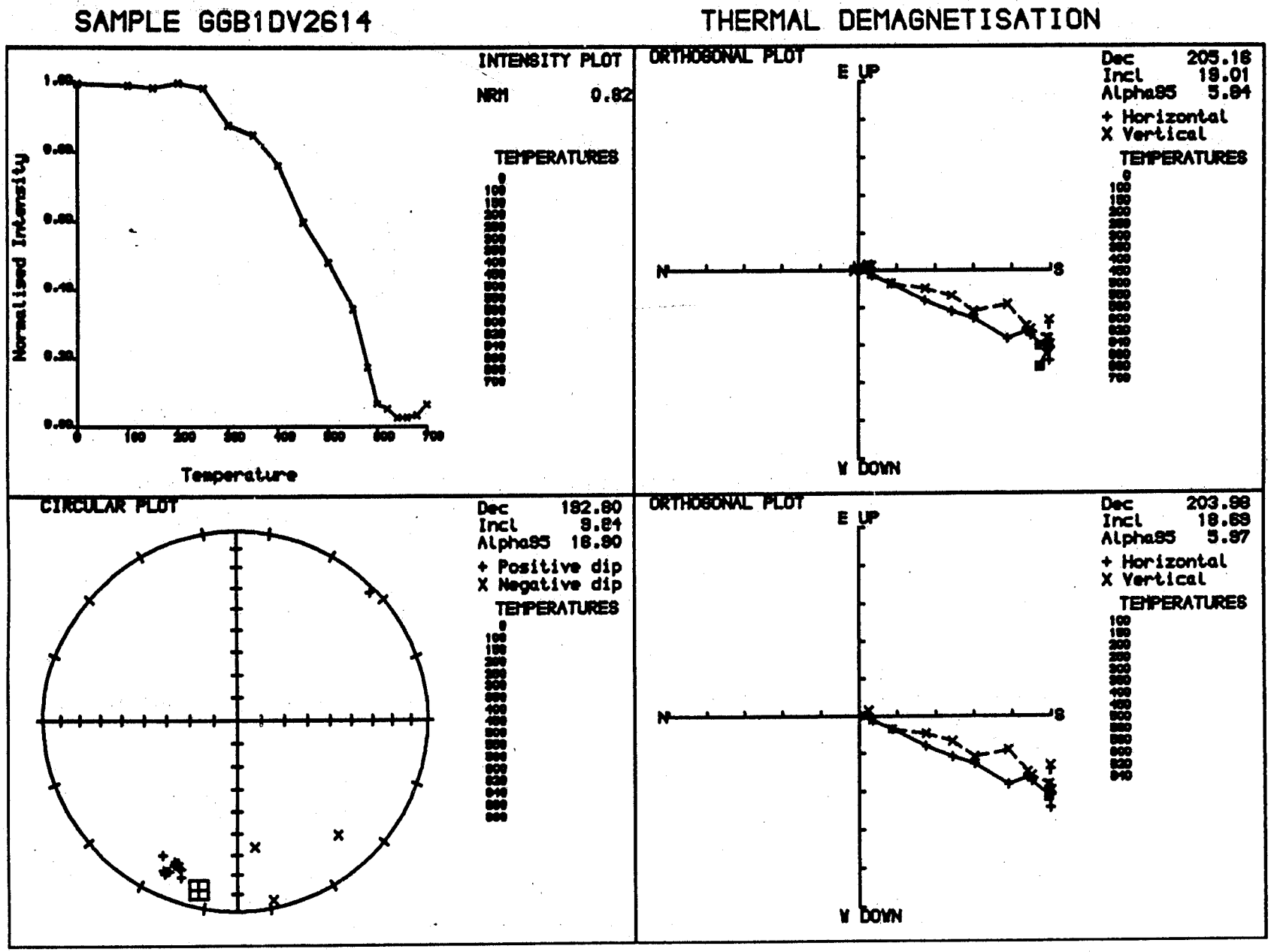
SAMPLE GGB1DV2614
THERMAL DEMAGNETISATION
INTENSITY PLOT
NRM 0.82
TEMPERATURES
Normalised Intensity
Temperature
ORTHOGONAL PLOT
E UP
N
S
W DOWN
Dec 205.16
Incl 19.01
Alpha95 5.84
+ Horizontal
X Vertical
TEMPERATURES
CIRCULAR PLOT
Dec 192.80
Incl 9.84
Alpha95 16.90
+ Positive dip
X Negative dip
TEMPERATURES
ORTHOGONAL PLOT
E UP
N
S
W DOWN
Dec 203.98
Incl 18.69
Alpha95 5.97
+ Horizontal
X Vertical
TEMPERATURES

Figure 3.8g.

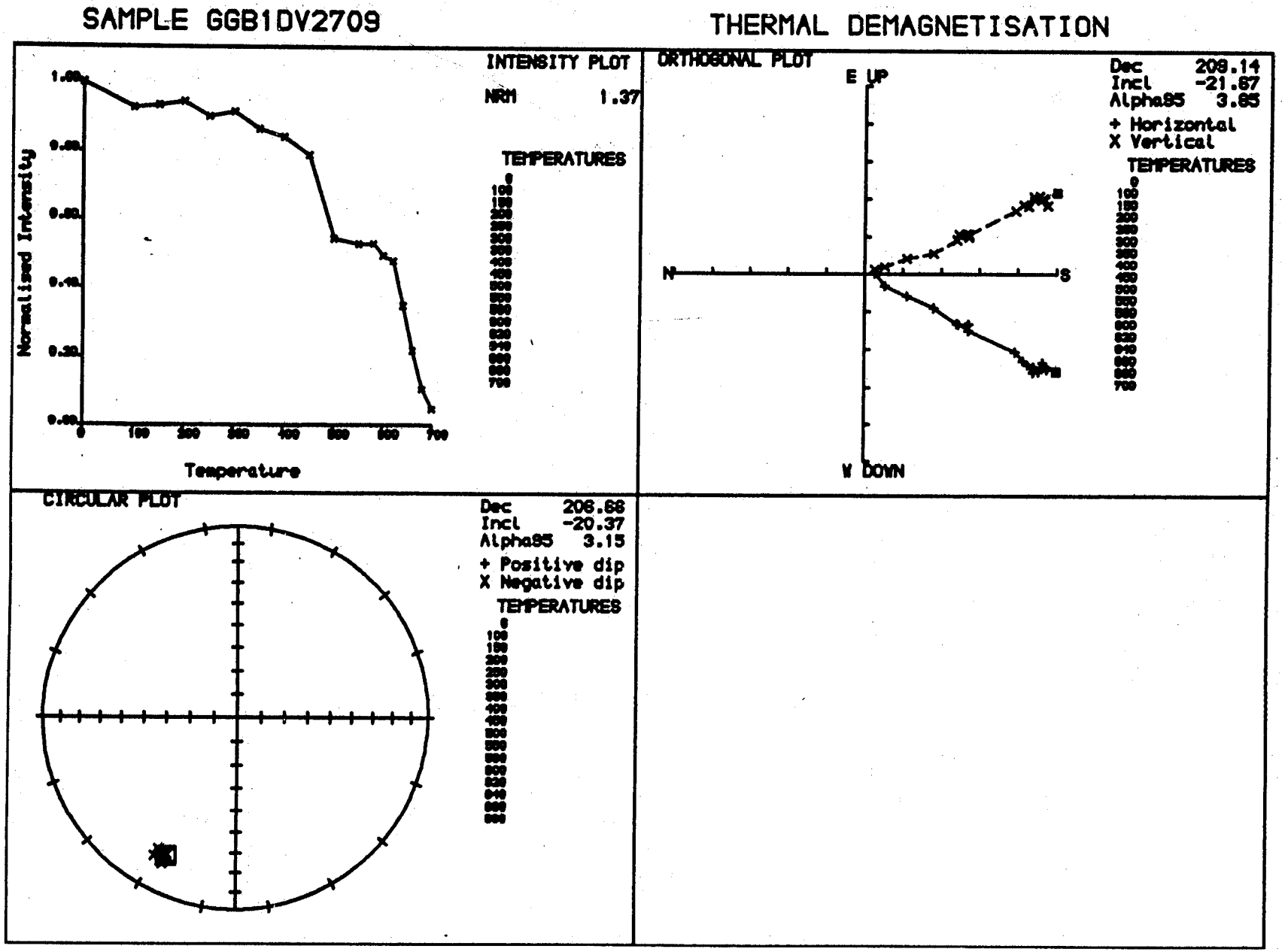
SAMPLE GGB1DV2709
THERMAL DEMAGNETISATION
INTENSITY PLOT
NRM 1.37
TEMPERATURES
Normalised Intensity
Temperature
ORTHOGONAL PLOT
E UP
N
S
W DOWN
Dec 209.14
Incl -21.67
Alpha95 3.85
+ Horizontal
X Vertical
TEMPERATURES
CIRCULAR PLOT
Dec 206.68
Incl -20.37
Alpha95 3.15
+ Positive dip
X Negative dip
TEMPERATURES

Figure 3.8h.

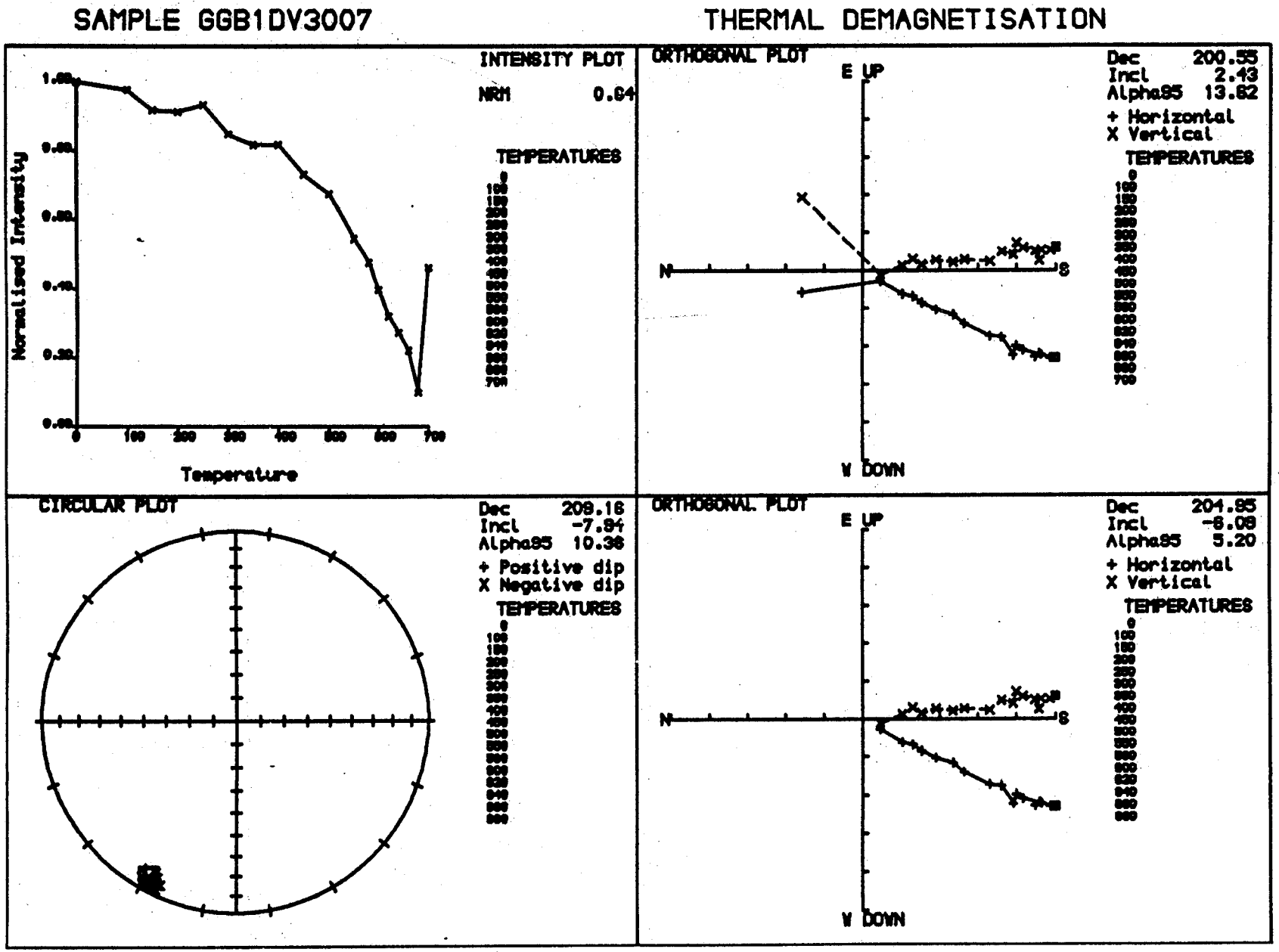
SAMPLE GGB1DV3007
THERMAL DEMAGNETISATION
INTENSITY PLOT
NRM 0.64
TEMPERATURES
Normalised Intensity
Temperature
ORTHOGONAL PLOT
E UP
W DOWN
N
S
Dec 200.55
Incl 2.43
Alpha95 13.62
+ Horizontal
X Vertical
TEMPERATURES
CIRCULAR PLOT
Dec 209.16
Incl -7.84
Alpha95 10.36
+ Positive dip
X Negative dip
TEMPERATURES
ORTHOGONAL PLOT
E UP
W DOWN
N
S
Dec 204.85
Incl -6.08
Alpha95 5.20
+ Horizontal
X Vertical
TEMPERATURES

Figure 3.8i.

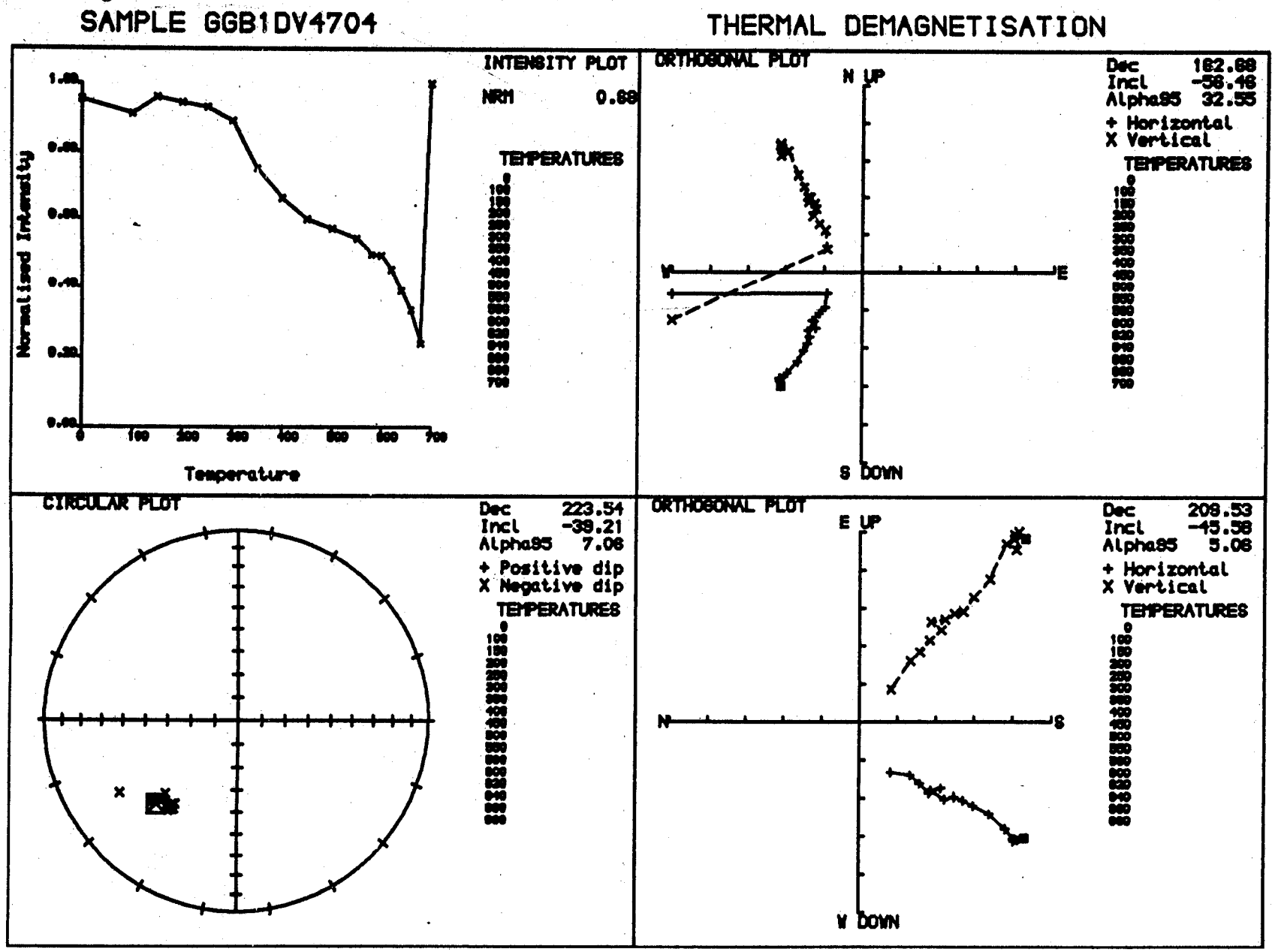
SAMPLE GGB1DV4704
THERMAL DEMAGNETISATION
INTENSITY PLOT
NRM 0.69
TEMPERATURES
Normalised Intensity
Temperature
ORTHOGONAL PLOT
N UP
S DOWN
Dec 182.69
Incl -58.46
Alpha95 32.55
+ Horizontal
X Vertical
TEMPERATURES
CIRCULAR PLOT
Dec 223.54
Incl -39.21
Alpha95 7.06
+ Positive dip
X Negative dip
TEMPERATURES
ORTHOGONAL PLOT
E UP
W DOWN
Dec 208.53
Incl -45.58
Alpha95 5.06
+ Horizontal
X Vertical
TEMPERATURES

Figure 3.9a Some examples of palaeomagnetic results from Group 3 (southern Pembrokeshire) (see caption Figure 3.7a).

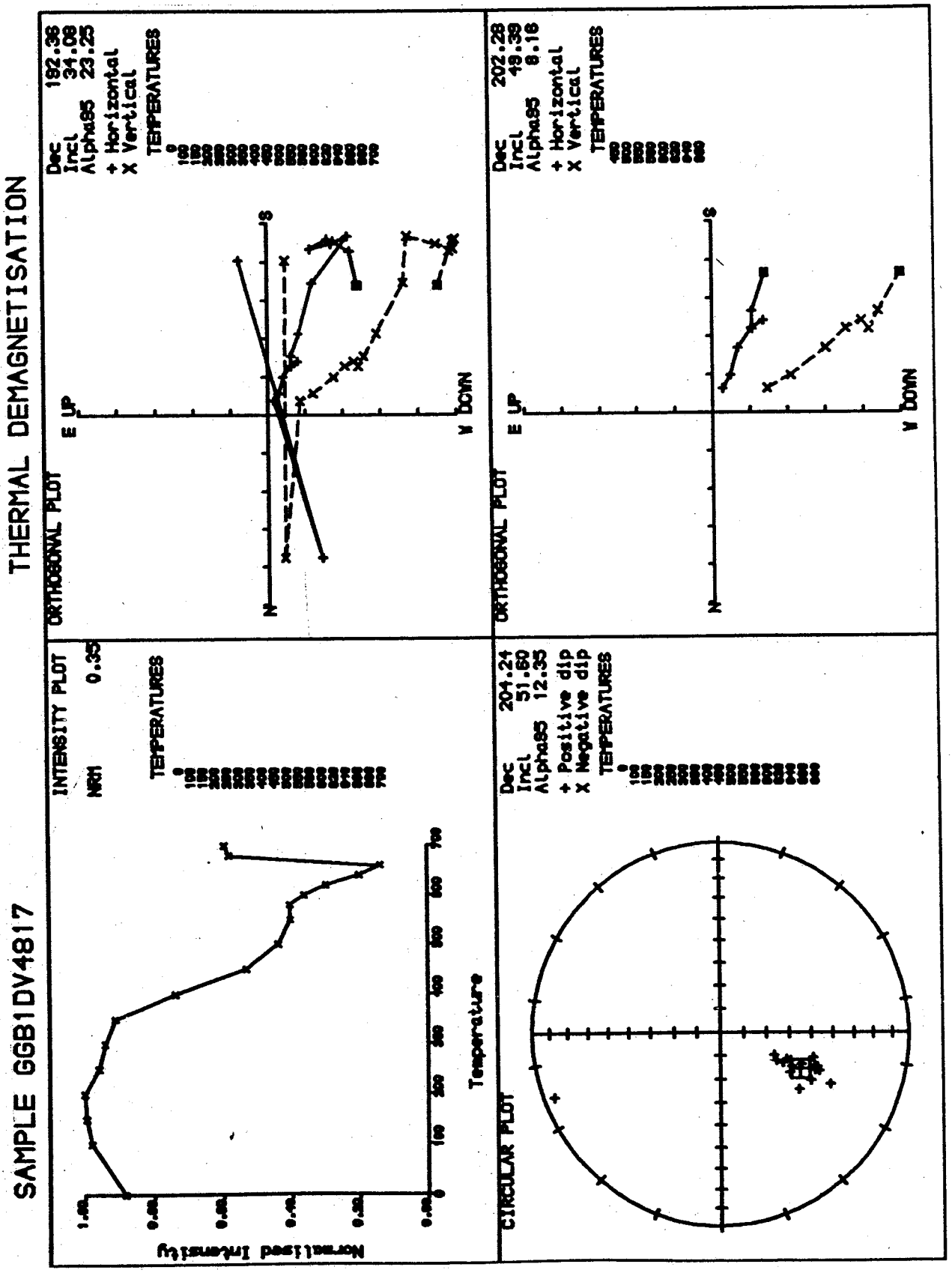

Figure 3.9b.

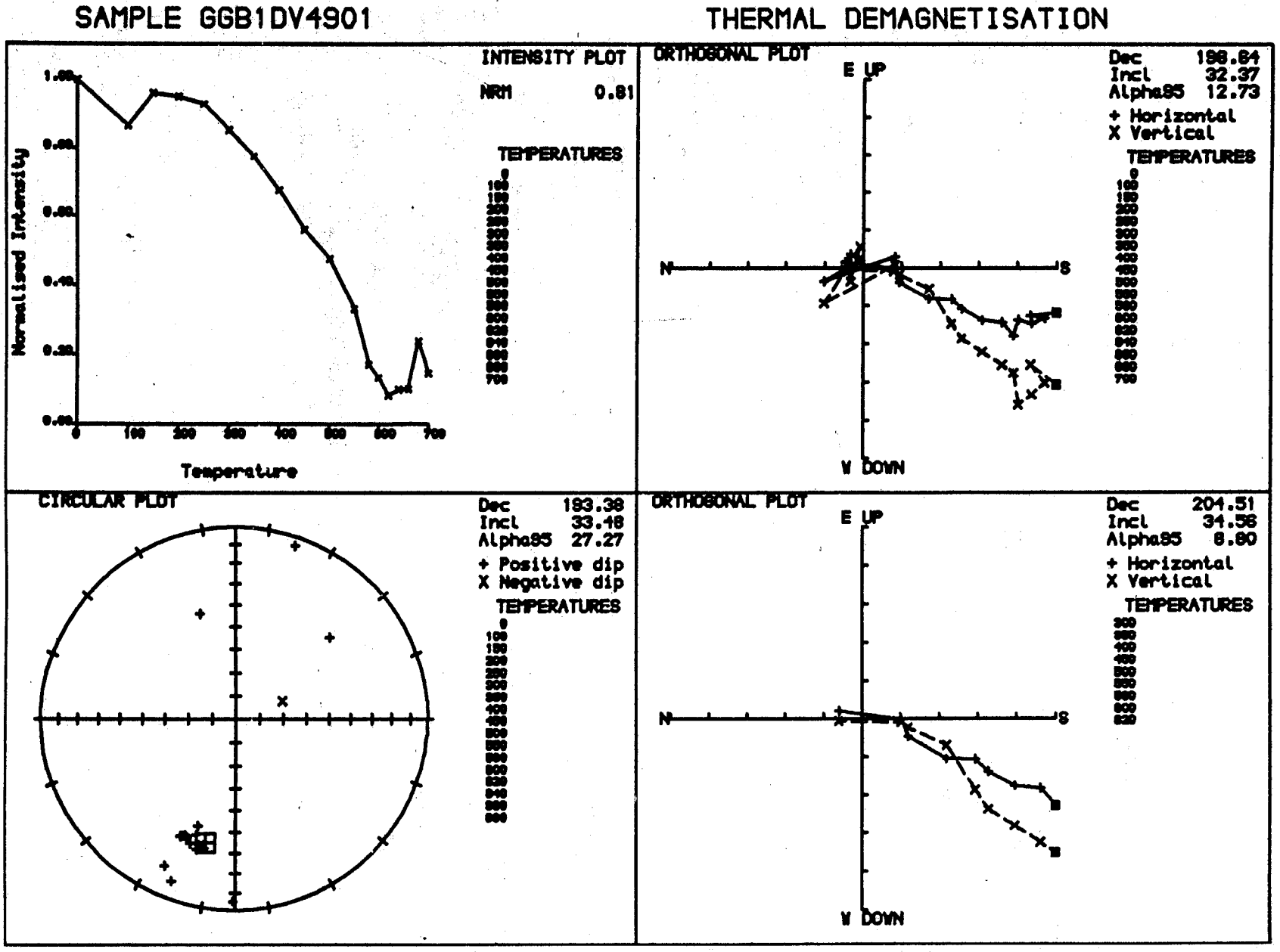
SAMPLE GGB1DV4901
THERMAL DEMAGNETISATION
INTENSITY PLOT
NRM 0.81
TEMPERATURES
Normalised Intensity
Temperature
ORTHOGONAL PLOT
E UP
N
S
W DOWN
Dec 198.64
Incl 32.37
Alpha95 12.73
+ Horizontal
X Vertical
TEMPERATURES
CIRCULAR PLOT
Dec 193.38
Incl 33.48
Alpha95 27.27
+ Positive dip
X Negative dip
TEMPERATURES
ORTHOGONAL PLOT
E UP
N
S
W DOWN
Dec 204.51
Incl 34.56
Alpha95 8.80
+ Horizontal
X Vertical
TEMPERATURES

Figure 3.9c.

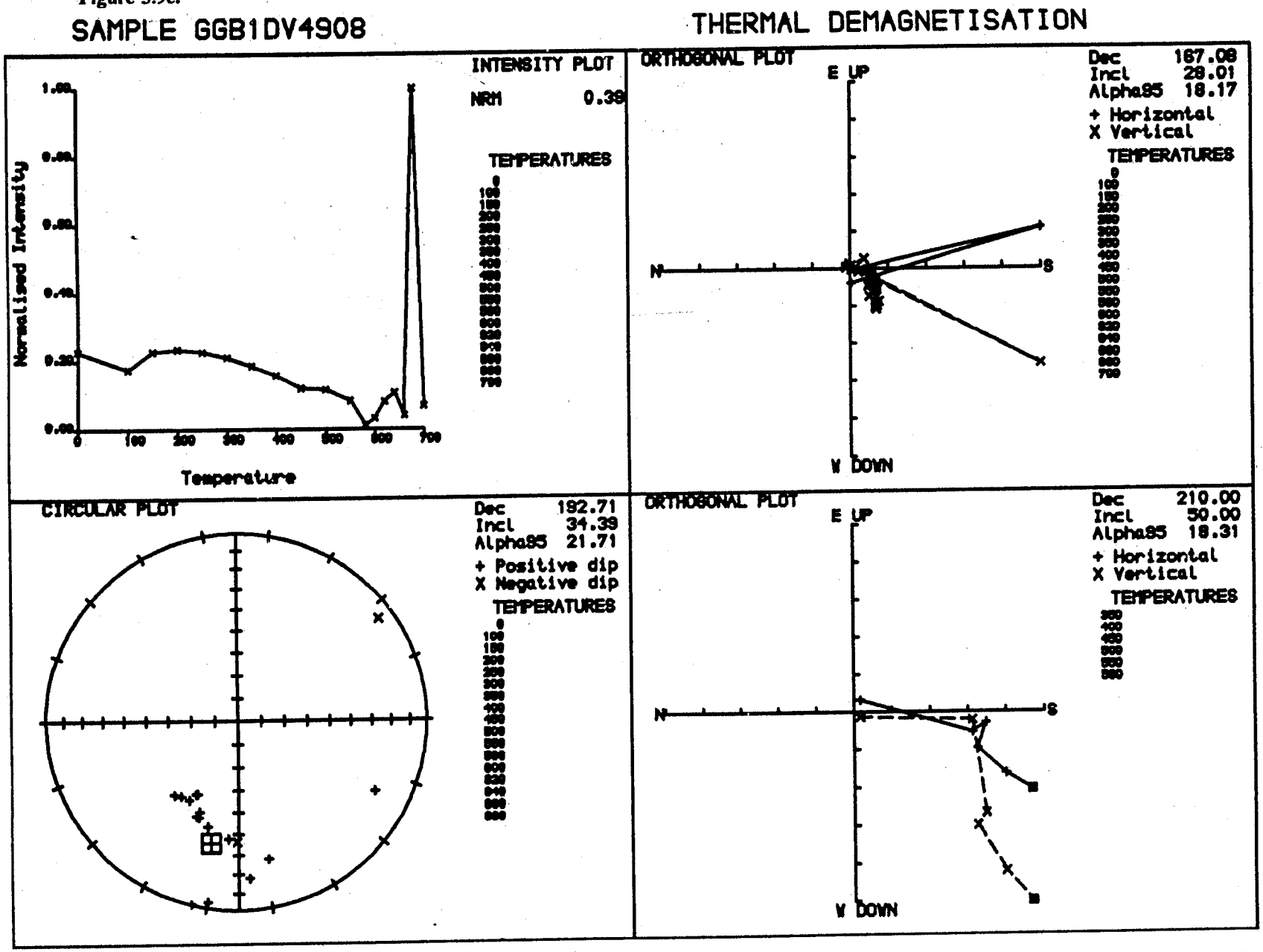
SAMPLE GGB1DV4908
THERMAL DEMAGNETISATION
INTENSITY PLOT
NRM 0.39
TEMPERATURES
Normalised Intensity
Temperature
ORTHOGONAL PLOT
E UP
N
S
W DOWN
Dec 167.08
Incl 28.01
Alpha95 18.17
+ Horizontal
X Vertical
TEMPERATURES
CIRCULAR PLOT
Dec 192.71
Incl 34.39
Alpha95 21.71
+ Positive dip
X Negative dip
TEMPERATURES
ORTHOGONAL PLOT
E UP
N
S
W DOWN
Dec 210.00
Incl 50.00
Alpha95 18.31
+ Horizontal
X Vertical
TEMPERATURES

Figure 3.9d.

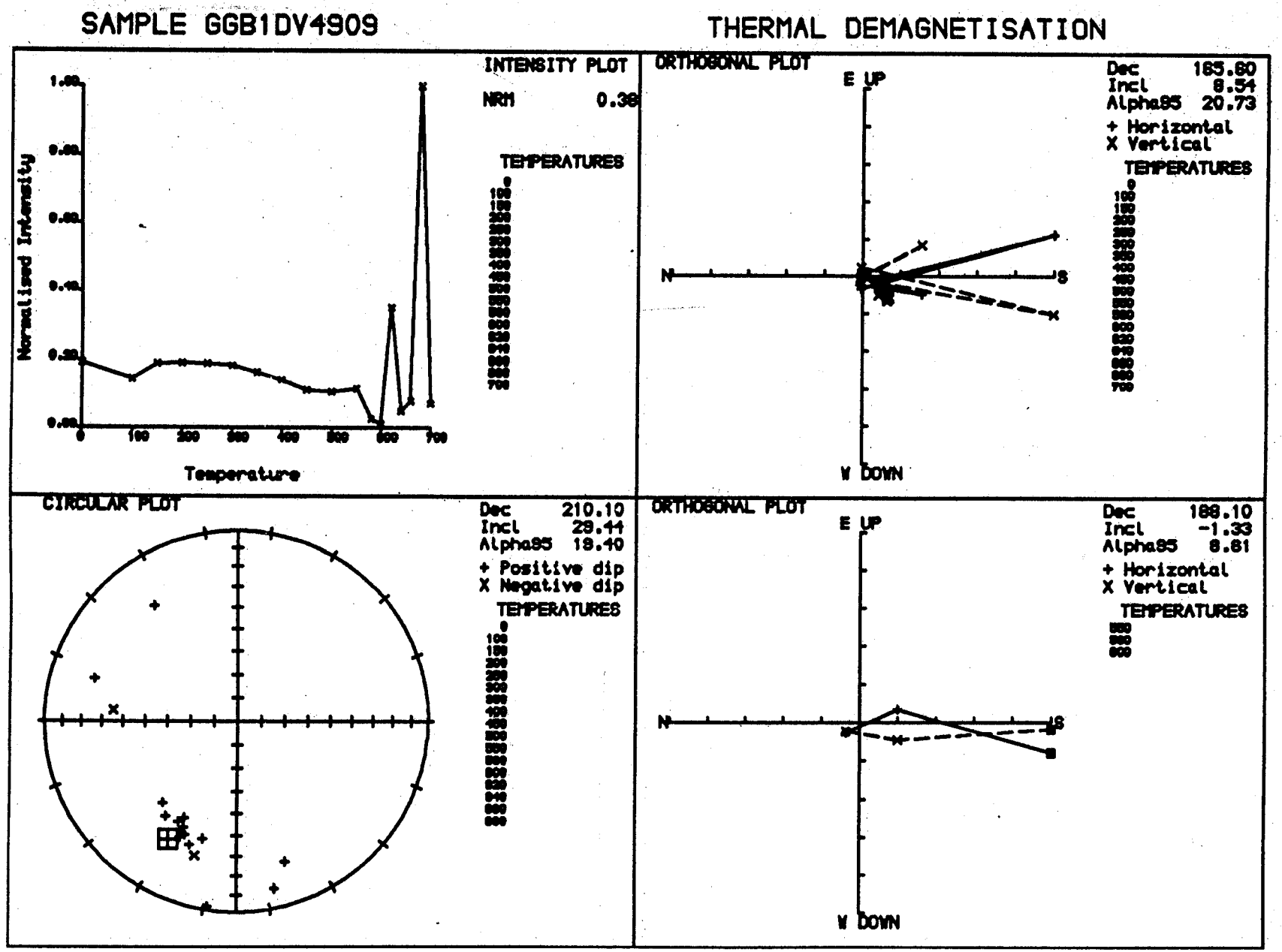
SAMPLE GGB1DV4909
THERMAL DEMAGNETISATION
INTENSITY PLOT
NRM 0.38
TEMPERATURES
Normalised Intensity
Temperature
ORTHOGONAL PLOT
E UP
N
S
W DOWN
Dec 165.60
Incl 8.54
Alpha95 20.73
+ Horizontal
X Vertical
TEMPERATURES
CIRCULAR PLOT
Dec 210.10
Incl 29.44
Alpha95 18.40
+ Positive dip
X Negative dip
TEMPERATURES
ORTHOGONAL PLOT
E UP
N
S
W DOWN
Dec 188.10
Incl -1.33
Alpha95 8.81
+ Horizontal
X Vertical
TEMPERATURES

Figure 3.9e.

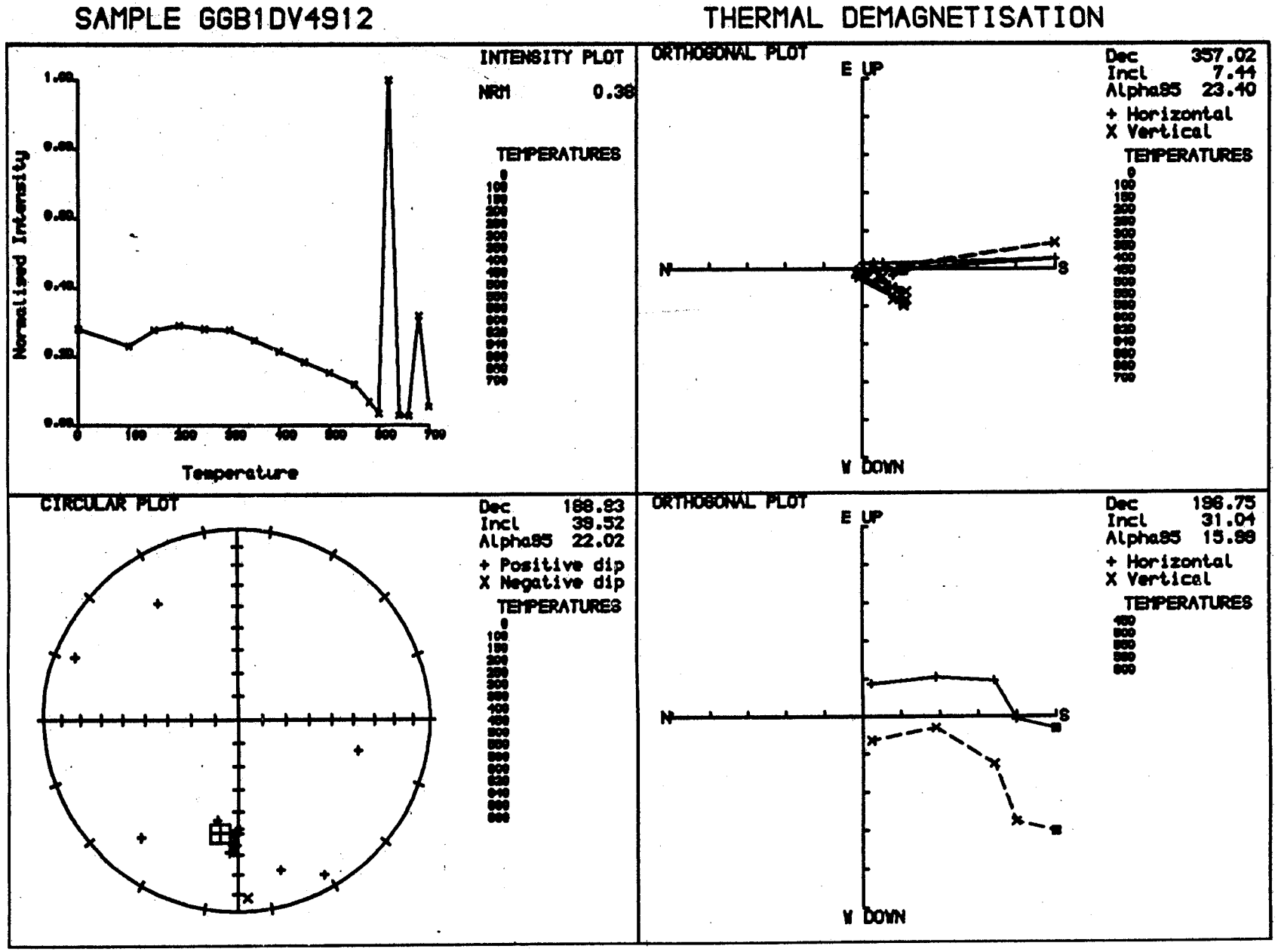
SAMPLE GGB1DV4912
THERMAL DEMAGNETISATION
INTENSITY PLOT
NRM 0.36
TEMPERATURES
Normalised Intensity
Temperature
ORTHOGONAL PLOT
E UP
N
S
W DOWN
Dec 357.02
Incl 7.44
Alpha95 23.40
+ Horizontal
X Vertical
TEMPERATURES
CIRCULAR PLOT
Dec 188.83
Incl 39.52
Alpha95 22.02
+ Positive dip
X Negative dip
TEMPERATURES
ORTHOGONAL PLOT
E UP
N
S
W DOWN
Dec 196.75
Incl 31.04
Alpha95 15.88
+ Horizontal
X Vertical
TEMPERATURES

Figure 3.9f.

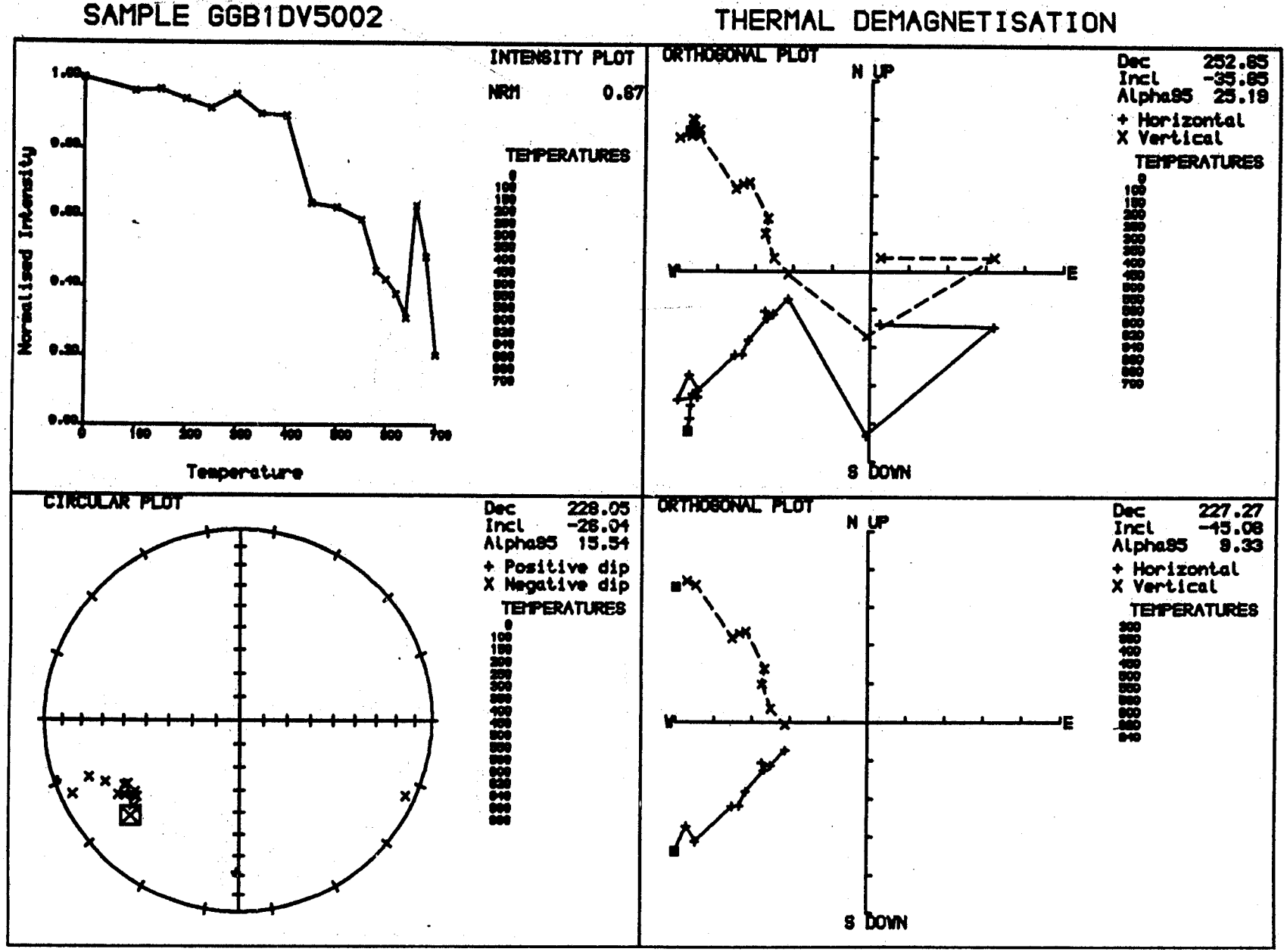
SAMPLE GGB1DV5002
THERMAL DEMAGNETISATION
INTENSITY PLOT
NRM 0.67
TEMPERATURES
Normalised Intensity
Temperature
ORTHOGONAL PLOT
N UP
W
E
S DOWN
Dec 252.65
Incl -35.85
Alpha95 25.19
+ Horizontal
X Vertical
TEMPERATURES
CIRCULAR PLOT
Dec 228.05
Incl -26.04
Alpha95 15.54
+ Positive dip
X Negative dip
TEMPERATURES
ORTHOGONAL PLOT
N UP
W
E
S DOWN
Dec 227.27
Incl -45.08
Alpha95 9.33
+ Horizontal
X Vertical
TEMPERATURES

Figure 3.9g.

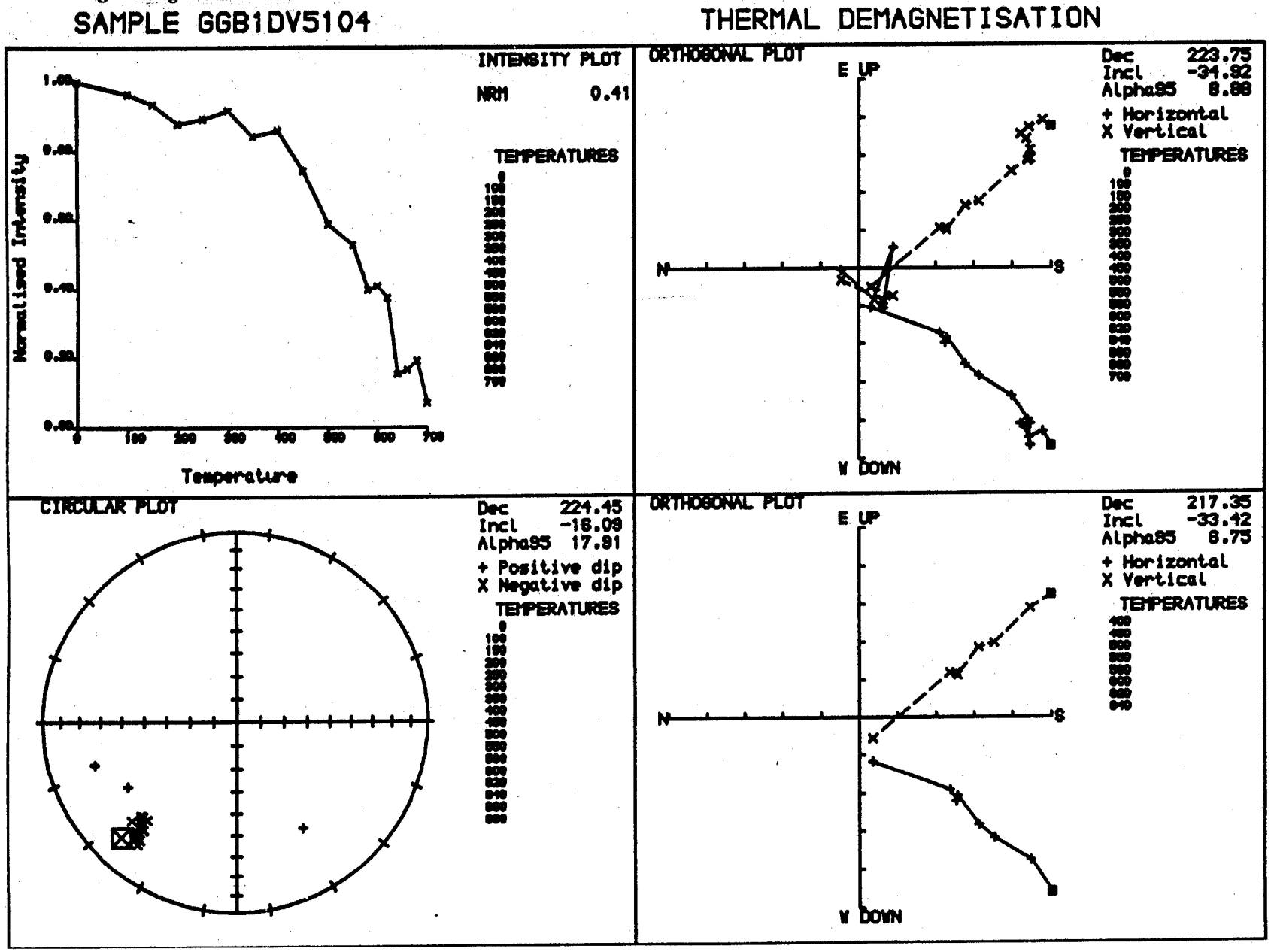
SAMPLE GGB1DV5104
THERMAL DEMAGNETISATION
INTENSITY PLOT
NRM 0.41
TEMPERATURES
Normalised Intensity
Temperature
ORTHOGONAL PLOT
E UP
N
S
W DOWN
Dec 223.75
Incl -34.82
Alpha95 8.88
+ Horizontal
X Vertical
TEMPERATURES
CIRCULAR PLOT
Dec 224.45
Incl -16.09
Alpha95 17.91
+ Positive dip
X Negative dip
TEMPERATURES
ORTHOGONAL PLOT
E UP
N
S
W DOWN
Dec 217.35
Incl -33.42
Alpha95 8.75
+ Horizontal
X Vertical
TEMPERATURES

Figure 3.9h.

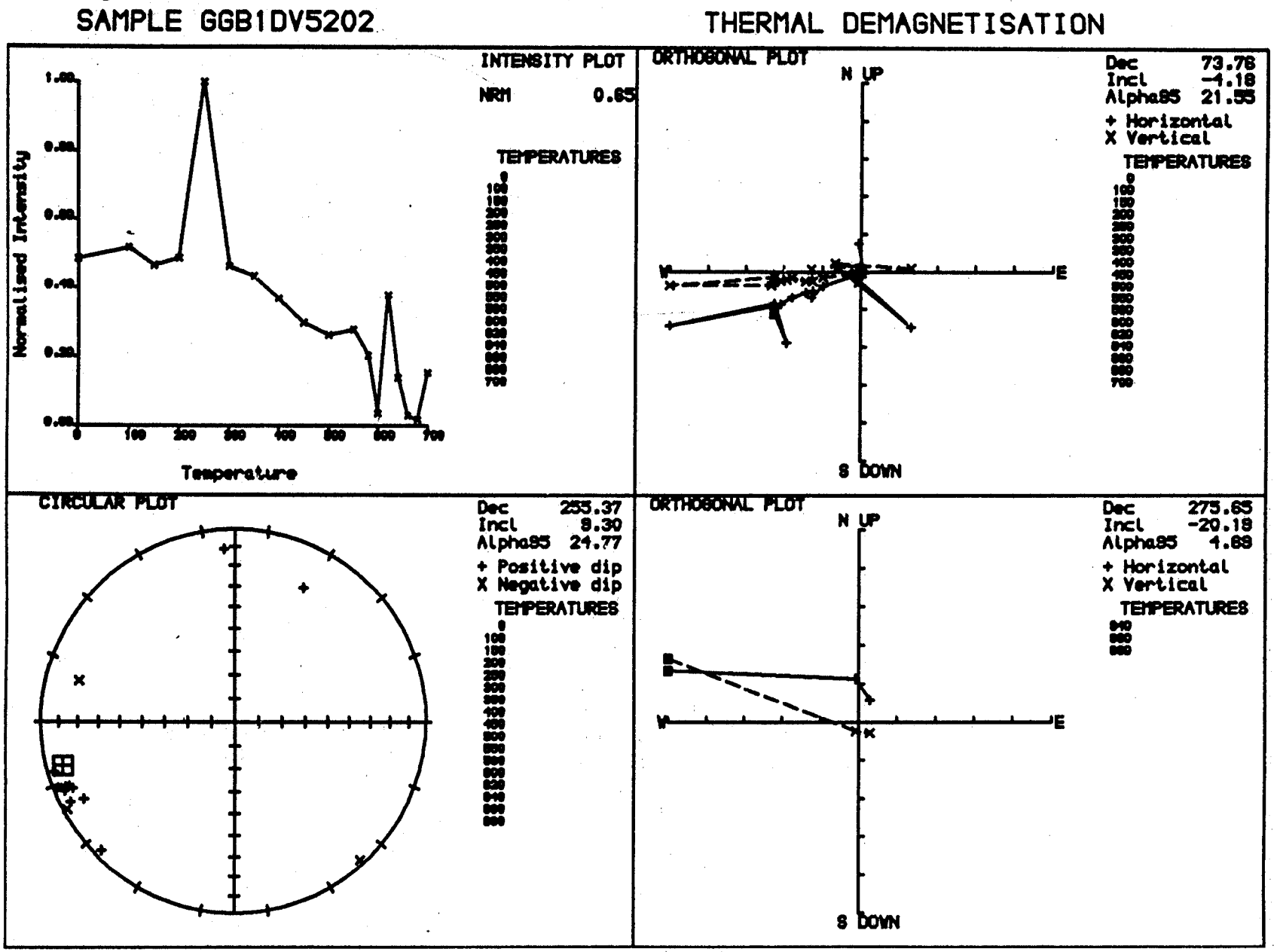
SAMPLE GGB1DV5202
THERMAL DEMAGNETISATION
INTENSITY PLOT
NRM 0.65
TEMPERATURES
Normalised Intensity
Temperature
ORTHOGONAL PLOT
N UP
S DOWN
W
E
Dec 73.78
Incl -4.18
Alpha95 21.55
+ Horizontal
X Vertical
TEMPERATURES
CIRCULAR PLOT
Dec 255.37
Incl 9.30
Alpha95 24.77
+ Positive dip
X Negative dip
TEMPERATURES
ORTHOGONAL PLOT
N UP
S DOWN
W
E
Dec 275.65
Incl -20.18
Alpha95 4.69
+ Horizontal
X Vertical
TEMPERATURES

Figure 3.9i.

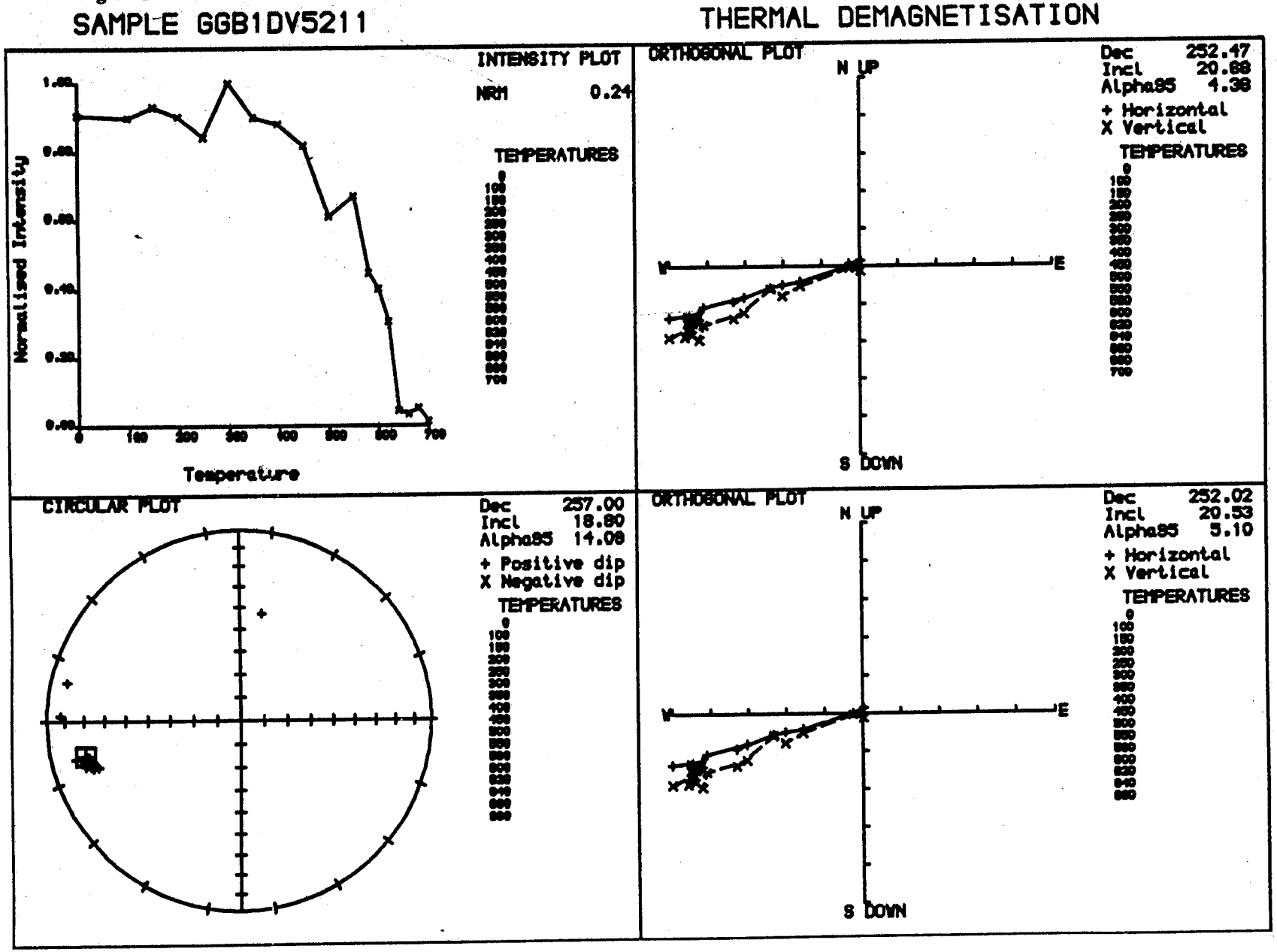
SAMPLE GGB1DV5211
THERMAL DEMAGNETISATION
INTENSITY PLOT
NRM 0.24
TEMPERATURES
Normalised Intensity
Temperature
ORTHOGONAL PLOT
N UP
W
E
S DOWN
Dec 252.47
Incl 20.68
Alpha95 4.38
+ Horizontal
X Vertical
TEMPERATURES
CIRCULAR PLOT
Dec 257.00
Incl 18.80
Alpha95 14.08
+ Positive dip
X Negative dip
TEMPERATURES
ORTHOGONAL PLOT
N UP
W
E
S DOWN
Dec 252.02
Incl 20.53
Alpha95 5.10
+ Horizontal
X Vertical
TEMPERATURES

Table 3.2 The expected reversed palaeomagnetic directions for Group 1 (Brecon/Abergavenny area), Group 2 (Carmarthen area) and Group 3 (southern Pembrokeshire) from 310 My up to present. The pole positions are from Piper (1987).

Age (My)	GROUP 1 Dec/Inc	GROUP 2 Dec/Inc	GROUP 3 Dec/Inc
310	187.0/17.4	185.8/17.6	185.3/18.0
300	188.2/07.5	187.1/07.7	186.6/08.2
290	189.2/-02.8	188.2/-02.5	187.8/-02.0
280	189.0/-06.7	188.0/-06.5	187.5/-06.0
270	193.4/-08.2	192.5/-07.8	192.0/-07.3
260	192.2/-13.6	191.2/-13.3	190.8/-12.8
250	191.6/-19.2	190.7/-18.9	190.3/-18.4
240	194.7/-27.5	193.8/-27.2	193.4/-26.7
230	204.0/-42.2	203.3/-41.7	203.0/-41.3
220	208.6/-46.7	207.9/-46.2	207.6/-45.8
210	206.6/-61.7	206.3/-61.4	206.0/-61.1
200	217.9/-69.0	217.7/-68.7	217.5/-68.4
190	213.4/-65.1	213.1/-64.7	212.8/-64.4
180	205.6/-59.5	205.2/-59.2	204.9/-58.9
170	210.7/-55.3	210.2/-54.9	209.9/-54.5
160	203.2/-55.2	202.7/-54.9	202.4/-54.6
150	197.0/-57.6	196.6/-57.4	196.3/-57.1
140	193.1/-60.1	192.7/-60.0	192.5/-59.7
130	181.6/-60.8	181.3/-60.8	181.2/-60.6
120	180.2/-60.8	179.9/-60.8	179.8/-60.6
110	181.6/-60.8	181.3/-60.8	181.2/-60.6
100	180.0/-54.3	179.5/-54.3	179.3/-54.1
90	181.2/-51.1	180.6/-51.1	180.4/-50.9
80	134.0/-55.5	183.6/-55.5	183.4/-55.3
70	187.7/-54.1	187.2/-54.0	187.0/-53.8
60	187.6/-57.2	187.2/-57.1	187.0/-56.9
50	187.0/-57.0	186.6/-56.9	186.4/-56.7
40	184.8/-59.4	184.5/-59.4	184.3/-59.2
30	176.4/-63.6	176.2/-63.6	176.1/-63.5
20	177.6/-65.0	177.4/-65.1	177.4/-64.9
10	178.4/-65.7	178.3/-65.7	178.3/-65.6

supports previous results reported by Creer in 1957 (for comparison, see Table 3.3).

Each figure usually consists of 4 graphs. They are the intensity plot in the top left, the circular plot in the bottom left, the orthogonal plot for all data points in the top right and if NOT all data points are used to determine the palaeomagnetic directions for the specimens, the bottom right shows the orthogonal plot by which the direction is calculated and listed in APPENDIX A. The intensity plot is used especially in judging the originality of the higher temperature components. If there is a significant increase in intensi-

ties, the component should be suspected. This can be seen in the orthogonal plot that the data points would direct not toward the origin of the graph or become unstable. The circular plots are mostly used only qualitatively (except if no linear segments on the orthogonal plots can be defined due to disintegration of the specimen during thermal treatment or the intensities resists to change with the temperature); sometimes the last data point is not plotted on the graph and possibly due to plotting errors.

In some specimens a linear segment generally below 300°C can be defined quite easily (see Table A-1a or Table A-1b, APPENDIX A). However, these directions (Lower Temperature (LT) components) are not consistent within sites and only those near the present Earth's field direction can be regarded as viscous magnetisations. No interpretation will be given concerning these components in this thesis. Hence, the term of "two components" usually refers to Permo-Carboniferous (PC) and Higher Temperature (HT) components unless otherwise stated. In this case, only the HT component is plotted in the bottom right of the figure. Single component specimens are those interpreted as Permo-Carboniferous overprints.

A detail explanation of Figures 3.7 to 3.9

Figure 3.7a to Figure 3.7i are representative for the specimens from Group 1. Almost 60 % out of 142 specimens show two components (PC and HT). Figures 3.7b, 3.7d, 3.7e, 3.7f, 3.7h and 3.7i are the examples of these specimens (cf Figure 3.13). Generally, the NRM intensities from this group decrease smoothly with temperatures. This shows that the HT component is real.

Figure 3.8a to Figure 3.8i are from Group 2. All show a single component (PC). Two (GGB1DV4402 and GGB1DV4403) out of 220 specimens (less than 1% of the population from this group) have HT component. The in situ and tilt-corrected both HT components disagree with any palaeomagnetic direction expected for this area (see Table A-1 and Table 3.2). The intensity plots generally are decreasing smoothly although for some specimens the intensities increase slightly after 600°C is reached (see Figures 3.8a, 3.8b, and 3.8f). Other specimens increase significantly before 700°C; for example, Figures 3.8h and 3.8i.

Mostly specimens from Group 3 show erratic intensity plots after 600°C (see Figure 3.9a to Figure 3.9i). There are only 2 out of 91 specimens (about 2%) from Group 3 which possibly show two component behaviour (see Figure 3.9d, (GGB1DV4909) and Figure 3.9h (GGB1DV5202)). A southwest-positive component of specimen GGB1DV4909 is subtracted to recover a south-shallow component. The substantial increase in the intensities above 600°C in this specimen, however, shows that a magnetic phase is being generated in the furnace above this temperature. It is possible therefore, that the south-shallow component is an artefact. The other specimen (GGB1DV5202) has westerly declination and negative inclination before and after bedding correction (this direction is not sensitive to bedding correction). This HT component is determined by three data points; at 640°, 660° and 680°. Since the position of the second point is much closer to the third than to the first, this component is apparently being determined by the first and second points only and in this case the direction is highly suspect.

In short, the HT components from Group 2 and 3 may be generated inside the oven during the thermal treatment for two main reasons. Firstly, the HT component specimens are only found in a very small percentage (about 1% and 2%; cf almost 60% for Group 1). Secondly, the directions are different to any palaeomagnetic directions expected for the area (see Table 3.2).

Figure 3.10 shows the in situ mean declinations from horizontal or southward dipping beds (which comprise the majority of the sites) of each locality. The numbers near the end of the arrows are the inclinations (which vary according to the dips of the beds since the remanence predates full folding). It can be clearly seen that the western sites have the more westerly directions. Any differences caused by orientation procedures of the samples from these sites can be ruled out. Almost half of the samples collected from Group 3 (southern Pembrokeshire) were oriented using both a magnetic and sun compass. Figure 3.11 shows a histogram of the differences in orientation of the samples using the magnetic and sun compass. A good agreement is shown which is mostly within a degree or two.

The maximum difference between the mean declination of the sites from Group 1 and Group 3 is more than 50° (see Table 3.3). There are two principal ways in which the difference in the mean declinations from the two groups may be explained:

1. Southern Pembrokeshire has been rotated by 40° clockwise (McClelland-Brown, 1983) or

Table 3.3 Palaeomagnetic results (in situ). Loc = locality, Lat = latitude, Lon = longitude, Tilt/Dir = bedding correction (Dir = direction of the tilt), Dec = declination, Inc = inclination, N(n) = number of specimens accepted (demagnetised), a-95 = the cone of 95% confidence, k = Fisher precision parameter.

Site	Loc	Lat(°)	Long(°)	Tilt(°)	Dir(°)	Dec(°)	Inc(°)	a95(°)	N(n)	k
GGB1DV01	2	51.81	356.85	15	165	193.2	-0.1	11.0	5(5)	48
GGB1DV02	2	51.81	356.85	15	177	192.8	10.8	15.1	5(5)	26
GGB1DV03	2	51.81	356.85	17	136	211.7	8.5	15.4	5(5)	25
GGB1DV04	2	51.81	356.85	19	160	14.1	-3.9	13.7	5(5)	32
GGB1DV05	9	51.76	355.59	18	167	210.4	-1.4	2.9	5(5)	701
GGB1DV06	9	51.76	355.59	10	190	208.8	1.2	4.1	5(5)	341
GGB1DV07	9	51.76	355.59	48	168	209.4	3.6	6.8	5(5)	126
GGB1DV08	9	51.76	355.59	40	340	206.8	-12.8	3.9	5(5)	380
GGB1DV09	9	51.76	355.59	64	333	203.1	-5.0	5.7	3(3)	476
GGB1DV10	9	51.76	355.59	45	349	208.6	-3.4	3.4	5(5)	512
GGB1DV12	9	51.76	355.59	65	342	197.7	-2.9	4.2	5(5)	327
GGB1DV14	2	51.81	356.85	15	165	190.5	-2.7	10.7	4(5)	74
GGB1DV15	2	51.81	356.85	15	165	190.9	6.7	11.5	5(5)	45
GGB1DV16	2	51.81	356.85	15	165	183.2	-3.2	9.8	5(5)	62
GGB1DV17	2	51.81	356.85	15	165	184.2	2.5	5.6	5(5)	186
GGB1DV18	2	51.81	356.85	15	165	186.4	-0.3	17.9	5(5)	19
GGB1DV19	2	51.81	356.85	15	165	187.2	-3.6	9.3	5(5)	68
GGB1DV20	2	51.81	356.85	15	165	190.4	-9.1	6.9	4(4)	177
GGB1DV21	6	51.82	355.72	19	132	186.4	-6.5	4.7	11(11)	93
GGB1DV22	6	51.82	355.72	24	123	188.5	-8.1	4.7	9(9)	123
GGB1DV23	6	51.82	355.72	14	140	192.1	-15.5	3.2	7(7)	361
GGB1DV24a	5	51.82	355.84	55	160	201.6	3.3	-	1(1)	-
GGB1DV24b	5	51.82	355.84	57	168	195.0	7.9	6.1	6(6)	121
GGB1DV24c	5	51.82	355.84	62	162	194.1	16.6	5.1	10(10)	90
GGB1DV25	5	51.82	355.84	62	162	196.2	10.2	4.6	10(10)	111
GGB1DV26	9	51.76	355.59	54	330	206.9	-13.5	3.8	8(15)	212
GGB1DV27	9	51.76	355.59	25	166	208.0	-6.3	2.2	18(18)	248
GGB1DV28	9	51.76	355.59	14	180	215.5	-4.8	23.4	2(3)	116
GGB1DV29	9	51.76	355.59	0	0	204.2	-10.5	8.8	7(7)	47
GGB1DV30	9	51.76	355.59	4	251	202.7	-3.0	3.2	8(8)	294
GGB1DV31	9	51.76	355.59	0	0	203.5	-2.9	5.6	7(7)	118
GGB1DV32	9	51.76	355.59	0	0	198.6	-3.4	7.4	7(7)	66
GGB1DV33	9	51.76	355.59	41	327	209.1	-18.4	5.6	5(5)	190
GGB1DV34	9	51.76	355.59	32	324	210.0	-12.8	5.2	9(9)	98
GGB1DV35	3	51.80	356.64	4	130	187.7	1.3	5.1	13(13)	67
GGB1DV36	3	51.80	356.64	4	130	190.5	-4.7	10.7	6(6)	40
GGB1DV37	1	51.92	356.97	40	140	189.2	17.1	6.8	13(13)	38
GGB1DV38	1	51.92	356.97	40	140	189.0	9.1	11.5	8(8)	24
GGB1DV39	1	51.92	356.97	2	275	190.3	-5.6	4.2	20(20)	62
GGB1DV40	4	51.88	356.51	6	130	190.7	2.4	10.9	7(7)	31
GGB1DV41	4	51.88	356.51	6	130	187.7	-11.2	6.3	12(12)	48
GGB1DV42	4	51.88	356.51	6	130	191.6	-14.0	12.1	8(9)	22
GGB1DV43	8	51.78	355.55	39	172	214.0	2.7	5.7	18(19)	38
GGB1DV44	8	51.78	355.55	39	172	206.6	5.4	5.5	6(6)	147
GGB1DV45	7	51.80	355.60	38	192	201.5	-7.4	7.0	5(5)	121
GGB1DV46	7	51.80	355.60	38	192	197.5	-3.7	4.1	9(9)	155
GGB1DV47	7	51.80	355.60	38	170	200.2	-13.3	4.5	15(15)	74
GGB1DV48	10	51.64	355.20	90	004	200.3	-52.2	7.3	24(24)	17
GGB1DV49	10	51.64	355.15	82	006	208.8	-38.6	4.1	19(19)	67
GGB1DV50	10	51.63	355.14	42	184	216.6	-6.3	5.5	13(13)	57
GGB1DV51	11	51.65	354.95	96	184	230.2	45.2	3.1	18(18)	129
GGB1DV52	11	51.66	354.94	52	022	244.8	-17.2	6.2	16(17)	35

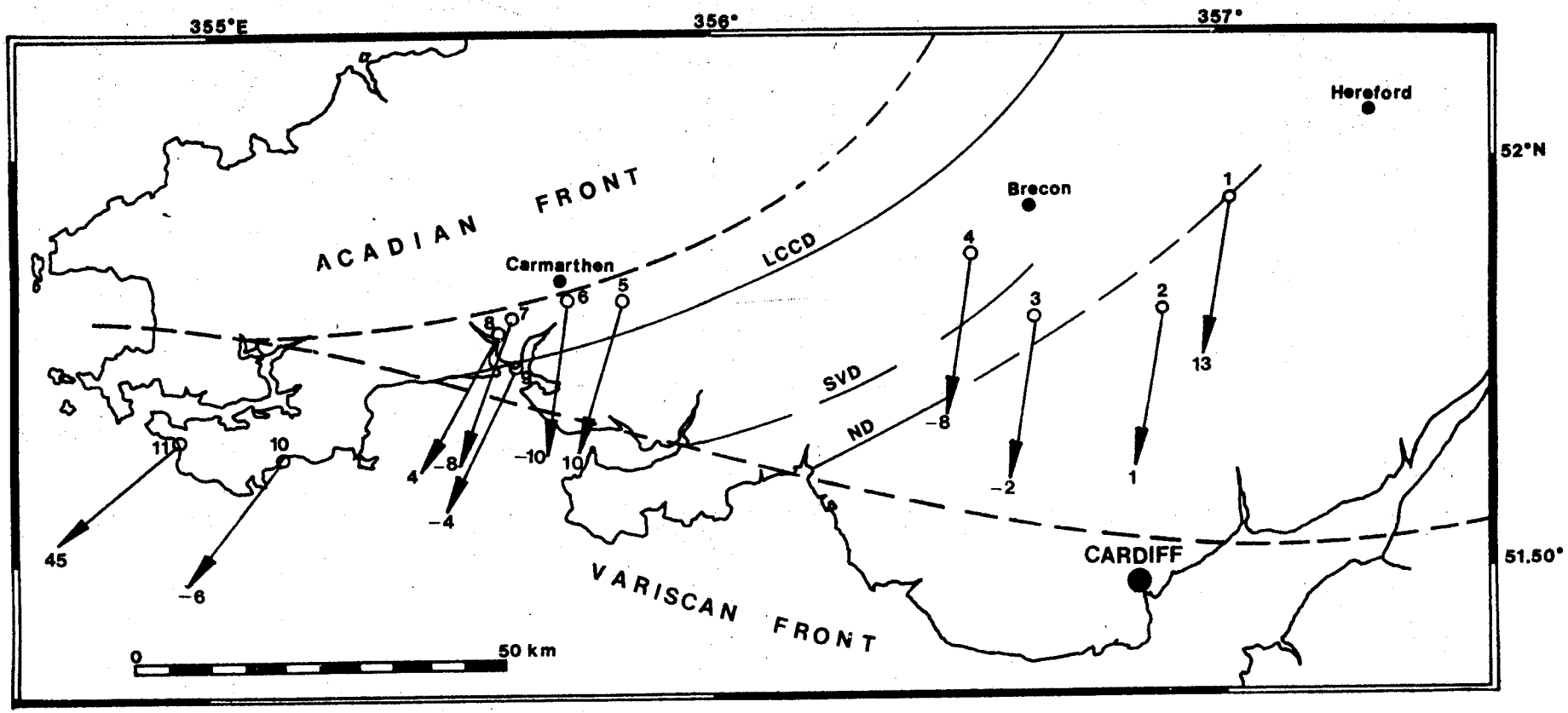

Figure 3.10 In situ mean directions from horizontal or southward dipping beds at each locality. The arrow are pointing to the declination directions and the number near the head of the arrow represents the inclination (see caption Figure 3.2 for locality information).

2. The folding in the west has had the resultant effect of rotating the palaeomagnetic directions due, for example, to incomplete plunge corrections.

Table 3.3 lists the in situ site mean directions. Twelve out of 453 specimens were excluded from the site mean calculation. Only site GGB1DV04 (from one block sample) has normal polarity. It is possible that there was some mistake during orientation for this block sample either during sample collection or re-orientation before drilling in the laboratory. Sites GGB1DV01 to GGB1DV03 and sites GGB1DV14 to GGB1DV20 (these sites were sampled to verify the polarity of site GGB1DV04) all from the same location have reversed polarity. In calculating the mean for this locality the GGB1DV04 site mean direction is converted to a reversed direction by adding 180° to its declination and giving an opposite sign to its inclination. It can therefore be concluded that the polarity of the secondary magnetisation found in the South Wales red beds is overwhelmingly reversed.

3.4.2 Fold Test

The FOLDCONT program has been used in this study and the output of the program can be seen in the APPENDIX C and APPENDIX B. The program calculates the mean direction associated with the highest k value (also see CHAPTER 2). There are two ways of finding the highest k; by unfolding both limbs of a fold simultaneously (usual fold test) or separately in a stepwise manner. The latter always gives higher k values than the former method. However, the mean direction derived from this k value does not necessarily represent the palaeomagnetic field at the time when the

Figure 3.12a Fold test without plunge correction (see Table B-1, APPENDIX B).
(a) samples from Llanthony (Locality 1)
(b) samples from LLanstephan (Locality 9)

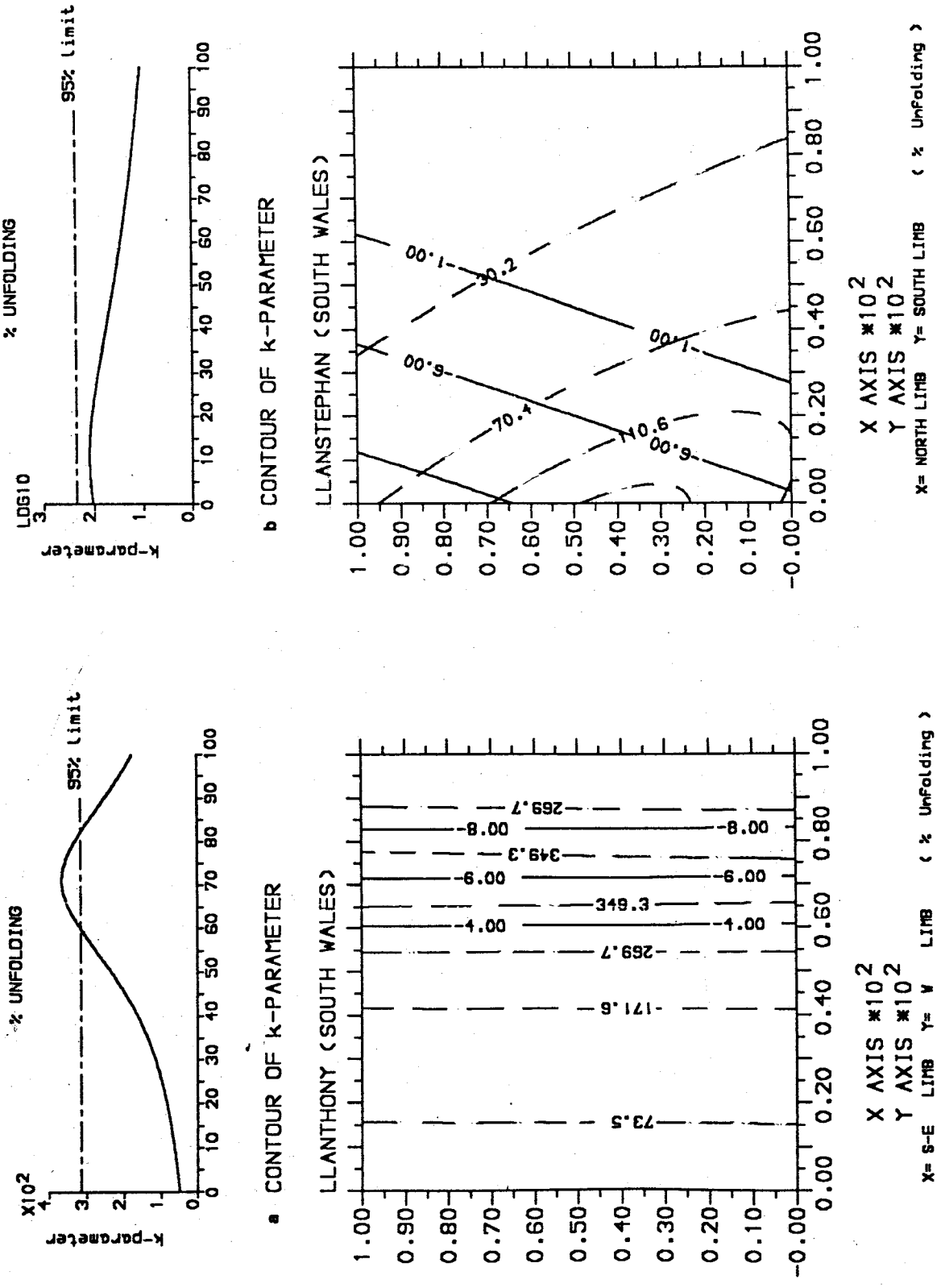

Figure 3.12b Fold test without plunge correction (see Table B-1, APPENDIX B).
(a) samples from Freshwater East (Locality 10)
(b) samples from Freshwater West (Locality 11)

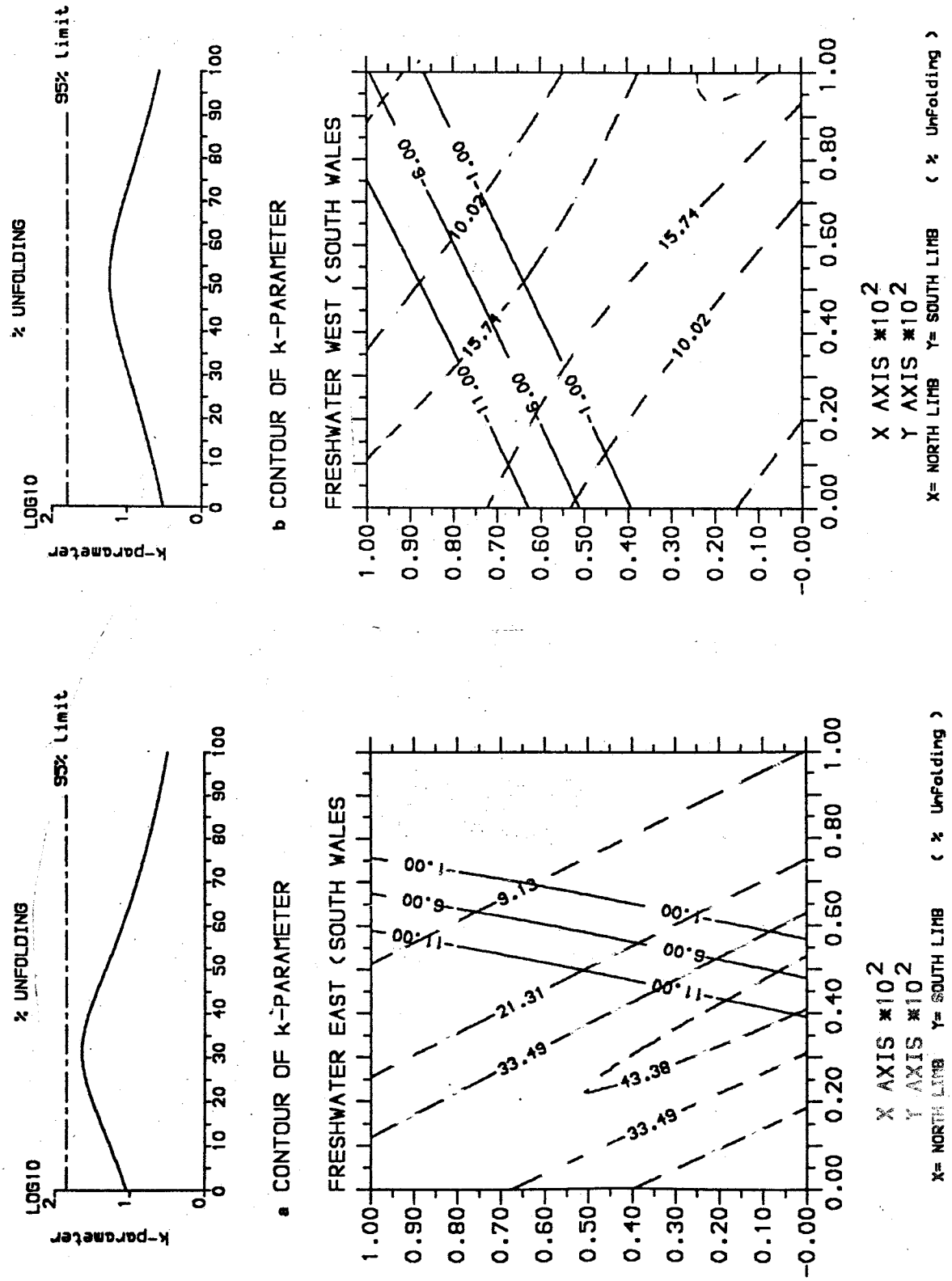

Figure 3.12c Fold test without plunge correction (see Table B-1, APPENDIX B).
(a) Orielton anticline (sites GGB1DV48, GGB1DV49 and GGB1DV51)
(b) Orielton syncline (sites GGB1DV50 and GGB1DV52)
See text and Figure 3.3b.

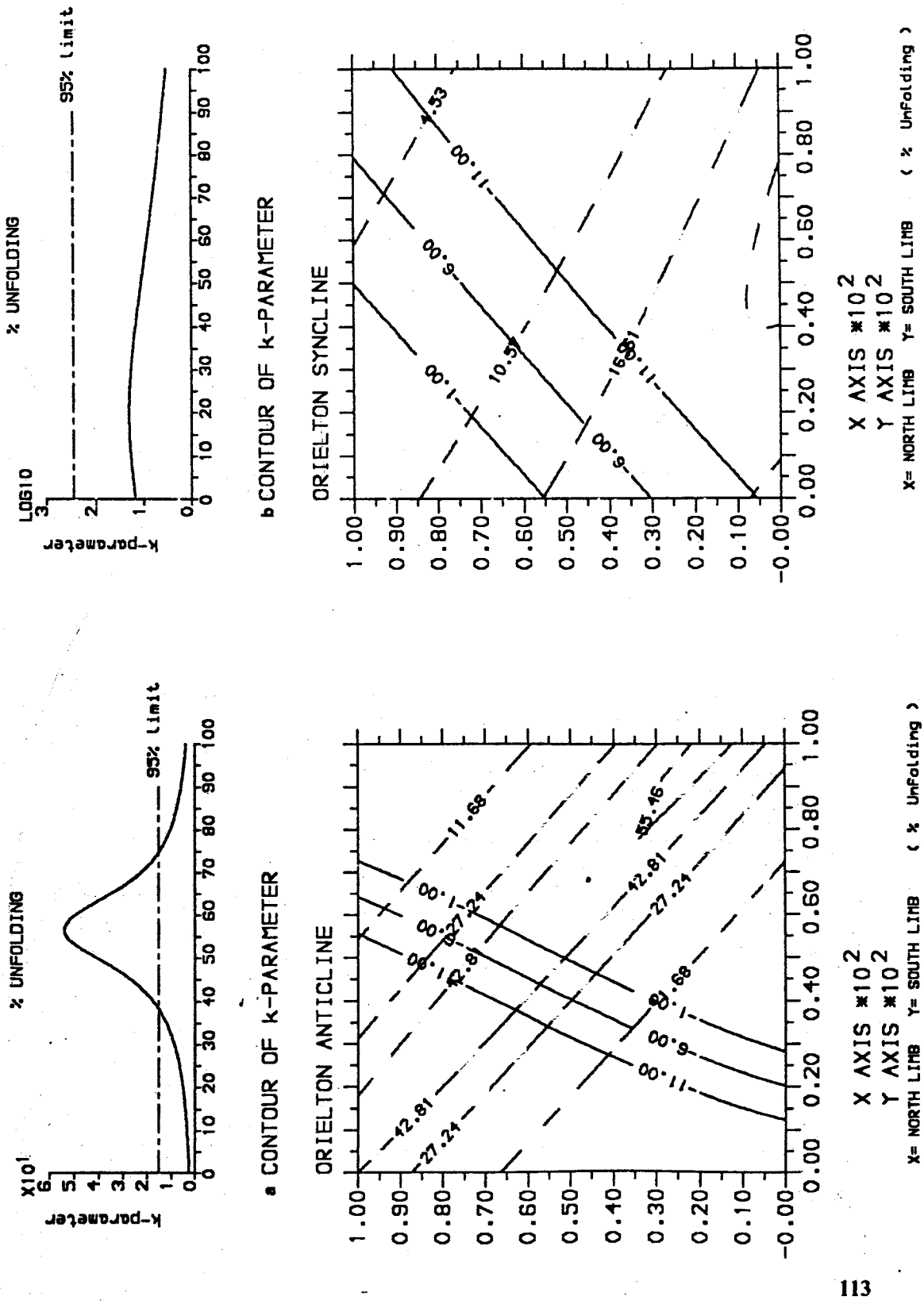

cluded that the plunge already existed when the magnetisation occurred or the direction of the plunge is to the east instead of to the west (in other words, the plunge is steeper than it is today). If the latter is correct, there would be slight increase in k values and the inclination line of -6° would be shifted toward the peak of the contour. This means that the derived inclination (using the new method) would be even closer to the expected inclination and the inclination derived from the one dimensional would deviate more from the expected direction (the inclination becomes more positive). However, since there is still no k values exceed the k_2, the former interpretation (the plunge was already existed) is considered as a valid one.

The inclinations from both methods are within the range of -11° to -1°. This fold test also indicates that the fold has been tightened-up slightly since the acquisition of the secondary magnetisation, possibly the southern limb has been folded more than the northern limb.

The results from Llanstephan yield a fold test which is close to negative (10% percent before fully folded) whereas the results from Llanthony can be close to positive (17% percent folded). There are two explanations for this. First, it is likely that the age of the deformation in Llanthony (Locality 1) is post-Variscan age, or at least younger than at Locality 9, since the age of the deformation in Llanstephan (Locality 9) is generally agreed to be of Variscan age. It has been assumed implicitly that the remagnetisation at both localities occurred at the same time (during the Variscan orogeny) and there is a geological evidence that the climax of the Variscan deformation moved northward with time (Owen, 1974). Second, the alpha-95 circles from both localities do not overlap. Hence the two palaeofield directions

possibly represent the Earth's magnetic fields at different times. The first explanation is likely to be more acceptable.

Figure 3.12b(a) shows the results of the fold test on specimens from Freshwater East. The fold is called the Freshwater East anticline (see Figure 3.3b). The northern limb is almost twice as steep as the southern limb. The southern limb has to be left in situ and the northern limb has to be unfolded by 46% to achieve an optimum grouping (Dec. = 204.8° and Inc. = -7.1° with alpha-95 = 6.4°). This implies that the fold was more symmetric when the rock acquired the secondary magnetisation. If both limbs are unfolded simultaneously, they have to be unfolded by 32% (Dec. = 205.9° and Inc. = -18.8° with alpha-95 = 6.5°). The inclination derived by this method lies outside the expected range (-11° to -1°). No k values, however, are greater than k_2 (= 70.8). If the in situ palaeomagnetic directions are corrected for the plunges of the fold (North limb = 08°/297° and South limb = 14°/095°), there is a decrease in k values and still below the k_2 (= 49.8; it is different to the previous one because two different plunges act on the same fold). However, if both plunges are in the same amount and direction (14°/095°), the k values are significantly increased and some of them exceed the k_2 (= 70.8; it is the same as without a plunge correction because all palaeomagnetic vector involved are corrected by the same plunge correction). If this plunge correction (14°/095°) is the correct one for both limbs of the anticline, the palaeomagnetic directions may then be considered as the valid ones. In this case, the northern and southern limbs have to be unfolded by 50% and 6% respectively to achieve the optimum grouping (Dec. = 211.5° and Inc. = -1.1° with alpha-95 = 4.0°). By applying the plunge correction to the east for both limbs, the palaeomagnetic directions are ro-

tated about 7° to the west. This direction cannot be rejected at 95% level of confidence because its k passes the McElhinny test. And if the amount of the plunge is increased progressively at that direction, the k-parameter reaches in a maximum at 24°. On the contrary, the k-parameter decreases if the plunge direction is to the west (297°). For this reason, the apparent direction for the northern limb of the Freshwater East anticline is to the east as for the other limb. Palaeomagnetically, this discrepancy could be explained by the possibility that the plunge was steeper when the rocks were remagnetised than it is today and the direction of the plunge is still to the west. In applying the plunge correction, a negative plunge should then be given. In this thesis, however, the amount and direction of the plunge of the northern limb of this anticline is assumed to be the same as the other limb so that there is no need to convert the sign of the plunge. It is probable that this problem cannot be analysed further here because the remanence in red beds has been shown to be rotated by the effects of penetrative deformation (Stamatakos, 1991) with the least rotated vectors coming from those sites with lowest internal strain. Hence a complete analysis would also require the measurement and analysis of strain indicators at each of the palaeomagnetic sites.

Figure 3.12b(b) shows the results of the fold test on the specimens from the Castlemartin Corse anticline, Freshwater West (Locality 11). The northern limb is less steep than the southern limb (see Figure 3.3b). There are two peaks on the contour plot; at the top left and at the bottom right. The former is close to the expected direction. If the expected inclination is not introduced in the fold test, the fold test would pick the latter peak because it is higher than the former. The mean direction derived from this k is close

to palaeofield during Lower Devonian times which is not correct (see APPENDIX B, the mean direction derived from "k maximum"). If both limbs are unfolded simultaneously, they have to be unfolded by 52% (Dec.=228.6° and Inc.=4.1° with alpha-95=14.1°). If the limbs are unfolded separately, the northern limb has to be unfolded by 20% and the southern limb by 72% (Dec.=229.3° and Inc.=-10.9° with alpha-95=13.9°) to achieve optimum grouping. The inclinations derived from the usual method are out of the (-11°, -1°) range. No k values exceed the k_2 (=62.7). However, if the in situ palaeomagnetic directions are corrected for the plunge (North limb=07°/275° and South limb=15°/310°), some k values become higher than the k_2 (=60.8). The palaeomagnetic direction derived from the fold test is Dec.=233.8° and Inc.=-10.8° with alpha-95=6.9°. It is about 20° more westerly than the mean direction for the Freshwater East anticline (Dec.=211.5°).

The directions derived from the fold tests at these two localities (Table 3.4b) support the observation that the declinations are more westerly for the more westerly sites (cf Locality 10 (Dec=211.5°) and Locality 11 (Dec=233.8°)) and therefore these results provide some support for McClelland-Brown's hypothesis that the southern Pembrokeshire area has been rotated. As mentioned earlier that in this thesis, a fold test is performed on each possible fold configuration in this area (see section 3.2.2) and the results of these fold tests should not contradict each other. The Freshwater East anticline (Locality 10) and the Castlemartin Corse anticline (Locality 11) can be considered as an anticline and a syncline (the Orielton anticline and the Orielton syncline). The following are the results of the fold tests on these folds.

Figure 3.12c(a) shows the results of the fold test for the anticlinal structure. In the contour plot, the inclination lines do not form straight lines and they are slightly bent. No explanation is given in this thesis concerning the unusual form of these inclination lines. The palaeomagnetic result is Dec. = 204.1° and Inc. = -1.1° with alpha-95 = 5.8°. This derivation is justifiable because its k is much higher than the k_2 (see APPENDIX B). Since there is a decrease in k-values (but some are still higher than its k_2) after applying the plunge correction (North limb = 08°/297° and South limb = 15°/310°), it may then be possible either that the plunge probably existed when the rocks acquired their magnetism or the plunge direction at the northern limb is not to the west (but 14° to the east; see also the fold test result for the Freshwater East anticline above). The latter gives the more westerly mean palaeomagnetic direction (Dec. = 214.4° and Inc. = -2.3° with alpha-95 = 6.2) with its k value comparable to the k without the plunge correction and higher than its k_2.

Figure 3.12c(b) shows the results of the fold test for the syncline. No k values exceed the k_2. The plunge correction (North limb = 14°/095° and South limb = 07°/275°) increases the k values slightly but all are still below the k_2. Both with and without the plunge correction the data yield a mean palaeomagnetic direction which is more westerly than the mean direction for the anticline.

In short, assessment of the results from the Orielton anticline and syncline indicates that southern Pembrokeshire has been rotated (relative to Locality 1, Llanthony) with a condition that the plunge direction at the northern limb of the Freshwater East is to the east (palaeomagnetically). This is in

Table 3.4a Usual fold test results (in situ).

Locality	Unfolded	Dec(°)/Inc(°)	a95	N(site)	k
Llanthony (1)	72%	188.6/ -6.1	2.2	3	366 p
Llanstephan (9)	10%	206.8/ -5.2	1.9	11	124
Freshwater E. (10)	32%	205.9/-18.8	6.5	3	44
Freshwater W. (11)	52%	228.6/ 4.1	14.1	2	17
Anticline (10+11)	56%	204.1/ 1.1	5.8	3	54 p
Syncline (10+11)	20%	230.4/-11.7	12.9	2	20

Note : p = passes the McElhinny test at 95% level of confidence.

the same sense as McClelland-Brown suggested in 1983, although the amount is varied according to how westerly the locations are. These results are over-shadowed by a larger rotation for more westerly sites and they could be refined further if the sites being analysed are not so widely separated.

It must be stressed that the mean direction derived from the highest k value does not necessarily represents the palaeomagnetic field at that time of ac-

quisition. Hence, the configuration of the fold should not be determined from this k parameter alone but instead by reference to the palaeofield direction predicted from the apparent polar wander path from adjoining stable crustal areas. From this study it can be seen clearly that the k value from this new method is usually close to the highest k. The following (Table 3.4a and 3.4b) is summary of the results of the fold tests based on unfolding both limbs of the fold simultaneously. The directions derived by this one dimensional method are not necessarily in agreement with the predicted palaeofield during Variscan times (~ 280 My when the inclinations must lie within a range of -11° and -1°, see Table 3.2). This can be refined further by the application of the two dimensional fold test (see Table 3.5).

The plunge correction is seen to play an important role in a fold test. The direction of the plunge or even the amount of the plunge itself will determine the outcome of the fold test. It would be interesting to see whether a very accurate plunge measurement is necessary in order to perform the fold test properly or whether the fold test can provide the information about the plunge of a fold more accurately than any other method. These results show that there is a clear relationship between the plunge correction and the McElhinny test. For example, before applying the plunge correction, no k values exceed the k_2 during partial tilt correction on the specimens from the Freshwater East and the Castlemartin Corse anticlines. However, after applying the appropriate plunge correction to each anticline, some k values are higher than the k_2 (the test becomes positive). This means that the plunge can also cause the McElhinny test to be negative. It may then be possible to use the McElhinny test for estimating the plunge of a fold in certain circumstances.

Table 3.4b Usual fold test results (plunge-corrected).

Locality	Unfolded	Dec(°)/Inc(°)	a95	N(site)	k
Llanstephan (9)	10%	206.3/ -8.6	1.9	11	121 f
Freshwater E. (10)	36%	201.9/-14.9	7.9	3	30 f
Freshwater E. (10)*	34%	212.1/-13.4	4.1	3	107
Freshwater W. (11)	54%	233.0/ 1.1	7.1	2	65
Anticline (10+11)	56%	204.3/ 0.8	10.6	3	17
Anticline (10+11)*	54%	214.4/ 1.8	6.1	3	49
Syncline (10+11)	30%	229.1/-10.8	11.6	2	25 f

Note : * the plunge correction for the northern limb is 14°/095° instead of 08°/297°.
f = fails the McElhinny test.

Relating the stage of unfolding at which the palaeomagnetic direction mostly grouped to the geometry of the folds in southern Pembrokeshire at the time of acquisition has been tried by previous workers. For example, Chamalaun (1964) suggested that the limbs being investigated made an angle of 30° with the horizontal when the remagnetisation occurred. McClelland-Brown (1983) suggested that the plunge varied during the evo-

lution the folds she investigated. However, these authors considered the structures as one major anticline which is not correct. In this study, the effort is restricted to the configuration of the fold based on the new fold test (two dimensional) results when the remagnetisation occurred. Table 3.5 lists the predicted attitude of the limbs of each fold from this study relative to the horizontal when the remagnetisation occurred by assuming that the inclination of the palaeomagnetic direction at that time was within the range of (-11° and -1°).

Table 3.5 The attitude of the limbs relative to the horizontal based on the two dimensional fold test (plunge-corrected except for Llanstephan). All k values pass the McElhinny test with the exception the k for the syncline and Llanstephan.

Locality	N(°)/S(°) dipping	Dec(°)/Inc(°)	k
Llanthony (1)	~ 0/11	188.6/-6.1	368
Llanstephan (9)	~ 49/16	207.3/-9.1	151
Freshwater E. (10)*	~ 43/41	211.5/-1.1	113
Freshwater W. (11)	~ 38/31	233.8/-10.8	71
Anticline (10+11)*	~ 43/44	214.4/-1.4	49
Syncline (10+11)	~ 38/31	229.1/-10.8	25

Note : * the plunge correction for the northern limb is 14°/095° instead of 08°/297°.

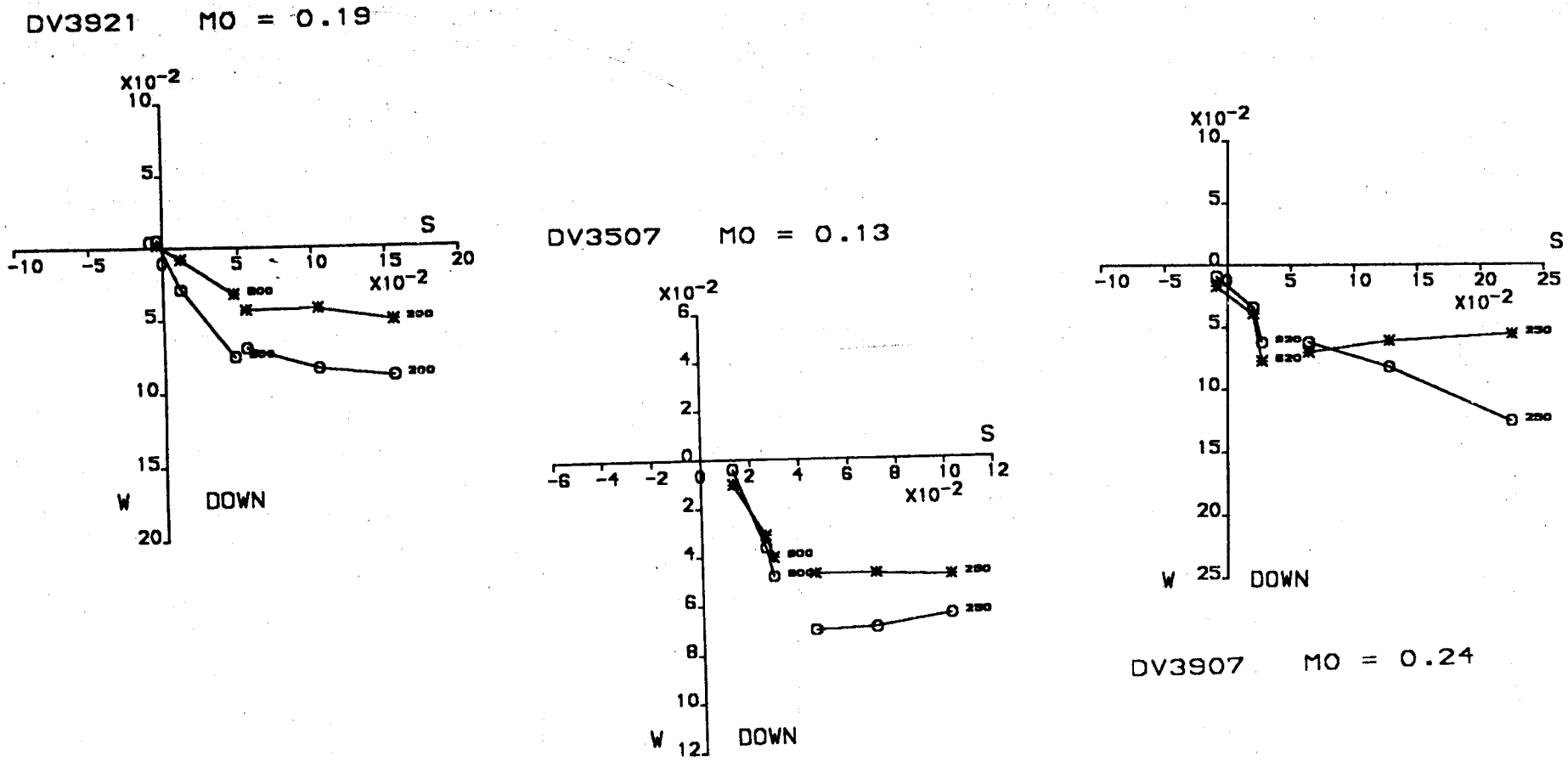

Figure 3.13a Orthogonal plots of specimens showing two components (positive inclinations, downward). The intensity unit is 10E-5 A m^2 / kg. Star symbol is vertical and circle symbol is horizontal.

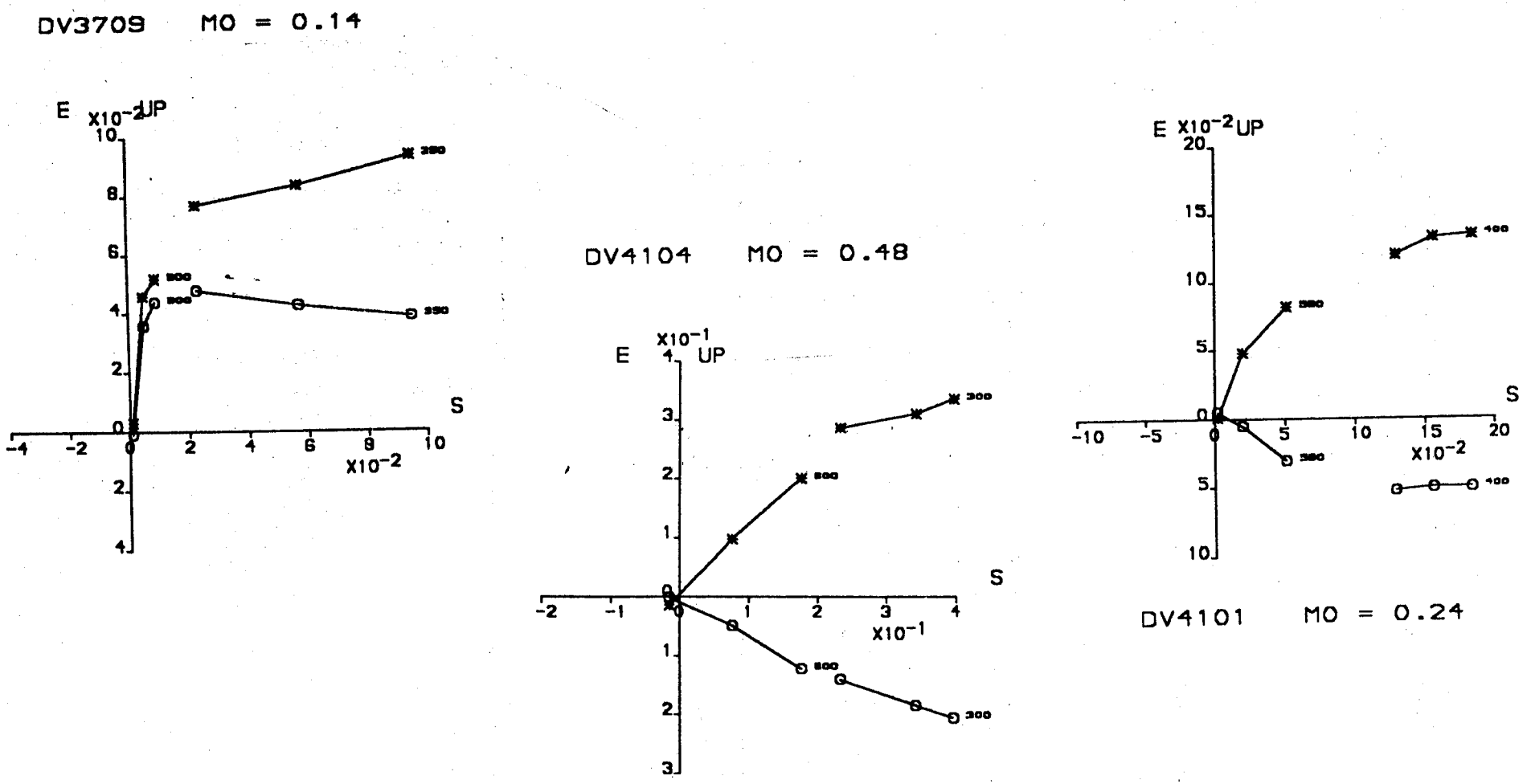

Figure 3.13b Orthogonal plots of specimens showing two components (negative inclinations, upward) (see caption Figure 3.13a).

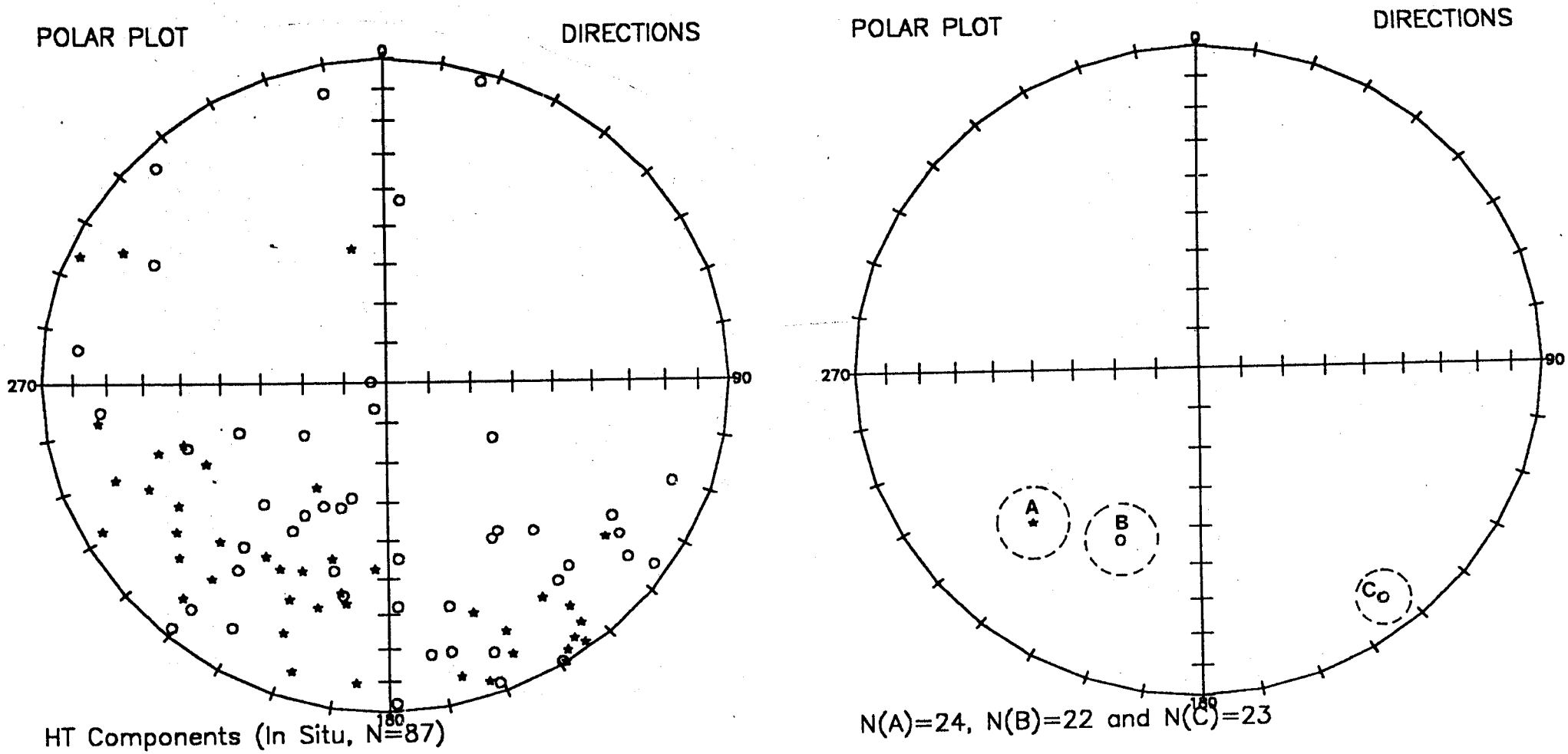

Figure 3.14 Equal area projection (polar) of higher temperature components
(a) specimen level (in situ)
(b) grouped into Category A, B and C (in situ). See text.

Star (circle) symbol = lower (upper) hemisphere.

3.4.3 Non-Permo-Carboniferous Component

Eighty seven specimens (about 19%) showed two component behaviour (Figures 3.13a and 3.13b, only three data points for each component are shown). Figure 3.13a shows some examples of positive inclinations (down) and Figure 3.13b negative inclinations (up). Of these, 18% come from Group 1 (Brecon/Abergavenny area). Group 2 (around Carmarthen) and Group 3 (southern Pembrokeshire) only contribute 0.5% each and are excluded from further discussion. These specimens (almost 60% of specimens from Group 1) are from Locality 1 (Llanthony), Locality 2 (Brynmawr), Locality 3 (Ponstiscill), and Locality 4 (Storey-Arms). The lithology of these rocks is sandstone and they are purple in colour. The formations are Lower Devonian Brownstones except the rock from Ponstiscill which is believed to be Upper Devonian. The higher temperature components from Locality 2 (Brynmawr) are sometimes difficult to isolate from the influence of the Permo-Carboniferous component. The room temperature susceptibility of these specimens seemed to remain constant or showed slight change throughout the demagnetisation process (see Room Temperature Susceptibility Results, Figure 3.19). Figure 3.14 shows the higher temperature components on a stereonet. There are three categories of consistent directions within a site; Category A, B and C.

In situ directions with moderate positive inclinations (downward) and declinations mostly within the SW quadrant fall into Category A and the negative inclinations (upward) within this quadrant belong to Category B. The rest belongs to Category C where their declinations lie mostly within the SE quadrant with negative inclinations (see Table 3.6a, 3.6b and 3.6c).

Table 3.6a Higher temperature components (Category A, N = 24).

SPECIMEN	Dec	Inc	Tilt	Dir	CDec	CInc	a95	Temp. range
GGB1DV0104	196.9	43.3	15	165	191.4	30.1	12.4	450 - 720
GGB1DV0202	203.7	37.5	15	177	199.9	23.9	05.7	625 - 720
GGB1DV0302	228.9	20.5	17	136	222.5	20.4	20.4	550 - 700
GGB1DV1503	225.3	31.9	15	165	218.6	23.7	04.8	550 - 700
GGB1DV1601	196.8	29.3	15	165	193.6	16.3	20.2	600 - 700
GGB1DV1704	244.9	41.6	15	165	232.9	37.4	08.8	625 - 700
GGB1DV1705	294.0	04.0	15	165	292.2	13.3	23.7	600 - 700
GGB1DV1905	209.2	35.5	15	165	203.5	24.2	28.5	500 - 700
GGB1DV3503	203.8	28.8	04	130	201.7	27.6	17.6	580 - 660
GGB1DV3507	252.3	31.1	04	130	250.2	33.2	17.5	600 - 700
GGB1DV3509	233.6	24.8	04	130	231.8	25.6	11.5	600 - 680
GGB1DV3601	202.1	19.1	04	130	200.8	17.9	06.9	550 - 680
GGB1DV3604	183.8	42.4	04	130	181.0	40.0	30.3	620 - 700
GGB1DV3901	192.3	34.8	02	275	193.6	34.5	14.3	640 - 700
GGB1DV3902	190.5	32.2	02	275	191.7	32.0	08.6	640 - 700
GGB1DV3905	214.0	36.5	02	275	215.2	35.5	23.8	580 - 700
GGB1DV3906	220.8	22.4	02	275	221.4	21.2	15.4	620 - 700
GGB1DV3907	252.5	38.1	02	275	253.1	36.3	12.4	600 - 700
GGB1DV3908	222.6	12.4	02	275	222.9	11.1	14.3	580 - 700
GGB1DV3909	238.4	29.5	02	275	239.0	27.9	27.0	600 - 700
GGB1DV3910	212.9	59.0	02	275	215.7	58.0	11.6	580 - 700
GGB1DV3911	298.1	15.4	02	275	297.9	13.6	25.5	620 - 700
GGB1DV3919	261.8	16.5	02	275	261.9	14.5	22.0	600 - 700
GGB1DV3921	245.2	24.8	02	275	245.6	23.1	21.4	580 - 700

Note :
Dec/CDec = in situ/tilt-corrected declination
Inc/CInc = in situ/tilt-corrected inclination
(or see APPENDIX, Table A-1 for more information).

Some specimens with positive inclinations (but negative after applying bedding corrections) in this quadrant are also included into Category C.

Eighteen specimens (including 4 specimens from Group 2 and Group 3) are excluded from site mean calculations. One specimen (GGB1DV4205) was probably wrongly oriented since it belongs to XX components. The rest are excluded due to having shallow inclinations (characteristic of a PC component) or having deviated from any categories defined above.

The in situ mean for Category A direction is Dec/Inc = 226.4°/33.3° and alpha-95 = 11.0°. This corresponds to a pole position situated at Lat/Lon = 9°S/313°E which lies within the APWP for southern Britain (see Piper, 1987). Therefore it is likely that Category A direction is the primary Lower Devonian direction for southern Britain. This direction is an agreement with the high temperature component observed by Channell and others (1991) from the Lower ORS from central South Wales (Dec = 232.2°, Inc = 31.9°). These authors reported that this component predates the Acadian (Middle Devonian) folding. The specimens falling in this category are from Locality 3 (Ponstiscill, 5 specimens), Locality 2 (Brynmawr, 8 specimens) and Locality 1 (Llanthony, 11 specimens). The bedding correction for these sites is almost negligible except for sites from Locality 2. However, the tilt-corrected mean (Dec/Inc = 223.6°/30.1° and alpha-95 = 11.2°) is not significantly different to the in situ mean direction.

The in situ mean B direction (Dec/Inc = 204.0°/-42.2° and alpha-95 = 11.3°) is close to a direction for younger times (~ 230 My, Triassic; see Table 3.2). The specimens falling in this category are mostly from Locality 4 (Storey Arms, 17 specimens). Five specimens are from Locality 2 and 3. As in Category A case, the bedding correction for these sites is also negligible. The tilt-corrected mean is Dec/Inc = 210.3°/-44.5° and alpha-95 = 11.7°.

The interpretation of Category C is still unclear. Category C comprises specimens mostly from Locality 1 (Llanthony, 17 specimens). Locality 3 and Locality 2 only contribute 1 and 5 specimens respectively. The bedding correction for these sites is significant since the strata in Locality 1 dip

Table 3.6b Higher temperature components (Category B, N = 22).

SPECIMEN	Dec	Inc	Tilt	Dir	CDec	CInc	a95	Temp. range
GGB1DV0303	171.5	-17.3	17	136	176.1	-30.7	13.5	600 - 700
GGB1DV1501	272.7	-86.4	15	165	332.9	-73.6	08.0	650 - 700
GGB1DV1702	236.6	-66.6	15	165	272.1	-66.7	17.6	550 - 700
GGB1DV3501	177.8	-32.2	04	130	179.8	-34.8	16.7	450 - 640
GGB1DV3511	220.5	-02.9	04	130	220.7	-02.9	12.4	600 - 700
GGB1DV4001	220.1	-11.5	06	130	221.3	-11.4	09.8	580 - 640
GGB1DV4002	217.7	-29.0	06	130	221.1	-29.1	09.6	580 - 620
GGB1DV4004	211.6	-13.9	06	130	213.1	-14.7	05.0	580 - 680
GGB1DV4007	224.3	-47.3	06	130	230.7	-46.6	27.6	500 - 640
GGB1DV4101	206.2	-55.5	06	130	214.9	-56.4	11.3	550 - 700
GGB1DV4102	196.5	-59.9	06	130	206.7	-61.8	11.2	550 - 700
GGB1DV4103	191.6	-34.2	06	130	195.5	-36.9	10.2	550 - 700
GGB1DV4104	211.0	-51.2	06	130	218.5	-51.8	07.8	600 - 700
GGB1DV4105	165.5	-30.1	06	130	167.8	-34.9	14.8	600 - 700
GGB1DV4107	250.8	-52.5	06	130	256.9	-49.1	14.4	600 - 660
GGB1DV4108	199.7	-56.8	06	130	208.8	-58.5	25.6	600 - 680
GGB1DV4109	251.2	-38.8	06	130	255.0	-35.6	24.6	450 - 680
GGB1DV4201	176.9	-45.2	06	130	181.8	-49.1	08.0	550 - 680
GGB1DV4202	220.2	-35.1	06	130	224.4	-34.9	05.2	580 - 680
GGB1DV4203	211.7	-46.1	06	130	218.0	-46.7	09.2	550 - 660
GGB1DV4207	195.5	-40.3	06	130	200.4	-42.6	02.6	500 - 580
GGB1DV4209	159.6	-13.1	06	130	160.4	-18.3	37.2	550 - 700

moderately to the southeast. However, both the in situ (Dec/Inc = 143.6°/-12.1°) and tilt-corrected (Dec/Inc = 144.5°/-44.9°) mean C directions are different to any expected palaeomagnetic directions for the area for the last 310 My (see Table 3.2 for Group 1). Table 3.6a, 3.6b and 3.6c list the palaeomagnetic directions for higher temperature components for Category A, Category B and Category C respectively.

3.4.4 IRM Results

From IRM (Isothermal Remanent Magnetisation) acquisition experiments, it can be concluded that the magnetic mineral responsible for the remanence is most likely to be haematite (Figures 3.15a, 3.15b and 3.15c). Figures

Figure 3.15a IRM acquisition for samples from Group 1 (Brecon/Abergavenny area). The intensity unit is 10E-5 A m^2 / kg (H = heated, UH = unheated).

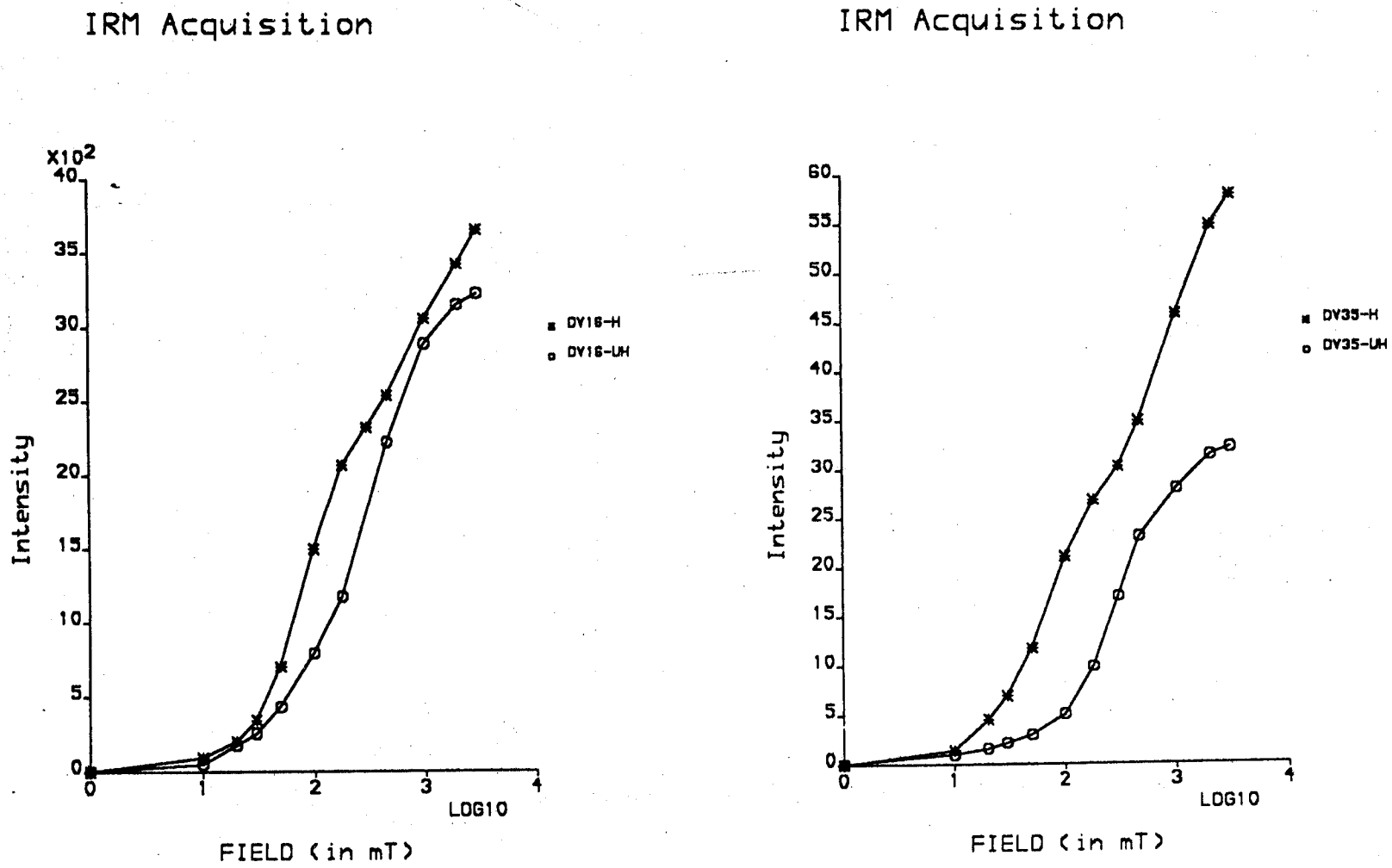

Figure 3.15b IRM acquisition for samples from Group 2 (Carmarthen area) (see caption Figure 3.15a).

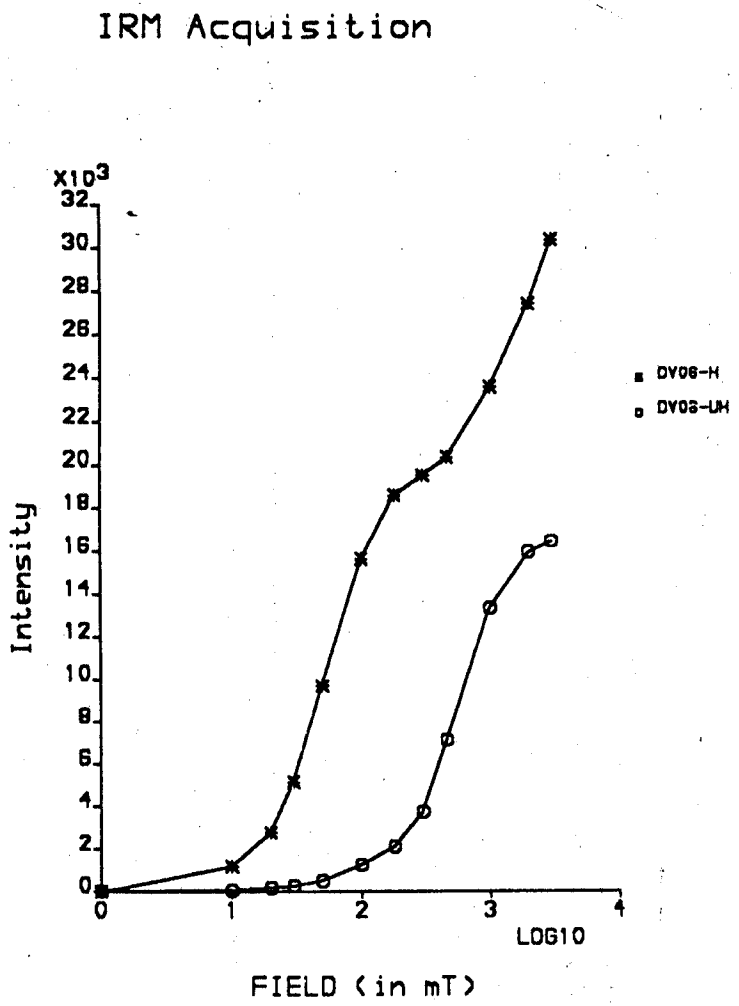

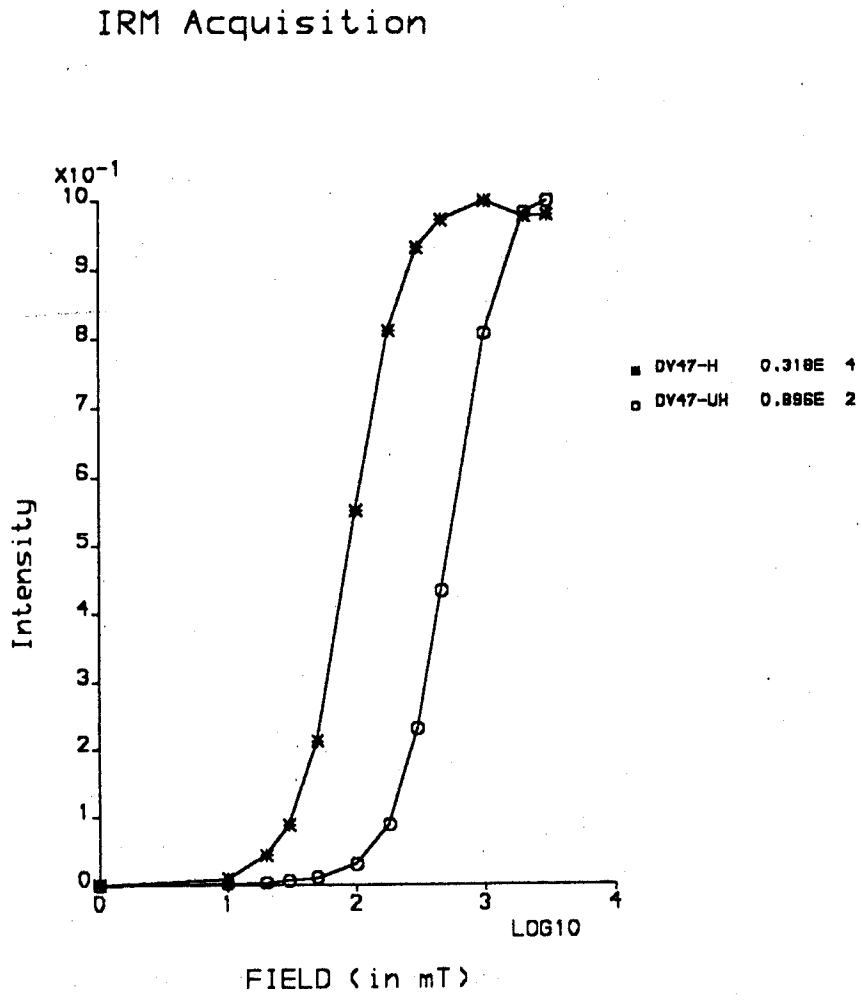

Figure 3.15c IRM acquisition for samples from Group 3 (southern Pembrokeshire) (see caption Figure 3.15a).

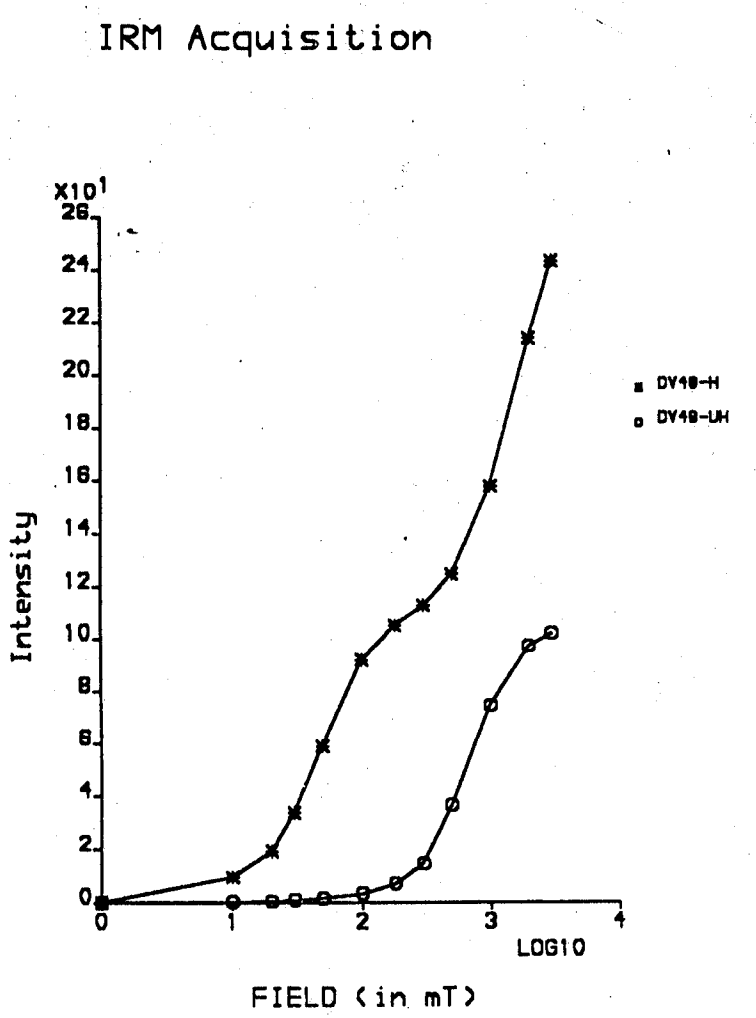

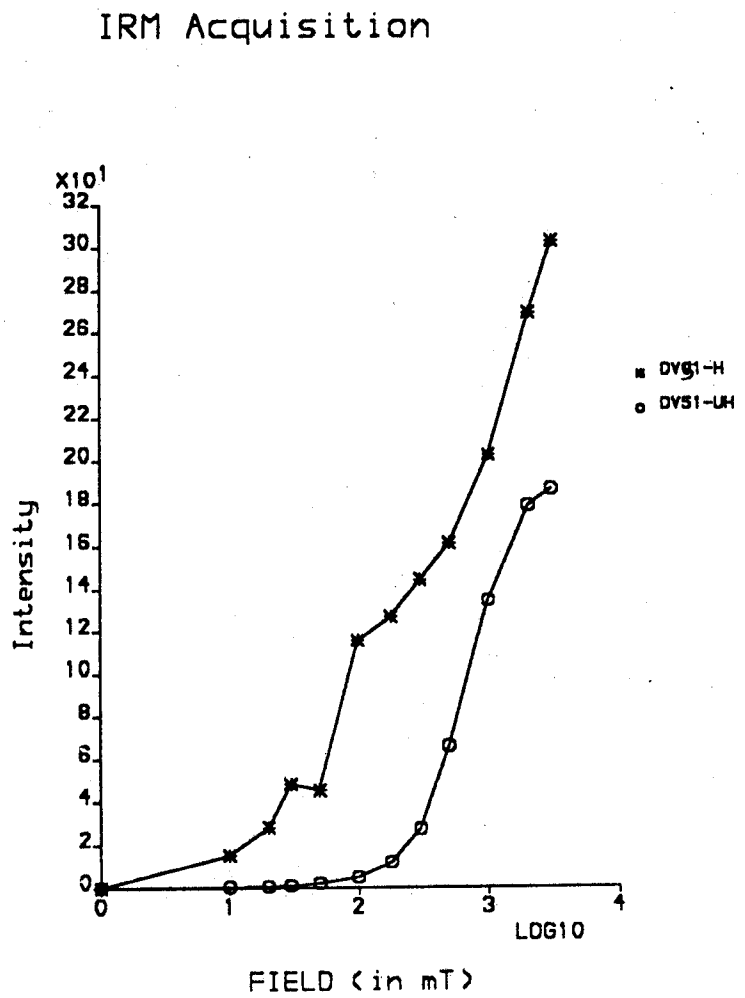

Table 3.6c Higher temperature components (Category C, N = 23).

SPECIMEN	Dec	Inc	Tilt	Dir	CDec	CInc	a95	Temp. range
GGB1DV0301	122.3	-24.0	17	136	119.5	-40.4	21.1	600 - 700
GGB1DV1604	124.8	-19.3	15	165	120.1	-30.4	43.3	450 - 700
GGB1DV1801	118.8	-61.3	15	165	090.2	-68.9	13.9	625 - 700
GGB1DV1903	144.3	02.3	15	165	143.9	-11.7	10.2	450 - 700
GGB1DV1904	147.6	03.4	15	165	147.3	-10.9	08.6	550 - 700
GGB1DV3506	148.9	00.3	04	130	148.9	-03.5	23.0	640 - 700
GGB1DV3701	141.0	-22.7	40	140	142.0	-62.6	12.5	580 - 680
GGB1DV3703	126.0	-05.0	40	140	120.7	-43.5	10.8	580 - 680
GGB1DV3705	145.4	05.4	40	140	146.5	-34.4	12.3	580 - 680
GGB1DV3706	160.6	-03.2	40	140	167.3	-40.1	14.7	580 - 700
GGB1DV3707	156.5	10.6	40	140	158.3	-27.7	19.7	550 - 700
GGB1DV3708	167.5	-17.0	40	140	183.7	-50.3	29.7	550 - 700
GGB1DV3709	110.3	-12.6	40	140	096.5	-45.4	11.5	580 - 700
GGB1DV3710	149.4	-01.0	40	140	152.3	-40.3	14.7	580 - 700
GGB1DV3711	144.9	-43.7	40	140	169.9	-82.9	15.2	550 - 700
GGB1DV3713	147.6	-42.8	40	140	178.7	-81.1	21.1	580 - 700
GGB1DV3801	127.6	-13.0	40	140	120.2	-51.7	09.0	580 - 680
GGB1DV3802	137.1	-24.0	40	140	133.9	-63.9	07.1	580 - 700
GGB1DV3803	178.8	-02.8	40	140	188.0	-32.6	04.0	600 - 700
GGB1DV3804	142.7	08.4	40	140	143.2	-31.6	15.4	580 - 680
GGB1DV3805	145.8	21.3	40	140	145.7	-18.5	19.5	550 - 700
GGB1DV3806	137.0	-37.9	40	140	128.8	-77.7	06.9	620 - 680
GGB1DV3808	162.2	04.8	40	140	166.3	-32.0	07.2	550 - 700

3.15a, 3.15b and 3.15c represent samples from Group 1, 2 and 3 respectively. The unheated samples started to saturate at 2 T. However, most heated samples became hardened and the field of 3 T was not enough to determine whether the increase in acquired remanence started to flatten out. Also, below 1 T the curves are concave instead of being convex. This probably results from breaking down of clay minerals to form magnetite which saturates at around 300 mT. It seems that samples from Group 1 exhibit the least chemical changes.

The thermal demagnetisation of the IRMs gave a better picture of the magnetic carrier in the red beds. Decay curves of the heated and unheated

samples show that the magnetic mineral is haematite. It can then be seen that the blocking temperatures are above 600°C. The unheated samples however, sometimes show less steeper inclination. This can be seen in samples from Group 1 (about 45° less, see Figure 3.16b) and indicates that haematite in these red beds is present as two components with broadly overlapping blocking temperature components. As a result thermal demagnetisation was not able to separate them. However, all heated specimens clearly show two component behaviour on the orthogonal plots (Figure 3.16, 3.17 and 3.18). This confirms that there was a chemical alteration during the heating process which appears to have produced magnetite since the blocking temperature for the lower blocking temperature component is generally below 600°C. Is new magnetite formed during demagnetisation responsible for the higher temperature components which were observed in some specimens ? This seems unlikely for three reasons:

1. These components are identified mainly in the haematite (550 - 700°C) range.

2. Since the specimens showing two component behaviour are only a very small proportion of the collection, a contribution of the new magnetite to the higher temperature component seems unlikely.

3. All specimens showing two components are from Group 1 which proved more resistant to the chemical changes during the laboratory experiments.

The low field cage and the modern thermal demagnetiser seem to be successful in creating a very low field environment. The system enables the higher temperature stage of demagnetisation to separate coherent components from spurious effects. This study failed to find the higher components

Figure 3.16a Thermal demagnetisation of the IRM from Group 1 (Brecon/Abergavenny area). The last two letters refer to a sample code ;16 means DV16 (IRM1-heated samples and IRM2-unheated (fresh) samples). The intensity unit is 10E-5 A m^2 / kg.

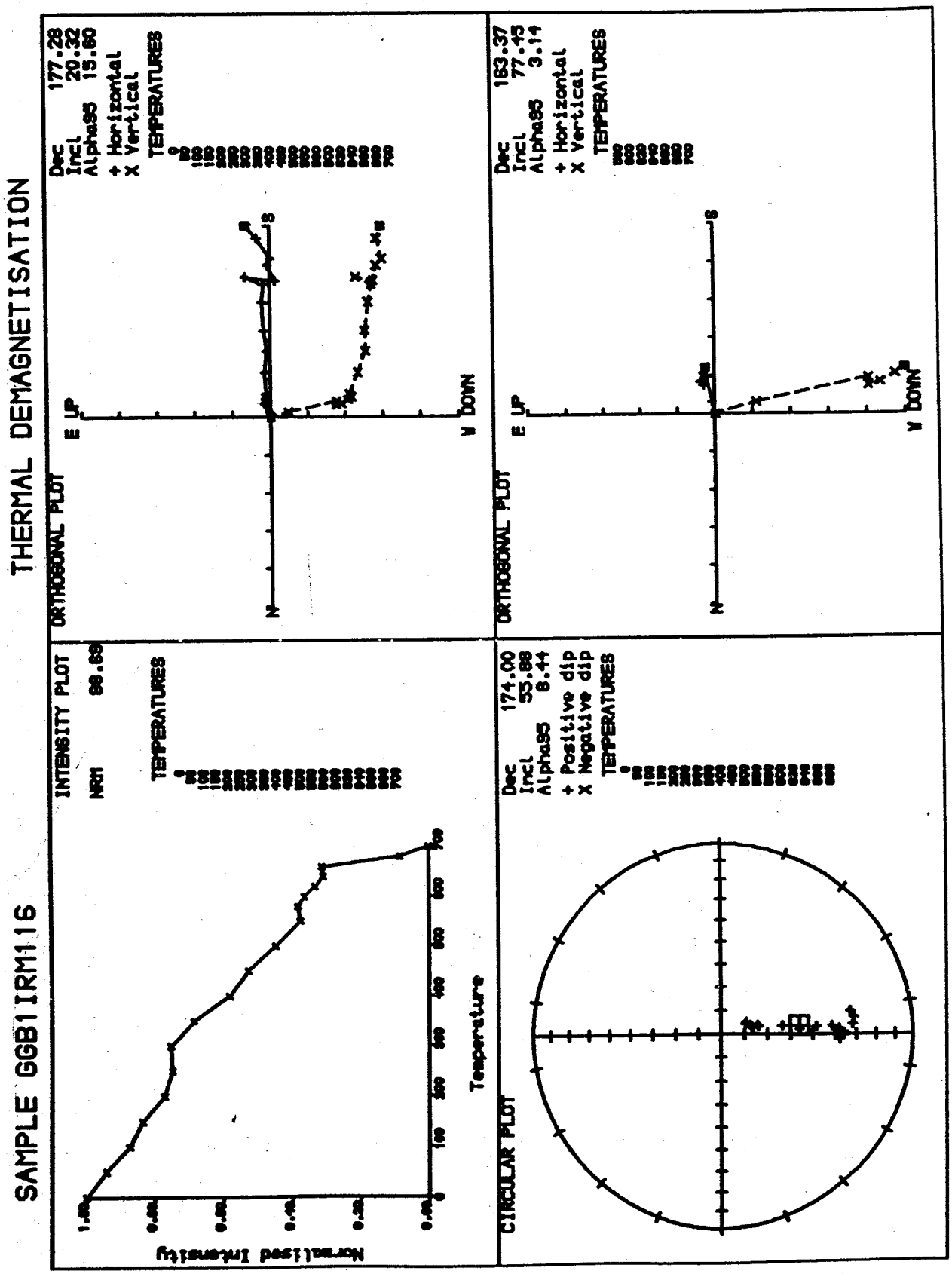

Figure 3.16b.

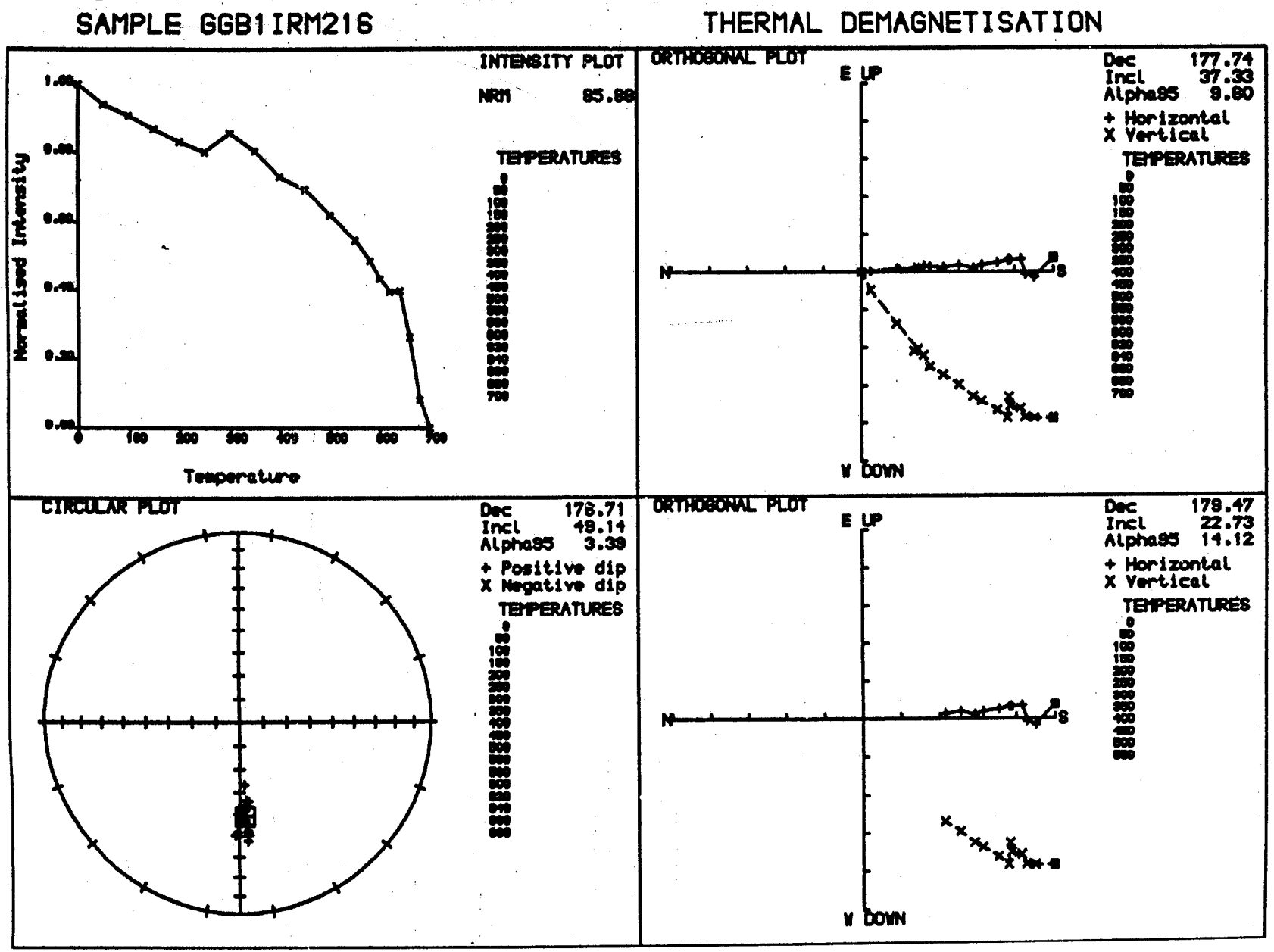
SAMPLE GGB1IRM216
THERMAL DEMAGNETISATION
INTENSITY PLOT
NRM 85.88
TEMPERATURES
Normalised Intensity
Temperature
ORTHOGONAL PLOT
E UP
N
S
W DOWN
Dec 177.74
Incl 37.33
Alpha95 9.80
+ Horizontal
X Vertical
TEMPERATURES
CIRCULAR PLOT
Dec 178.71
Incl 49.14
Alpha95 3.39
+ Positive dip
X Negative dip
TEMPERATURES
ORTHOGONAL PLOT
E UP
N
S
W DOWN
Dec 178.47
Incl 22.73
Alpha95 14.12
+ Horizontal
X Vertical
TEMPERATURES

Figure 3.16c.

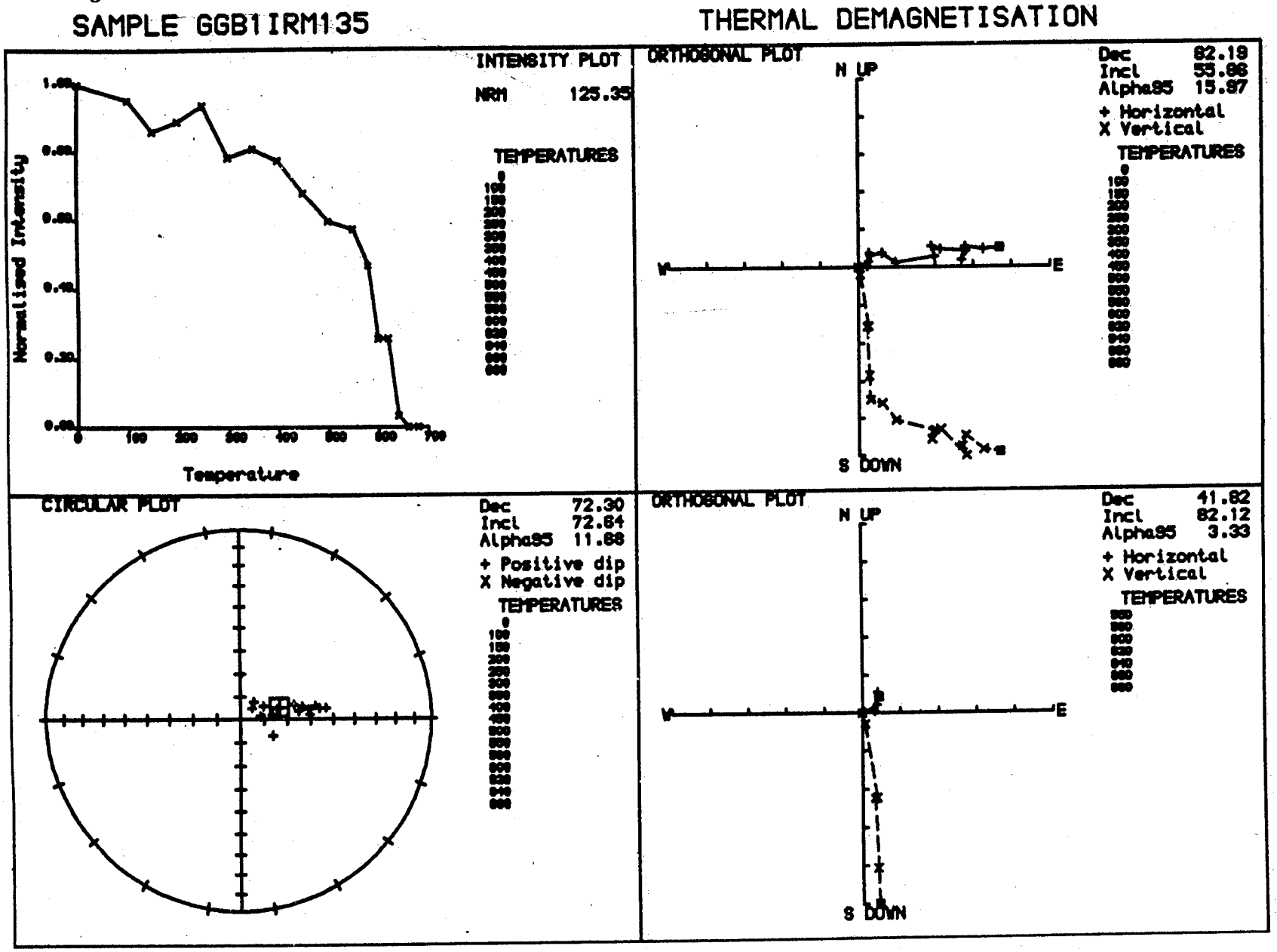
SAMPLE GGB1IRM135
THERMAL DEMAGNETISATION
INTENSITY PLOT
NRM 125.35
TEMPERATURES
Normalised Intensity
Temperature
ORTHOGONAL PLOT
N UP
W
E
S DOWN
Dec 82.19
Incl 55.66
Alpha95 15.97
+ Horizontal
X Vertical
TEMPERATURES
CIRCULAR PLOT
Dec 72.30
Incl 72.64
Alpha95 11.68
+ Positive dip
X Negative dip
TEMPERATURES
ORTHOGONAL PLOT
N UP
W
E
S DOWN
Dec 41.82
Incl 82.12
Alpha95 3.33
+ Horizontal
X Vertical
TEMPERATURES

Figure 3.16d.

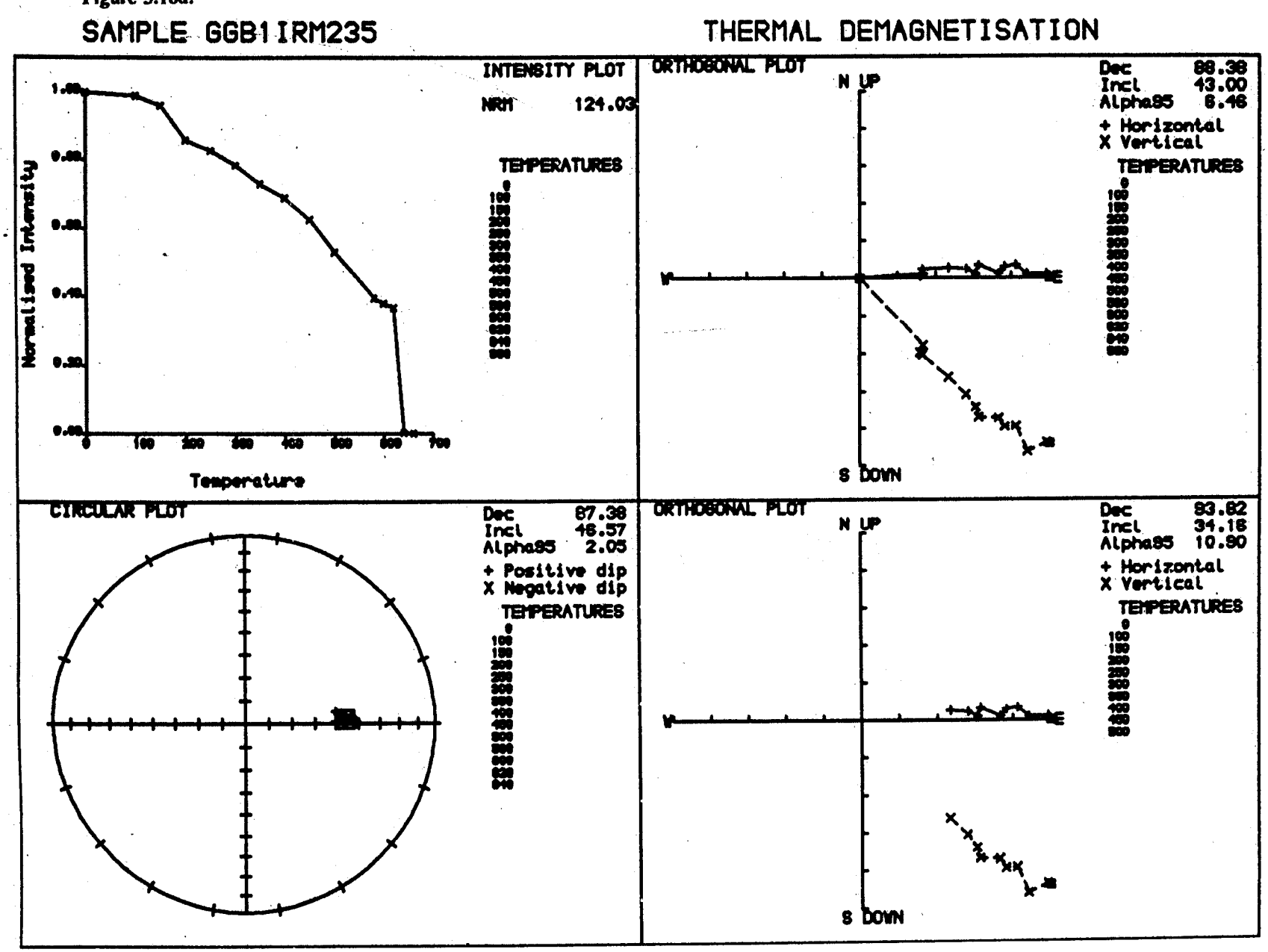
SAMPLE GGB1IRM235
THERMAL DEMAGNETISATION
INTENSITY PLOT
NRM 124.03
TEMPERATURES
Normalised Intensity
Temperature
ORTHOGONAL PLOT
N UP
W
E
S DOWN
Dec 88.38
Incl 43.00
Alpha95 6.46
+ Horizontal
X Vertical
TEMPERATURES
CIRCULAR PLOT
Dec 87.38
Incl 46.57
Alpha95 2.05
+ Positive dip
X Negative dip
TEMPERATURES
ORTHOGONAL PLOT
N UP
W
E
S DOWN
Dec 83.82
Incl 34.16
Alpha95 10.90
+ Horizontal
X Vertical
TEMPERATURES

Figure 3.17a Thermal demagnetisation of the IRM from Group 2 (Carmarthen area) (see caption Figure 3.16a).

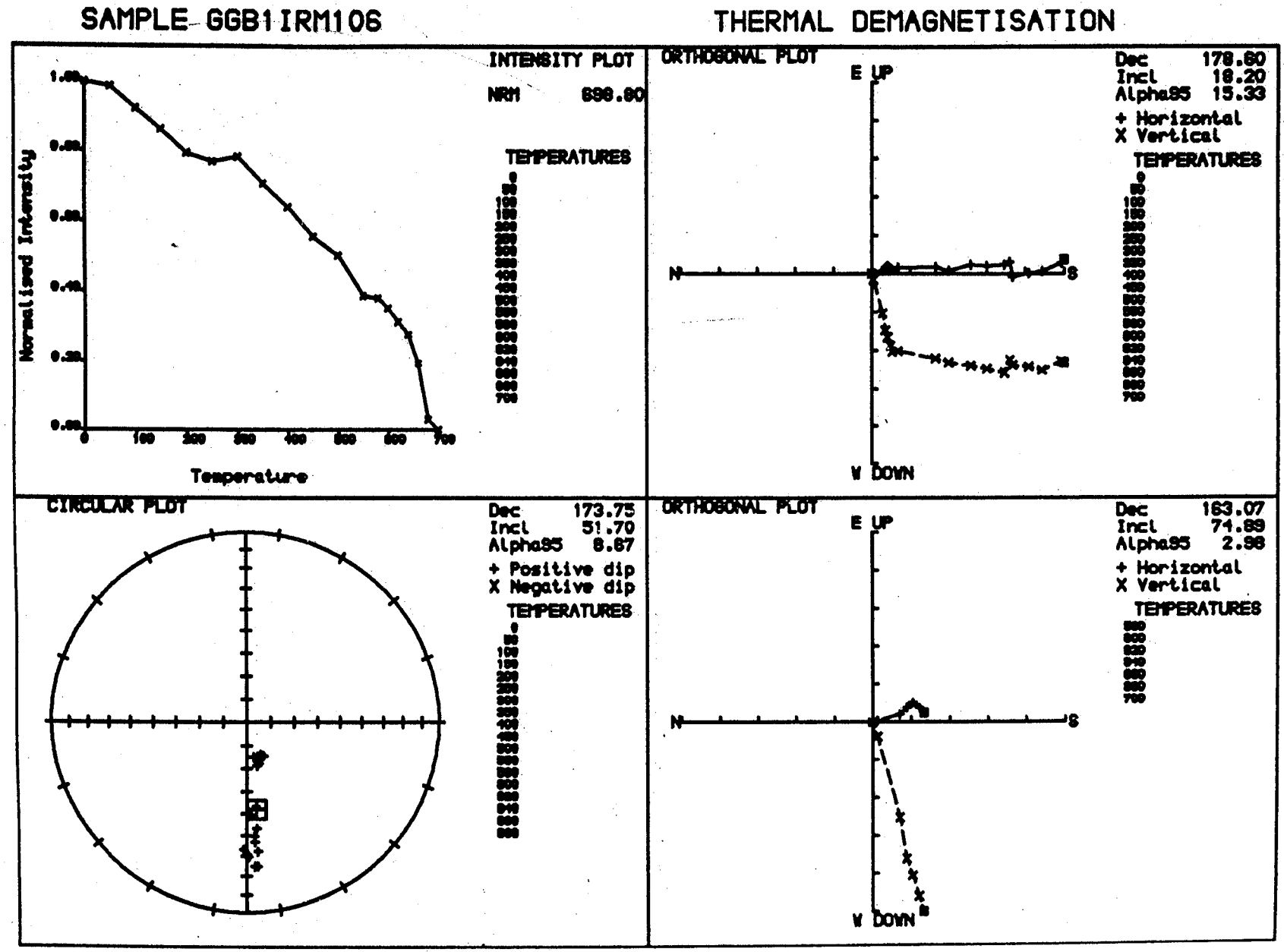

Figure 3.17b.

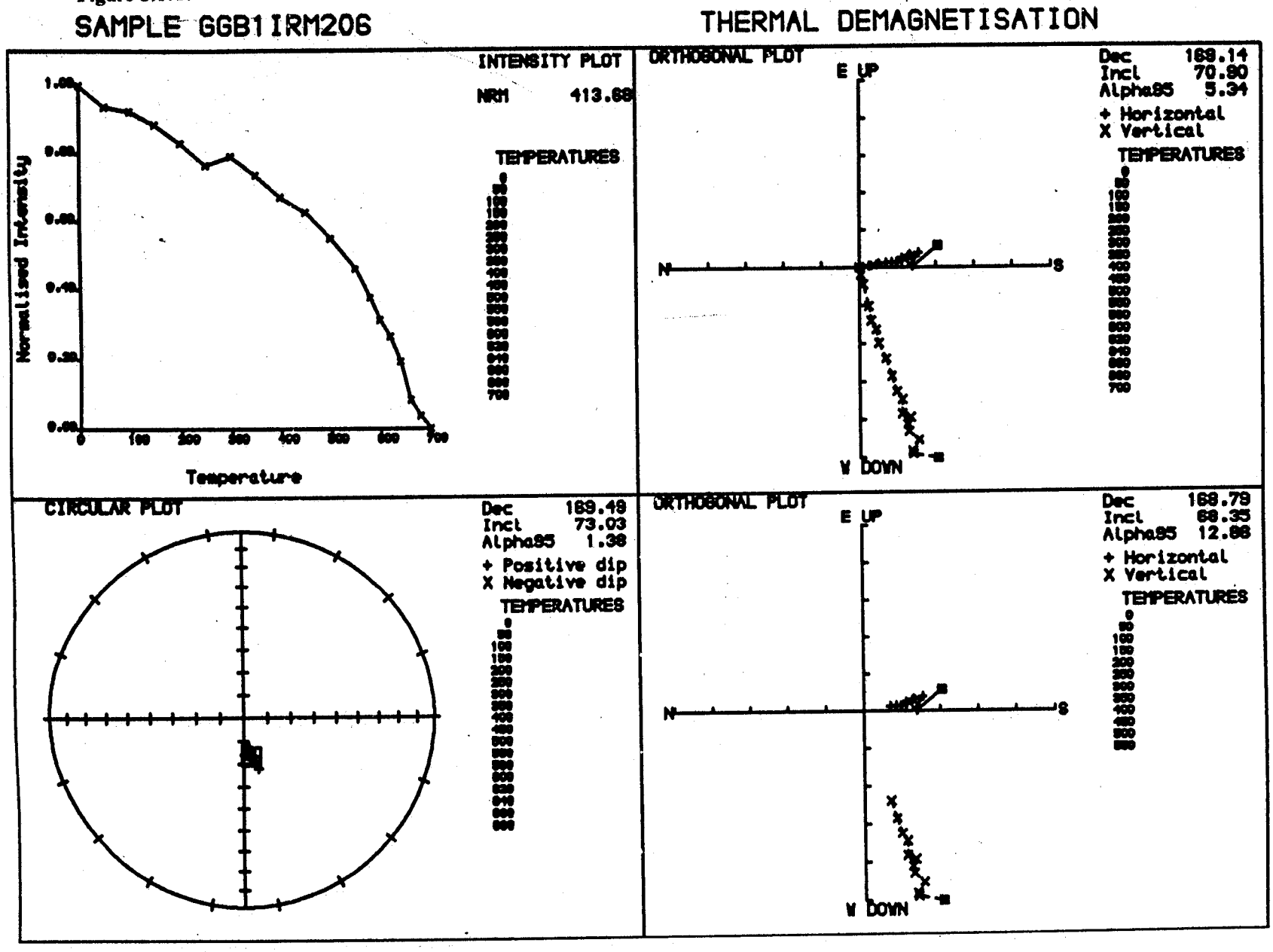
SAMPLE GGB1IRM206
THERMAL DEMAGNETISATION
INTENSITY PLOT
NRM 413.68
TEMPERATURES
Normalised Intensity
Temperature
ORTHOGONAL PLOT
E UP
N
S
W DOWN
Dec 169.14
Incl 70.90
Alpha95 5.34
+ Horizontal
X Vertical
TEMPERATURES
CIRCULAR PLOT
Dec 169.48
Incl 73.03
Alpha95 1.38
+ Positive dip
X Negative dip
TEMPERATURES
ORTHOGONAL PLOT
E UP
N
S
W DOWN
Dec 168.79
Incl 68.35
Alpha95 12.88
+ Horizontal
X Vertical
TEMPERATURES

Figure 3.17c.

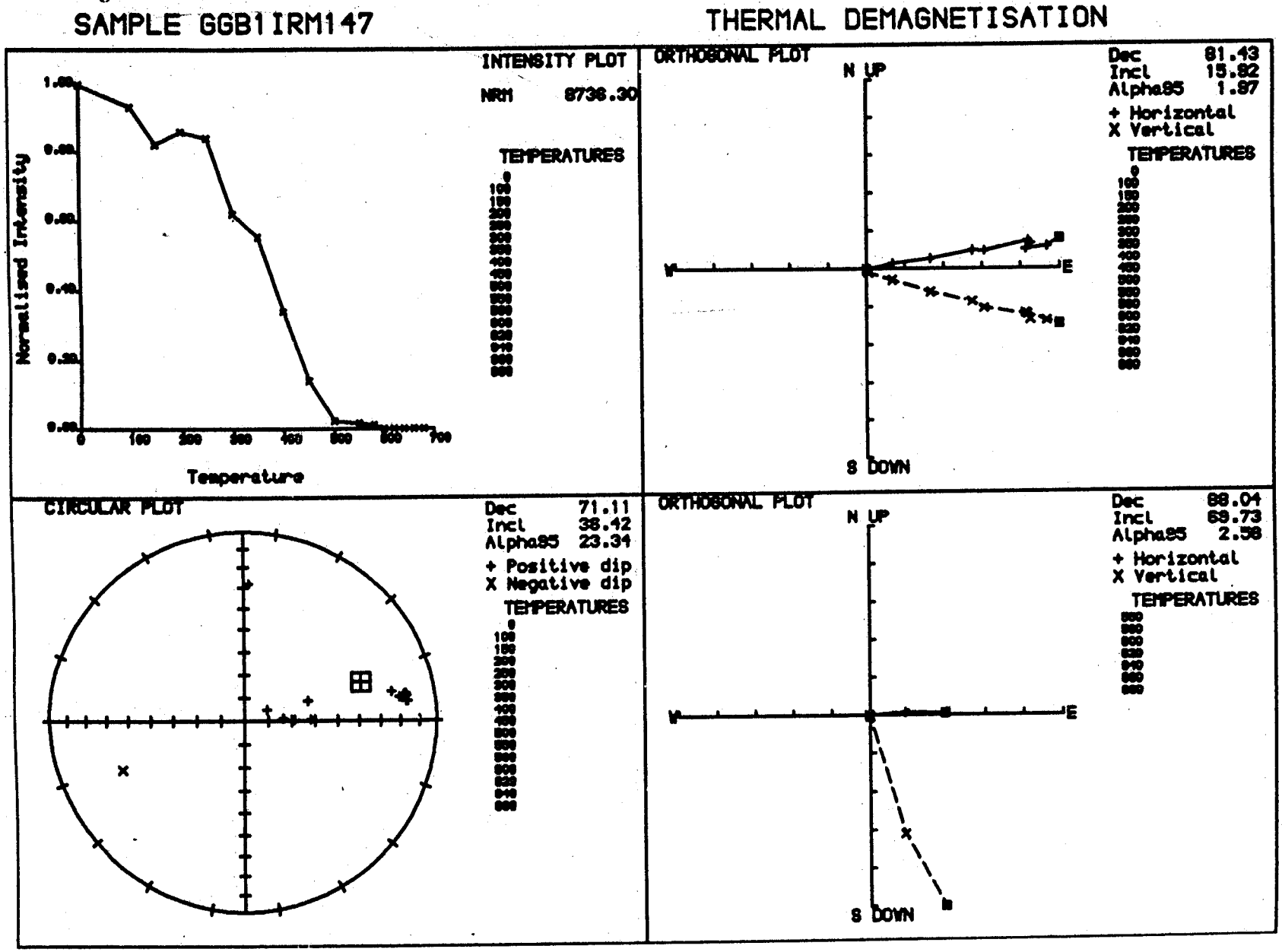
SAMPLE GGB1IRM147
THERMAL DEMAGNETISATION
INTENSITY PLOT
NRM 8736.30
TEMPERATURES
Normalised Intensity
Temperature
ORTHOGONAL PLOT
N UP
W
E
S DOWN
Dec 81.43
Incl 15.82
Alpha95 1.87
+ Horizontal
X Vertical
TEMPERATURES
CIRCULAR PLOT
Dec 71.11
Incl 38.42
Alpha95 23.34
+ Positive dip
X Negative dip
TEMPERATURES
ORTHOGONAL PLOT
N UP
W
E
S DOWN
Dec 88.04
Incl 69.73
Alpha95 2.58
+ Horizontal
X Vertical
TEMPERATURES

Figure 3.17d.

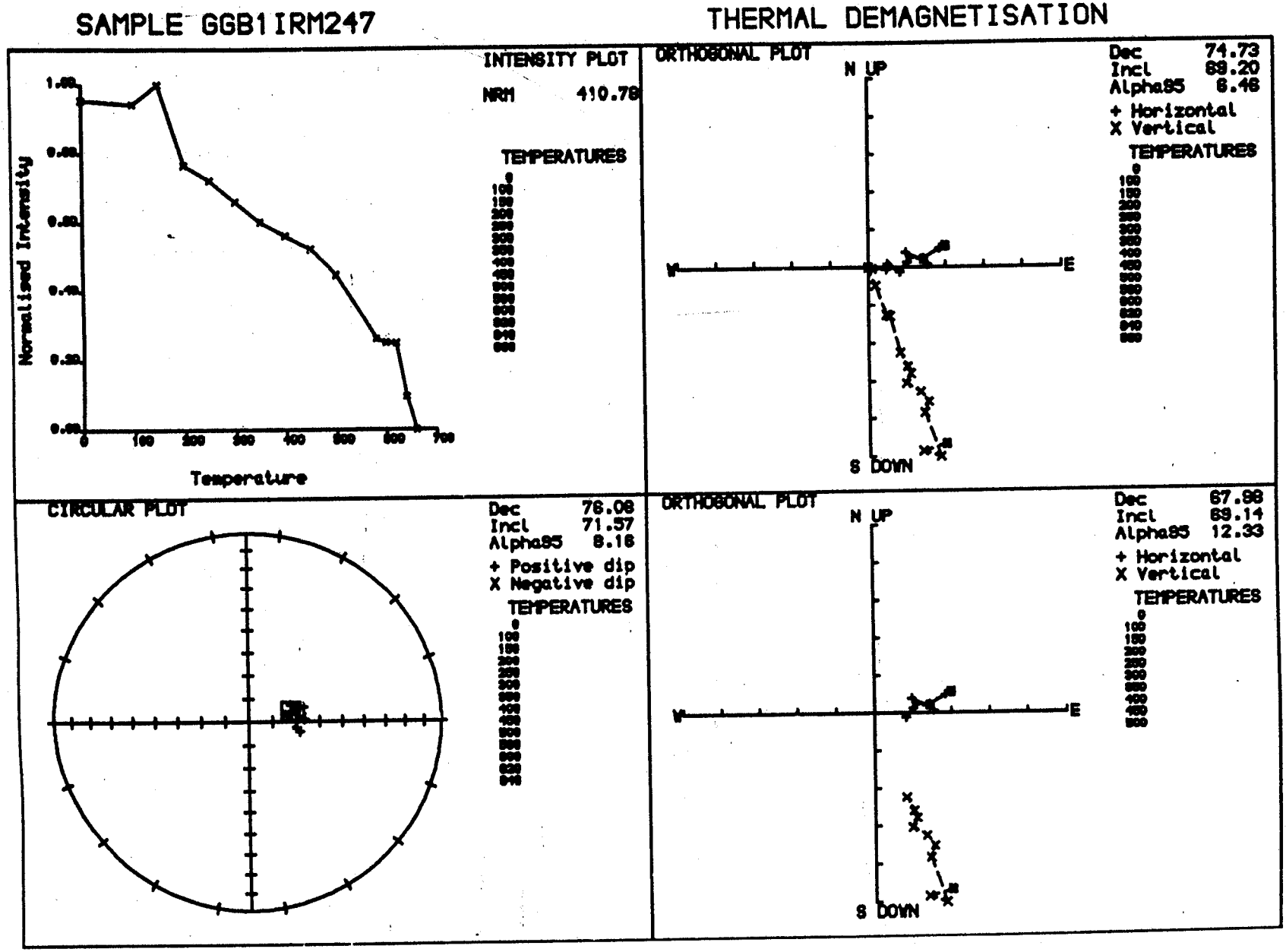
SAMPLE GGB1IRM247
THERMAL DEMAGNETISATION
INTENSITY PLOT
NRM 410.78
TEMPERATURES
Normalised Intensity
Temperature
ORTHOGONAL PLOT
N UP
W
E
S DOWN
Dec 74.73
Incl 69.20
Alpha95 6.46
+ Horizontal
X Vertical
TEMPERATURES
CIRCULAR PLOT
Dec 76.08
Incl 71.57
Alpha95 8.16
+ Positive dip
X Negative dip
TEMPERATURES
ORTHOGONAL PLOT
N UP
W
E
S DOWN
Dec 67.98
Incl 69.14
Alpha95 12.33
+ Horizontal
X Vertical
TEMPERATURES

Figure 3.18a Thermal demagnetisation of the IRM from Group 3 (southern Pembrokeshire) (see caption Figure 3.16a).

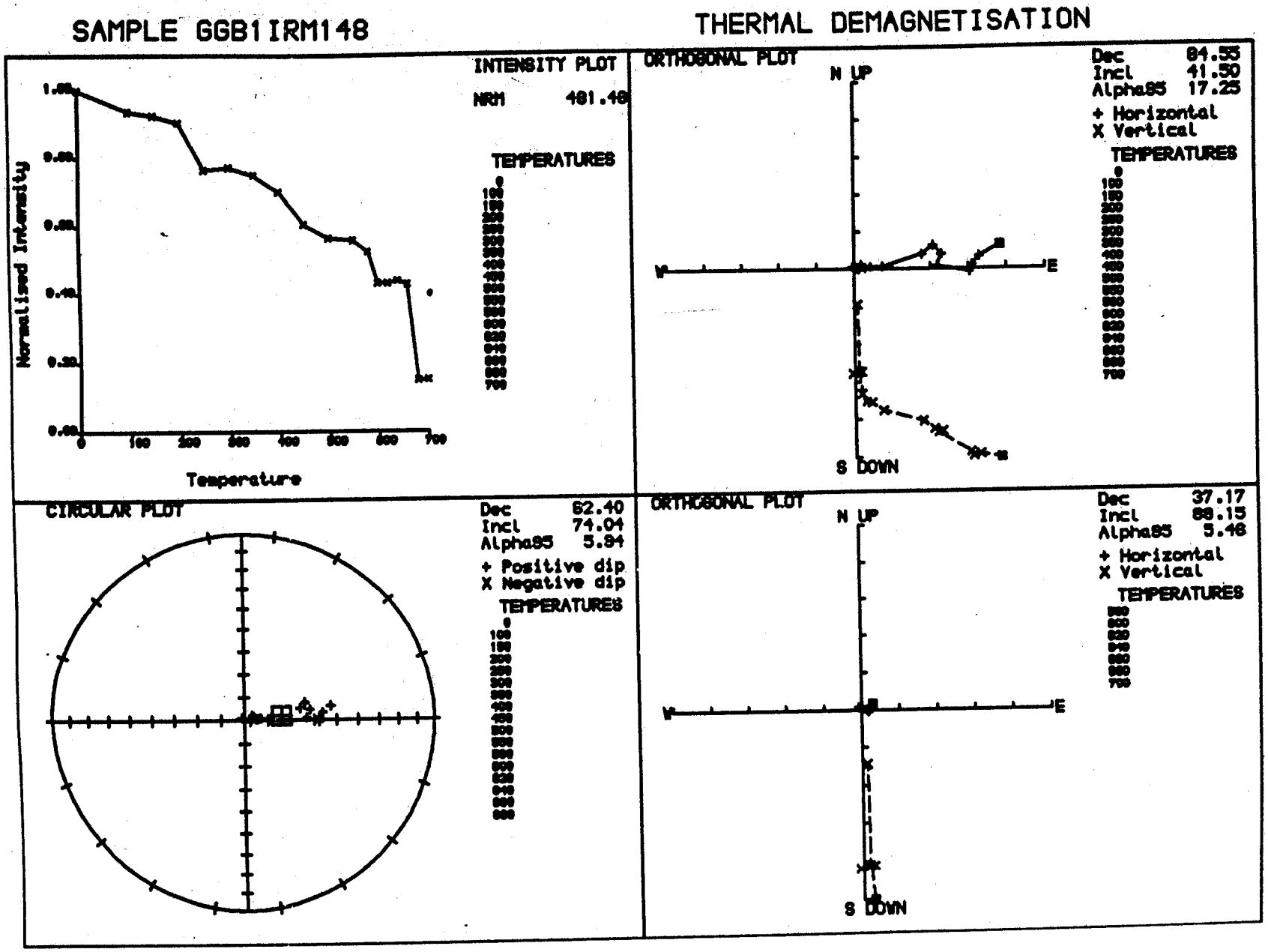

Figure 3.18b.

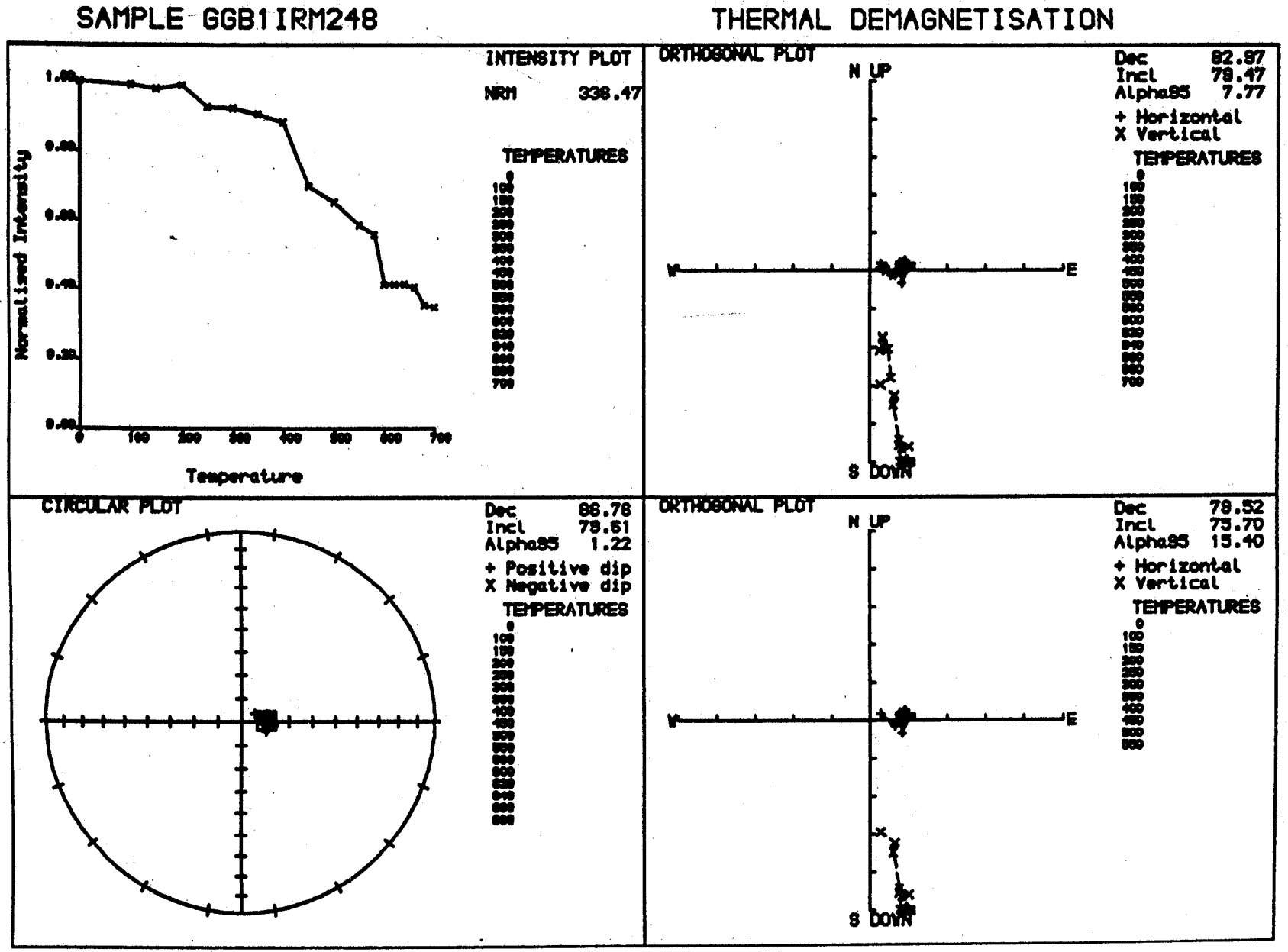
SAMPLE GGB1IRM248
THERMAL DEMAGNETISATION
INTENSITY PLOT
NRM 336.47
TEMPERATURES
Normalised Intensity
Temperature
ORTHOGONAL PLOT
N UP
W
E
S DOWN
Dec 82.87
Incl 79.47
Alpha95 7.77
+ Horizontal
X Vertical
TEMPERATURES
CIRCULAR PLOT
Dec 86.76
Incl 79.61
Alpha95 1.22
+ Positive dip
X Negative dip
TEMPERATURES
ORTHOGONAL PLOT
N UP
W
E
S DOWN
Dec 78.52
Incl 75.70
Alpha95 15.40
+ Horizontal
X Vertical
TEMPERATURES

Figure 3.18c.

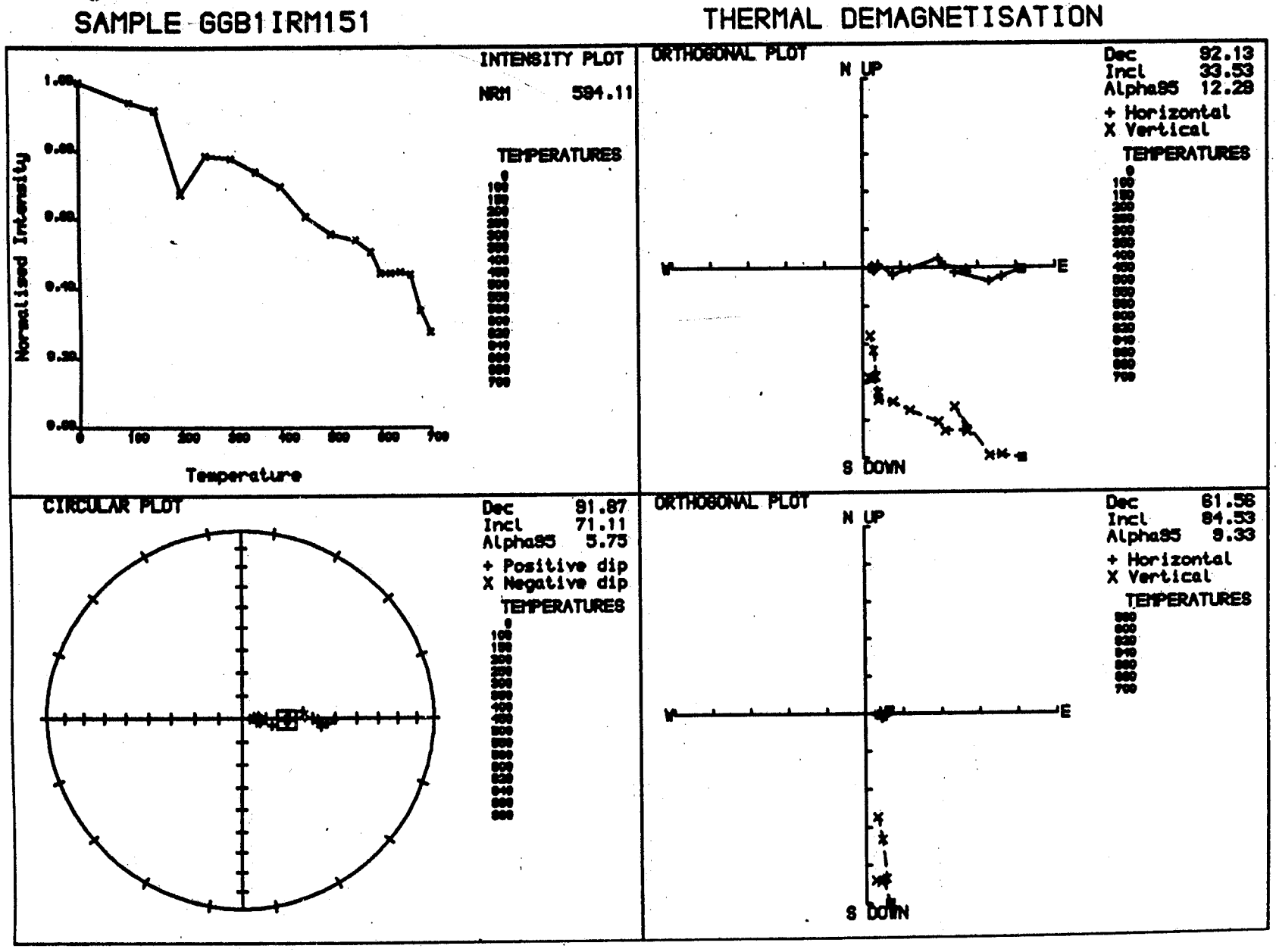
SAMPLE GGB1IRM151
THERMAL DEMAGNETISATION
INTENSITY PLOT
NRM 594.11
TEMPERATURES
Normalised Intensity
Temperature
ORTHOGONAL PLOT
N UP
S DOWN
W
E
Dec 92.13
Incl 33.53
Alpha95 12.29
+ Horizontal
X Vertical
TEMPERATURES
CIRCULAR PLOT
Dec 91.87
Incl 71.11
Alpha95 5.75
+ Positive dip
X Negative dip
TEMPERATURES
ORTHOGONAL PLOT
N UP
S DOWN
W
E
Dec 61.56
Incl 84.53
Alpha95 9.33
+ Horizontal
X Vertical
TEMPERATURES

Figure 3.18d.

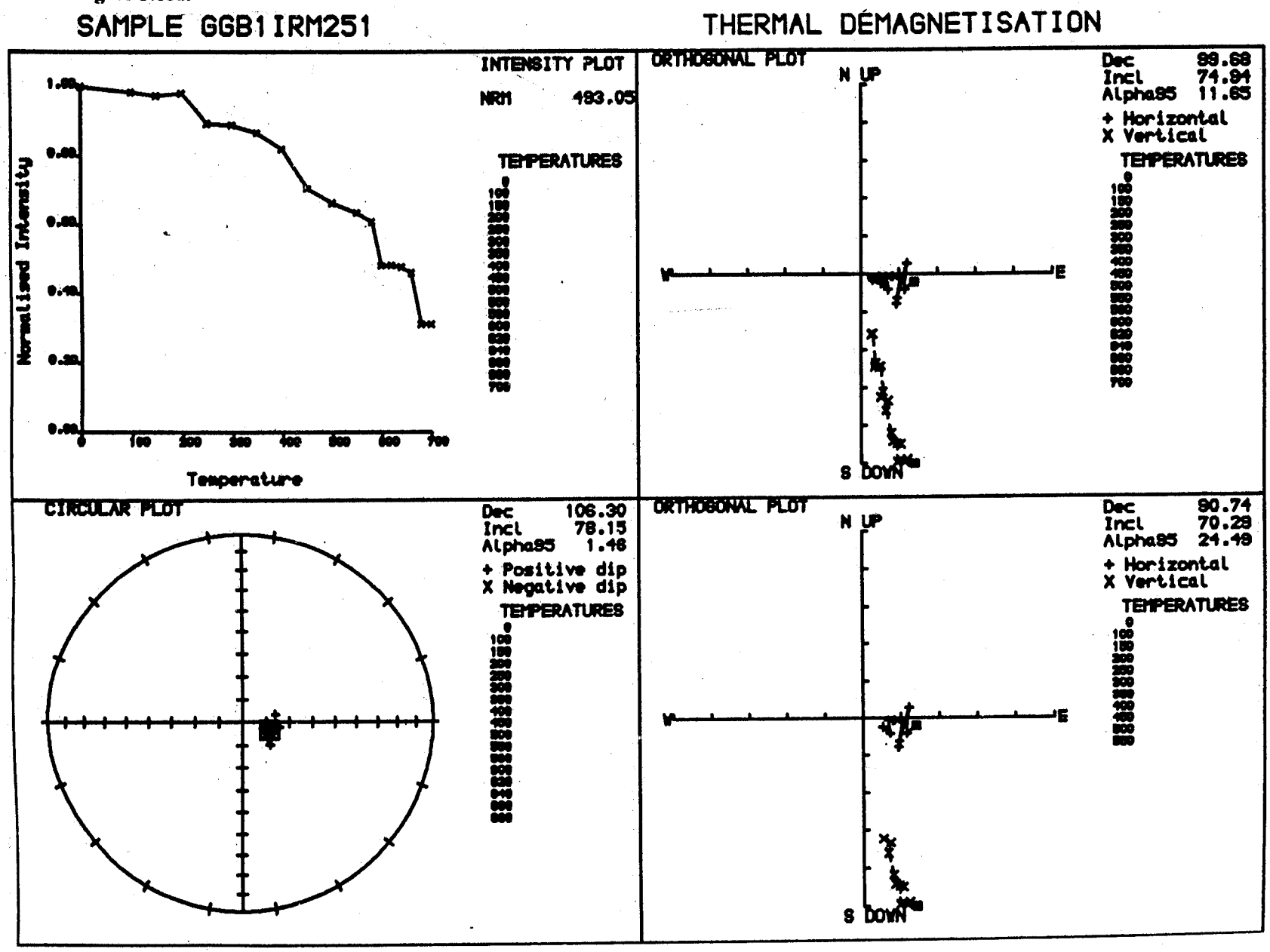
SAMPLE GGB1IRM251
THERMAL DÉMAGNETISATION
INTENSITY PLOT
NRM 483.05
TEMPERATURES
Normalised Intensity
Temperature
ORTHOGONAL PLOT
N UP
W
E
S DOWN
Dec 99.68
Incl 74.94
Alpha95 11.65
+ Horizontal
X Vertical
TEMPERATURES
CIRCULAR PLOT
Dec 106.30
Incl 78.15
Alpha95 1.48
+ Positive dip
X Negative dip
TEMPERATURES
ORTHOGONAL PLOT
N UP
W
E
S DOWN
Dec 90.74
Incl 70.29
Alpha95 24.48
+ Horizontal
X Vertical
TEMPERATURES

which were reported by several earlier workers (Chamalaun and Creer, 1964; McClelland-Brown, 1983) and it seems possible that the components observed by these authors were IRM's introduced in the demagnetising ovens used and/or acquired prior to measurement.

3.4.5 Room Temperature Susceptibility Results

During the thermal treatment 203 specimens had their susceptibilities monitored (Figure 3.19). Some specimens exhibited no change in susceptibility. This includes those showing two component behaviour (Group 1). The lithology is sandstone and purple in colour. The rest show increase in their susceptibility values to about 10 times their original values. The lithology of the rock in these cases is mudstone or siltstone. It can therefore be concluded that the possibility of creating the new mineral (magnetite) through the breaking down of clay minerals is more likely to be the cause than any reduction process from haematite to magnetite. This former transformation in red beds happens at temperature above 500°C.

3.4.6 AMS Results

Figure 3.20 is a histogram of the magnitude of the anisotropy. The magnitude is defined as the difference between the maximum and the minimum relative to the minimum susceptibility. From this study, 12% is the average magnitude of the anisotropy for South Wales red beds but it is rarely as much as 32%. The relationship between the susceptibility axes is described below.

Figure 3.19 Histograms of room temperature susceptibility during thermal treatment (SI volume unit).

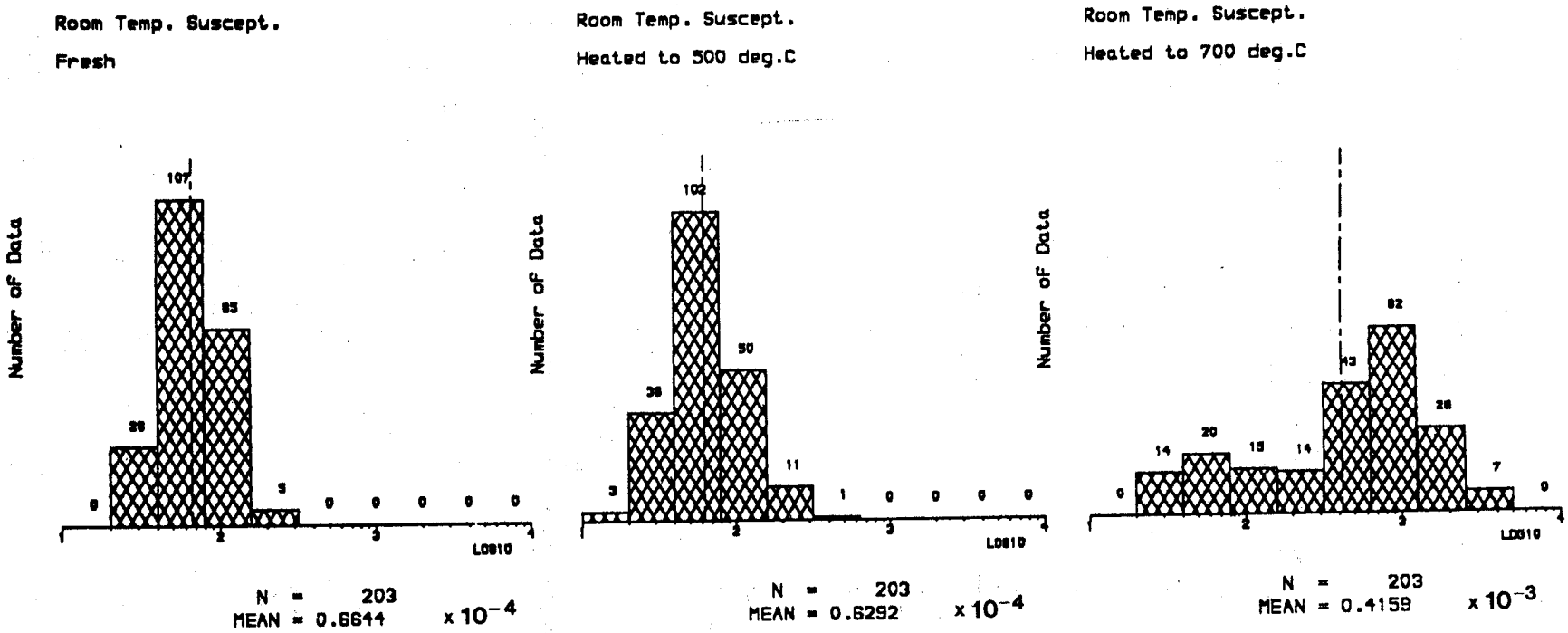

Figure 3.20 Histogram of the magnitude of anisotropy in per cent. k1 and k3 are the maximum and minimum susceptibility axis.

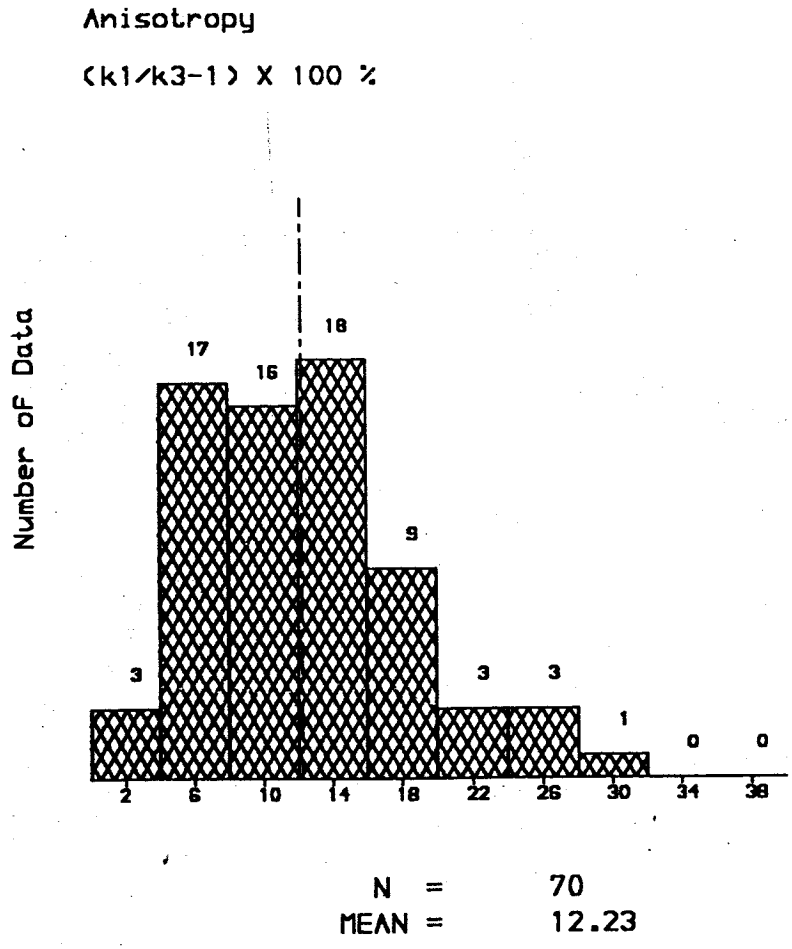

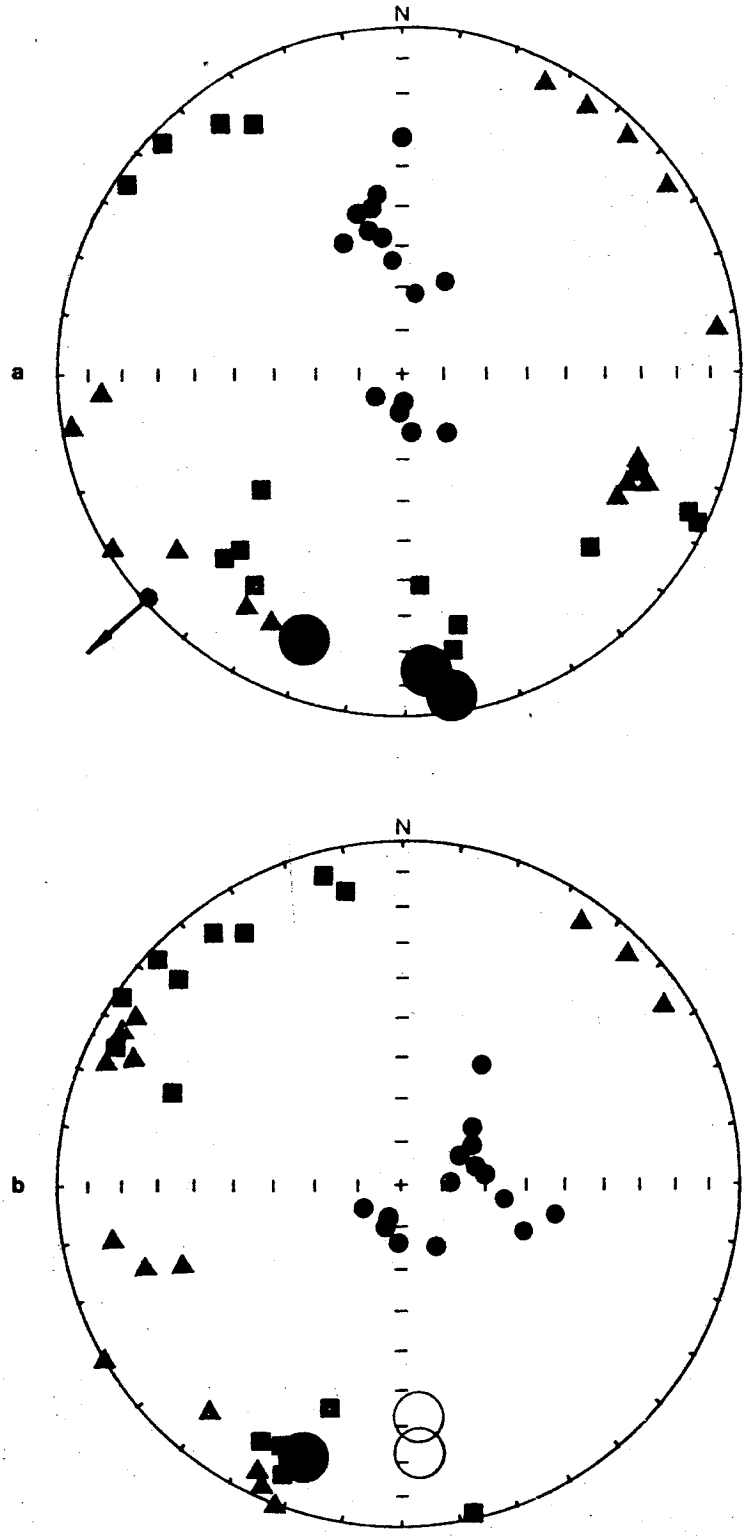

Figure 3.21 Equal area projection of susceptibility axis for core samples from Locality 1 (Llanthony). Triangle, square and small circle symbols are for maximum, intermediate and minimum susceptibility axis. Large circle symbols are for mean NRM directions. Solid = lower hemisphere
(a) in situ (the orientation of the fold axis is represented by the arrow)
(b) tilt-corrected

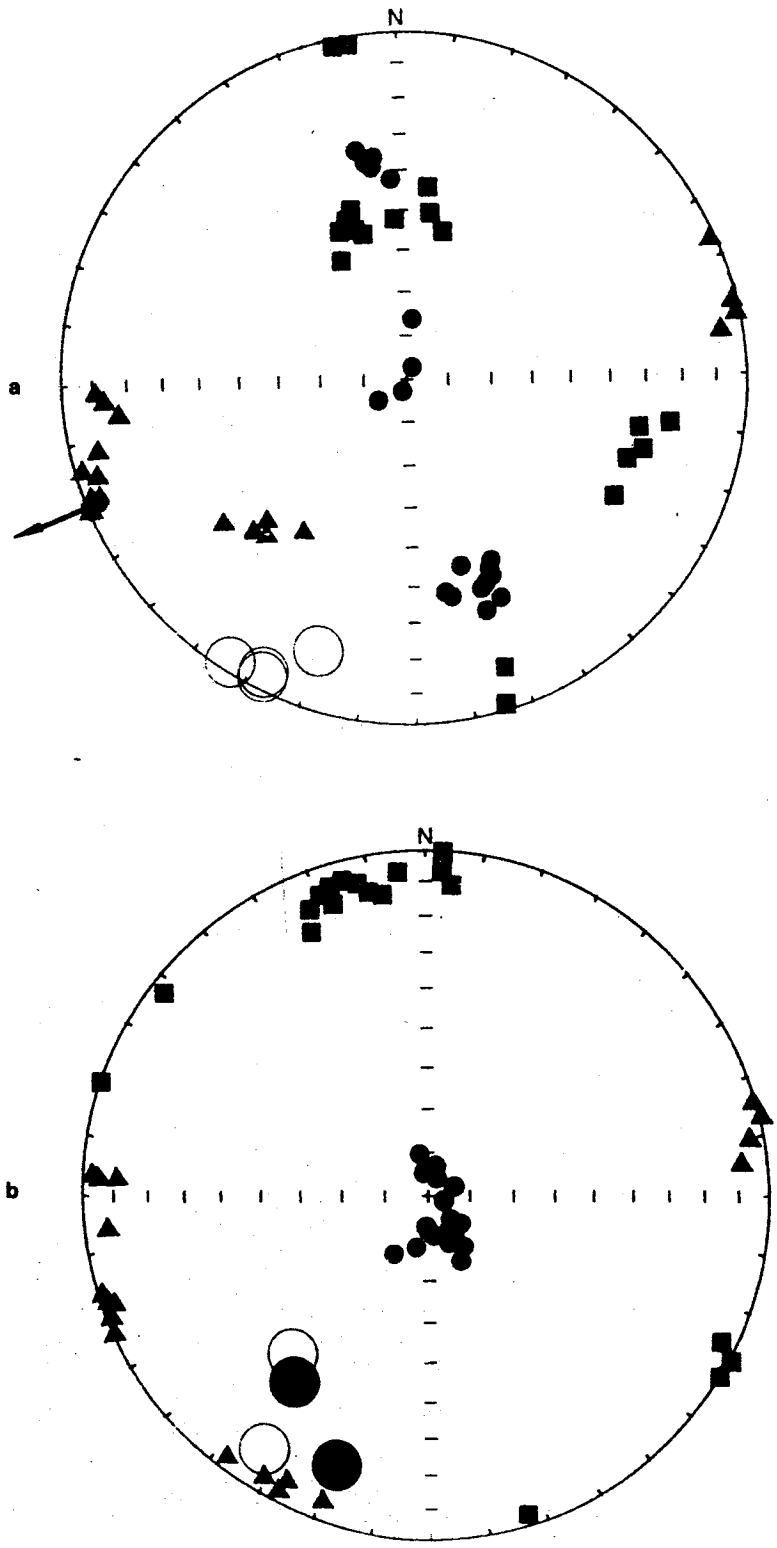

Figure 3.22 Equal area projection of susceptibility axis for block samples from Locality 9 (Llanstephan) (see caption Figure 3.21).
(a) in situ (the orientation of the fold axis is represented by the arrow)
(b) tilt-corrected

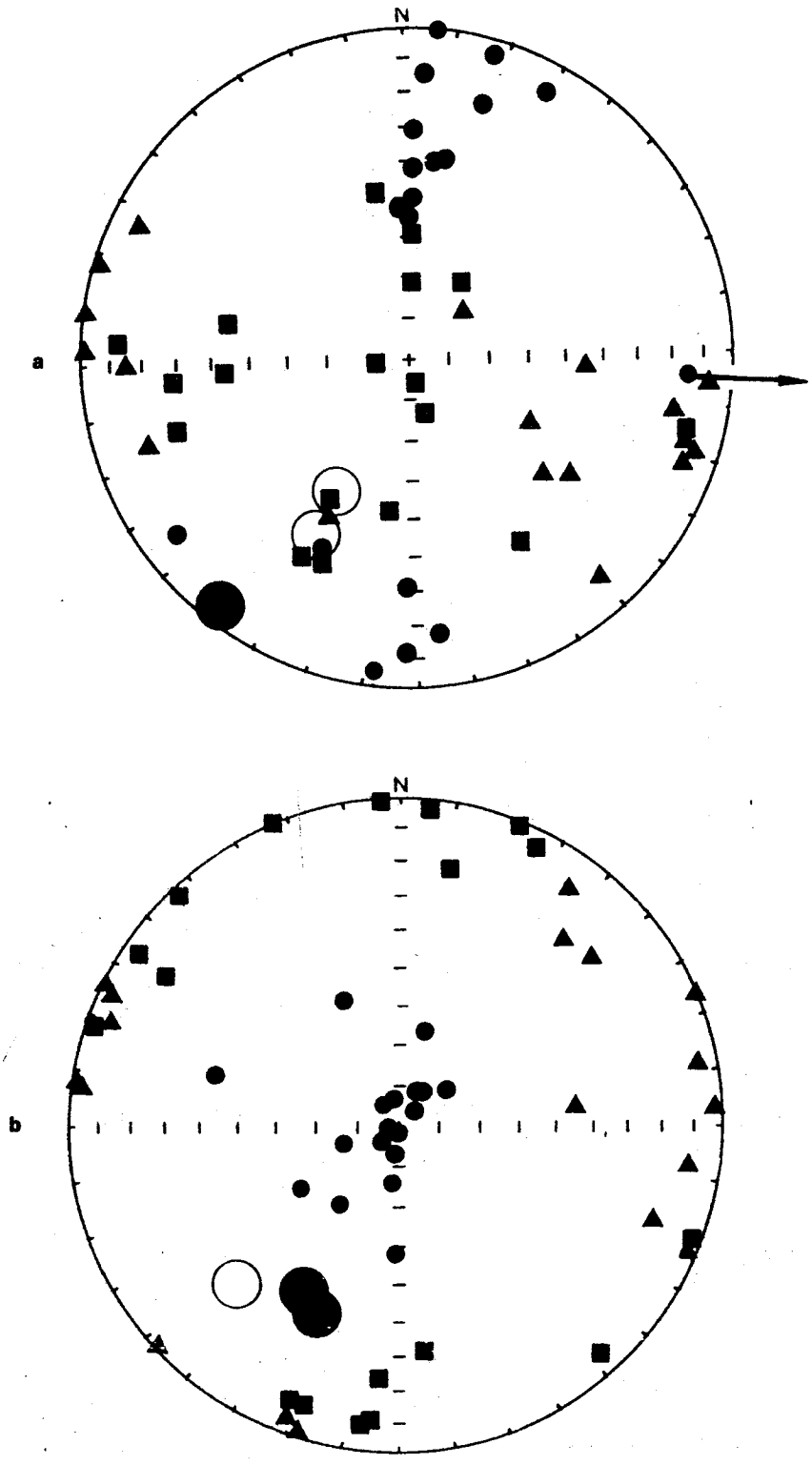

Figure 3.23 Equal area projection of susceptibility axis for core samples from Locality 10 (Freshwater East) (see caption Figure 3.21).
(a) in situ (the orientation of the fold axis is represented by the arrow)
(b) tilt-corrected

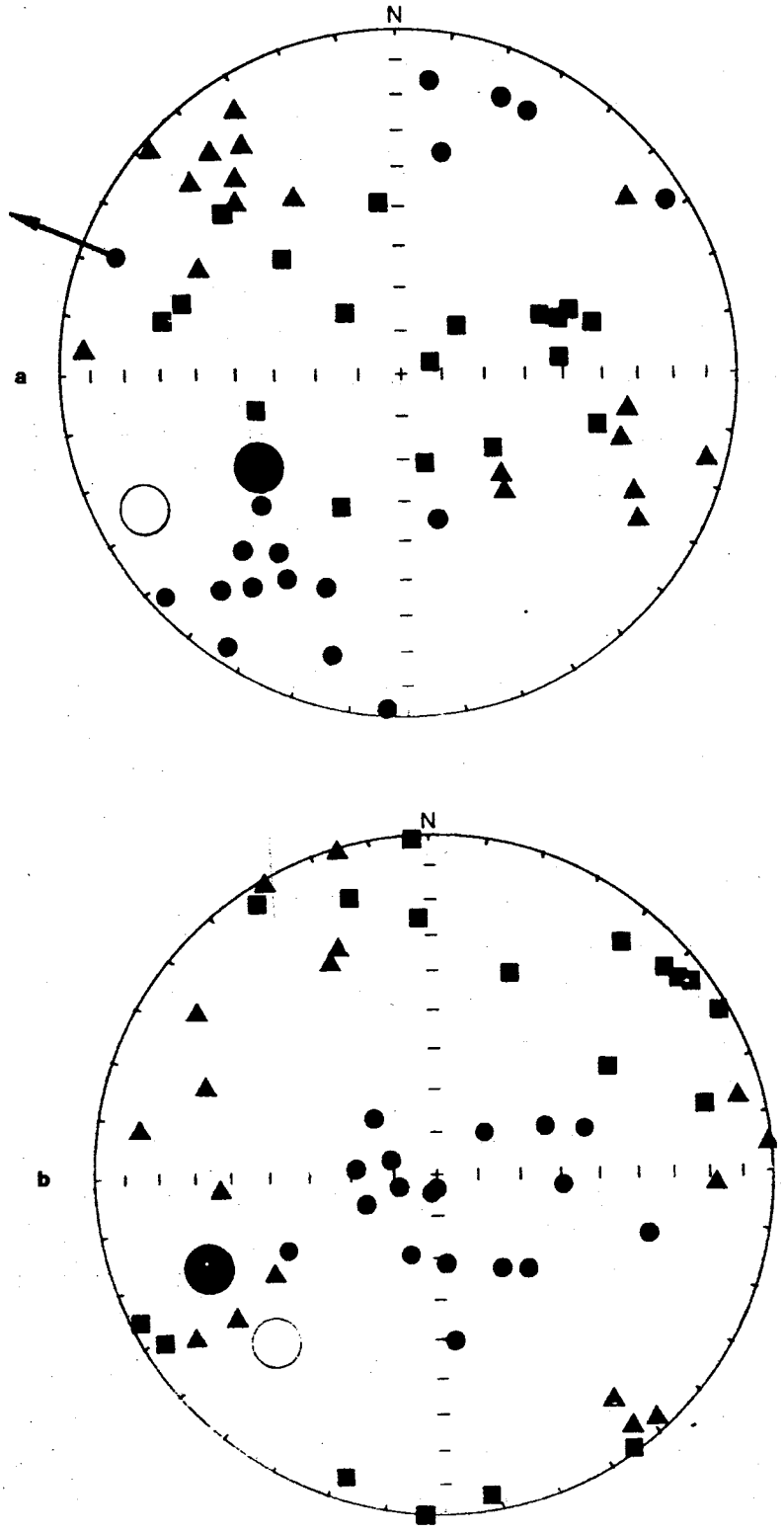

Figure 3.24 Equal area projection of susceptibility axis for core samples from Locality 11 (Freshwater West) (see caption Figure 3.21).
(a) in situ (the orientation of the fold axis is represented by the arrow)
(b) tilt-corrected

Table 3.7a The summary of AMS studies. N = number of specimens. The definition of A, L, F and E is given in CHAPTER 2, Basic Palaeomagnetism (section 2.7.4). P = percentage of prolate ellipsoids in %.

Locality	N	A	L	F	E	P
Llanthony	15	1.073	1.020	1.053	1.032	7
Llanstephan	19	1.133	1.037	1.094	1.055	16
Freshwater E.	18	1.122	1.024	1.095	1.069	6
Freshwater W.	18	1.140	1.055	1.080	1.025	39

Figures 3.21, 3.22, 3.23 and 3.24 show the results of AMS (Anisotropy of Magnetic Susceptibility) studies. The big circle is the average of the NRM directions for each site. The arrow (only shown in in situ stereographic projections) is pointing to the bearing of the fold axis and the position of the arrow on the projections shows the plunge of the axis. The fold axes of the Freshwater East and the Castlemartin Corse anticlines shown in Figure 3.23 and Figure 3.24 are the average values of four plunges on each limb (see section 3.4.2 Fold Test). These plunges are calculated by means of the orientation of the bedding/cleavage intersection lineation (Dr. P.L. Hancock, written communication).

In general, after bedding correction, the minimum susceptibility axis tend to cluster around the pole to the bedding. This means that the nature of the susceptibility is most probably of primary origin and has evidently not been

appreciably reoriented by later straining of the rocks. The other axes (maximum k_1 and intermediate k_2) tend to orientate themselves parallel to the bedding plane. These axes are about perpendicular to each other (see Table 3.7b). This result seems to contradict the palaeomagnetic results which show a predominance of secondary magnetisations. This is evidently because the AMS experiment is not measuring the magnetic fabric of the minerals responsible for the remanence. The AMS results show that depositional origin of the fabric has to be interpreted independently of the results from NRM measurements. AMS presumably resides in paramagnetic and/or ferromagnetic compounds which do not contribute to a magnetic remanence. As a result, there is no clear relationship between the AMS axes and the direction of the NRMs.

Table 3.7b The mean maximum and intermediate axes (tilt-corrected).

Locality	k1 Dec(°)/Inc(°)	k2 Dec(°)/Inc(°)
Llanthony (1)	245/ 8	155/-2
Llanstephan (9)	246/ 3	156/-7
Freshwater E. (10)	257/-8	167/3
Freshwater W. (11)	296/12	206/-10

Note : k1 and k2 are the maximum and intermediate axis respectively.

Since the specimens of Locality 9 (Llanstephan) were taken from the same single block samples, they do not sample a large volume of rock. It is probably for this reason that the AMS results show a better grouping than the rest (the k-parameters are about 10, see Table 3.7c). To provide more

Table 3.7c Fisherian statistics for the mean maximum and intermediate principal axes.

Locality	N	k1 k /a95	k2 k/a95
Llanthony (1)	15	4/19°	4/19°
Llanstephan (9)	19	11/11°	10/11°
Freshwater E. (10)	18	5/16°	5/17°
Freshwater W. (11)	18	4/20°	4/18°

information on the way that this anisotropy is acquired it would be necessary to undertake more systematic sampling; for example the samples being investigated could be restricted to only one bed where the conditions (e.g. current flow velocity and direction of sediment source) were possibly uniform. Table 3.7a, 3.7b and 3.7c list the summary of the AMS studies. In general, the magnitude of the anisotropy for specimens from Group 2 and Group 3 is about 6% higher than for specimens from Group 1. The AMS observed at all localities suggests that it is primary in origin.

The percentage of the prolate ellipsoids (where $E < 1$) in Locality 11 (Freshwater West) is very much higher than in other localities (39%, see Table 3.7a). Some samples are most prominently of fine grained argillaceous facies. It is possible that this lithology is responsible for the higher percentage of the prolate ellipsoids in responding to horizontal stresses before the folding episode started. This can be seen by grouping the maximum susceptibility axes in the direction of the fold axis (see Figure 3.21a, Figure 3.22a, Figure 3.23a and Figure 3.24a).

Although the principal axes (the maximum and intermediate) of susceptibility do not exhibit the tight groupings of the overprinted component of remanence, there is a clear indication that they have been rotated in the same sense as the inferred remanence rotation (see Table 3.7b and 3.7c). The declinations of the maximum and intermediate axes at Locality 11 (Freshwater West) are about 40° more westerly than those at Locality 10 (Freshwater East). The amount is twice as much as the rotation of the remanence vector between these localities (Table 3.5 and Figure 3.10).

3.5 Conclusion and Discussion

Analysis of the Permo-Carboniferous overprinted components has yielded a variety of results when subjected to fold tests and has enabled the geometry of the folds at the time of this remanence acquisition to be determined. At Locality 1 (Llanthony), the beds were apparently sub-horizontal when the rocks acquired the secondary magnetisation. However in Locality 9 (Llanstephan), the beds were approximately in their present in situ positions when the remagnetisation occurred. In other words, the fold already existed when this overprinting episode took place. If the rocks in both localities were remagnetised at the same time, it is therefore likely that the deformation in the Locality 1 (Llanthony) is younger than the fold in Locality 9 (Llanstephan). This hypothesis is in agreement with the geological evidence showing that the climax of the Variscan orogeny moved northwards with time (Owen, 1974). The slight differences in the palaeomagnetic directions from both localities may be explained by possible unaccommodated plunge components, block rotations within the area and/or associated experimental errors.

The fold test results from Locality 10 (Freshwater East) are more difficult to interpret. The northern limb has to be unfolded by 50% with the southern limb retained nearly in situ (~ 6% unfolding) to achieve optimum grouping. The fold then becomes more symmetrical with both limbs dipping moderately to the north and south. In comparison to the fold at Locality 9 (Llanstephan), both northern limbs were dipping 40°-50° relative to the horizontal when the overprinting event took place. However the southern limb of the fold in Locality 9 (Llanstephan) was sub-horizontal. It therefore seems that later north-south stresses have tightened-up the structures at both localities in terms of steepening the northern limb of the fold in Locality 10 and the southern limb of the fold in Locality 9. The appropriate plunge corrections improve the in situ palaeomagnetic directions at Locality 9 and Locality 10. Hence, the axis of this fold was approximately horizontal when the secondary magnetisation was acquired. If the direction of the observed plunges are correct, the fold test suggests that the fold axes were steeper than they are today.

Probably, the fold test results from Locality 11 (Freshwater West) are the most difficult to interpret. There are two peaks on the k-parameter contour plot. Since the inclination lines are unique, only the correct one is chosen by the fold test. This shows that the fold test based on the k-parameter alone may lead to incorrect mean directions.

In the eastern part of the study area, no declination anomalies were detected. It seems that the movement of the major Variscan structures since the acquisition of magnetism of the rocks does not contribute to any palaeomagnetically-detectable rotations in the area. Table 3.8a lists the in

situ locality means except for the localities where a fold test can be carried out. For these localities the mean directions derived from the fold tests are given. After being tilt-corrected (with respect to the results of the fold test in each group), the group mean direction is calculated by averaging the site means (see Table 3.8b and Figure 3.25). Figure 3.26 shows the pole position for specimens from Group 1, Group 2 and Group 3. Only the pole from Group 3 (southern Pembrokeshire) deviates from the APWP for southern Britain.

From the AMS studies, the difference of the magnitude of anisotropy between specimens from Group 1 and Group 2 and/or Group 3 is very small ($\sim$ 6%). It can be concluded therefore that the difference in NRM directions between the groups cannot be explained in term of remanence deflection by the susceptibility anisotropy. However, this conclusion is made with the reservation that the AMS studies determined a depositional (primary) effect whereas NRM in South Wales red beds is of secondary origin. AMS appears to be rotated clockwise in the western part of the study area by a somewhat larger amount than the overprinted remanence. This suggests that some rotation took place before this remanence was acquired.

The Permo-Carboniferous overprinting appears to have completely replaced the primary Lower Devonian component in these red beds in the south-western part of the study area whilst this secondary remanence has evidently survived any overprinting influences in Triassic or later times. Partial overprinting of Permo-Carboniferous age is also widely recognised in igneous rocks as far north as Central Wales (Briden and Mullan, 1984; McCabe and Channel, 1990). Maximum palaeotemperatures of the order

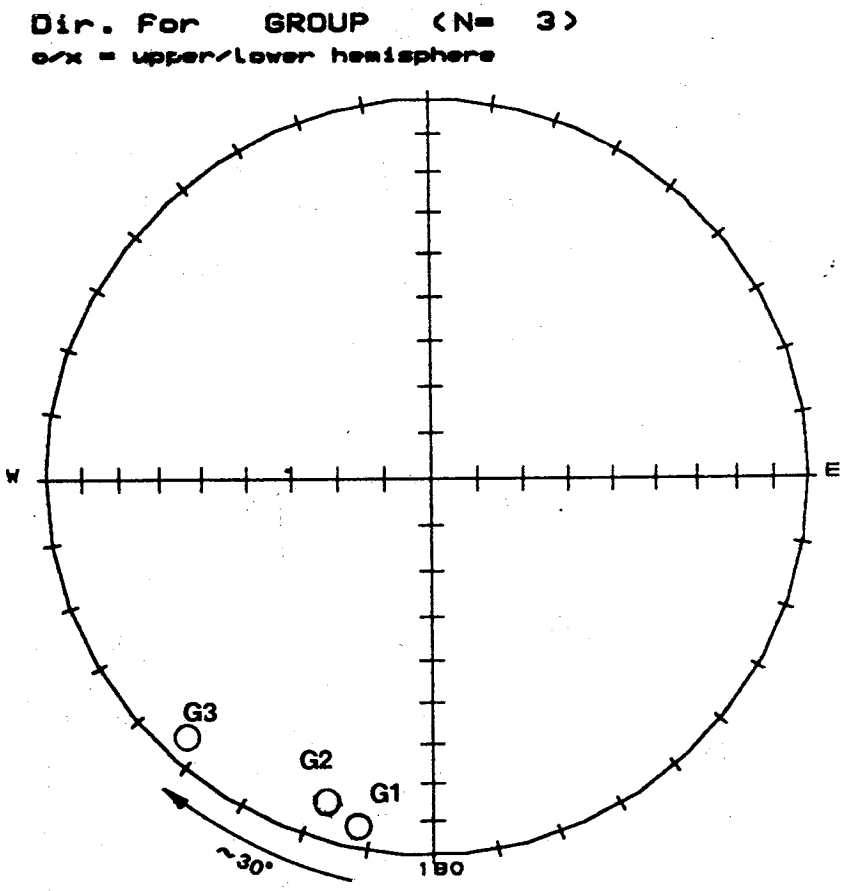

Figure 3.25 Group means in a stereonet. G1 is the group mean for the Brecon/Abergavenny area (Group 1), G2 for the Carmarthen area (Group 2) and G3 for the southern Pembrokeshire area (Group 3).

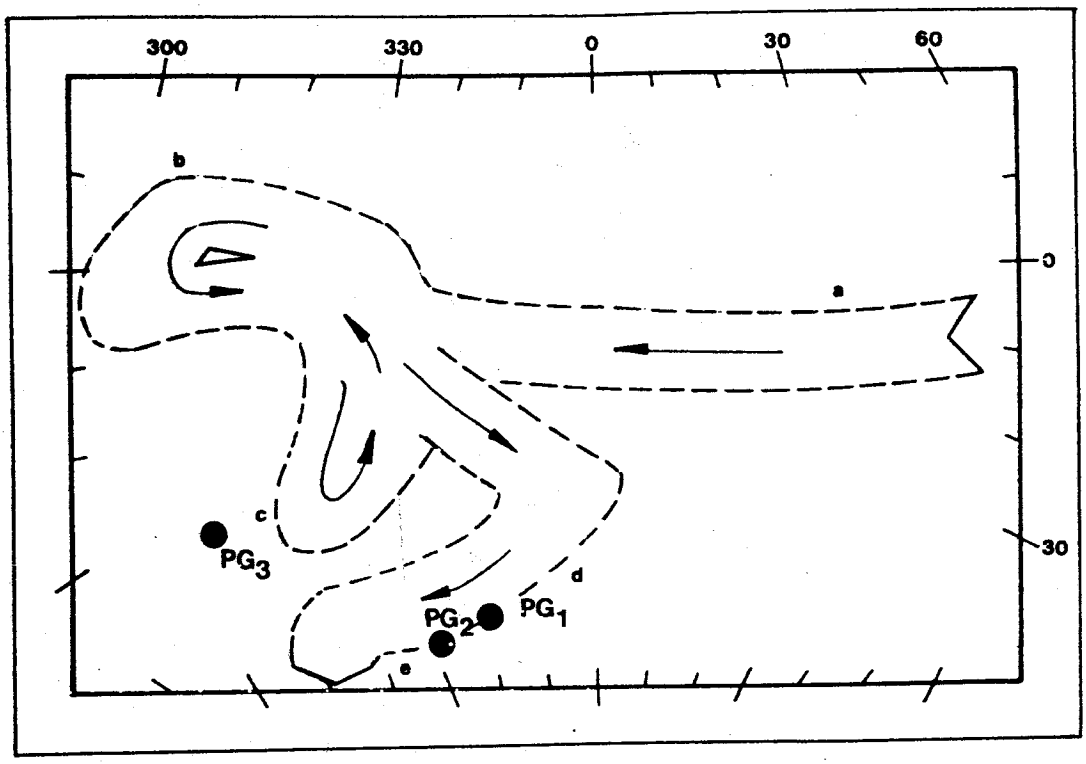

Figure 3.26 Palaeomagnetic poles from Group 1 (PG1), Group 2 (PG2) and Group 3 (PG3). Only PG3 deviates from the APWP for southern Britain (redrawn from Piper, 1987).

Table 3.8a Locality means (in situ except Locality 1,9,10 and 11).

Loc	Dec(°)	Inc(°)	a95	N(site)	k
1	186.6	-6.1	2.2	3	366
2	191.3	1.2	5.5	11	69
3	189.1	-1.7	15.3	2	270
4	190.0	-7.6	13.9	3	79
5	196.7	9.5	7.5	4	151
6	189.0	-10.1	8.8	3	196
7	199.7	-8.1	8.2	3	224
8	210.3	4.0	17.9	2	196
9	207.3	-9.1	1.7	11	124
9*	202.2	-4.9	5.3	4	306
10	211.5	-1.1	4.0	3	113
11	233.8	-10.8	6.9	2	71

Note : * from the hinge zone area

Table 3.8b Group means.

GROUP	Site Lat(°)/Lon(°)	Dec(°)/Inc(°)	a95	k	Pole Lat(°)/Lon(°)
1	51.8/356.9	193/ -4	7	86	-39/340
2	51.8/355.6	198/-10	5	111	-41/332
3	51.6/355.0	223/ -6	55	22	-30/304

of 200° - 300°C were apparently attained in southern Wales during these times (Oliver, 1988), and remagnetisation was probably motivated by fluid motion during orogenic loading.

In contrast, in the north-eastern part of the study area some specimens appear to show a primary Devonian component and a Triassic (?) compo-

nent, although in each case these are sporadic in occurrence. The Permo-Carboniferous overprinting episode here and the location of the area relative to the Variscan front evidently resulted in a less complete replacement and precipitation of remanence-carrying phases. The higher temperature components (95% found in the north-eastern area) represent the acquisition by haematite deposited during the Lower Devonian and the possibly Triassic times. A different type of remanence acquisition is possibly represented by the palaeomagnetic direction of Category C.

The Triassic overprinting and syn-deformational magnetisation at the early stages of folding in the north-eastern area are possibly inter-related. According to the results of the fold test, the age of the deformation in this area is younger than that of the south-western area but still Variscan in age. The Triassic overprinting could be a side effect of later deformation.

CHAPTER 4 MAGNETOSTRATIGRAPHY OF THE WESTPHALIAN A

4.1 Introduction

Magnetostratigraphy is the study of changes in the Earth's magnetic field recorded through stratigraphic successions of sediments and bedded igneous rocks (Turner,1987). One of the areas encompassed by magnetostratigraphy is geomagnetic polarity reversal stratigraphy. By convention the present-day polarity is normal with the N-seeking compass needle pointing to geographic north. Since the work of Matuyama it has been known that the polarity of the Earth's magnetic field has changed from normal to reversed during geological time; these are geomagnetic field reversals (Cox and Hart,1986). The last established reversal occurred about 730,000 years ago from reversed to normal polarity. When rocks are magnetised, they may record and preserve the polarity of the Earth's magnetic field at that time. Since polarity reversals are global, geomagnetic polarity stratigraphy can potentially be used as a means of worldwide correlation of rock units. The correlation would be meaningful if there is some stratigraphic control on the rock being correlated and the magnetisation is essentially a primary phenomenon. The stratigraphic control is achieved by means of fossil or isotopic dating.

4.1.1 Permo-Carboniferous Reversed Superchron

Table 4.1 Nomenclature (Cox and Hart, 1986; Piper, 1987).

duration (My)	name
0.1 - 1	subchron (event)
1 - 10	chron (epoch)
10 - 100	superchron

The chronology of reversals is referred to the polarity time scale (Piper,1987). Table 4.1 shows the nomenclature used to define polarity intervals in the polarity time scale. Prior to times older than ca. 4 - 5 My (million years) it has been established from the chronology of marine magnetic anomalies. Since there is no ocean floor older than 200 My preserved for study, the extension of the polarity time scale to Palaeozoic times requires palaeomagnetic studies of continental sedimentary rocks. Although the palaeomagnetism of Palaeozoic rocks has been studied since the 1950's, much of the remanence record which has been resolved is either composite or secondary and worldwide correlation of magnetic polarities is difficult. It is generally agreed that palaeomagnetic techniques used three decades ago are sub-standard compared to modern techniques and they often failed to recognise remagnetisations. As a consequence, any palaeomagnetic results derived prior to the advent of modern cleaning techniques and component analysis should be re-examined thoroughly.

The duration of the Permo-Carboniferous Reversed (PCR) superchron is believed to be about 70 My long and is the longest period of constant polarity recognised in the Phanerozoic eon. Palaeomagnetists generally agree that the upper boundary of the superchron lies between the Lower and the

Upper Tartarian or within the Upper Tartarian stages of Upper Permian times (Irving and Pullaiah,1976). Recently, Molina-Garza and others (1989) took the upper boundary to be about 251 +/- 4 My based on palaeomagnetic study of the Dewey Lake formation (Late Permian), Northwest Texas. However, the base of the superchron had been a controversial topic for some time and two possible solutions have been proposed. An age younger than Westphalian D was suggested by McMahon and Strangway (1968) while an older age has been proposed by other authors (see below). McMahon reported 4 zones of normal polarity in the Maroon and the Minturn Formation - Vail, Colorado, and she placed the base of the superchron within the Maroon Formation (reported by Miller and Opdyke, 1985). Miller and Opdyke (1985) re-studied the same section and failed to find the normal zones within this section. They proposed that the normal zones recognised by the earlier workers were overprints and suggested that the base of the PCR must lie within the Westphalian C and D or older formations. Roy and Morris (1983) prefer to locate the base of the superchron within the Westphalian A (see Palmer and others, 1985). Irving and Pullaiah (1976) suggested that the lower boundary should be within the Namurian or between the Namurian and Westphalian. Recently, Harland and others (1990) accepted a base for the PCR superchron at 323 My (Kinderscoutian, Namurian).

4.1.2 Previous Results

Palaeomagnetism of British Carboniferous rocks has been studied since the 1950s (Belshé,1957; Everitt and Belshé,1960). However, the reliability of the results has been over-shadowed by identification of the importance of

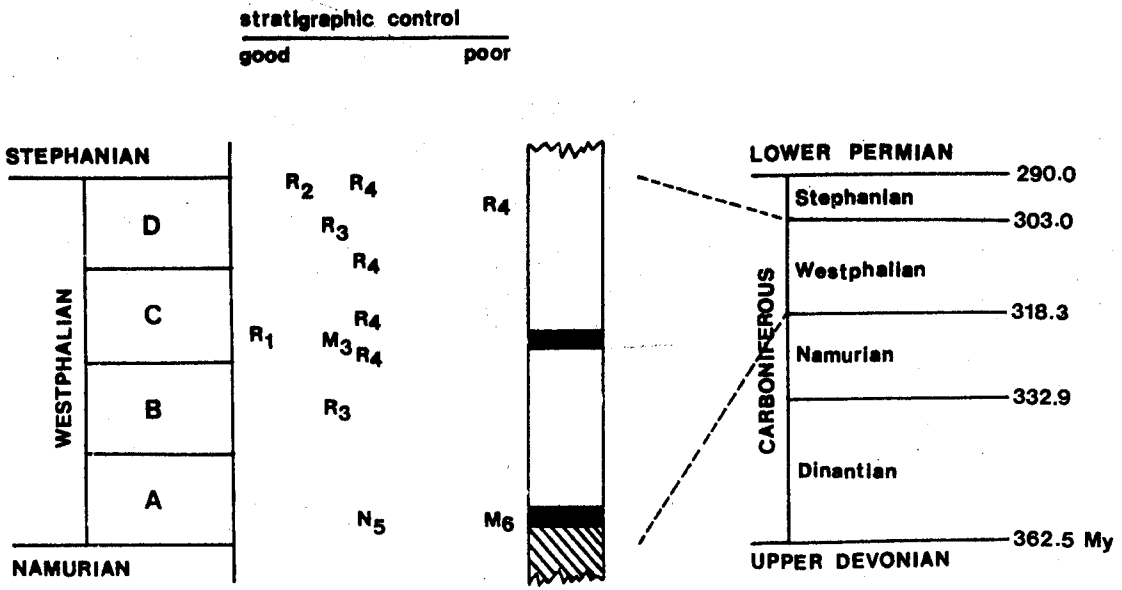

Figure 4.1 Westphalian Magnetostratigraphical Time Scale for the British Isles and north-western Europe. (modified and redrawn from Palmer and others,1985). The age information was taken from Harland and others (1990).

Note :
white strip = reversed polarity (R),
black strip = normal or mixed polarity (N or M).
hatched strip = unreliable published data
Subscripts after R,N or M are referred to
(1) Belsy & Turner (1983)
(2) Tarling and others (1973)
(3) Noltimier & Ellwood (1977)
(4) Birkenmajer and others (1968)
(5) Belshé (1957)
(6) Titman (1971)

remagnetisation in Palaeozoic rocks. Palmer and others (1985) attempted to construct the Carboniferous polarity time scale for the British Isles and northwestern Europe and to correlate this time scale on a worldwide basis. Figure 4.1 shows the Westphalian section of this time scale. Westphalian A is indicated by normal or mixed polarity. However some disagreement can be detected in the palaeomagnetic results which Palmer and others referred to.

For example, the palaeomagnetic direction reported by Titman (1971) from intrusive igneous Carboniferous rocks from Derbyshire does not record a remanence dating from Upper Carboniferous times (Piper and others, 1991). The characteristic Upper Carboniferous palaeomagnetic direction for Britain is shallow in inclination (see Table 3.2, CHAPTER 3) and the steep inclination (-60.7°) derived from these rocks is clearly not an Upper Carboniferous direction although the isotopic age of the rock is 313 +/- 16 My. The age given is probably on the low side due to argon loss and the rock unit is presumed to be older than the Westphalian A and to correlate with Lower Carboniferous lavas in the same area.

Belshé (1957) reported normal polarity within Westphalian A sediments from Lancashire. A better grouping of the palaeomagnetic directions after bedding correction indicated a positive fold test. This suggested that the magnetism pre-dates the deformation. However, the palaeomagnetic direction from these sediments is close to the Triassic direction from Britain. Everitt and Belshé (1960) suggested that these sediments may have been remagnetised during Triassic times. In addition, the remanence may be

composite because it was derived from NRM directions and not studied with thermal or AF magnetic cleaning.

It is therefore concluded that the British Westphalian A rocks have not been studied palaeomagnetically in a proper way, or thoroughly tested in a way sufficient to produce a polarity time scale for these times. The following sections describe a palaeomagnetic study of the Westphalian A rocks from South Wales which has aimed to contribute to this objective. The stratigraphic age of these rocks is well-defined by the faunal content of marine bands.

4.2 Location and Sampling

Figure 4.2 is a generalised geological map of the South Wales Coal measures of Westphalian age. They occur within three separate outcrops: The Pembrokeshire coalfield in the west, the South Wales coalfield main basin in the middle and the small Forest of Dean coalfield in the east (to the east of the area shown on Figure 4.2) (Thomas,1974). The strata lie conformably on the underlying Namurian sediments. Lithostratigraphically, these sedimentary successions are divided broadly into Lower Coal Measures, Middle Coal Measures and Upper Coal Measures. The Lower Coal Measures are equivalent to the Westphalian A, the Middle Coal Measures to the Westphalian B/C and the Upper Coal Measures to the Westphalian C/D divisions used within continental Europe. The boundaries between these divisions are now defined by well dated marine bands although the boundary between Westphalian C and D is not precisely positioned (Barclay,1989). The Gastrioceras Subcrenatum and the Amman (Vanderbeckei) marine

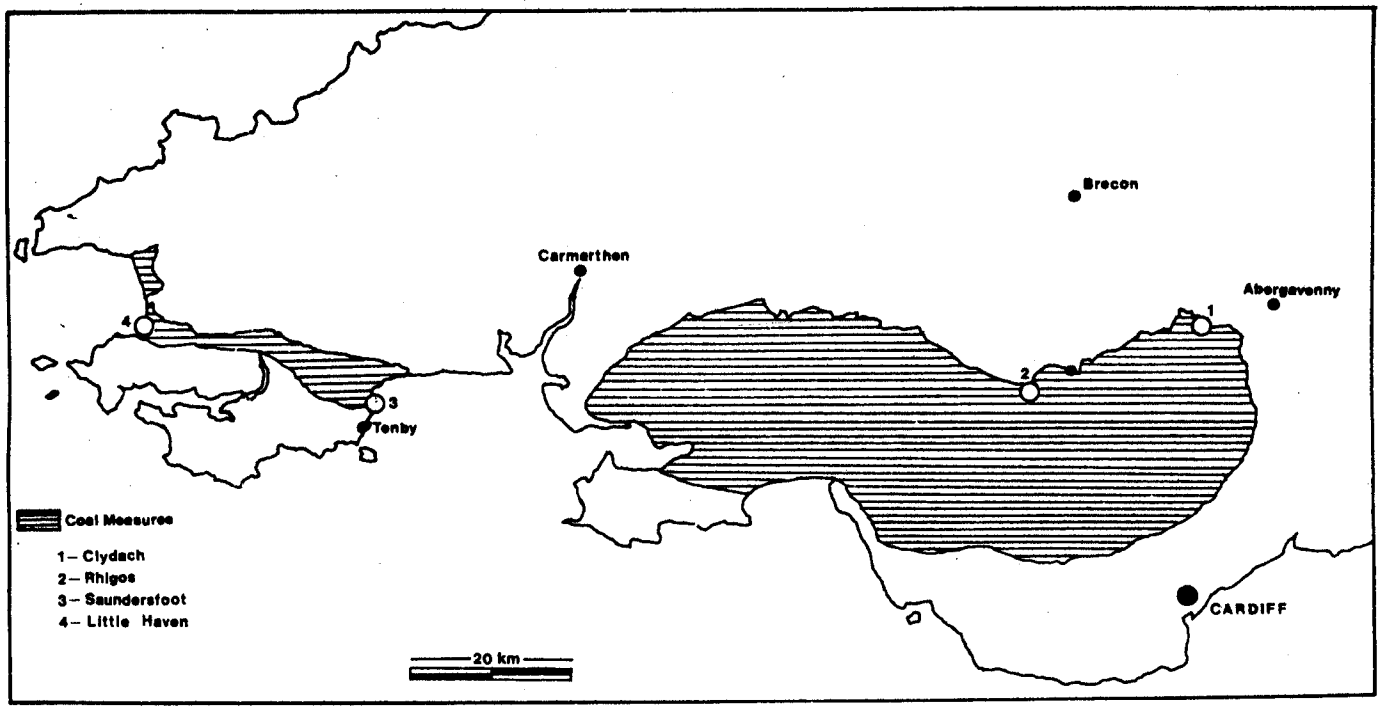

Figure 4.2 Outcrops of Coal Measures in South Wales (George, 1970). Numbers refer to sampling localities

(a)

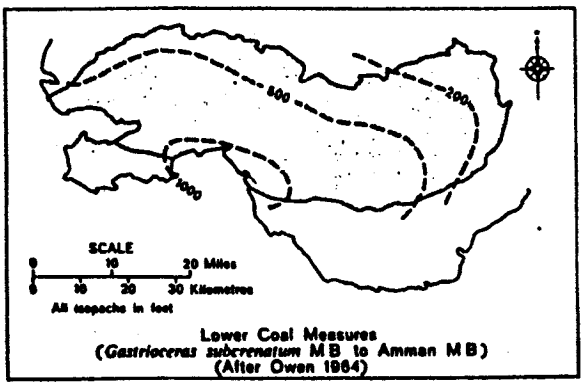

(b)

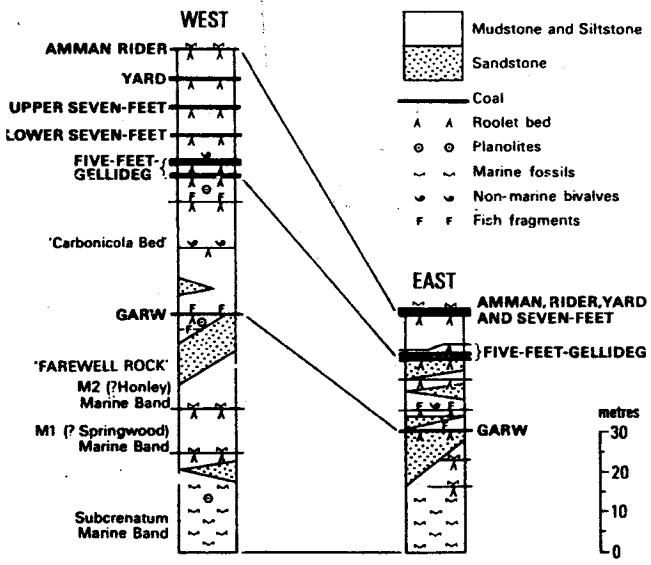

Figure 4.3 Thickness variations of the Westphalian A rocks in the main basin.
(a) Isopachyte diagram (Thomas,1974)
(b) Generalised vertical section (Barclay,1989)

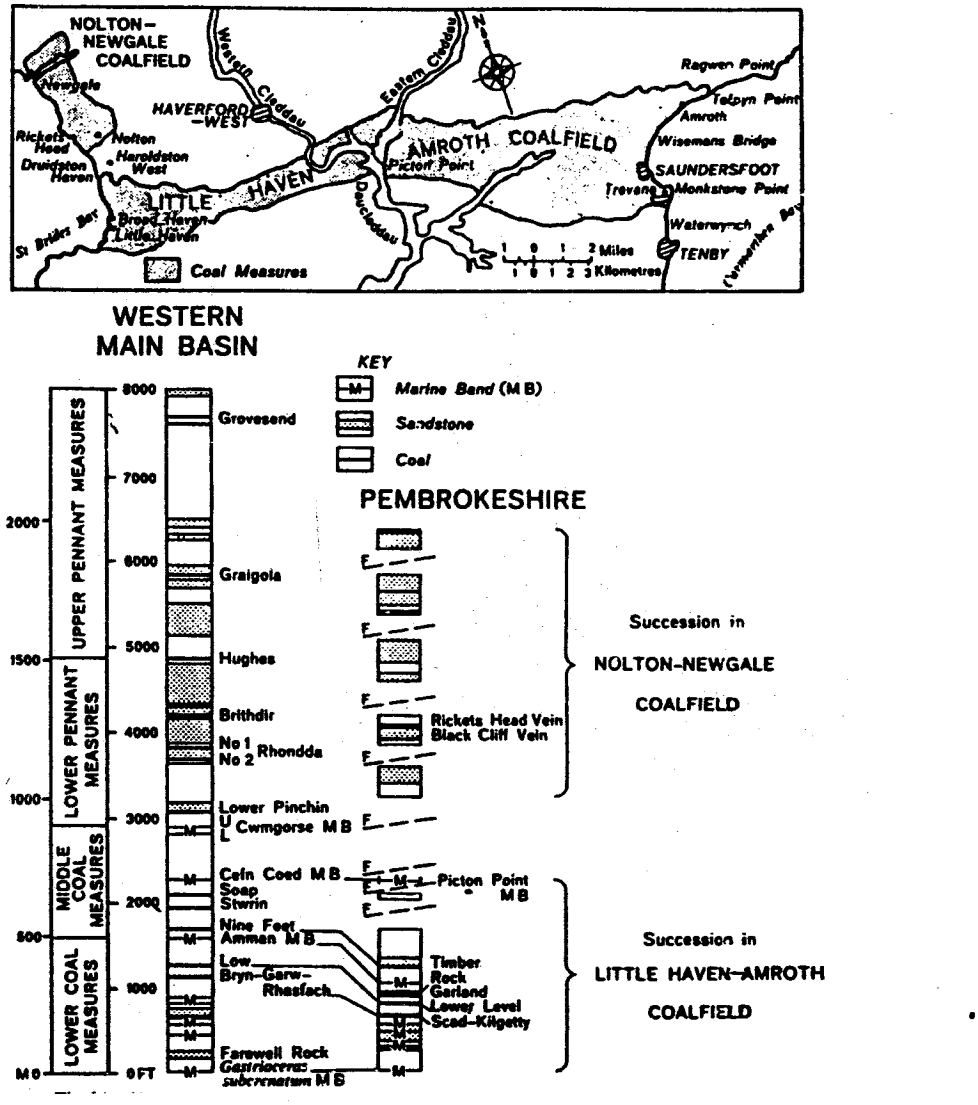

Figure 4.4 Correlation of the Westphalian A rocks in the main basin and in the Pembrokeshire coalfields (Thomas, 1974).

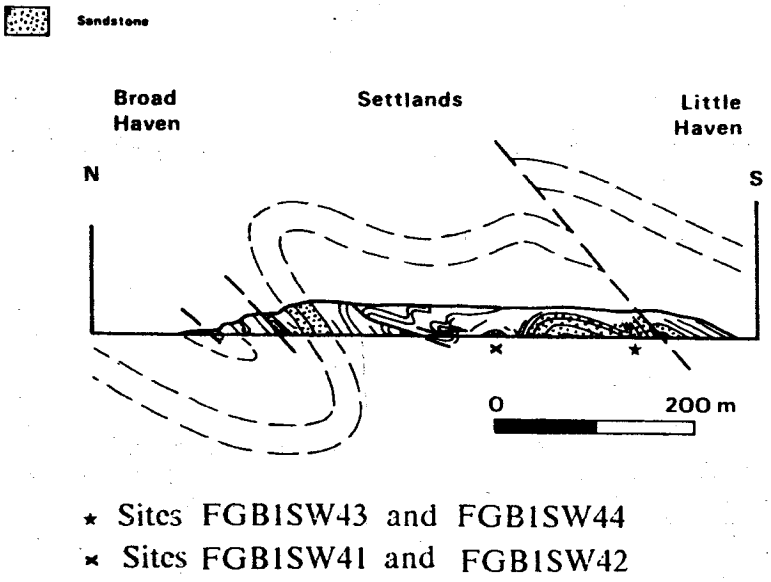

Figure 4.5 Locality 4 (Little Haven). The vertical section is from Hancock and others (1982).

bands are used internationally as the lower and upper boundaries of the Lower Coal measures (Westphalian A).

The Lower Coal Measures can be considered to record an environmental transition from mainly marine recorded by the Namurian deposits to mainly paralic as recorded by the Westphalian. Strata below the Garw coal have few coal seams and plenty of marine bands. In contrast, marine bands are rare and coal seams are thick and common above the Garw coal. A thick sandstone layer just below the Garw coal is known as the 'Farewell Rock'. It indicates that there is no workable coal seam beneath it. Figure 4.3 shows variations in the thickness of the Lower Coal Measures in the main basin. Since some horizons have been preserved and the thinning happened in one direction (to the northeast), it is that likely these variations are not due to erosion only but reflect the extent of the former sedimentary environment.

The Lower Coal Measures in the Pembrokeshire coalfields are found in the Little Haven - Amroth coalfield. The coalfield is a narrow belt stretching from Little Haven (St. Bride Bay) in the west to Amroth (Carmarthen Bay) in the east. The strata have been severely deformed. The correlation of the measures with those in the main basin is shown in Figure 4.4

Four localities were chosen as the sampling areas. Accessibility and exposed outcrops were major constraints in choosing the sampled areas. Locality 1 (Clydach,Brynmawr) yields an almost complete section of Westphalian A rocks. The thickness of these rocks is about 60 metres. The bottom part of the section is exposed in the southern side of the Valley road (A465) and in both banks of a small stream near Llanelly Hill

(Clydach,Brynmawr) the upper part of the section is exposed. The Clydach section seemed to be the best section for the following reasons :

1. Clydach is located in the northeastern part of the main coalfield where the thickness of the Westphalian A rocks is thinner (~ 60 m).

2. Some marker horizons like the Gastrioceras Subcrenatum Marine Band, Farewell Rock and Garw Coal are well defined in the Clydach gorge.

3. At the time of the fieldwork, coal mining activities were mainly on seams above Westphalian A.

However, in the event the resolution of the sampling depended largely on the rock type. The shales which are the dominant lithology in the Lower Coal Measures proved to be too thinly bedded for drilling for palaeomagnetic study. Hence, most of the sampled material is siltstone and sandstones.

Core sampling was used on the bottom part of the section on both sides of the Valley road. Two sites (FGB1SW02 and FGB1SW03) were sampled from two thick beds of Namurian rocks in the northern side of the Head of the Valley road. In the southern side of the road, Westphalian A rocks crop out. Site FGB1SW04 to FGB1SW14 were spread stratigraphically from the base to half-way through the upper boundary. The upper parts of this section can be found in the stream section, near Llanelly Hill. It proved inconvenient to employ core sampling in this part of the section since the location of the rocks proved difficult to locate and the terrain is quite rough.

Hence, block sampling was used on these parts (sites FGB1SW28 to FGB1SW32). The position of these sites from Locality 1 on a stratigraphic column is shown in Figure 4.9.

Only five block samples could be retrieved from the rocks above the Garw coal from Locality 1. To get a better resolution of sampling above the Garw coal. Locality 2 (Rhigos,near Merthyr Tydfil) which comprises a stream section was sampled. Outcrop is found on both side of the stream bank. The rocks sampled from this locality are above the Garw Coal up to the upper boundary of the measures comprising the Amman (Vanderbeckei) marine band (sites FGB1SW20 to FGB1SW26). Site FGB1SW27 is within the Westphalian B but the rock proved very hard to drill in the laboratory and no cores could be retrieved from this sample.

To determine the age of the magnetisation with respect to deformational events, it is advantageous to sample folded beds (section 2.7.1, CHAPTER 2). Since folded beds are rare in the main basin, the sampling was extended to Pembrokeshire where rocks of this age are significantly deformed. Five block samples (site FGB1SW15 to FGB1SW19) from Saundersfoot (Locality 3) were kindly provided by Dr.A.Hartley (University of Wales, Cardiff) from his collection. The results of the fold test ,however, was inconclusive. Core sampling of this area was then carried out in order to clarify the previous results (sites FGB1SW33 to FGB1SW40). Sites FGB1SW33 to FGB1SW36 are from both limbs of the Ladies Cave anticline and the remainder are from a small syncline which is located a few tens of metres from the anticline to the north. The sampling was extended to Locality 4 (Little Haven) (sites FGB1SW41 and FGB1SW44). Sites FGB1SW43 and

FGB1SW44 were sampled from both limbs of a major fold whereas sites FGB1SW41 and FGB1SW42 were from a smaller fold, north of the major fold (see Figure 4.5).

Table 4.2 is a summary of the location and sampling technique used in the field work.

Table 4.2 Locality and National Grid Reference.

Loc.	area	Nat.Grid	Lat./Lon.	sampling
1	Clydach	c.SO(2320,1350)	51.80/356.85	core
1	Clydach	c.SO(2180,1170)	51.80/356.85	block
2	Rhigos	c.SN(9210,0580)	51.73/356.42	block
3	Saundersfoot	c.SS(1390,0440)	51.71/355.31	core
4	Little Haven	c.SM(8520,1250)	51.76/354.90	core

The results from Clydach (Locality 1) were chosen as a reference for the other localities for the following reasons :

- block and core sampling were used
- the area has not been disturbed severely
- a complete section of Westphalian A rocks was sampled.

However, the age and the stability of the magnetisation would be inferred from the results of a fold test from the Pembrokeshire samples.

4.3 Laboratory Measurement

Palaeomagnetic measurements were carried out in the Geomagnetism Laboratory, Department of Earth Sciences and Isothermal Remanence Magnetisation (IRM) acquisition in the Rock Magnetic Laboratory, Department of Geography, University of Liverpool. Most cores were measured with a Molspin spinner magnetometer and the measurements were carried out in a low field cage (see section 2.5, CHAPTER 2). Since previous AF demagnetisation studies of these specimens as part of an undergraduate project had shown that this method was not effective (Dr. J. Shaw, personal communication), thermal demagnetisation was then chosen as a cleaning method in the present study. Thermal demagnetisation was also employed by Noltimier and Ellwood (1977) in palaeomagnetic studies of South Wales coals (within Westphalian B, C and D). The maximum temperature at which the NRMs of their samples could be tested was 330°C. Above this temperature the direction became unstable.

Three hundred and thirty two specimens (74 from block samples) were measured for their NRMs and 239 specimens (64 from block samples) were subjected to stepwise thermal demagnetisation. Twenty of these were measured on a SQUID magnetometer since their intensities were below, or close to, the noise level of the Molspin spinner magnetometer. An MM (Magnetic Measurement) thermal demagnetiser located in the cage was used to demagnetise the specimens. On average the specimens were subjected to stepwise thermal demagnetisation up to 500°C in steps of 50°C. Sixteen cores were further demagnetised to temperatures above 650°C.

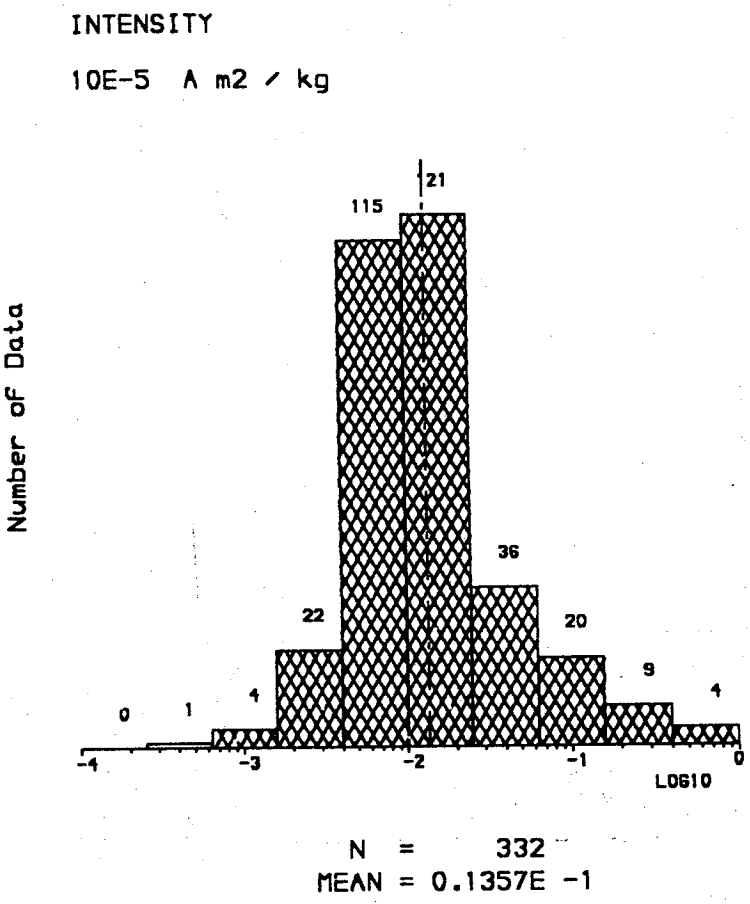

Figure 4.6 Histogram of the NRM intensities. The mean is comparable to the noise level of the spinner.

10E-5 A m²/kg.

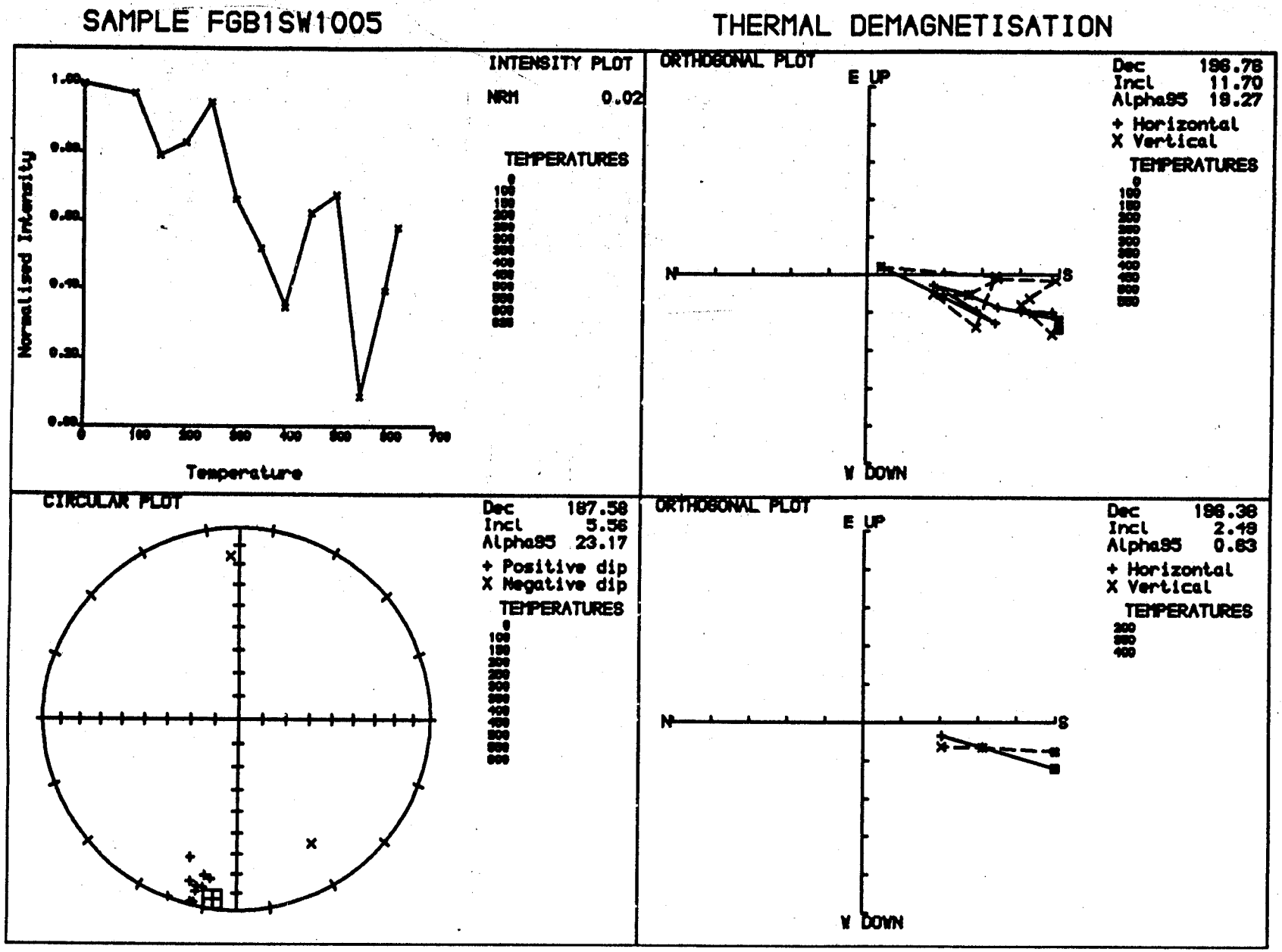
SAMPLE FGB1SW1005
THERMAL DEMAGNETISATION
INTENSITY PLOT
NRM 0.02
TEMPERATURES
Normalised Intensity
Temperature
ORTHOGONAL PLOT
E UP
N
S
W DOWN
Dec 196.76
Incl 11.70
Alpha95 18.27
+ Horizontal
X Vertical
TEMPERATURES
CIRCULAR PLOT
Dec 187.58
Incl 5.56
Alpha95 23.17
+ Positive dip
X Negative dip
TEMPERATURES
ORTHOGONAL PLOT
E UP
N
S
W DOWN
Dec 196.38
Incl 2.49
Alpha95 0.63
+ Horizontal
X Vertical
TEMPERATURES

Figure 4.7b A typical example of palaeomagnetic results (SQUID). The intensity unit is 10E-8 A m^2/kg.

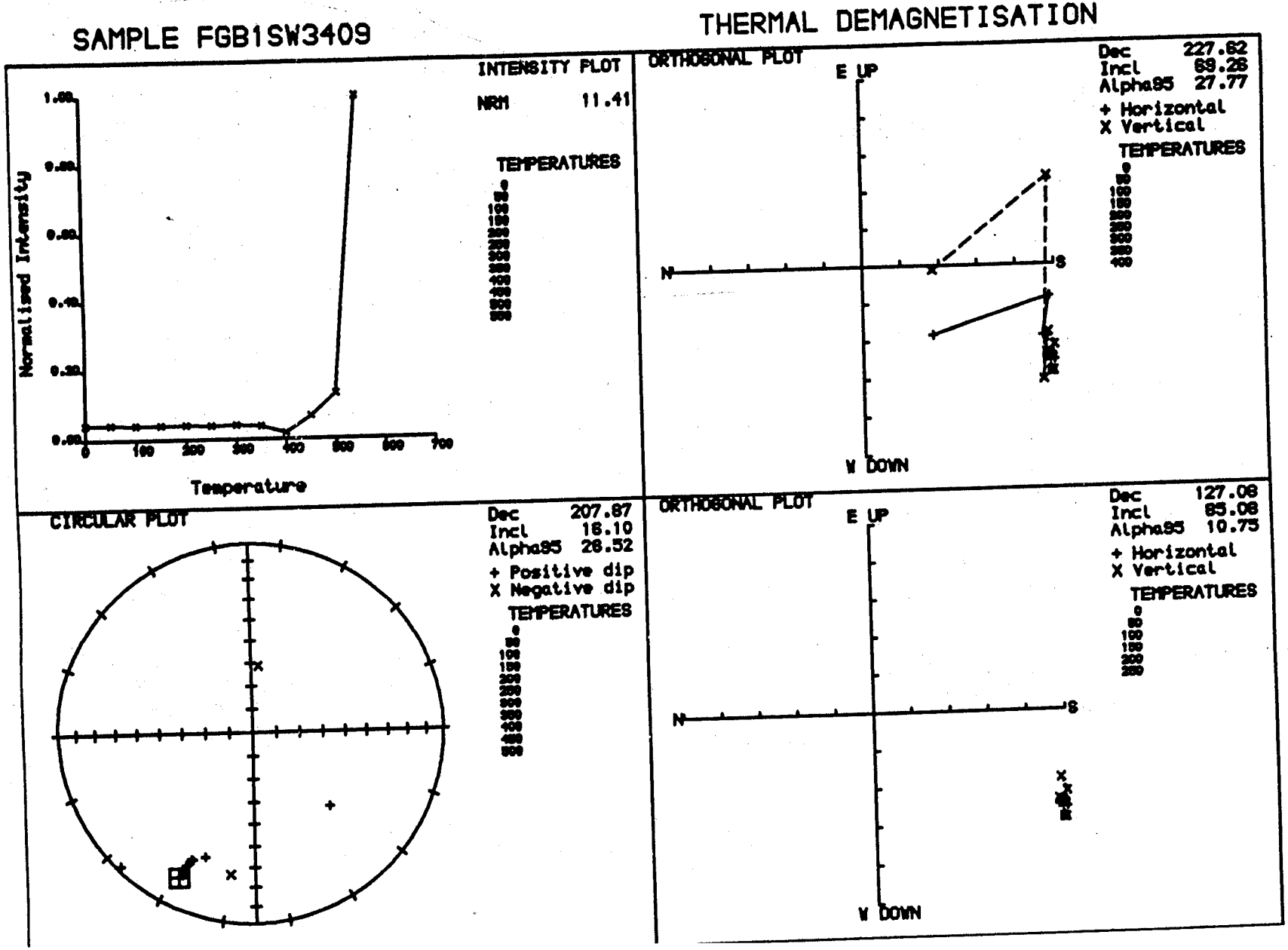

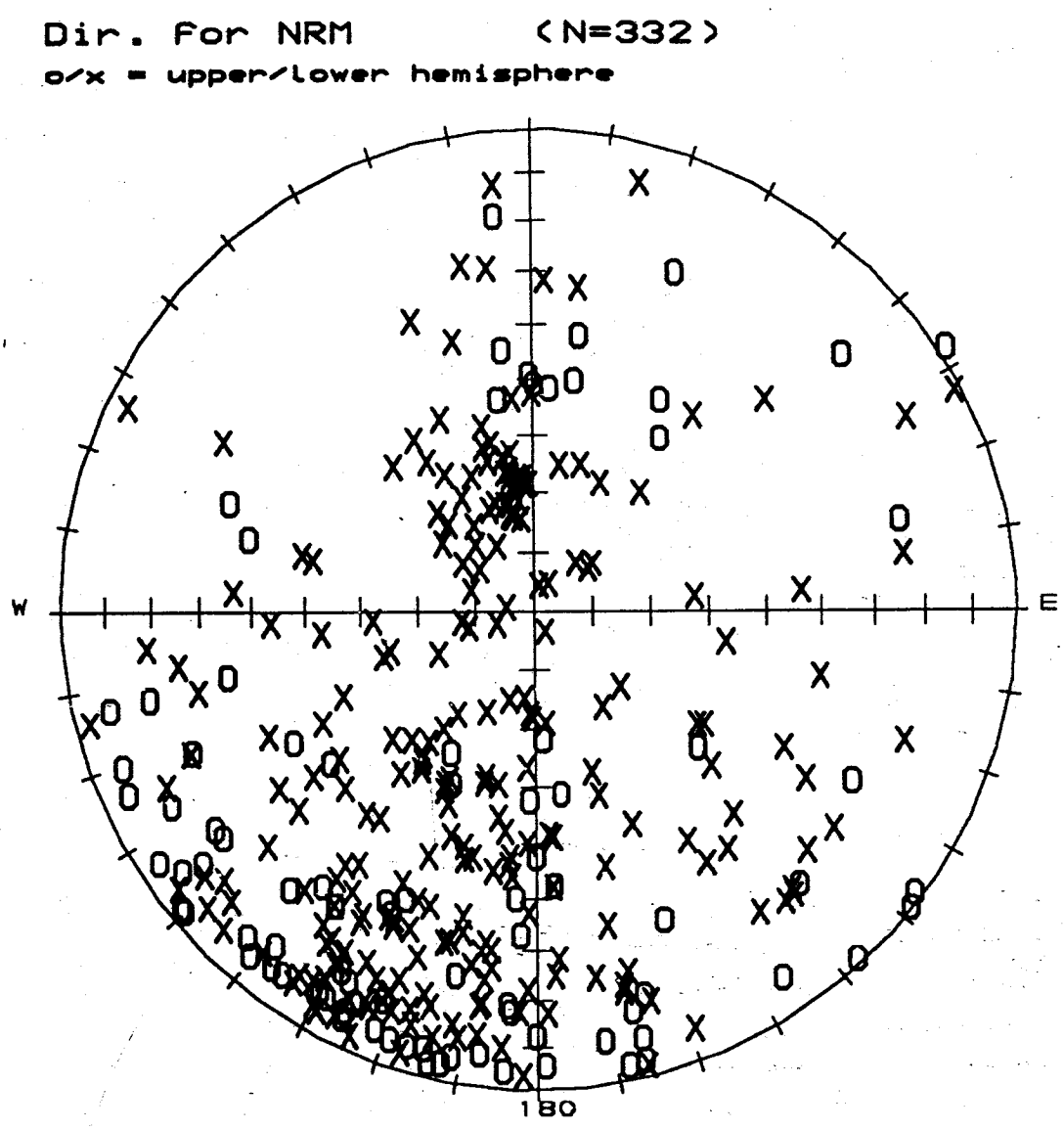

Figure 4.8a Equal area projection of in situ NRM directions. Some directions are clustered about the present Earth's field direction.

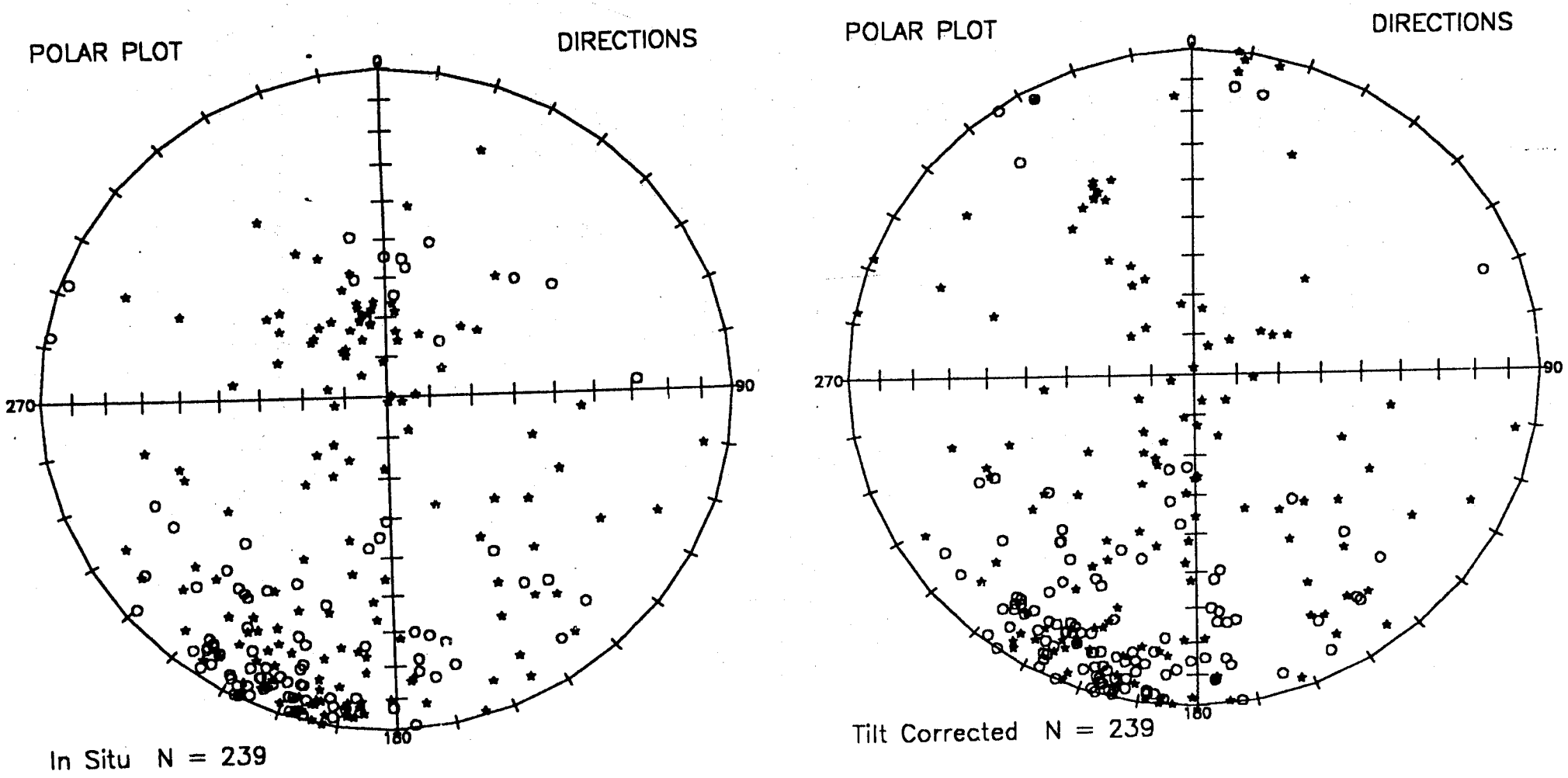

Figure 4.8b Equal area projection (polar) of specimen directions (in situ and tilt corrected). Star (circle) symbol = lower (upper) hemisphere.

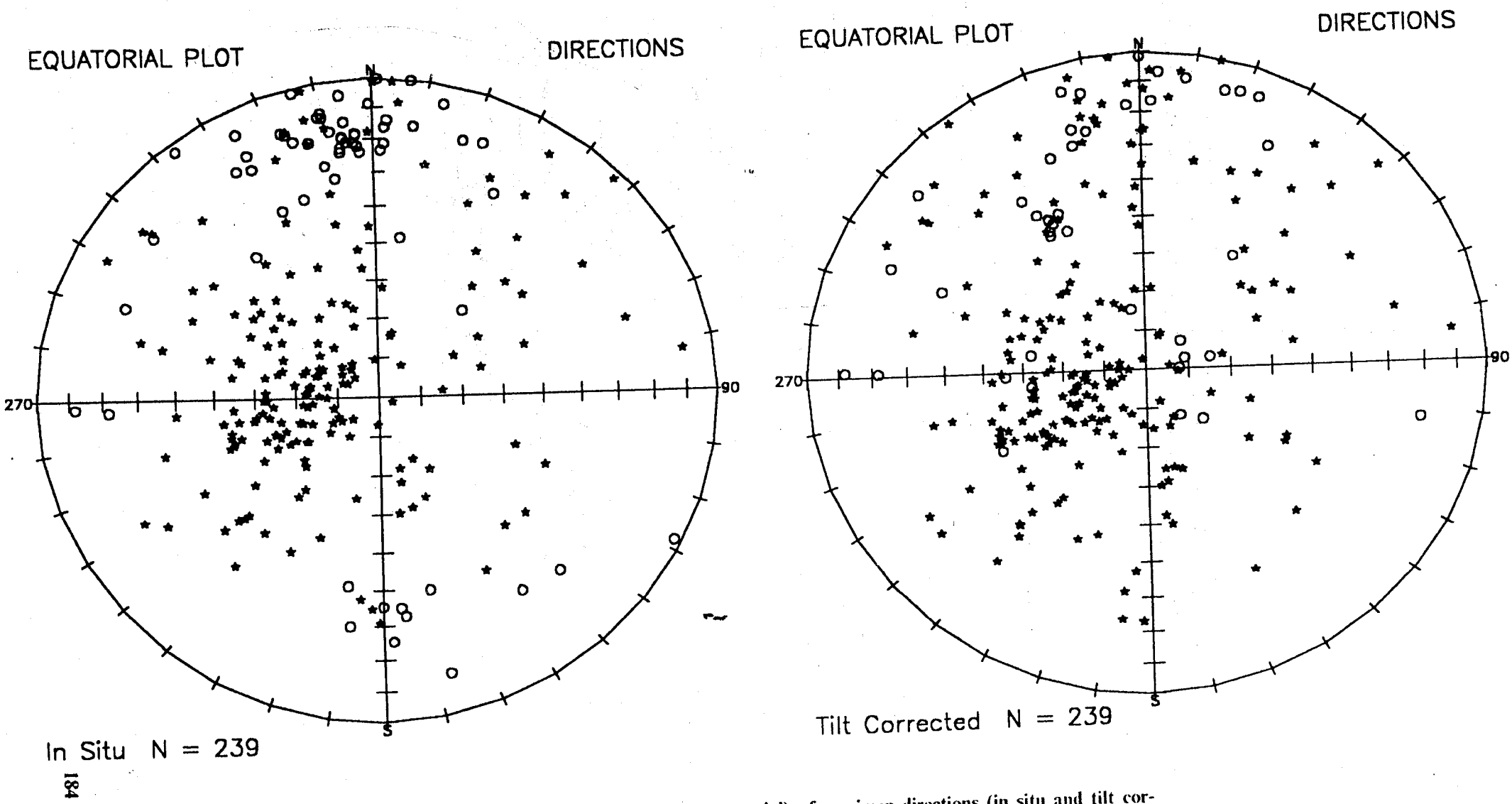

Figure 4.8c Equal area projection (equatorial) of specimen directions (in situ and tilt corrected). Star (circle) symbol = near (far) side.

Due to their low NRM intensities (see Figure 4.6), most samples did not produce smoothly decreasing intensity plots or single components on orthogonal plots. Figure 4.7 shows some examples of the results. Hence, the orthogonal plots could not be used to isolate components and the mean direction at specimen level had to be determined by application of Fisherian analysis to directional groupings to find the mean direction. In general, most specimens were stable up to 350°C-400°C. The mean direction for each specimen was taken by averaging these stable directions (see Table A-2, APPENDIX A). Figure 4.8a shows the individual NRM directions before cleaning. Figure 4.8b and Figure 4.8c show the directions after cleaning. It is observed that the essentially continuous distribution between present Earth's field directions and a SSW directed shallow direction becomes more clearly bimodal with cleaning so that some directions remain close to the present Earth's field but most of the others become more concentrated in the SSW shallow direction.

One hundred and twenty eight specimens show shallow inclinations in a direction SSW - NNE which is a characteristic of the Upper Carboniferous field direction for this area (see Table 3.2, CHAPTER 3). Only one specimen from site FGB1SW02 (Upper Namurian) has normal polarity (FGB1SW0217,see Table A-2,APPENDIX A) and the rest, including the whole section of the Westphalian A rocks, have reversed polarity.

The in situ (except sites FGB1SW15,FGB1SW17 and FGB1SW19 which are fully tilt-corrected; see the end of this section) mean direction for these Westphalian A directions (109 cores) is Dec/Inc = 194.5°/3.7° with alpha-95 = 7°, N=26 sites (sites FGB1SW02 and FGB1SW03 are ex-

cluded since they are from Upper Namurian rocks, see Table 4.3). This corresponds to a pole position at Lat/Lon = 35° S/339° E. However, it is apparent that this analysis can be more refined. The geology in the Pembrokeshire area is very complex and it seems that the tilt adjustment influences many of the palaeomagnetic directions. For example, sites FGB1SW15, FGB1SW17 and FGB1SW19 have to be fully tilt-corrected in order to give the Upper Carboniferous direction while, sites FGB1SW35 and FGB1SW36 have to be left in situ to stay in this direction (see Table 4.3).

To exclude the results from this area as later overprints may be justified. Most specimens from Rhigos (Locality 2, site FGB1SW22 to FGB1SW24) are poorly-stable and showed large alpha-95 values; only 3 specimens out of 25 contribute to the site means (see Table A-2, APPENDIX A). The palaeomagnetic results from this locality are therefore also excluded. The mean direction from Locality 1 (Clydach, Brynmawr) may be considered as representative of the Westphalian A direction from South Wales although a primary origin cannot be confirmed by a fold test. Figure 4.9 shows results from the Clydach section. The in situ mean direction for 16 sites (69 specimens) is Dec/Inc = 193.7°/2.2° with alpha-95 = 6.1°. This corresponds to a pole position at Lat/Lon = 35.9° S / 339.9° E (dp=3.1° and dm=6.1°) which is close to other pole positions from Upper Carboniferous rocks from southern Britain (see Figure 4.10). However, if this palaeofield in situ direction is compared to the expected directions for the area (see Table3.2 for Group 1), it is close to younger times (~ 295 My; cf Westphalian A (319-310 My)). Since the strata are dipping to the south (see Table 4.3), the bedding correction will rotate the palaeomagnetic vector

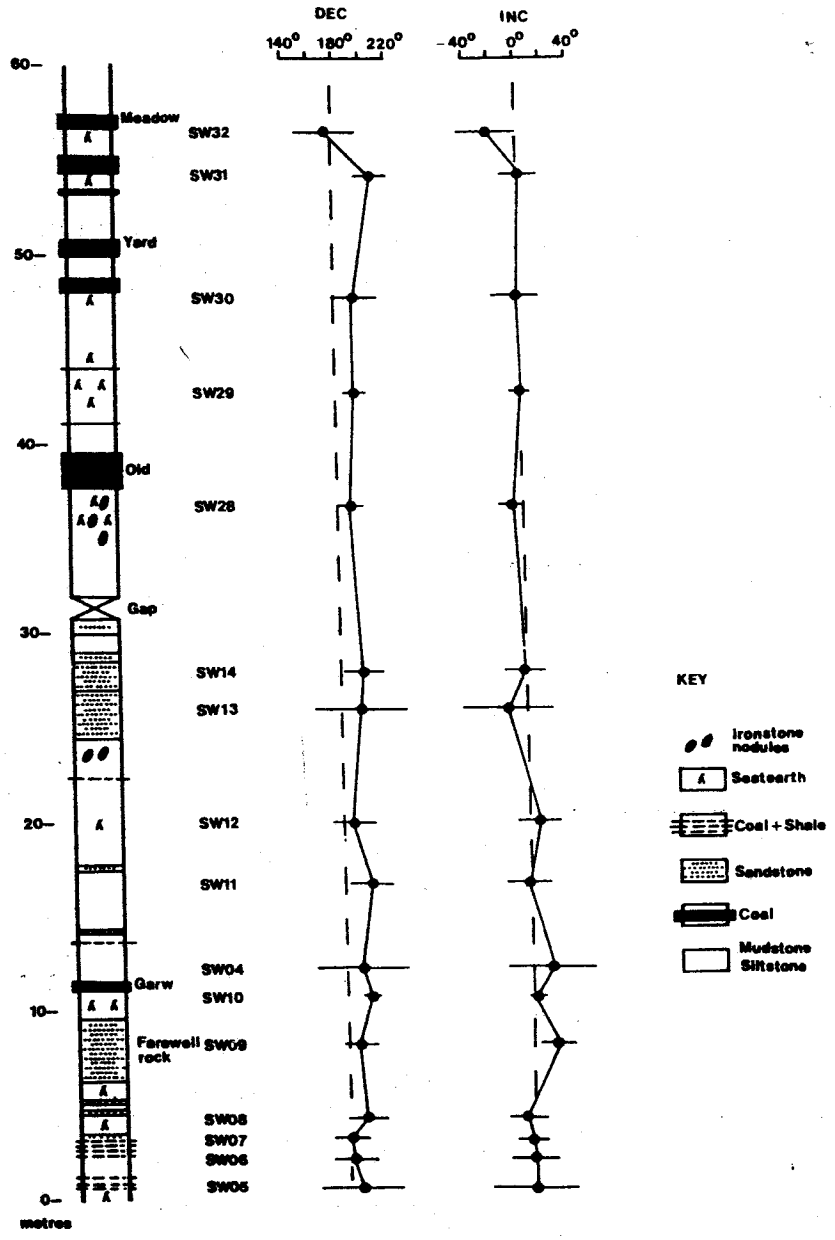

Figure 4.9 In situ palaeomagnetic results from the Clydach section. The information on the lithology is from Barclay (1989). The lower part is from the Clydach gorge section and the upper part is from a borehole section in Blaenant (the nearest section for sites FGB1SW28 - FGB1SW32).

Figure 4.10 The position of the Westphalian A pole from this study on the APWP for southern Britain (modified and redrawn from Piper, 1987). The position of the pole reflects that the Westphalian A rocks from Clydach (Brynmawr) escape from younger overprints.

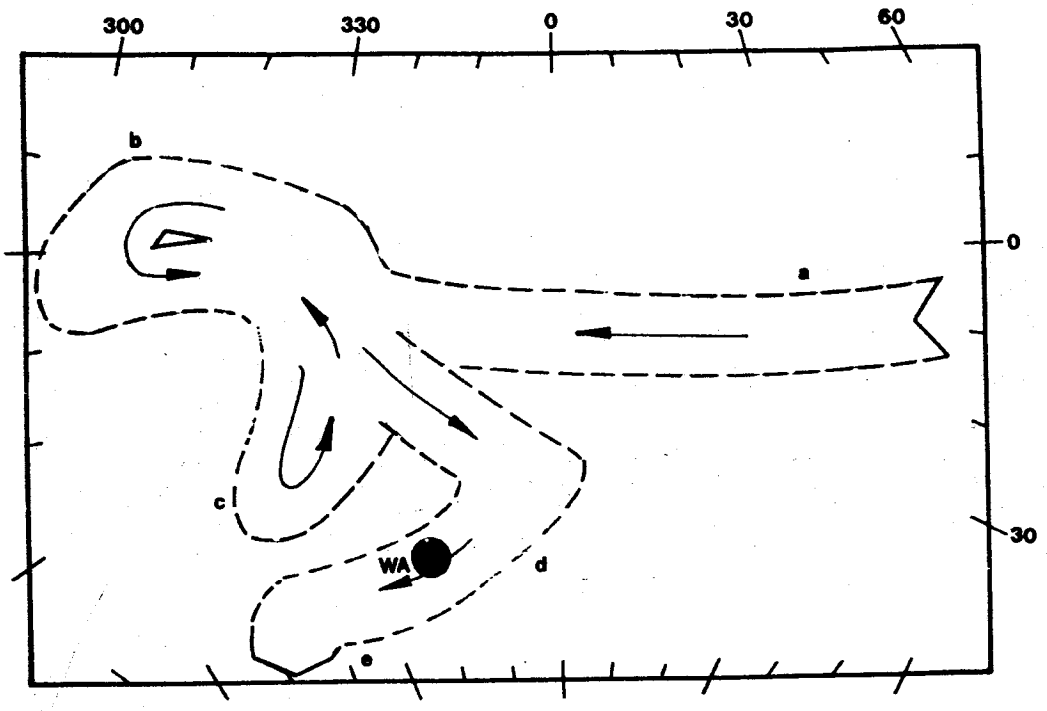

WA : Westphalian A (South Wales) pole

a – U. Ordovician / L. Silurian
b – M. Silurian / L. Devonian
c – M. / U. Devonian
d – U. Carboniferous
e – Permian

Table 4.3 Site means directions.

SITE	Dec	Inc	Tilt	Dir	CDec	CInc	N(n)	k
FGB1SW02	208.1	2.5	8	173	208.1	-4.0	7(22)	17
FGB1SW03	206.5	-2.6	8	173	206.9	-9.2	12(22)	10
FGB1SW04	193.3	18.7	7	175	192.7	12.1	3(12)	14
FGB1SW05	189.9	4.0	7	175	189.8	-2.8	4(8)	9
FGB1SW06	185.8	5.0	7	175	185.8	-1.9	1(4)	-
FGB1SW07	199.7	1.9	7	175	199.7	-4.4	6(9)	26
FGB1SW08	194.8	-1.9	7	175	195.0	-8.5	6(9)	22
FGB1SW09	191.7	24.2	7	175	190.9	17.5	1(4)	-
FGB1SW10	199.5	6.7	7	175	199.3	0.4	9(10)	93
FGB1SW11	201.5	1.9	7	175	201.6	-4.4	4(6)	33
FGB1SW12	188.3	10.9	7	175	188.1	4.0	5(8)	24
FGB1SW13	195.9	-11.7	7	175	196.6	-18.3	3(6)	13
FGB1SW14	198.2	1.1	7	175	198.3	-5.4	6(7)	20
FGB1SW15	357.7	-55.3	110	359	179.8	-14.7	5(5)	124
FGB1SW17	035.3	-56.3	104	4	166.7	-15.0	5(5)	21
FGB1SW19	207.6	-9.5	38	17	208.9	27.8	5(5)	21
FGB1SW22	194.9	16.1	10	79	191.9	20.2	2(5)	42
FGB1SW24	209.7	21.4	15	154	206.0	12.5	1(5)	-
FGB1SW28	189.5	-6.1	8	155	190.2	-12.7	5(5)	69
FGB1SW29	193.3	1.6	7	200	193.3	-5.4	5(5)	89
FGB1SW30	194.1	-1.0	10	183	194.3	-10.8	5(5)	20
FGB1SW31	207.6	2.4	6	172	207.6	-2.4	4(5)	49
FGB1SW32	173.6	-23.1	12	161	175.1	-34.8	2(4)	113
FGB1SW33	210.5	13.7	38	180	211.5	-19.2	5(7)	9
FGB1SW34	206.9	35.0	47	178	201.5	-7.7	5(5)	23
FGB1SW35	200.5	5.9	71	18	208.8	76.6	4(9)	7
FGB1SW36	196.2	-25.0	82	18	194.9	57.00	5(7)	15
FGB1SW42	186.5	-5.5	47	188	185.5	-52.4	1(4)	-

Note :
N(n) = number of specimens accepted (demagnetised)
Dec/CDec = in situ/tilt-corrected declination
Inc/CInc = in situ/tilt-corrected inclination
k = Fisher precision parameter
Tilt/Dir = bedding correction (Dir = direction of the tilt)

even closer to the expected palaeofield direction at the times when the climax of the Variscan orogeny in South Wales occurred (~ 280 My).

In summary, although the phenomenon of the geomagnetic field for staying in one polarity for a long time is not uncommon one, the palaeomagnetic result presented here is unable to confirm whether the palaeofield during the Westphalian A times is overwhelmingly in a reversed state or not. The reason for this is that the observed palaeofield is close to a palaeofield for younger times. If these rocks was remagnetised during the climax of the

Variscan orogeny, the remagnetisation in South Wales probably occurred in most types of rocks except coals. Noltimier and Ellwood (1977) reported normal and reversed horizons within the Westphalian B, C and D coals from South Wales (see also Figure 4.1). If these coals were also remagnetised, the normal horizons would not have been detected by these authors since the polarity of the geomagnetic field at the times of remagnetisation is known to be in a reversed state (see CHAPTER 3 Palaeomagnetism of Old Red Sandstones, South Wales). The study of magnetostratigraphy during Westphalian A times must still be carried out elsewhere in the country where younger overprints are thought to be unknown or to restricted to special type of rocks which escaped from remagnetisation, for example South Wales coals (Westphalian A).

Directions for site FGB1SW15, FGB1SW17 and FGB1SW19 (block samples from Locality 3 (Saundersfoot)) are more scattered before bedding correction (see Figure 4.11). A better grouping is achieved if the site means are fully tilt-corrected. The results of this fold test indicate that this remanence has been essentially stable at least since the deformation occurred although it should be noted that it was not possible to resolve a component structure in these samples.

However, another fold test on 20 core samples from the same locality suggests that the magnetisation occurred during folding (Figure 4.12). The specimens were measured with a SQUID magnetometer (see Table 4.4 and Table A-2, APPENDIX A). The SQUID magnetometer is about ten times more sensitive than the Molspin magnetometers. Due to the shortage of time, however, only 20 cores were measured with this instrument (see Table

4.4 or Table A-2, APPENDIX A). The process of demagnetising the specimens was also stopped at 550°C since the intensities of the specimens were consistently increasing and above 400°C the directions became unstable. It was clear that chemical changes were taking place in the furnace and that this was the maximum temperature to which the NRM could be tested. Linear segments in the orthogonal plots could still not be recognised to isolate components and the mean direction for each specimen was calculated in the same way as for those measured on the spinner magnetometer.

Specimens were taken from limbs of a chevron fold (the Ladies Cave anticline; sites FGB1SW33 to FGB1SW36). The fold possesses long straight limbs and a narrow hinge zone. The anticline is inclined with the axial surface dipping steeply south (Hancock and others,1982). The northern limb is steeper than the southern limb. It can be seen clearly (see Figure 4.12a and 4.12b and Table B-2, APPENDIX B) that the palaeomagnetic directions from both limbs are in better agreement if both limbs are unfolded by 32% (with or without plunge correction). Although no k-values pass the McElhinny test, there is a slight increase in the values and the peak of the contour is shifted toward more positive inclination. More sites are needed in order that the k_2 value becomes lowered. If each limb is unfolded separately (the new method, see section 2.7.1, CHAPTER 2) the results will depend on the chosen inclination used as the expected palaeomagnetic direction. However, from the contour of the k-parameter (see Figure 4.12), it is clear that the k values which are higher than 30 ($\sim$ 5% less than the k maximum) cover a quite wide area. This suggests that there is uncertainty in the expected palaeomagnetic direction, in this case especially in the inclination. The expected in situ inclination could be from about -10° to +25°

Figure 4.11 Equal area projection of the site mean directions from sites FGB1SW15, FGB1SW17 and FGB1SW19 (block samples from Saundersfoot, Pembrokeshire). The directions are better grouping after bedding correction.

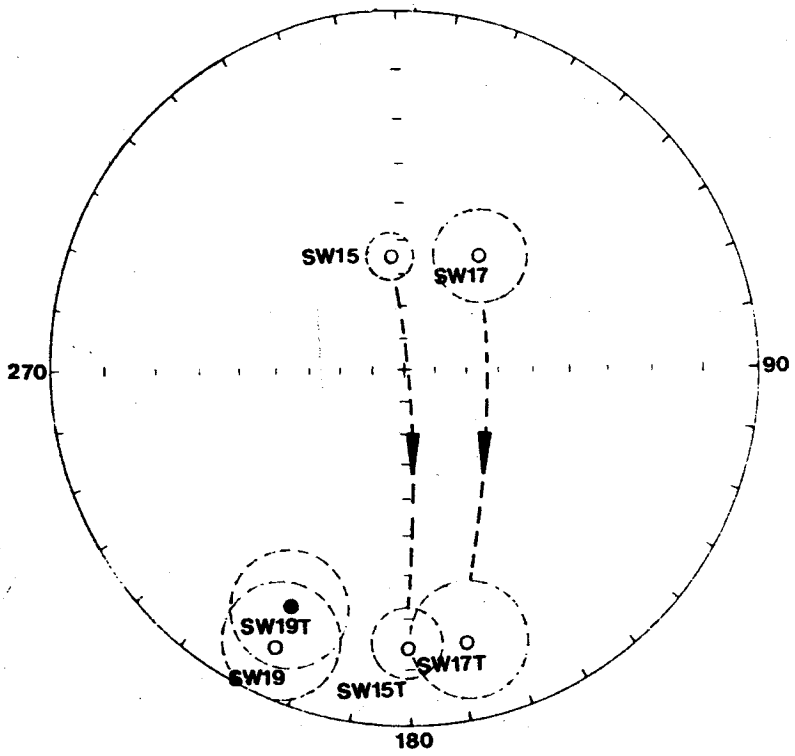

Figure 4.12 The fold test on the specimens from the Ladies Cave anticline, Saundersfoot (Locality 3). The rock acquired magnetisation during folding (Variscan). See text.

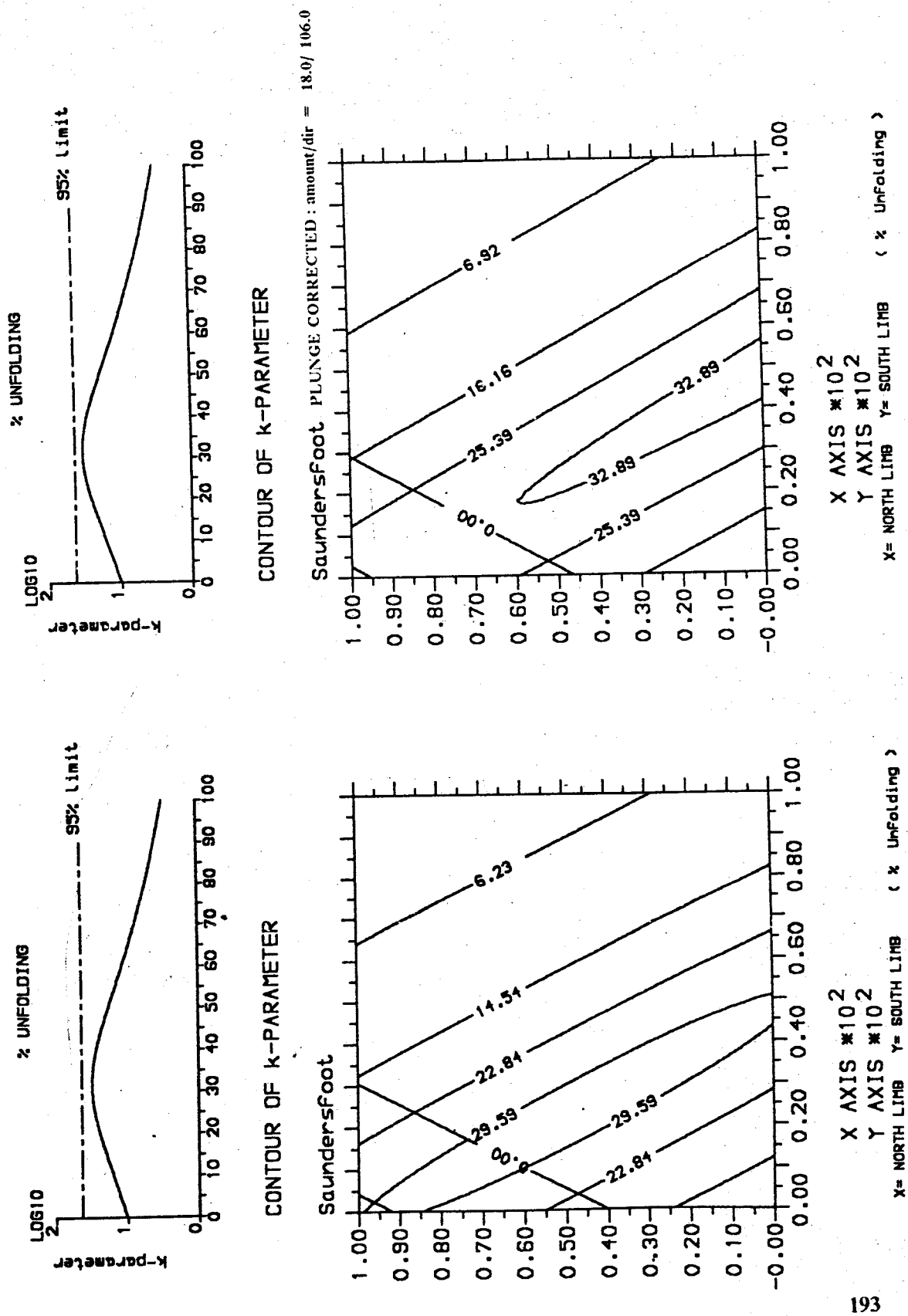

without any significant differences resulting in the k values. One conclusion that can be drawn from this fold test is that the age of the magnetisation is syn-deformational which in turn will constrain further the range of the expected inclination, say from about -10° to +10°. The interpretation here is, therefore, that the age of magnetisation of the Westphalian A is syn-deformational not pre-folding as suggested by the result from the block samples (sites FGB1SW15, FGB1SW17 and FGB1SW19). Results discussed below indicate the reason why the fold test result from the block samples is doubtful.

Core samples from Pembrokeshire fall into two groups; the first group (29 specimens) are those with intensities well-above the noise level of the spinner and a second group (the majority: 90 specimens) which have very weak intensities. Twenty specimens from the second group were measured with the SQUID magnetometer. The specimens from Pembrokeshire show a large within-site scatter (see Table 4.4). The in situ directions of specimens measured with the spinner have steep inclinations. In contrast, the specimens measured with the SQUID have shallow inclinations. One possible explanation of this observation is that the specimens which have higher intensities have been remagnetised recently due to weathering. This is probable because their palaeomagnetic directions (in situ) are very close to the present Earth's magnetic field. Due to the attitude of some beds, some directions after bedding correction show shallow inclinations which could mistakenly be interpreted as an Upper Carboniferous direction. Hence, only the shallow in situ directions are accepted here as ancient remanences. When these directions are adjusted for tilt (without plunge correction) within the expected inclination range of -10° to +10°, the fold test yields Dec/Inc =

Figure 4.13a IRM acquisition curves for samples SW08 and SW10. The intensity unit used is 10E-5 A m^2/kg.

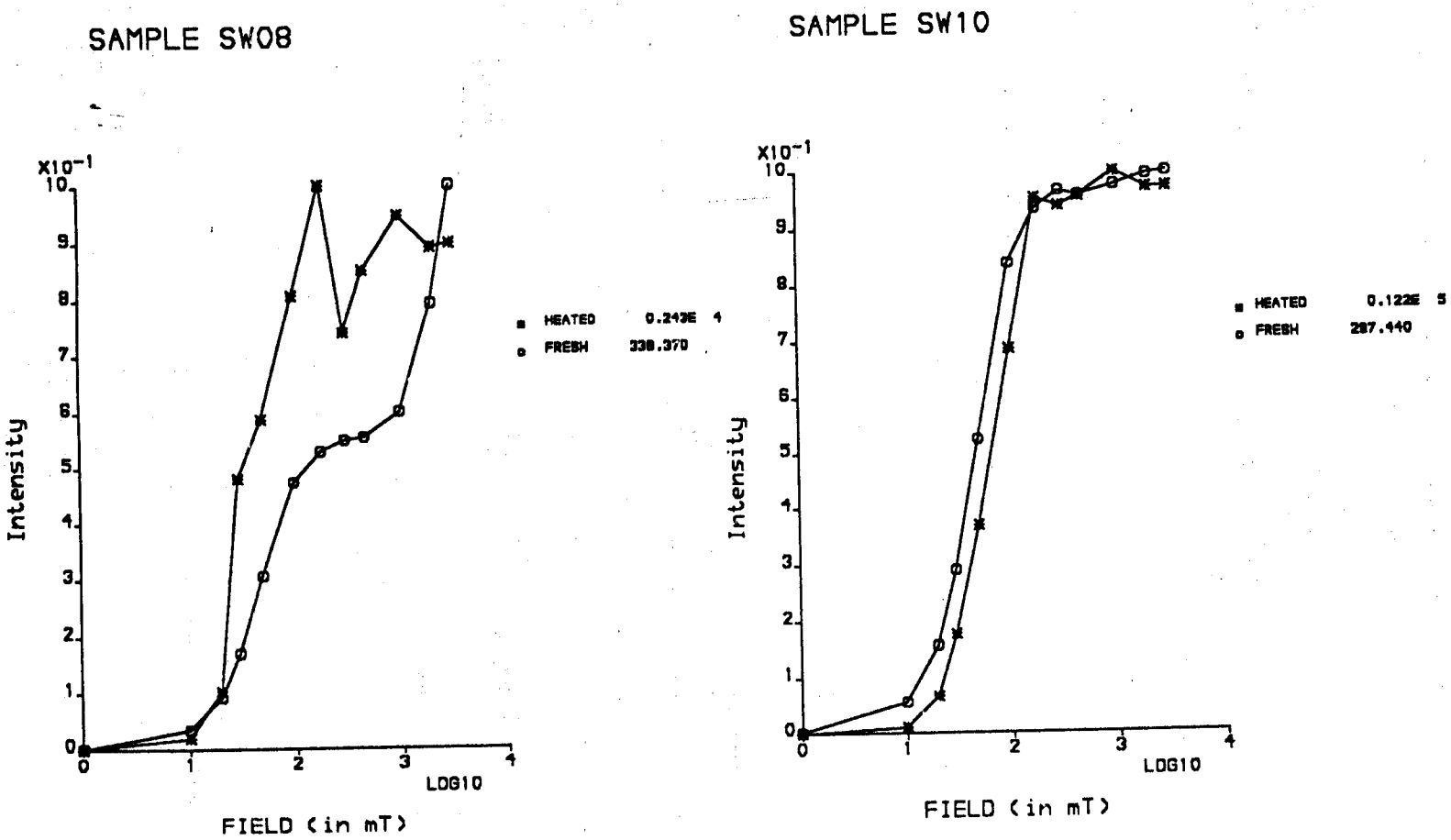

Figure 4.13b IRM acquisition curves for samples SW17 and SW18. The intensity unit used is 10E-5 A m^2/kg.

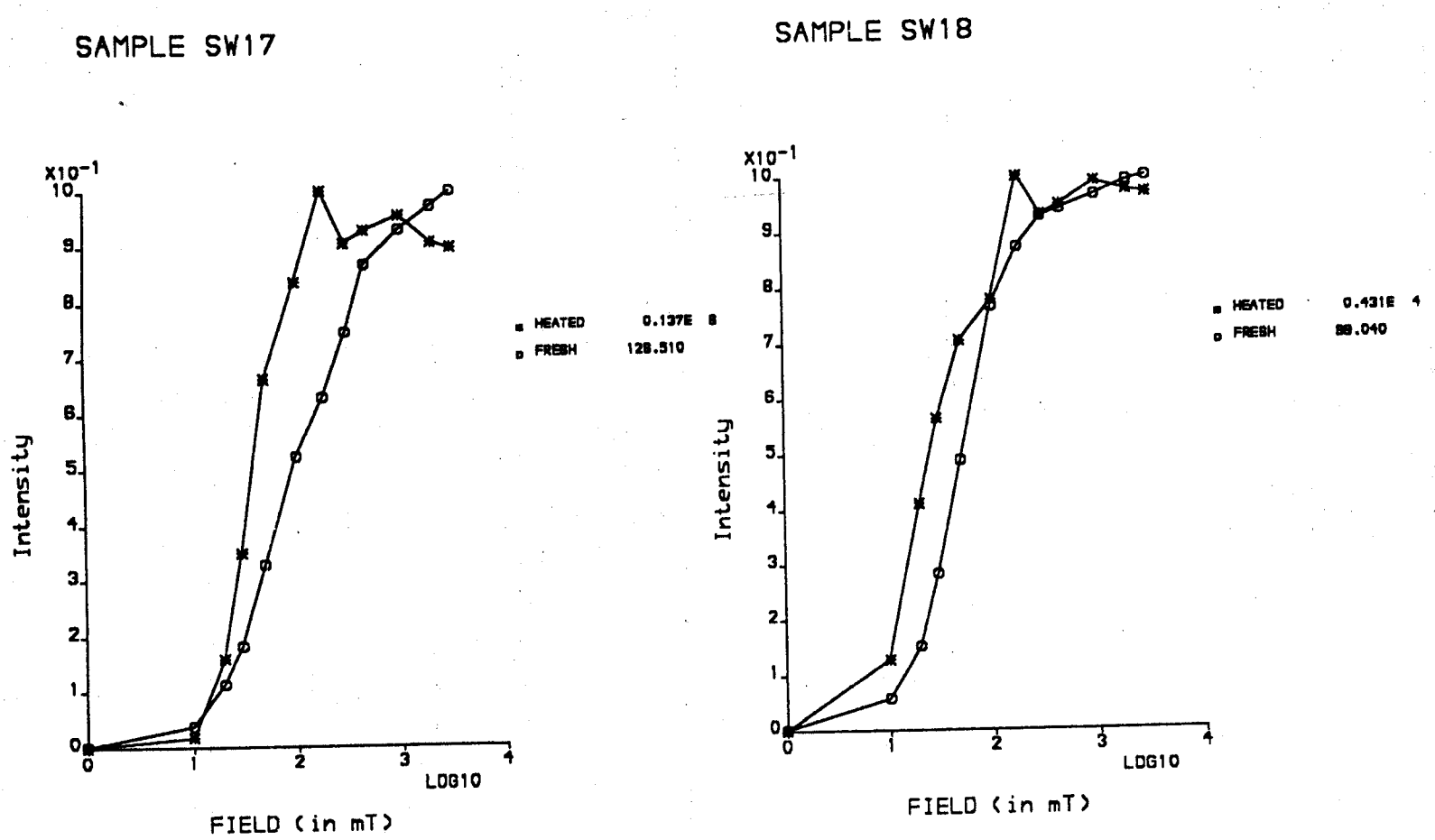

Figure 4.14a Thermal demagnetisation of IRM for sample SW08 (heated). The intensity unit used is 10E-5 A m^2/kg.

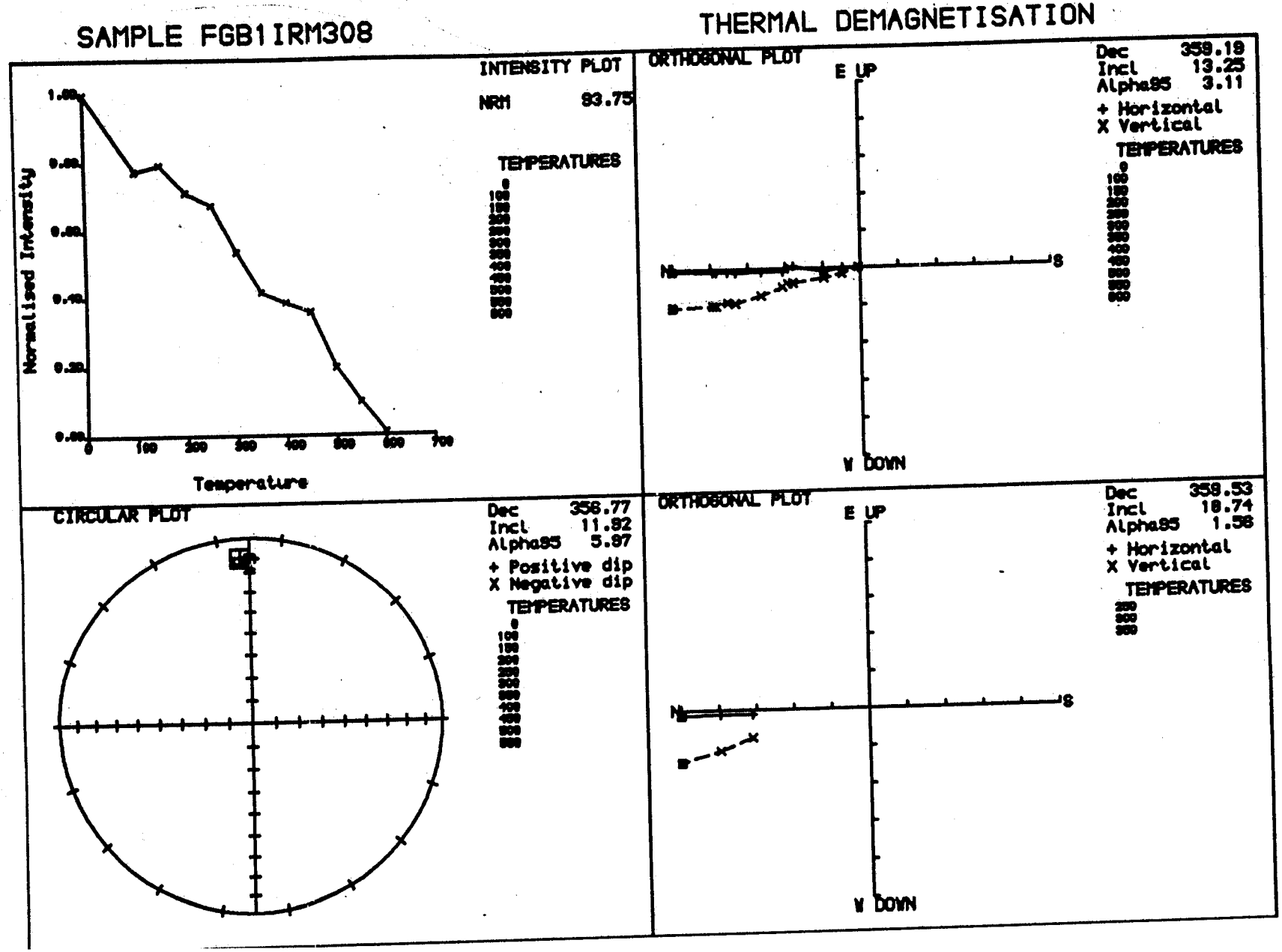

Figure 4.14b Thermal demagnetisation of IRM1 for sample SW10 (heated). The intensity unit used is 10E-5 A m^2/kg.

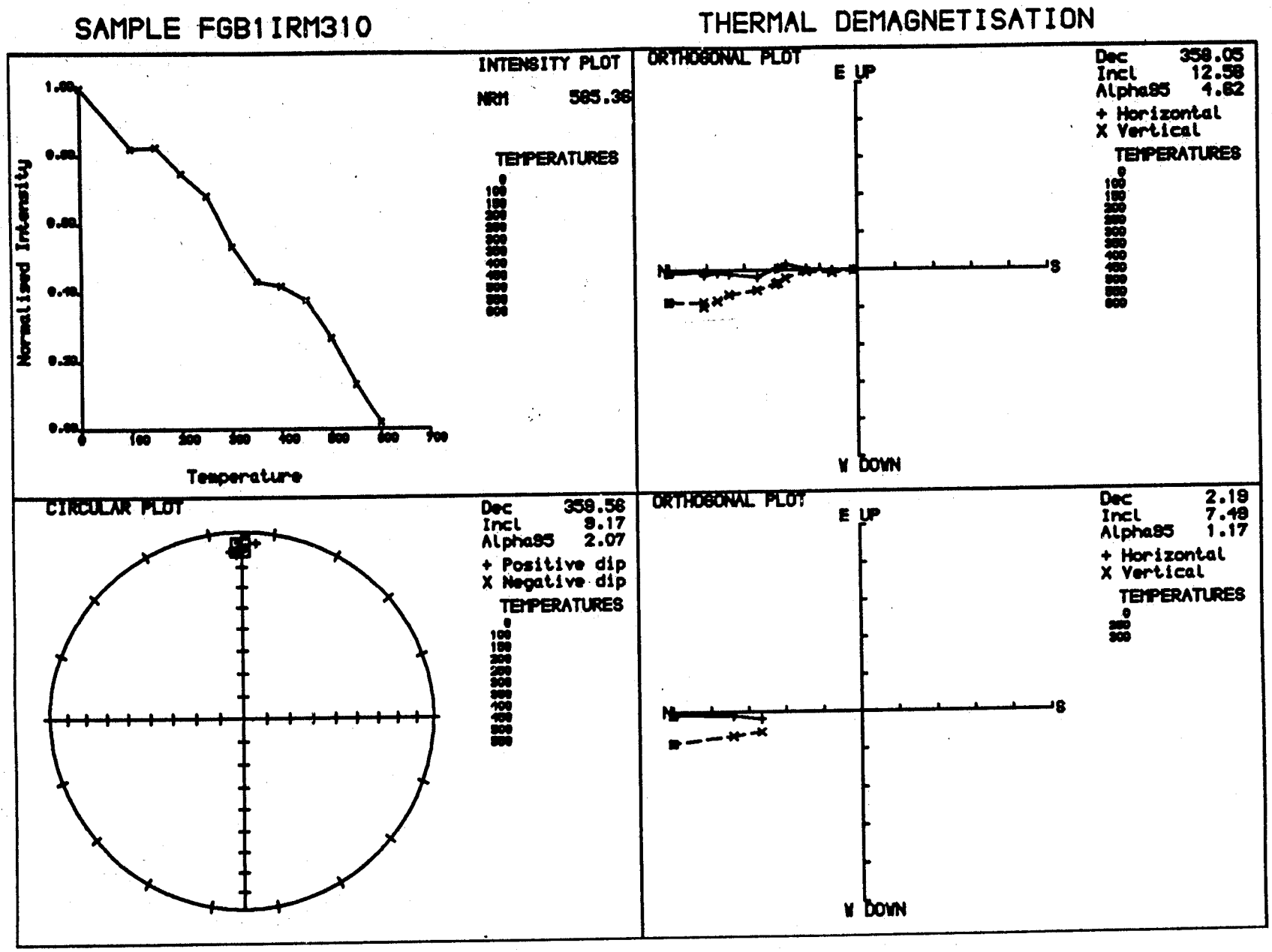

Figure 4.14c Thermal demagnetisation of IRM for sample SW17 (heated). The intensity unit used is 10E-5 A m^2/kg.

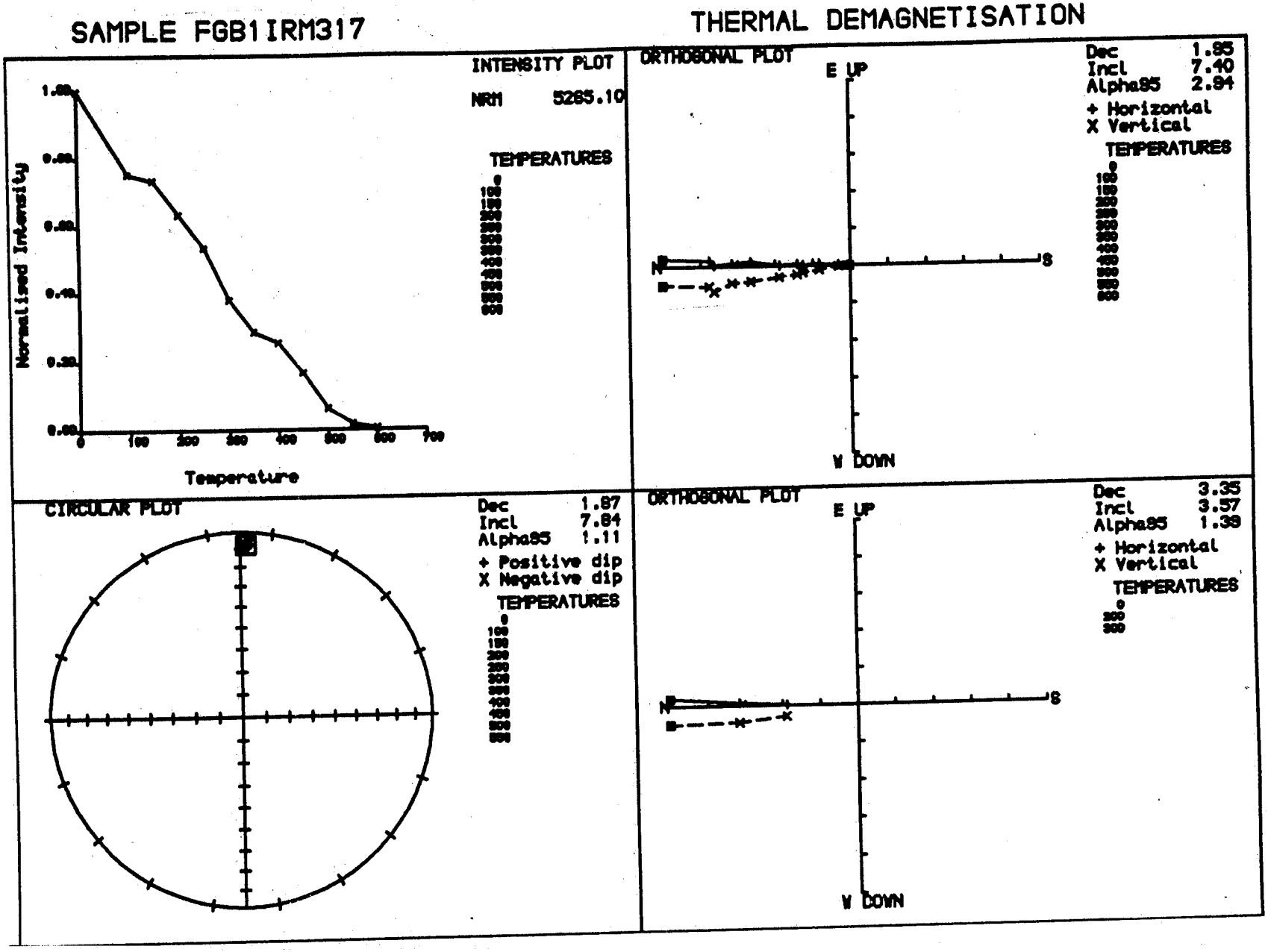

Figure 4.14d Thermal demagnetisation of IRM for sample SW18 (heated). The intensity unit used is 10E-5 A m^2/kg.

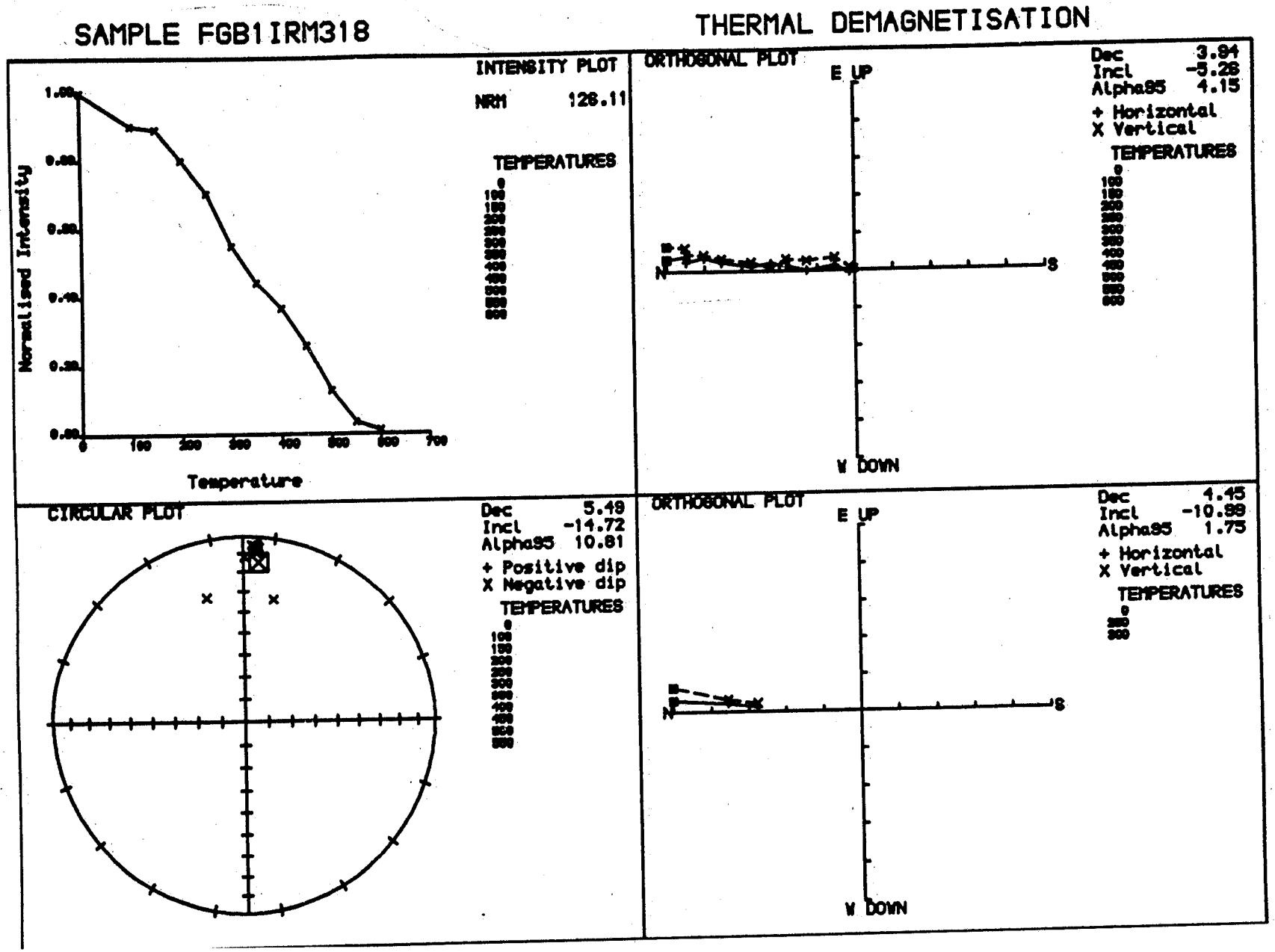

Figure 4.15a Thermal demagnetisation of IRM for sample SW08 (unheated). The intensity unit used is 10E-5 A.m^2/kg.

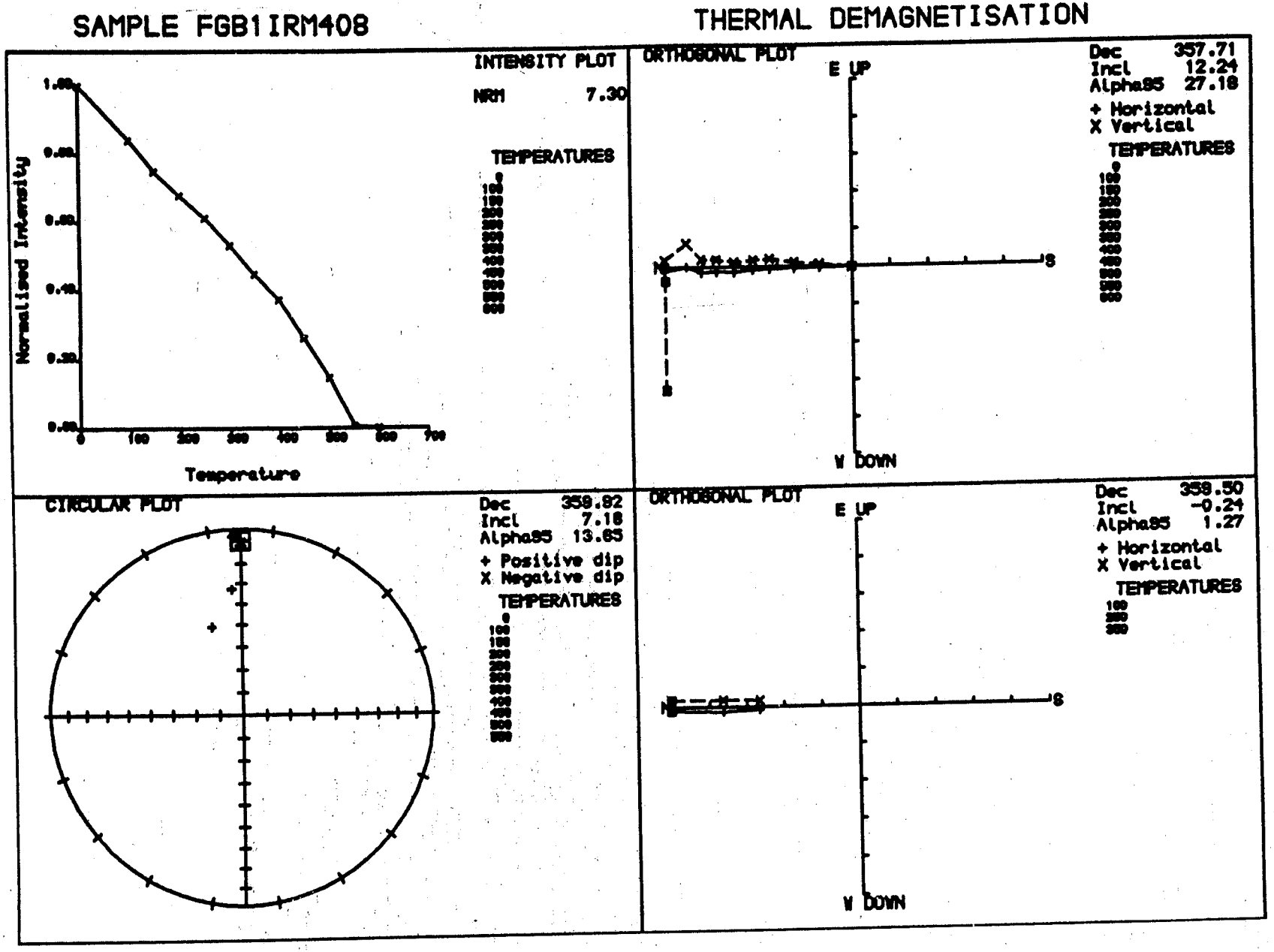

Figure 4.15b Thermal demagnetisation of IRM for sample SW10 (unheated). The intensity unit used is 10E-5 A.m^2/kg.

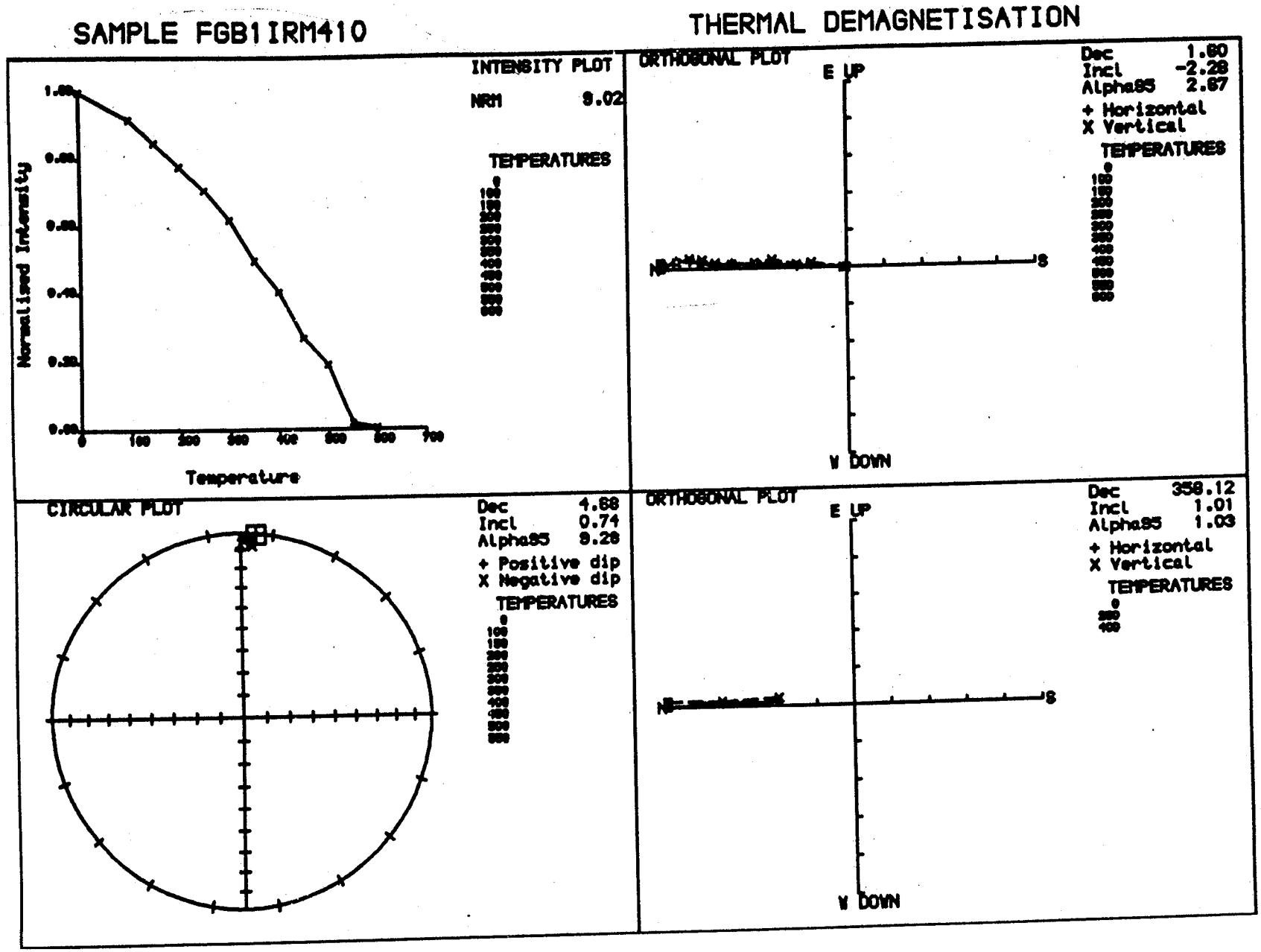

unit used is 10E-5 A.m^2/kg.

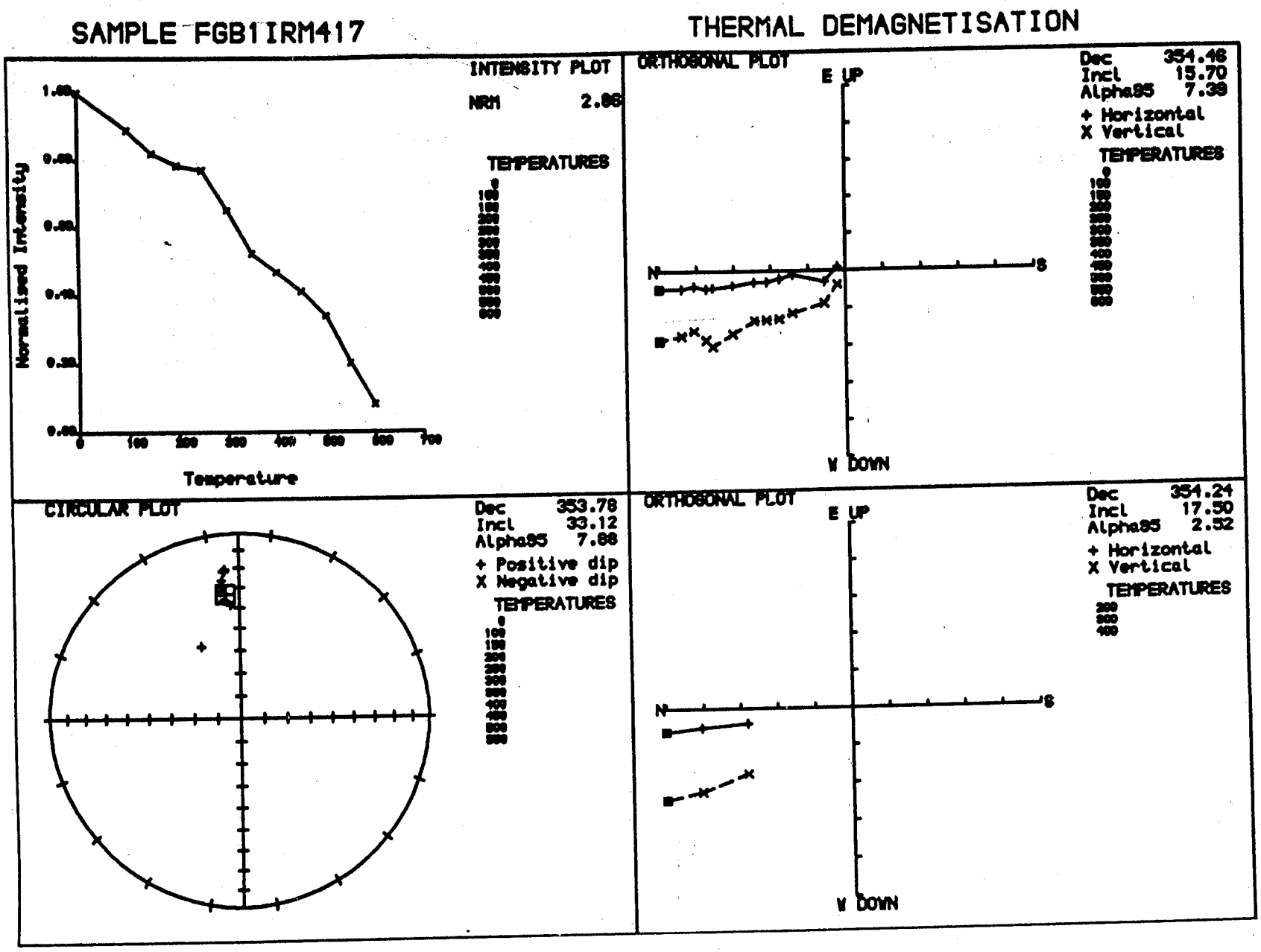

Figure 4.15d Thermal demagnetisation of IRM for sample SW18 (unheated). The intensity unit used is 10E-5 A.m^2/kg.

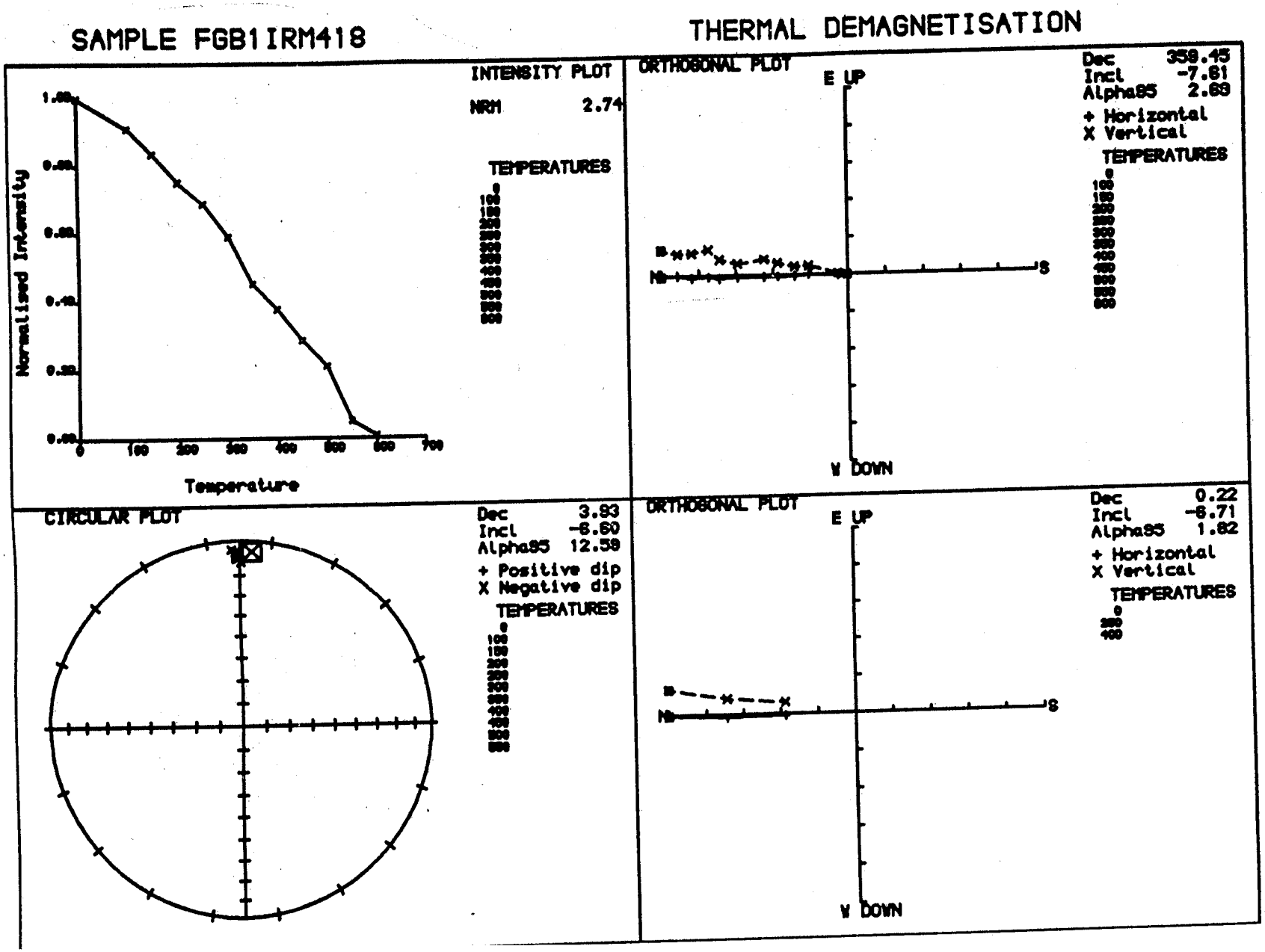

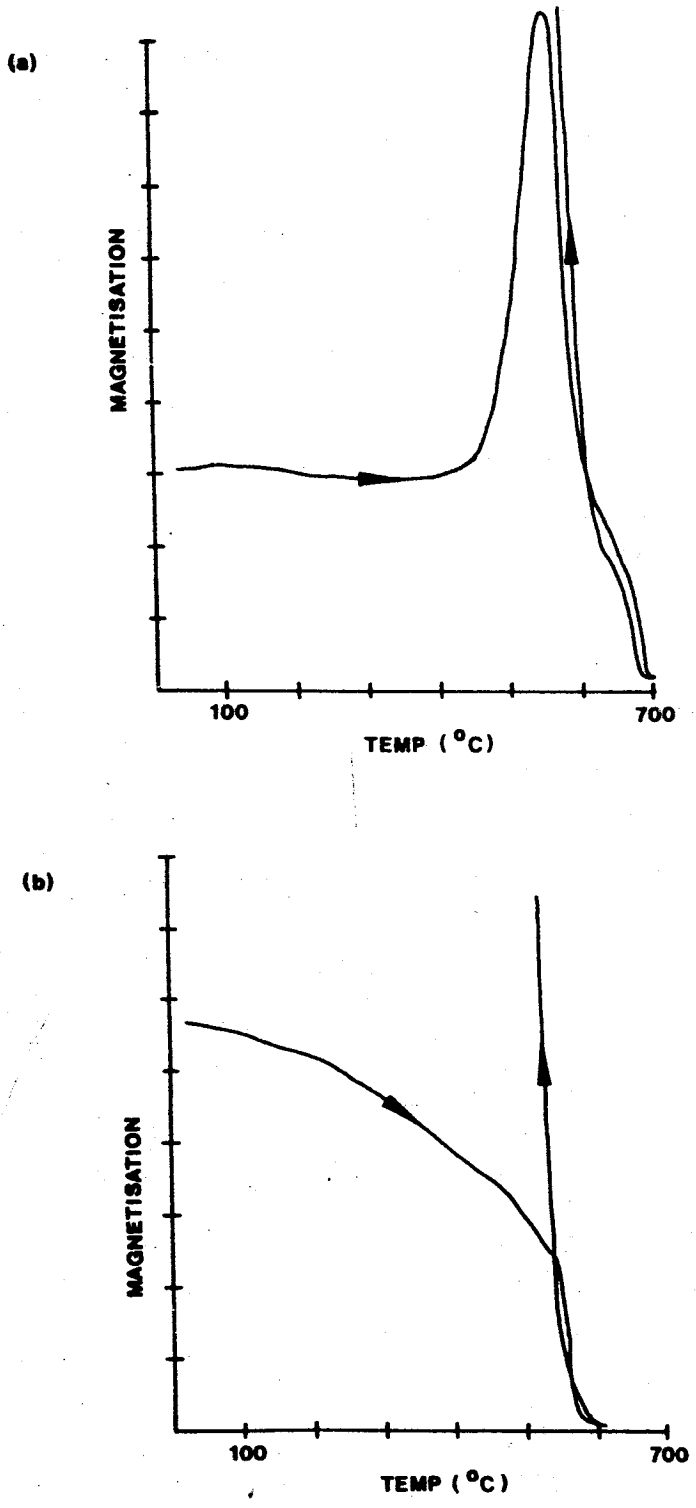

Figure 4.16 Thermomagnetic curves for unheated (a) and heated (b) samples. Heating and cooling curves are different for both samples.

Table 4.4 Palaeomagnetic results from Pembrokeshire (core samples). Specimens measured with a SQUID are given symbol +. The figures illustrate the results.

The unit of NRM intensity used is 10E-5 A m^2 / kg.

SPECIMEN	Dec	Inc	Tilt	Dir	CDec	CInc	NRM	
FGB1SW3303	303.68	59.76	38	180	233.35	58.51	0.0134	
FGB1SW3305	223.61	27.21	38	180	217.87	-02.07	0.0028	+
FGB1SW3306	261.49	77.48	38	180	198.89	48.55	0.0207	
FGB1SW3308	234.05	11.45	38	180	234.04	-11.41	0.0030	+
FGB1SW3309	185.31	38.03	38	180	184.18	00.15	0.0110	+
FGB1SW3310	209.71	-04.69	38	180	218.02	-36.68	0.0053	+
FGB1SW3311	196.24	-06.43	38	180	202.14	-42.50	0.0045	+
FGB1SW3403	211.93	24.18	47	178	209.97	-15.92	0.0088	+
FGB1SW3406	223.34	60.99	47	178	199.58	20.31	0.0114	+
FGB1SW3407	203.41	31.34	47	178	200.01	-12.09	0.0093	+
FGB1SW3408	196.15	33.24	47	178	193.45	-11.97	0.0088	+
FGB1SW3409	206.18	24.52	47	178	204.80	-17.67	0.0114	+
FGB1SW3501	338.55	74.66	71	018	008.25	06.94	0.1733	
FGB1SW3502	348.83	68.69	71	018	007.80	00.19	0.1314	
FGB1SW3503	348.70	71.47	71	018	009.04	02.67	0.1136	
FGB1SW3505	193.55	07.16	71	018	177.34	77.39	0.0052	+
FGB1SW3506	146.21	-32.10	71	018	153.32	18.81	0.0058	+
FGB1SW3507	189.86	-04.88	71	018	178.64	64.81	0.0056	+
FGB1SW3508	234.08	-12.69	71	018	249.05	42.37	0.0060	+
FGB1SW3509	184.10	33.16	71	018	056.52	71.16	0.0052	+
FGB1SW3510	007.74	73.51	71	018	015.10	02.76	0.0949	
FGB1SW3601	005.70	68.53	82	018	013.41	-12.98	0.1369	
FGB1SW3602	351.22	67.75	82	018	007.96	-11.88	0.3032	
FGB1SW3604	205.06	-08.97	82	018	220.66	71.63	0.0072	+
FGB1SW3605	216.59	-28.68	82	018	223.32	49.17	0.0066	+
FGB1SW3608	206.57	-38.10	82	018	207.26	43.21	0.0054	+
FGB1SW3610	167.82	-18.28	82	018	149.67	50.28	0.0057	+
FGB1SW3611	186.56	-25.64	82	018	180.03	54.57	0.0070	+
FGB1SW4106	318.02	74.48	32	325	322.47	42.56	0.0297	
FGB1SW4109	343.58	65.55	32	325	334.19	34.34	0.3214	
FGB1SW4110	353.01	66.02	32	325	338.61	35.78	0.1967	
FGB1SW4111	348.94	71.10	32	325	334.91	40.20	0.0453	
FGB1SW4113	341.70	70.03	32	325	332.21	38.59	0.0332	
FGB1SW4114	345.15	68.59	32	325	334.11	37.44	0.0538	
FGB1SW4115	342.99	66.74	32	325	333.61	35.46	0.0597	
FGB1SW4116	342.25	69.64	32	325	332.55	38.24	0.1908	
FGB1SW4117	333.17	71.22	32	325	328.39	39.35	0.0910	
FGB1SW4118	007.24	41.18	32	325	356.63	15.25	0.0456	
FGB1SW4119	326.19	35.17	57	304	323.03	-18.73	0.0824	
FGB1SW4120	317.14	75.72	57	304	307.40	19.05	0.0816	
FGB1SW4201	087.25	-28.35	47	188	070.03	-11.76	0.0230	
FGB1SW4202	186.48	-05.45	47	188	185.52	-52.43	0.0095	
FGB1SW4204	107.48	86.33	47	188	183.10	42.29	0.0281	
FGB1SW4214	075.65	89.04	30	186	184.19	60.32	0.0473	
FGB1SW4303	308.30	67.52	71	336	325.76	-01.10	0.0498	
FGB1SW4309	321.03	74.65	71	336	332.07	04.14	0.0897	
FGB1SW4310	325.83	66.98	71	336	332.03	-03.69	0.2250	
FGB1SW4409	344.77	57.66	48	179	204.09	71.93	0.0227	
FGB1SW4411	339.00	61.13	48	179	204.43	67.39	0.0265	

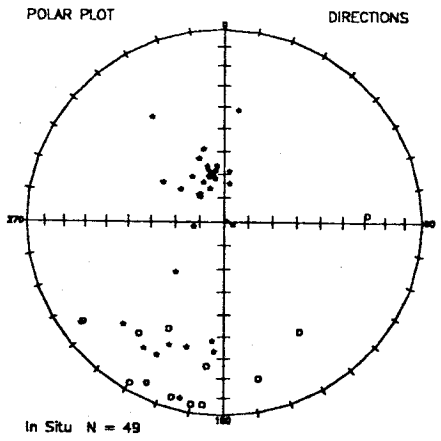

Star (circle) symbol = lower (upper) hemisphere.

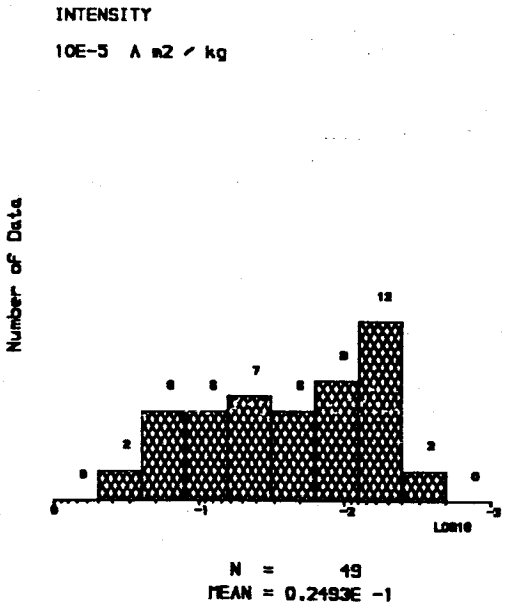

202.2°/7.9° with alpha-95 = 6.5°. In summary, the results of the fold test on the core samples are more meaningful than those from the block samples and the age of the magnetisation is syn-deformational.

4.4 Rock Magnetism

One of the magnetic methods used to identify the magnetic carriers in this investigation is IRM (Isothermal Remanent Magnetisation) study (see section 2.7.3, CHAPTER 2 and section 3.3.2, CHAPTER 3). Heated and unheated samples were studied including cases where there was chemical change during thermal treatment. Thirty six samples (from 18 sites) consisting of 18 heated and 18 unheated samples were given IRMs of 3000 mT through several steps. Another IRM of 300 mT was given to the samples, after the 3000 mT IRM but in an orthogonal direction. The IRMs were stepwise thermally demagnetised. Figures 4.13, 4.14 and 4.15 show some examples of the results. The terms IRM3 and IRM4 refer to heated and unheated samples and the last two digits represent the site numbers. Table 4.5 shows the maximum temperature experienced by the heated samples during the thermal demagnetisation of the NRM

Table 4.5 Maximum temperatures reached during thermal demagnetisation of the NRM.

Sample	T(°C)	Area
SW08	550	Clydach
SW10	625	Clydach
SW17	500	Saundersfoot
SW18	100	Saundersfoot

Most samples were saturated around 100 mT. Four heated samples from sites FGB1SW21, FGB1SW24, FGB1SW29 and FGB1SW30 acquired very

strong IRMs in a field as low as 20 mT. The acquisition experiment for these samples was terminated at 20 mT since the IRM intensity gained by the samples were out of the range of the spinner.

It seems likely that the magnetic mineral which is responsible for the remanence is magnetite, although the presence of haematite, a mineral requiring high remanences to saturate it, cannot be ruled out (see IRM Acquisition for Sample SW08 (unheated)). The thermal demagnetisation of the IRM (see Figure 4.15a) shows that this mineral it is likely to be goethite (instead of haematite) because a phase is present which loses its remanence after being heated at 100°C. Generally, there is no significant difference between heated and unheated samples. Most samples show single component behaviour on the orthogonal plots and a few per cent their IRM intensity is left after 600°C. This indicates that magnetite is the dominant magnetic carrier. The presence of magnetite as the predominant magnetic phase in these sediments implies alkaline and mildly reducing conditions during deposition and/or diagenesis (Piper, 1987 p. 64-65). Time considerations have not permitted study of the size or domain structure of this magnetite, but it has clearly been susceptible to acquisition of secondary components as shown by the smearing of NRM directions. A few samples were measured to study their magnetic hysteresis with a VSM magnetometer. This proved to be unsuccessful due to the very low quantity of magnetite in the samples and the dominance of the paramagnetic constituents.

Figure 4.16 shows thermomagnetic curves of a unheated and heated sample. At 400°C the unheated sample experienced a chemical change. The new

mineral also appears to be magnetite. However, for the heated sample nothing happened at that temperature. And the Curie temperature for this new mineral is about 575°C, which is the Curie temperature of magnetite. The heating and the cooling curves for the heated samples are not exactly the same. This indicates further chemical change.

4.5 Discussion

From rock magnetic studies, the magnetic mineral which is responsible for the remanence is shown to be magnetite. Magnetite is also a product of chemical alteration due to heating. This happens at about 400°C. It is possible that the clay minerals are the source of this alteration, which is also observed in red beds (Collinson,1983). However, from a previous chapter (CHAPTER 3 Palaeomagnetism of Old Red Sandstones, South Wales) the breakdown of the clay minerals is observed to happen at higher temperatures. Another explanation is that it is due to the presence of pyrite. The presence of pyrite in the specimens are indicated by the physical appearance of the specimens showing grey-black in colour and rich in organic content. Above 350°C pyrite changes to magnetite (Tarling,1983) and it seems that this mineral was produced under reducing conditions during the diagenesis of these sediments.

The age of the magnetisation remains uncertain. The main difficulty is in finding rocks which are appropriate for a fold test in the main basin. The complexity of the geology of the area adds another problem in interpreting the fold test. The problems become worse because some samples have been overprinted in a Recent field. This overprint component has an intensity

well above the noise level of the spinner. After bedding correction, some directions are close to an Upper Carboniferous direction and some have normal polarity. If this problem is not acknowledged, the fold test yields an incorrect conclusion. However, the arrival of a new SQUID magnetometer enabled 20 very weak samples of 1 inch diameter (from 4 sites) to be measured. The scatter within sites is less than those obtained with the spinner. All of them have a reversed polarity and the fold test applied to these samples indicates that the remanence was acquired during folding. Since the age of the folding is Variscan, the age of the magnetisation is probably late Carboniferous. The possibility of later remagnetisation during Triassic or Permian times can be excluded because a contrasting field direction would then be expected (Table 3.2, CHAPTER 3) and causative geological events are not so obvious. The palaeopole position (see Figure 4.10) reflects a magnetisation recording a palaeomagnetic direction for Upper Carboniferous times in southern Britain.

The polarity of all palaeomagnetic directions which could be considered to be primary from this study of Westphalian A rocks is reversedly magnetised. Although the palaeofield derived from this study suggests that it represents geomagnetic field for younger times, this result supersedes previous studies reported by Belshé (1957) and Titman (1971) both in term of the stratigraphic control and of the palaeomagnetic techniques used, including modern instrumentations. Therefore, the Westphalian magnetostratigraphy for the British Isles and northwestern Europe proposed by Palmer and others in 1985 must be revised. The palaeomagnetic results from contemporaneous rocks from other parts of the country or from

Westphalian A coals (which are thought to be escaped from remagnetisation) from South Wales are desirable to test this result.

CHAPTER 5 CONCLUSION

5.1 Summary

5.1.1 Fold Test

A new method for applying a fold test to a collection of palaeomagnetic directions has been discussed. It has been reported by some workers (e.g Hudson and others, 1989) that the mean palaeomagnetic direction derived from the highest value of the k-parameter in a fold test employing a partial tilt correction does not necessarily coincide with the expected palaeomagnetic direction for the area being investigated. Therefore, any conclusion drawn from such studies may be incorrect.

The highest k can be obtained either by unfolding both limbs of a fold simultaneously (the usual method) or by unfolding the limbs separately (this study) in a stepwise manner. The latter method will give the true highest k. It has been demonstrated in this study that the palaeomagnetic directions derived from both methods may be incorrect.

A simple solution to this problem is that the expected palaeomagnetic direction must be determined first before applying the fold test. The expected palaeomagnetic direction can be predicted either from palaeomagnetic results from adjoining horizontal strata of the same rocks from the same area

or from an established apparent polar wander path (APWP) which is valid for the area. For the sake of simplicity, in this study, only the inclination is used for finding the mean direction. The mean inclination of palaeomagnetic directions from both limbs of a fold has a simple distribution in responding to partial unfolding of each limb; each possible inclination is usually represented by a straight line. The direction with the highest k-value within the accepted inclination is considered as the mean palaeomagnetic direction. Using this new method, the fold test yields a mean direction which is close to the expected direction. Thus if a remanence can be linked to a specific magnetisation event, this implies that the geometry of the fold at the time the rock acquired its magnetism can be determined.

5.1.2 The Results of the Fold Test

Permo-Carboniferous (secondary) components from Locality 1 (Llanthony), Locality 9 (Llanstephan), Locality 10 (Freshwater East) and Locality 11 (Freshwater West) were subjected to the fold test. The results from Locality 1 and Locality 9 are almost in the opposite sense to each other. At Locality 1 the remagnetisation occurred at the earliest stage of folding whereas at Locality 9 it took place at the latest stage of folding. The age of magnetisation is still syn-deformational. The age of the deformation in Locality 1 could be Late Caledonian, Variscan or post-Variscan and in Locality 9 it is possibly Variscan (Dr.R. Gayer, personal communication; Owen and Weaver, 1983).

There are two possible explanation for this puzzle :

1. The age of the deformation in Locality 1 is younger than that of the deformation in Locality 9 (but still possibly Variscan in age), if the overprinting event occurred at the same time in both localities.

2. Alternatively, if the deformation at both localities took place at the same time, the remagnetisation process in Locality 1 must have taken place earlier than in Locality 9.

The results of the fold test from Locality 10 and Locality 11 (southern Pembrokeshire) suggest that the age of magnetisation is syn-deformational. The plunge for the northern limb of the Freshwater East anticline in Locality 10 is directed to the west whereas the plunge for the southern limb is to the east. No specific geological explanation for this discrepancy is given here because it is beyond the scope of the thesis and it is possible that the remanence in this area has been variably rotated by the effects of penetrative deformation. The results of the fold test suggest that the the direction of the plunge for the northern limb should be in the opposite direction in order that the plunge correction improves the grouping of the palaeomagnetic vectors and some of the k values pass the McElhinny test. For this ground, in this thesis it is assumed that the plunge for this limb is the same as for the other limb (i.e. to the east). The direction of the plunge for the Castlemartin Corse anticline in Locality 11 is to the west. The plunge correction for both anticlines bring the scattered directions between limbs into agreement and significantly increase the k values. The mean palaeomagnetic direction for Locality 11 (Freshwater West) is more westerly than for Locality 10 (Freshwater East). These directions cannot be rejected at 95% level of confidence since their k values pass the McElhinny test.

However, these anticlines are part of a bigger anticlinal structure called the Orielton anticline which is a compound fold comprising the Castlemartin Corse and the Freshwater East anticlines and the intervening Orielton syncline (Hancock and others, 1983). The result of the fold test applied to the Orielton anticline is ambiguous since the McElhinny test is positive with or without the plunge correction. Without the plunge correction, the mean palaeomagnetic direction is close to the results from Locality 9 (Llanstephan) which suggests that there is no rotation of the area. With the appropriate plunge correction, the fold test gives a more westerly direction implying that rotation has occurred. This ambiguity is likely to be caused by a wide separation of the sites being analysed so that the k_1 is very low (less than 3). On the other hand, the results of the fold test on the Orielton syncline show that there are no k-values passing the McElhinny test. However, both results could be refined if the sites involved in the assessment were increased in number and not widely separated.

5.1.3 Rotation

It has been proved, palaeomagnetically, that there is no rotation involved in the movement between major blocks (separated by major Variscan disturbances) in the main basin (Group 1) since Late Carboniferous times.

The mean of Group 2 (the Carmarthen area) and Group 3 (the southern Pembrokeshire area) are about 5° and 30° more westerly than the mean of Group 1 (the Brecon/Abergavenny area) respectively. These discrepancies cannot be explained in terms of remanence deflection by the susceptibility anisotropy. From the AMS studies, the magnitude of the anisotropy rarely

Table 5.1 Group means.

Area	Lat(°)	Lon(°)	Dec(°)	Inc(°)	deflection(°)
Group 1	51.8	356.9	193	-4	0
Group 2	51.8	355.6	198	-10	5
Freshwater East	51.6	355.1	211	-1	18
Freshwater West	51.7	355.0	234	-11	41
Mill Haven *	51.8	354.8	241	-21	52

Note : * McClelland-Brown (1983)

exceeds 30% and the average value is 12%. McElhinny (1973) pointed out that even the magnitude is 50%, the total deflection of a magnetisation direction is only 11.6°. Most anisotropy is perpendicular to the bedding plane (oblate, E > 1). Hence, most of this effect would be perpendicular to the bedding plane and not sensitive to the declinations in the bedding. These more westerly declinations for western sites must, therefore, be explained in terms of a rotation of the area. It is more likely that tectonic rotation caused palaeomagnetic directions in the area to be deflected more for more westerly sites Table 5.1 lists the amount of the deflection relative to the mean palaeomagnetic direction for Group 1. The mean direction of Group 3 is the average value of the mean directions for Freshwater East (Locality 10) and Freshwater West (Locality 11).

5.1.4 Polarity of Westphalian A Sediments

From this study, the polarity of the palaeomagnetic direction for the Westphalian A is overwhelmingly reversed although the palaeofield direction is applicable to younger times and cannot be unambiguously tested by means of a fold test. The mean direction from Locality 1 (Clydach, Bryn.mawr) may be considered as a representative of the Westphalian A direction from South Wales. The dip of the strata is sub-horizontal (0° - 12°). The mean in situ direction for 16 sites (69 specimens) is Dec/Inc = 193.7°/2.2° with alpha-95 = 6.1°. This corresponds to a pole position at Lat/Lon = 35.9°S/339.9°E (dp = 3.1° and dm = 6.1°) which is very close to the expected pole position for the Upper Carboniferous rocks from southern Britain.

The palaeomagnetic results from other localities show a large within-site scatter. Most specimens from Locality 2 (Rhigos) showed large alpha-95 values and most specimens from Pembrokeshire (Locality 3 (Saundersfoot) and Locality 4 (Little Haven)) had very weak NRMs which are below the noise level of a Molspin spinner magnetometer. Some specimens from this area which had their intensities well above the noise level showed Recent overprints. Due to the time available, only 20 very weak specimens from Locality 3 (Saundersfoot) were able to be measured with a SQUID magnetometer. These specimens were sampled from a chevron fold called the Ladies Cave anticline. All are reversed and the mean direction (the expected inclination is within -10° and 10°) is Dec/Inc = 202.2°/ 7.9° with alpha-95 = 6.5° which is close to the results from Locality 1 (Clydach,

Brynmawr). However, the age of magnetisation for these specimens appears to be syn-deformational.

5.1.5 Rock Magnetic Studies

Owing to very low concentrations of magnetic minerals within the samples from both red beds and Westphalian A sediments, only IRM techniques yielded positive results. The IRM acquisition technique accompanied by thermal demagnetisation of two different IRMs (which are orthogonal to each other) revealed that haematite is responsible for the remanence in the red beds and magnetite in the Westphalian A sediments from South Wales.

The technique was also employed to detect any possible chemical changes in red bed samples during thermal treatment. It was found that the chemical changes happened above 500°C for the majority of samples. The new mineral is likely to be magnetite. This result is in agreement with the results reported by earlier workers (e.g. Dunlop, 1972; Collinson, 1983).

5.2 Discussion and Suggestions

- Since the magnetisation from folded beds may be acquired during the straining associated with folding, the classic fold test based on two k-values (in situ and 100% unfolded) may provide an incomplete analysis of progressive tilt adjustment and, if possible, consideration of the plunge correction should be routinely employed in palaeomagnetic studies.

- There is an obvious relationship between the McElhinny test and the plunge correction in this study. Failure of the McElhinny test does not necessarily mean that the remanence is post-folding or that the test is too stringent. Plunging of the fold axes may also cause the McElhinny test to be negative.

- The result of the fold test suggests that the age of the Neath Disturbance at Locality 1 (Llanthony, Group 1) is probably younger (Triassic (?)) than the age of the deformation in Locality 9 (Llanstephan, Group 2). Some specimens from this group also yielded higher temperature components which are close to the expected Triassic palaeomagnetic direction for the area. This study has therefore recognised regional variations in the influence of overprinted and identified temporal variations.

- Further palaeomagnetic results from the eastern end of the Castlemartin Corse anticline and the western end of the Freshwater East anticline are desirable. In conjunction with the results from this research, the results could be used to fully confirm a regional rotation suggested by McClelland-Brown in 1983 and to determine the amount of the rotation involved (this study yields a mean estimate of about 10° less than McClelland-Brown's hypothesis, see Table 5.1). No general record of a Devonian remanence is present to establish the magnitude of rotations between Devonian and Permo-Carboniferous times although AMS results suggest that some measure of rotation took place between these times.

- Since no normal horizons within the Westphalian A sediments from South Wales are found in this study and the observed palaeofield direction is close to those for younger times, magnetostratigraphy of the Westphalian A remains unresolved. However, further studies of coals from South Wales or palaeomagnetic studies of contemporaneous rocks from other parts of the country are desirable because palaeomagnetic studies of coals seem to be successful for magnetostratigraphic purposes according to Noltimier and Ellwood (1977).

- The palaeomagnetic results from the Westphalian A from Locality 3 (Saundersfoot, Pembrokeshire) suggest that there is no rotation of the area being investigated. This area is located within Zone Ic of Hancock and others (1983). Further palaeomagnetic investigation is desirable in this zone to confirm this results and attempt to delineate the zone of rotational deformation at the Variscan Front in the Southwest Wales area using palaeomagnetic techniques. Since there is no general agreement between geologists on the positioning of the Variscan Front in this area (see Hancock and others, 1983), palaeomagnetic investigations might be used as a constraint for solving this disagreement.

- The IRM studies suggest that the magnetic mineral responsible for the remanence in the Westphalian A sediments is magnetite. It would be interesting to study the genesis and domain state of this mineral in these sediments since the samples from the western area are found to be more susceptible to a Recent field acquisition than the samples from the eastern area.

References

1. Addison, F.T., Turner, P. and Tarling, D.H. (1985). Magnetic Studies of the Pendleside Limestone : Evidence for Remagnetization and Late-Diagenetic Dolomitization during a Post-Asbian Normal Event. J. geol. Soc. London ,142, 983-994.

2. Allen, J.R.L. (1974). The Devonian Rocks of Wales and the Welsh Borderland. In The Upper Palaeozoic and Post-Palaeozoic Rocks of Wales. Owen, T.R. (editor), Univ. of Wales Press, Cardiff.

3. Barclay, W.J. (1989). Geology of the South Wales Coalfield, Part II, the Country around Abergavenny, 3rd edition. Mem. Br. Geol. Surv. Sheet 232 (England and Wales).

4. Belshé, J.C. (1957). Palaeomagnetic Investigation of Carboniferous Rocks in England and Wales. Adv. Phys. ,6, 187-191.

5. Birkenmajer, K., Krs, M. and Nairn, A.E.M. (1968). A Palaeomagnetic Study of Upper Carboniferous Rocks from the Inner Sudetic and Bohemian Massif. Bull. Geol. Soc. Amer. ,79, 589-608.

6. Briden, J.C. and Mullan, A.J. (1984). Superimposed Recent, Permo-Carboniferous and Ordovician Palaeomagnetic Remanence in the Builth Volcanic Series, Wales. Earth Planet. Sci. Lett. ,69, 413-421.

7. Burmester, R.F., Bazard, D.R. and Beck, Jr. M.E. (1990) Post-folding Remagnetisation that Passes the Fold Test. Geophys. J. Int. ,102, 455-463.

8. Chamalaun, F.H. (1963). Thermal Demagnetization of Red Sediments. Ph.D thesis. King's College. Newcastle-upon-Tyne.

Besly, B.M. & Turner, P. (1983). Origin of Red Beds in a moist tropical climate (Etruria Formation, Upper Carboniferous, U.K.) Spec. Publ. geol. Soc. Lond, 11, 131-47 R1

9. Chamalaun, F.H. (1964). Origin of the Secondary Magnetization of the Old Red Sandstones of the Anglo-Welsh Cuvette. J. Geophys. Res. ,69, 4327-4337.

10. Chamalaun, F.H. and Creer, K.M. (1964). Thermal Demagnetisation Studies on the Old Red Sandstone of the Anglo-Welsh Cuvette. J. Geophys. Res. ,69, 1607-1616.

11. Channell, J.E.T., McCabe, C. and Woodcock, N.H. (1991). An Early Devonian (pre-Acadian) Magnetization Component Recorded in the Lower Old Red Sandstone of South Wales (UK). Geophys. J. Int. in press.

12. Cox, A. and Hart, R.B. (1986). Plate Tectonics : How It Works. Blackwell Scientific Publications, Oxford.

13. Creer, K.M. (1957). The Natural Remanent Magnetization of Certain Stable Rocks from Great Britain. Phil. Trans. Roy. Soc. London ,A, ,250 (974) ,111-129.

14. Creer, K.M. (1962). A Statistical Enquiry into the Partial Remagnetisation of Folded Old Red Sandstones Rocks. J. Geophys. Res. ,67, 1899-1906.

15. Creer, K.M. (1968). Palaeozoic Palaeomagnetism. Nature ,219, 246-250.

16. Diehl, J.F. and Shive, P.N. (1981). Palaeomagnetic Results from the Late Carboniferous / Early Permian Casper Formation : Implications for Northern Appalachian Tectonics. Earth. Planet. Sci. Lett. ,54, 281-292.

17. Dunlop, D.J. (1972). Magnetic Mineralogy of Unheated and Heated Red Sediments by Coercivity Spectrum Analysis. Geophys. J. R. astr. Soc. ,27, 37-55.

11.a. Collinson, D.W. (1983). Methods in Rock Magnetism and Palaeomagnetism : Techniques and Instrumentation. Chapman and Hall Ltd, London.

18. Dunlop, D.J. (1979). On the Use of Zijderveld Vector Diagrams in Multi Component Palaeomagnetic Studies. Phys. Earth Planet. Intr. ,20, 12-24.

19. Dunne, W.M. (1983). Tectonic evolution of SW Wales During the Upper Palaeozoic. J. geol. Soc. London ,140, 257-265.

20. Edel, J.B. (1987). Paleoposition of the Western Europe Hercynides during the Late Carboniferous Deduced from Palaeomagnetic Data: Consequences for "Stable Europe". Tectonophysics ,139, 31-41

21. Evans, M.E. (1976). Test of the Dipolar Nature of the Geomagnetic Field throughout Phanerozoic Time. Nature ,262, 676-678.

22. Everitt, C.W.F. and Belshé, J.C. (1960). Palaeomagnetism of the British Carboniferous System. Phil. Mag. ,5, 675-685.

23. Facer, R.A. (1983). Folding, strain and Graham's Fold Test in Palaeomagnetism. Geophys. J. R. astr. Soc. ,72, 165-171.

24. Fisher, R.A. (1953). Dispersion on a Sphere. Proc. R. Soc. ,A217, 295-305.

25. George, T.N. (1970). British Regional Geology : South Wales (3rd edition). HMSO for Institute for Geological Sciences. London.

26. Graham J.W. (1949). The Stability and Significance of Magnetism in Sedimentary Rocks. J. Geophys. Res. ,54, 131-167.

27. Hancock, P.L. , Dunne, W.M. and Tringham, M.E. (1981). Variscan Structures in Southwest Wales. In The Variscan Orogen in Europe. Zwart, H.J. and Dornsiepen, U.F. (editors), Geol. Minjbouw ,60, 81-82.

28. Hancock, P.L. , Dunne, W.M. and Tringham, M.E. (1982). Variscan Structures in South-West Dyfed. In Geological Excursion in Dyfed, South-West Wales. Bassett, M.G. (editor), The National Museum of Wales for the Geologists' Assoc., South Wales Group, Cardiff.

29. Hancock, P.L. , Dunne, W.M. and Tringham, M.E. (1983). Variscan Deformation in Southwest Wales. In The Variscan Fold Belt in the British Isles. Hancock, P.L. (editor), Adam Hilger Ltd. , Bristol.

30. Harland, W.B. , Armstrong R.L., Cox, A.V., Craig, L., Smith, A.G., and Smith, D.G., (1990). A Geologic Time Scale 1989. Cambridge University Press, Cambridge.

31. Hrouda, F. and Janak, F. (1971). A Study of the Hematite Fabric of Some Red Sediments on the Basis of Their Magnetic Susceptibility Anisotropy. Sediment. Geol. ,6, 187 - 199.

32. Hudson, M.R., Reynolds, R.L., Fishman, N.S. (1989). Synfolding Magnetization in the Jurassic Preuss Sandstone, Wyoming-Idaho-Utah Thrust Belt. J. Geophys. Res. ,94, 13681-13705.

33. Irving, E. and Pullaiah, G. (1976). Reversals of the Geomagnetic Field, Magnetostratigraphy and Relative Magnitudes of Palaeosecular Variation in the Phanerozoic. Earth Sci. Revs. ,12, 35-64.

34. Kirschvink, J.L. (1980). The Least-Square Line and Plane and the Analysis of Palaeomagnetic Data. Geophys. J. R. astr. Soc. ,62, 699-718.

35. Li, Z.X., Powell, C.M. and Schmidt, P.W. (1989). Syn-deformational Remanent Magnetization of the Mount Eclipse Sandstone, Central Australia. Geophys. J. Int. ,99, 205-222.

36. MacDonald, W.D. (1980). Net Tectonic Rotation, Apparent Tectonic Rotation and the Structural Tilt Correction in Paleomagnetic Studies. J. Geophys. Res. ,85, 3659-3669.

37. McCabe, C. and Elmore, R.D. (1989). The Occurrence and Origin of Late Palaeozoic Remagnetisation in the Sedimentary Rocks of North America. Rev. Geophys. ,27, 471-494.

38. McCabe, C. and Channell, J.E.T. (1990). Palaeomagnetic Results from Volcanic Rocks of the Shelve Inlier, Wales : Evidence for a Wide Late Ordovician Iapetus Ocean in Britain. Earth Planet. Sci. Lett. ,96, 458-468.

39. McClelland-Brown, E. (1983). Palaeomagnetic Studies of Fold Development and Propagation in the Pembrokeshire Old Red Sandstone. In Palaeomagnetism of Orogenic Belts. McClelland-Brown, E. and Vanden Berg, J. (editors), Tectonophysics ,98, 131-149.

40. McClelland, E. (1987). Palaeomagnetic Results from the Lower Devonian Llandstadwell Formation, Dyfed, Wales - Discussion. Tectonophysics ,143, 335-336.

41. McElhinny, M.W. (1964). Statistical Significance of the Fold Test in Palaeomagnetism. Geophys. J. R. astr. Soc. ,54, 131-167. 328-340

42. McElhinny, M.W. (1973). Palaeomagnetism and Plate Tectonics. Cambridge University Press, Cambridge.

43. McFadden, P.L. and Jones, D.L. (1981). The Fold Test in Palaeomagnetism. Geophys. J. R. astr. Soc. ,67, 53-58.

44. McMahon, B.E. and Strangway, D.W. (1968). Investigation of Kiaman Magnetic Division in Colorado Red Beds. Geophys. J. R. astr. Soc. ,15, 265-285.

45. Merrill, R.T. and McElhinny, M.W. (1983). The Earth's Magnetic Fields. (International Geophysics Series, vol.32). Academic Press, London.

46. Miller, J.D. and Opdyke, N.D. (1985). Magnetostratigraphy of the Red Sandstone Creek Section, Vail, Colorado. Geophys. Res. Lett. ,12, 133-136.

47. Miller, J.D. and Kent, D.V. (1986). Synfolding and Prefolding Magnetizations in the Upper Devonian Catskill Formation of Eastern

Pennsylvania : Implication for the Tectonic History of Acadia. J. Geophys. Res. ,91, 12791-12803.

48. Molina-Garza, R.S., Geissman, J.W. and Van der Voo, R. (1989). Palaeomagnetism of the Dewey Lake Formation (Late Permian), Northwest Texas: End of the Kiaman Superchron in North America. J. Geophys. Res. ,94, 17881-17888.

49. Noltimier, H.C. and Ellwood, B.B. (1977). The Coal Pole : Palaeomagnetic Results from Westphalian B, C and D Coals, Wales. Trans. Amer. Geophys. Union (abstr.) ,58, 375.

50. Oliver, G.J.H. (1988). Arenig to Wenlock Regional Metamorphism in the Paratectonic Caledonides of the British Isles : a Review. In The Caledonian-Appalachian Orogen. Harris, A.L. and Fettes, D.J. (editors), Geol. Soc. Spec. Publ. no. 38, 347-363, Blackwell Scientific for the Geological Society, Oxford.

51. Oliver, J. (1986). Fluids Expelled Tectonically from Orogenic Belts: Their Role in Hydrocarbon Migration and Other Geologic Phenomena. Geology ,14, 99-102.

52. O'Reilly, W. (1983). Rock and Mineral Magnetism. Blackie & Son, Glasgow.

53. Owen, T.R. (1974). The Variscan Orogeny in Wales. In The Upper Palaeozoic and Post-Palaeozoic Rocks of Wales. Owen, T.R. (editor), Univ. of Wales Press, Cardiff.

54. Owen, T.R. and Weaver, J.D. (1983). The Structure of the Main South Wales Coalfield and its Margins. In The Variscan Fold Belt in the British Isles. Hancock, P.L. (editor), Adam Hilger Ltd. , Bristol.

55. Palmer, J.A. , Perry, S.P.G. and Tarling, D.H. (1985). Carboniferous Magnetostratigraphy. J. geol. Soc. London ,142, 945-956.

56. Perroud, H., Van der Voo, R. and Bonhommet, N. (1984). Palaeozoic evolution of the Armorica Plate on the Basis of Palaeomagnetic Data. Geology ,12, 579-582.

57. Piper, J.D.A. (1987). Palaeomagnetism and the Continental Crust. Open University Press, Milton Keynes.

58. Piper, J.D.A. and Grant, S. (1989). A Palaeomagnetic Test of the Axial Dipole Assumption and Implication for Continental Distribution through Geological Time. Phys. Earth Planet. Intr. ,55, 37-53.

59. Piper, J.D.A., Atkinson, D., Norris, S. and Thomas, S. (1991). Palaeomagnetic Study of the Derbyshire Lavas and Intrusions, Central England : Definition of Carboniferous Apparent Polar Wander. Phys. Earth Planet. Intr. in press.

60. Powell, C.M. (1989). Structural Controls on Palaeozoic Basin Evolution and Inversion in Southwest Wales. J. geol. Soc. London ,146, 439-446.

61. Press, F. and Siever, R. (1985) Earth (4th Edition) W.H. Freeman, New York.

62. Rast, N. (1983). Variscan Orogeny. In The Variscan Fold Belt in the British Isles. Hancock, P.L. (editor), Adam Hilger Ltd. , Bristol.

63. Roy, J.L. and Morris, W.A. (1983). A Review of Palaeomagnetic Results from the Carboniferous of North America; the Concept of Carboniferous Geomagnetic Field Horizon Markers. Earth Planet. Sci. Lett. ,65, 167-181.

64. Schwartz, S.Y. and Van der Voo, R. (1984). Palaeomagnetic Study of Thrust Sheet Rotation during Foreland Impingement in the Wyoming-Idaho Overthrust Belt. J. Geophys. Res. ,89, 10,077-10,086.

65. Sherwood, G.J. (1989). MATZIJ - A Basic Program to Determine Paleomagnetic Remanence Directions Using Principal Component Analysis. Computers & Geosciences ,15, 1173-1182.

66. Stamatakos, J. (1991). Kiaman Remagnetisation as a Test of Oroclinal Bending in the Central Appalachian Valley and Ridge Province. IUGG Proceeds (abstr.) ,p. 100, XX General Assembly, Vienna.

67. Stearns, C. and Van der Voo, R. (1987). Palaeomagnetic Results from the Lower Devonian Llandstadwell Formation, Dyfed, Wales. Tectonophysics ,143, 329-334.

68. Storetvedt, K.M., Tveit, E., Deutsch, E.R. and Murthy, G.S. (1990). Multicomponent Magnetizations in the Foyers Old Red Sandstone (Northern Scotland) and Their Bearing on Lateral Displacements along the Great Glen Fault. Geophys. J. Int. ,102, 151-163.

69. Tarling, D.H., Mitchell, J.G. and Spall, H. (1973). A Palaeomagnetic and Isotopic Age for the Wackerfield Dyke of Northern England. Earth Planet. Sci. Lett. ,18, 427-432.

70. Tarling, D.H. (1983). Palaeomagnetism. Principles and Application in Geology, Geophysics and Archeology. Chapman & Hall, London.

71. Thomas, L.P. (1974). The Westphalian (Coal Measures) in South Wales. In The Upper Palaeozoic and Post-Palaeozoic Rocks of Wales. Owen, T.R. (editor), Univ. of Wales Press, Cardiff.

72. Thompson, R. and Oldfield, F. (1986). Environmental Magnetism. Allen & Unwin, London.

73. Titman, D.J. (1971). A Palaeomagnetic Study of Some Upper Palaeozoic Rocks. MSc. thesis. Univ. Newcastle-upon-Tyne.

74. Torsvik, T.H., Lyse, O., Atterás, G. and Bluck, B.J. (1989). Palaeozoic Palaeomagnetic Results from Scotland and Their Bearing on the British Apparent Polar Wander Path. Phys. Earth Planet. Intr. ,55, 93-105.

75. Turner, P. and Tarling, D.H. (1975). Implications of New Palaeomagnetic Results from the Carboniferous System in Britain. J. geol. Soc. London ,131, 469-488.

76. Turner, P. and Archer, R. (1977). The Role of Biotite in the Diagenesis of Red Beds from the Devonian of Northern Scotland. Sediment. Geol. ,19, 241-251.

77. Turner, P. and Archer, R. (1978). Palaeomagnetic and Mineralogical Studies of Devonian Lacustrine Sediments from Caithness, Scotland. Phys. Earth Planet. Intr. ,16, 73-83.

78. Turner, P. (1979). The Palaeomagnetic Evolution of Continental Red Beds. Geol. Mag. ,116, 289-301. Elsevier Publication Co., Amsterdam.

79. Turner, P. (1980). Continental Red Beds. Developments in Sedimentology No.29. Elsevier Publication Co., Amsterdam.

80. Turner, P., Vaughan, D.J. and Besly, B. (1985). Remanence Acquisition in Red Beds from the Coal Measures of Central England. J. geol. Soc. London ,142, 000-000.

81. Turner, P. (1987). Magnetostratigraphy. Geology Today ,July-August, 127-132.

82. Van den Ende, C. (1977). Palaeomagnetism of Permian Red Beds of the Dome de Barrot - (S. France). PhD. thesis. Univ. Utrecht.

83. Van der Pluijm, B.A. (1987). Grain-scale Deformation and the Fold Test - Evaluation of Syn-folding Remagnetisation. Red Sandstone Creek Section, Vail, Colorado. Geophys. Res. Lett. ,14, 155-157.

84. Walker, T.R., Larson, E.E. and Hoblitt, R.P. (1981). Nature and Origin of Hematite in the Moenkopi Formation (Triassic), Colorado Plateau : A Contribution to the Origin of Magnetisation in Red Beds. J. Geophys. Res. ,86, 317-333.

APPENDIX A

Table A-1a Palaeomagnetic results from South Wales red beds.
Dec/CDec = in situ/tilt-corrected declination.
Inc/CInc = in situ/tilt-corrected inclination.
Tilt/Dir = bedding correction where Dir = direction of the tilt.
a95 = maximum angular deviation from the straight line determined by the three or more points in orthogonal plots (except specimens : (GGB1)DV3104, DV4702, DV4703 and DV4716 (using Fisher statistics)).
The unit of the temperature is °C (except 000 denotes before the treatment).
Comp = Component; LT = Lower Temperature, HT = Higher Temperature
PC = Permo-Carboniferous and XX = excluded from PC site mean calculation.

SPECIMEN	Comp	Dec	Inc	Tilt	Dir	CDec	CInc	a95	Temp. range
GGB1DV0101	LT	321.0	52.0	15	165	308.5	65.1	11.1	000 - 150
GGB1DV0101	PC	204.4	00.3	15	165	205.3	-11.3	04.9	200 - 625
GGB1DV0102	LT	228.2	78.4	15	165	192.7	67.3	16.6	000 - 150
GGB1DV0102	PC	201.0	-00.4	15	165	202.0	-12.5	05.6	200 - 625
GGB1DV0103	LT	266.5	52.5	15	165	246.5	52.9	25.4	000 - 150
GGB1DV0103	PC	192.5	09.6	15	165	192.1	-03.7	07.2	200 - 720
GGB1DV0104	PC	184.9	-09.0	15	165	186.4	-23.1	07.3	000 - 400
GGB1DV0104	HT	196.9	43.3	15	165	191.4	30.1	12.4	450 - 720
GGB1DV0105	LT	119.2	-52.9	15	165	099.8	-61.6	23.8	000 - 150
GGB1DV0105	PC	183.1	-01.0	15	165	183.8	-15.2	07.6	200 - 720
GGB1DV0201	LT	211.2	37.3	15	177	206.4	24.5	20.1	000 - 300
GGB1DV0201	PC	191.5	11.2	15	177	191.3	-03.3	06.5	350 - 600
GGB1DV0202	LT	290.5	78.9	15	177	221.6	75.4	27.3	000 - 350
GGB1DV0202	PC	197.7	15.6	15	177	197.0	01.5	07.5	400 - 600
GGB1DV0202	HT	203.7	37.5	15	177	199.9	23.9	05.7	625 - 720
GGB1DV0203	LT	016.2	83.2	15	177	162.4	81.1	40.0	000 - 350
GGB1DV0203	PC	211.0	-04.4	15	177	212.6	-16.7	06.2	400 - 600
GGB1DV0203	HT	186.1	09.1	15	177	186.0	-05.8	06.2	625 - 720
GGB1DV0204	LT	298.3	72.1	15	177	247.6	73.8	31.3	000 - 350
GGB1DV0204	PC	187.4	10.3	15	177	187.3	-04.4	09.8	400 - 720
GGB1DV0205	LT	198.5	64.0	15	177	191.4	49.7	33.0	000 - 350
GGB1DV0205	PC	175.7	20.0	15	177	175.7	05.0	02.9	400 - 500
GGB1DV0205	HT	160.6	26.4	15	177	162.0	11.9	19.4	550 - 720
GGB1DV0301	PC	210.3	10.1	17	136	208.1	05.1	10.3	100 - 550
GGB1DV0301	HT	122.3	-24.0	17	136	119.5	-40.4	21.1	600 - 700
GGB1DV0302	PC	192.4	23.5	17	136	187.7	13.4	28.7	000 - 500
GGB1DV0302	HT	228.9	20.5	17	136	222.5	20.4	20.4	550 - 700
GGB1DV0303	PC	219.1	-04.4	17	136	220.7	-06.2	14.4	000 - 550
GGB1DV0303	HT	171.5	-17.3	17	136	176.1	-30.7	13.5	600 - 700
GGB1DV0304	LT	025.7	-05.3	17	136	025.0	00.8	04.7	100 - 200
GGB1DV0304	PC	208.5	05.9	17	136	207.5	00.7	03.5	250 - 700
GGB1DV0305	LT	035.5	-30.8	17	136	026.4	-26.4	02.7	100 - 200
GGB1DV0305	PC	226.7	06.8	17	136	224.7	06.7	05.8	250 - 675
GGB1DV0401	LT	044.7	08.5	19	160	048.6	16.1	41.0	000 - 300
GGB1DV0401	PC	006.4	11.6	19	160	009.7	28.4	07.9	350 - 700
GGB1DV0402	PC	020.5	-16.3	19	160	018.6	-01.6	13.9	000 - 550
GGB1DV0402	HT	017.1	-03.3	19	160	018.0	11.8	08.9	600 - 675
GGB1DV0403	PC	012.7	02.7	19	160	014.7	18.6	16.6	000 - 600
GGB1DV0403	HT	315.3	-06.9	19	160	315.1	10.4	08.2	625 - 700
GGB1DV0404	PC	006.3	-14.5	19	160	005.4	02.6	13.6	000 - 550
GGB1DV0404	HT	004.5	-43.0	19	160	359.6	-25.3	17.1	600 - 700
GGB1DV0405	PC	024.5	-02.6	19	160	025.5	10.9	13.6	000 - 500
GGB1DV0405	HT	249.5	17.0	19	160	243.9	15.9	36.7	550 - 700

GGB1DV0501	PC	211.2	-00.5	18	167	212.7	-13.3	02.7	000 - 720
GGB1DV0502	PC	209.2	00.4	18	167	210.5	-12.9	02.0	000 - 720
GGB1DV0503	PC	212.9	-02.2	18	167	214.9	-14.5	02.4	000 - 720
GGB1DV0504	PC	211.9	-01.5	18	167	213.7	-14.1	05.5	000 - 550
GGB1DV0505	PC	206.9	-03.2	18	167	209.0	-16.9	03.8	000 - 550
GGB1DV0601	PC	208.6	03.5	10	190	208.7	-05.9	04.6	000 - 700
GGB1DV0602	PC	208.5	-01.3	10	190	208.8	-10.8	04.5	000 - 700
GGB1DV0603	PC	204.0	01.4	10	190	204.2	-08.3	03.0	000 - 700
GGB1DV0604	PC	208.4	02.1	10	190	208.5	-07.4	03.9	000 - 700
GGB1DV0605	PC	214.6	00.3	10	190	214.9	-08.8	03.3	000 - 700
GGB1DV0701	LT	019.0	71.4	48	168	150.5	56.9	28.5	000 - 250
GGB1DV0701	PC	209.1	00.9	48	168	219.8	-33.3	03.3	300 - 720
GGB1DV0702	LT	106.7	-74.1	48	168	009.0	-47.8	24.7	000 - 200
GGB1DV0702	PC	208.7	00.7	48	168	219.7	-33.7	03.8	250 - 720
GGB1DV0703	LT	310.0	75.8	48	168	182.4	52.4	06.8	000 - 200
GGB1DV0703	PC	206.4	-02.1	48	168	219.3	-37.3	03.2	250 - 720
GGB1DV0704	LT	224.8	33.3	48	168	212.4	01.5	25.8	000 - 250
GGB1DV0704	PC	210.0	15.1	48	168	211.9	-21.0	03.0	300 - 700
GGB1DV0705	LT	287.2	45.0	48	168	232.5	46.8	20.3	000 - 200
GGB1DV0705	PC	212.6	03.6	48	168	221.3	-29.1	04.7	250 - 700
GGB1DV0801	PC	209.8	-11.6	40	340	210.6	14.6	02.4	000 - 720
GGB1DV0802	PC	201.2	-14.9	40	340	201.4	15.7	02.1	000 - 720
GGB1DV0803	PC	210.5	-11.3	40	340	211.4	14.6	03.0	000 - 720
GGB1DV0804	PC	205.4	-12.2	40	340	206.5	16.2	03.7	000 - 700
GGB1DV0805	PC	206.8	-13.7	40	340	206.9	14.2	02.6	000 - 675
GGB1DV0901	PC	200.1	-04.4	64	333	216.4	35.2	03.3	000 - 720
GGB1DV0902	PC	206.8	-05.7	64	333	219.6	29.0	04.8	000 - 720
GGB1DV0903	PC	202.5	-04.8	64	333	217.7	33.0	03.8	000 - 720
GGB1DV1001	PC	213.5	-00.3	45	349	223.1	30.1	02.8	000 - 700
GGB1DV1002	PC	207.1	-04.4	45	349	214.3	30.1	02.6	000 - 700
GGB1DV1003	PC	207.8	-03.4	45	349	215.5	30.5	02.8	000 - 675
GGB1DV1004	PC	207.8	-03.9	45	349	215.2	30.1	03.3	000 - 700
GGB1DV1005	PC	206.8	-05.2	45	349	213.5	29.5	02.5	000 - 675
GGB1DV1201	PC	199.0	-03.9	65	342	218.4	43.9	04.6	000 - 720
GGB1DV1202	PC	199.9	-01.5	65	342	221.9	44.8	03.8	000 - 700
GGB1DV1203	PC	195.7	-04.9	65	342	214.3	45.6	04.9	000 - 675
GGB1DV1204	PC	194.5	-06.5	65	342	211.4	45.3	05.9	000 - 700
GGB1DV1205	PC	199.6	02.5	65	342	226.2	47.3	07.0	000 - 700
GGB1DV1401	PC	197.3	-09.2	15	165	199.6	-21.8	05.5	100 - 700
GGB1DV1402	LT	186.1	71.1	15	165	177.2	56.6	10.2	000 - 200
GGB1DV1402	XX	187.2	-40.3	15	165	194.2	-53.9	09.3	250 - 700
GGB1DV1403	LT	201.4	60.6	15	165	190.6	47.7	18.8	000 - 250
GGB1DV1403	PC	189.9	-06.1	15	165	191.4	-19.6	04.3	300 - 700
GGB1DV1404	LT	237.0	86.2	15	165	177.8	73.4	21.2	000 - 250
GGB1DV1404	PC	194.1	01.9	15	165	194.7	-11.2	04.8	300 - 700
GGB1DV1405	LT	247.1	74.6	15	165	207.7	67.2	15.0	000 - 250
GGB1DV1405	PC	180.6	02.6	15	165	180.9	-11.8	07.0	300 - 700
GGB1DV1501	PC	181.6	04.4	15	165	181.8	-10.0	05.9	100 - 625
GGB1DV1501	HT	272.7	-86.4	15	165	332.9	-73.6	08.0	650 - 700
GGB1DV1502	PC	194.6	-02.1	15	165	195.7	-15.1	09.8	150 - 700
GGB1DV1503	PC	186.9	09.9	15	165	186.6	-04.0	13.5	100 - 500
GGB1DV1503	HT	225.3	31.9	15	165	218.6	23.7	04.8	550 - 700
GGB1DV1504	PC	192.0	-01.0	15	165	193.0	-14.3	09.3	100 - 700

GGB1DV1505	LT	167.9	19.5	15	165	167.7	04.5	36.5	000 - 350
GGB1DV1505	PC	199.8	22.0	15	165	197.4	09.5	05.8	400 - 700
GGB1DV1601	PC	183.6	03.8	15	165	183.9	-10.4	09.9	100 - 550
GGB1DV1601	HT	196.8	29.3	15	165	193.6	16.3	20.2	600 - 700
GGB1DV1602	PC	173.8	03.0	15	165	174.0	-11.8	12.0	100 - 700
GGB1DV1603	PC	189.9	-00.5	15	165	190.7	-14.0	02.6	150 - 350
GGB1DV1603	HT	349.1	-09.8	15	165	349.1	05.1	28.1	400 - 675
GGB1DV1604	LT	312.3	76.6	15	165	228.2	81.9	05.8	000 - 150
GGB1DV1604	PC	189.5	-08.8	15	165	191.3	-22.4	07.5	200 - 400
GGB1DV1604	HT	124.8	-19.3	15	165	120.1	-30.4	43.3	450 - 700
GGB1DV1605	LT	334.2	67.8	15	165	314.3	82.0	07.3	000 - 150
GGB1DV1605	PC	179.3	-13.3	15	165	180.7	-27.8	11.6	200 - 400
GGB1DV1605	HT	346.7	55.2	15	165	347.9	70.2	19.8	450 - 700
GGB1DV1701	LT	162.5	72.1	15	165	163.6	57.1	09.8	000 - 150
GGB1DV1701	PC	182.3	02.9	15	165	182.6	-11.4	06.8	200 - 700
GGB1DV1702	PC	186.2	06.2	15	165	186.2	-07.8	09.4	100 - 500
GGB1DV1702	HT	236.6	-66.6	15	165	272.1	-66.7	17.6	550 - 700
GGB1DV1703	PC	188.3	05.6	15	165	188.5	-08.2	06.7	100 - 700
GGB1DV1704	LT	215.4	73.2	15	165	192.6	61.3	10.6	000 - 150
GGB1DV1704	PC	180.4	-05.9	15	165	181.3	-20.3	06.0	200 - 600
GGB1DV1704	HT	244.9	41.6	15	165	232.9	37.4	08.8	625 - 700
GGB1DV1705	PC	183.9	03.7	15	165	184.2	-10.5	07.8	100 - 550
GGB1DV1705	HT	294.0	04.0	15	165	292.2	13.3	23.7	600 - 700
GGB1DV1801	LT	241.2	86.9	15	165	176.1	74.0	17.8	000 - 250
GGB1DV1801	PC	197.8	-13.4	15	165	200.9	-25.8	08.2	300 - 600
GGB1DV1801	HT	118.8	-61.3	15	165	090.2	-68.9	13.9	625 - 700
GGB1DV1802	LT	321.2	73.1	15	165	259.7	83.2	04.4	000 - 150
GGB1DV1802	PC	189.9	-07.6	15	165	191.5	-21.2	09.7	200 - 500
GGB1DV1802	HT	127.0	22.0	15	165	129.6	10.0	41.3	550 - 700
GGB1DV1803	LT	332.9	73.8	15	165	269.7	86.5	11.1	000 - 100
GGB1DV1803	PC	165.3	02.8	15	165	165.3	-12.2	07.1	250 - 675
GGB1DV1804	LT	337.1	75.1	15	165	249.1	88.0	14.2	000 - 250
GGB1DV1804	PC	200.9	16.8	15	165	199.3	04.5	15.1	300 - 650
GGB1DV1805	LT	315.6	81.3	15	165	195.0	81.5	19.3	000 - 250
GGB1DV1805	PC	178.6	00.1	15	165	179.0	-14.4	10.8	300 - 700
GGB1DV1901	PC	178.0	-00.7	15	165	178.5	-15.3	06.8	150 - 700
GGB1DV1902	PC	191.2	03.0	15	165	191.6	-10.4	09.4	150 - 550
GGB1DV1902	HT	241.5	06.5	15	165	240.3	02.8	08.3	600 - 700
GGB1DV1903	LT	277.7	67.0	15	165	240.6	68.1	22.6	000 - 200
GGB1DV1903	PC	189.1	-05.3	15	165	190.4	-18.9	01.9	250 - 400
GGB1DV1903	HT	144.3	02.3	15	165	143.9	-11.7	10.2	450 - 700
GGB1DV1904	PC	196.4	-01.6	15	165	197.6	-14.4	05.6	100 - 500
GGB1DV1904	HT	147.6	03.4	15	165	147.3	-10.9	08.6	550 - 700
GGB1DV1905	PC	181.2	-13.4	15	165	182.8	-27.8	02.9	100 - 450
GGB1DV1905	HT	209.2	35.5	15	165	203.5	24.2	28.5	500 - 700
GGB1DV2001	LT	040.5	66.3	15	165	078.1	70.6	10.6	000 - 200
GGB1DV2001	PC	193.8	-11.9	15	165	196.3	-24.9	11.2	250 - 625
GGB1DV2002	LT	060.2	72.8	15	165	106.3	70.4	16.4	000 - 200
GGB1DV2002	PC	196.0	-06.3	15	165	197.8	-19.1	11.2	250 - 700
GGB1DV2003	PC	187.6	-10.4	15	165	189.4	-24.2	05.1	100 - 700
GGB1DV2004	PC	184.3	-07.6	15	165	185.6	-21.7	11.4	100 - 650
GGB1DV2101	PC	185.5	-15.0	19	132	191.4	-25.6	03.2	000 - 660
GGB1DV2102	PC	188.0	-04.5	19	132	190.7	-14.9	09.0	000 - 620
GGB1DV2103	PC	184.5	-07.6	19	132	188.2	-18.8	03.9	000 - 620
GGB1DV2104	PC	187.5	-09.8	19	132	191.8	-20.0	03.0	000 - 620
GGB1DV2105	PC	187.7	-04.7	19	132	190.5	-15.1	03.0	000 - 640

GGB1DV2106	PC	186.5	-08.6	19	132	190.4	-19.2	03.8	000 - 640
GGB1DV2107	PC	196.6	12.2	19	132	194.2	03.6	14.5	000 - 580
GGB1DV2108	PC	183.5	-00.8	19	132	185.3	-12.5	08.5	000 - 700
GGB1DV2109	PC	182.6	-11.1	19	132	187.2	-22.6	10.8	000 - 580
GGB1DV2110	PC	181.3	-09.0	19	132	185.3	-21.0	08.2	000 - 580
GGB1DV2111	PC	186.4	-11.8	19	132	191.3	-22.3	10.3	000 - 680
GGB1DV2201	PC	184.8	-17.2	24	123	193.9	-27.0	18.9	000 - 580
GGB1DV2202	PC	192.0	-04.1	24	123	195.3	-12.2	05.2	000 - 640
GGB1DV2203	PC	189.8	-09.9	24	123	195.6	-18.3	03.5	000 - 660
GGB1DV2204	PC	186.4	-10.8	24	123	192.6	-20.5	05.2	000 - 680
GGB1DV2205	PC	185.9	-19.6	24	123	196.1	-28.8	05.8	000 - 640
GGB1DV2206	PC	193.3	-02.7	24	123	195.9	-10.4	08.2	000 - 620
GGB1DV2207	PC	189.1	-02.7	24	123	192.1	-12.0	03.8	000 - 660
GGB1DV2208	PC	188.6	-02.5	24	123	191.4	-11.9	05.6	000 - 680
GGB1DV2209	PC	186.3	-03.7	24	123	189.7	-14.0	04.1	000 - 640
GGB1DV2301	LT	278.8	-79.2	14	140	301.7	-66.7	17.5	000 - 200
GGB1DV2301	PC	195.4	-18.6	14	140	200.2	-26.1	08.2	250 - 700
GGB1DV2302	PC	194.3	-19.1	14	140	199.3	-26.8	03.4	000 - 640
GGB1DV2303	PC	189.1	-16.7	14	140	193.3	-25.5	03.1	000 - 640
GGB1DV2304	PC	188.8	-14.7	14	140	192.6	-23.6	04.5	000 - 640
GGB1DV2305	PC	194.7	-10.0	14	140	197.6	-17.8	03.4	000 - 640
GGB1DV2306	PC	190.3	-15.8	14	140	194.4	-24.4	02.9	000 - 640
GGB1DV2307	PC	192.3	-13.8	14	140	195.9	-22.0	09.5	000 - 700
GGB1DV2401	LT	007.2	-12.5	55	160	013.5	36.0	31.3	000 - 300
GGB1DV2401	PC	201.6	03.3	55	160	214.4	-35.4	02.1	350 - 640
GGB1DV2402	LT	219.0	52.4	57	168	196.5	06.3	41.1	000 - 300
GGB1DV2402	PC	200.4	02.5	57	168	215.2	-43.1	02.2	350 - 620
GGB1DV2403	LT	008.7	42.9	57	168	115.4	70.9	14.0	000 - 250
GGB1DV2403	PC	201.2	14.9	57	168	206.9	-32.5	06.3	300 - 580
GGB1DV2404	PC	192.6	08.1	57	168	202.1	-42.7	05.0	100 - 640
GGB1DV2405	PC	196.3	03.0	57	168	210.1	-45.1	04.6	000 - 680
GGB1DV2406	LT	203.9	19.8	57	168	206.3	-27.1	21.4	000 - 300
GGB1DV2406	PC	193.2	08.1	57	168	202.9	-42.4	03.2	350 - 660
GGB1DV2407	LT	229.5	-33.3	57	168	276.3	-39.3	16.1	000 - 200
GGB1DV2407	PC	186.2	10.7	57	168	192.8	-42.9	04.4	250 - 700
GGB1DV2408	PC	205.9	16.3	62	162	211.3	-28.7	16.3	100 - 700
GGB1DV2409	PC	197.9	27.0	62	162	197.2	-25.1	08.7	100 - 680
GGB1DV2410	LT	356.[illegible]	23.6	62	162	057.1	76.0	46.5	000 - 200
GGB1DV2410	PC	202.3	16.3	62	162	208.4	-31.0	04.1	250 - 620
GGB1DV2411	LT	192.9	39.8	62	162	186.2	-16.4	16.0	000 - 300
GGB1DV2411	PC	201.5	13.5	62	162	209.9	-33.6	02.2	350 - 620
GGB1DV2412	LT	198.7	12.4	62	162	208.3	-36.2	33.4	000 - 300
GGB1DV2412	PC	191.9	13.1	62	162	201.1	-39.7	05.3	350 - 620
GGB1DV2413	LT	180.7	50.5	62	162	174.0	-09.8	33.9	000 - 300
GGB1DV2413	PC	190.4	20.1	62	162	194.9	-34.6	04.1	350 - 620
GGB1DV2414	LT	192.8	17.2	62	162	199.1	-35.9	20.7	000 - 300
GGB1DV2414	PC	187.1	17.6	62	162	193.0	-38.3	06.0	350 - 600
GGB1DV2415	LT	173.3	49.4	62	162	169.5	-11.9	30.5	000 - 300
GGB1DV2415	PC	187.3	18.2	62	162	192.8	-37.7	03.6	350 - 600
GGB1DV2416	LT	030.2	59.2	62	162	129.5	44.8	40.1	000 - 200
GGB1DV2416	PC	190.0	08.6	62	162	202.6	-44.4	06.9	350 - 620
GGB1DV2417	LT	045.5	53.4	62	162	119.6	37.7	35.9	000 - 250
GGB1DV2417	PC	186.9	13.9	62	162	195.2	-41.7	05.8	300 - 600
GGB1DV2501	LT	339.8	19.9	62	162	327.9	81.6	24.4	000 - 250
GGB1DV2501	PC	194.1	10.2	62	162	205.7	-40.8	03.2	300 - 660
GGB1DV2502	LT	024.5	52.2	62	162	121.6	50.3	21.3	000 - 250
GGB1DV2502	PC	194.0	03.4	62	162	211.6	-46.0	04.0	300 - 660
GGB1DV2503	LT	020.7	-02.0	62	162	039.6	42.2	20.2	000 - 300

GGB1DV2503	PC	198.0	09.2	62	162	210.3	-39.0	13.6	350 - 700
GGB1DV2504	LT	003.1	69.0	62	162	151.1	47.1	30.0	000 - 300
GGB1DV2504	PC	189.1	12.3	62	162	198.7	-41.9	04.8	350 - 680
GGB1DV2505	LT	020.4	68.3	62	162	143.4	43.8	42.7	000 - 200
GGB1DV2505	PC	194.6	18.1	62	162	200.2	-34.1	05.7	250 - 680
GGB1DV2506	LT	027.2	57.1	62	162	127.5	47.1	31.7	000 - 250
GGB1DV2506	PC	192.2	05.7	62	162	207.5	-45.4	05.2	300 - 660
GGB1DV2507	LT	016.5	-04.3	62	162	033.3	43.7	05.6	000 - 200
GGB1DV2507	PC	195.7	08.2	62	162	209.0	-41.3	05.5	250 - 700
GGB1DV2508	PC	208.3	03.6	62	162	224.3	-35.4	04.1	000 - 700
GGB1DV2509	LT	016.3	-08.9	62	162	029.0	40.4	07.4	000 - 200
GGB1DV2509	PC	200.1	10.8	62	162	210.9	-36.5	05.0	250 - 700
GGB1DV2510	PC	195.4	20.0	62	162	199.7	-32.2	05.8	000 - 700
GGB1DV2601	LT	175.6	-81.6	54	330	154.1	-28.4	21.7	000 - 200
GGB1DV2601	PC	200.6	-11.1	54	330	205.4	23.0	23.0	250 - 640
GGB1DV2602	LT	087.0	-25.4	54	330	096.2	04.6	20.5	000 - 200
GGB1DV2602	PC	205.1	-11.9	54	330	208.3	19.4	05.0	250 - 600
GGB1DV2603	LT	007.2	73.4	54	330	340.8	22.3	22.2	000 - 200
GGB1DV2603	XX	035.4	-05.8	54	330	049.9	-23.2	05.3	250 - 640
GGB1DV2604	LT	344.6	72.1	54	330	334.7	18.6	16.0	000 - 200
GGB1DV2604	XX	065.6	-12.3	54	330	073.2	-02.8	03.9	250 - 640
GGB1DV2605	PC	207.8	-13.3	54	330	209.2	16.5	05.7	000 - 640
GGB1DV2606	LT	323.2	59.0	54	330	326.5	05.2	13.0	000 - 150
GGB1DV2606	PC	211.1	-12.4	54	330	212.2	14.8	05.8	200 - 640
GGB1DV2607	PC	216.1	-09.9	54	330	217.5	12.8	04.0	000 - 700
GGB1DV2608	XX	116.9	-17.6	54	330	114.0	27.9	03.6	000 - 700
GGB1DV2609	LT	303.8	-31.9	54	330	243.0	-67.9	25.0	000 - 200
GGB1DV2609	XX	295.4	-03.5	54	330	277.4	-44.5	05.2	250 - 700
GGB1DV2610	XX	359.8	09.0	54	330	007.9	-37.0	05.7	000 - 700
GGB1DV2611	LT	048.2	04.9	54	330	049.0	-06 6	13.3	000 - 250
GGB1DV2611	XX	337.3	-07.4	54	330	345.0	-60.7	04.3	300 - 700
GGB1DV2612	LT	294.9	-22.0	54	330	254.9	-56.5	28.9	000 - 200
GGB1DV2612	PC	205.5	-16.6	54	330	205.1	15.7	04.7	250 - 700
GGB1DV2613	LT	168.6	07.6	54	330	185.3	56.9	33.8	000 - 250
GGB1DV2613	XX	355.1	-01.7	54	330	009.9	-48.5	04.3	300 - 700
GGB1DV2614	PC	202.6	-15.2	54	330	204.0	18.7	06.0	100 - 640
GGB1DV2615	LT	300.3	-26.9	54	330	251.4	-63.2	35.7	000 - 200
GGB1DV2615	PC	206.4	-17.0	54	330	205.5	14.9	04.7	250 - 700
GGB1DV2704	PC	208.1	-02.0	25	166	211.6	-20.2	03.4	000 - 700
GGB1DV2706	PC	207.3	-11.9	25	166	214.1	-29.8	02.6	000 - 700
GGB1DV2707	PC	207.1	-05.1	25	166	211.5	-23.5	04.7	000 - 700
GGB1DV2708	PC	208.0	-06.8	25	166	213.0	-24.8	06.0	000 - 700
GGB1DV2709	PC	205.5	-02.8	25	166	209.1	-21.7	03.9	000 - 700
GGB1DV2710	PC	213.0	-09.5	25	166	219.2	-25.7	04.1	000 - 700
GGB1DV2711	PC	208.1	-01.3	25	166	211.3	-19.5	03.4	000 - 640
GGB1DV2712	PC	216.8	-10.0	25	166	223.2	-24.9	03.6	000 - 700
GGB1DV2713	PC	209.8	-06.6	25	166	214.9	-24.0	02.8	000 - 700
GGB1DV2714	LT	228.2	82.7	25	166	179.4	60.9	26.5	000 - 200
GGB1DV2714	PC	211.2	-03.6	25	166	215.2	-20.7	05.0	250 - 640
GGB1DV2715	LT	121.4	39.7	25	166	130.8	20.4	29.6	000 - 200
GGB1DV2715	PC	209.8	-09.6	25	166	215.9	-26.9	03.6	250 - 660
GGB1DV2716	LT	121.7	-04.5	25	166	117.4	-21.8	33.0	000 - 250
GGB1DV2716	PC	210.5	-10.7	25	166	217.0	-27.7	04.6	300 - 700
GGB1DV2717	LT	164.0	60.4	25	166	164.8	35.4	17.2	000 - 200
GGB1DV2717	PC	200.7	-04.3	25	166	204.6	-24.5	02.3	250 - 700
GGB1DV2718	LT	276.0	27.7	25	166	261.3	33.3	35.3	000 - 200
GGB1DV2718	PC	207.1	-07.9	25	166	212.5	-26.1	02.7	250 - 700
GGB1DV2719	LT	027.8	-69.8	25	166	006.1	-47.9	21.9	000 - 200
GGB1DV2719	PC	210.4	-08.0	25	166	216.0	-25.2	04.0	250 - 700
GGB1DV2720	LT	012.0	29.3	25	166	023.2	50.8	21.4	000 - 200

GGB1DV2720	PC	206.2	-04.2	25	166	210.3	-22.9	03.9	250 - 700
GGB1DV2721	LT	121.4	37.0	25	166	129.9	17.7	01.8	000 - 150
GGB1DV2721	PC	202.7	-05.7	25	166	207.1	-25.3	03.8	200 - 700
GGB1DV2722	LT	020.7	06.1	25	166	025.1	26.2	09.7	000 - 150
GGB1DV2722	PC	202.2	-03.5	25	166	206.0	-23.3	03.9	200 - 700
GGB1DV2801	LT	148.2	74.5	14	180	162.8	61.7	25.7	000 - 250
GGB1DV2801	XX	133.5	19.1	14	180	136.0	09.3	03.1	300 - 700
GGB1DV2802	LT	038.6	57.5	14	180	058.8	67.0	25.6	000 - 150
GGB1DV2802	PC	220.5	-03.3	14	180	221.9	-13.8	07.3	200 - 700
GGB1DV2803	LT	185.5	-33.4	14	180	186.8	-47.3	26.3	000 - 200
GGB1DV2803	PC	210.5	-06.3	14	180	212.1	-18.3	05.3	250 - 700
GGB1DV2901	LT	231.3	09.1	00	000	231.3	09.1	30.9	000 - 350
GGB1DV2901	PC	206.9	-18.4	00	000	206.9	-18.4	04.8	400 - 580
GGB1DV2902	LT	134.5	06.9	00	000	134.5	06.9	20.1	000 - 150
GGB1DV2902	PC	206.2	-11.5	00	000	206.2	-11.5	03.0	200 - 580
GGB1DV2903	LT	326.4	-13.7	00	000	326.4	-13.7	32.8	000 - 150
GGB1DV2903	PC	190.4	-10.1	00	000	190.4	-10.1	05.6	200 - 550
GGB1DV2904	LT	127.3	02.4	00	000	127.3	02.4	23.4	000 - 150
GGB1DV2904	PC	197.9	06.2	00	000	197.9	06.2	09.3	200 - 550
GGB1DV2905	PC	210.1	-14.9	00	000	210.1	-14.9	06.3	000 - 700
GGB1DV2906	LT	192.2	10.4	00	000	192.2	10.4	23.3	000 - 300
GGB1DV2906	PC	200.4	-13.3	00	000	200.4	-13.3	05.2	350 - 550
GGB1DV2907	LT	289.1	-45.5	00	000	289.1	-45.5	06.6	100 - 250
GGB1DV2907	PC	217.4	-10.2	00	000	217.4	-10.2	06.4	300 - 700
GGB1DV3001	LT	125.5	59.6	04	251	131.5	61.8	19.9	000 - 150
GGB1DV3001	PC	203.0	-05.5	04	251	202.6	-08.2	07.4	200 - 600
GGB1DV3002	LT	260.8	73.2	04	251	258.9	69.3	17.4	000 - 150
GGB1DV3002	PC	199.6	-07.5	04	251	199.1	-10.0	08.3	200 - 600
GGB1DV3003	LT	261.5	-60.5	04	251	263.0	-64.4	38.3	000 - 350
GGB1DV3003	PC	206.7	00.4	04	251	206.6	-02.4	14.3	400 - 620
GGB1DV3004	LT	283.6	-67.7	04	251	289.9	-71.0	43.6	000 - 350
GGB1DV3004	PC	199.0	-00.7	04	251	198.9	-03.2	14.9	400 - 620
GGB1DV3005	LT	152.8	72.2	04	251	165.4	72.3	19.8	000 - 200
GGB1DV3005	PC	200.0	-02.1	04	251	199.8	-04.6	05.3	250 - 580
GGB1DV3006	PC	199.4	-03.5	04	251	199.2	-05.9	05.6	000 - 700
GGB1DV3007	PC	205.2	-03.3	04	251	204.9	-06.1	05.2	000 - 680
GGB1DV3008	PC	208.7	-01.7	04	251	208.6	-04.6	04.2	000 - 700
GGB1DV3101	LT	179.2	23.5	00	000	179.2	23.5	21.7	100 - 300
GGB1DV3101	PC	204.9	01.9	00	000	204.9	01.9	07.6	350 - 580
GGB1DV3102	PC	204.0	01.0	00	000	204.0	01.0	06.4	000 - 550
GGB1DV3103	LT	002.7	14.7	00	000	002.7	14.7	38.5	000 - 300
GGB1DV3103	PC	208.8	-07.7	00	000	208.8	-07.7	04.1	350 - 550
GGB1DV3104	PC	207.2	-08.1	00	000	207.2	-08.1	02.9	000 - 350
GGB1DV3105	LT	045.5	42.5	00	000	045.5	42.5	35.4	000 - 300
GGB1DV3105	PC	195.7	-06.9	00	000	195.7	-06.9	04.3	350 - 550
GGB1DV3106	LT	054.6	-11.0	00	000	054.6	-11.0	46.3	000 - 350
GGB1DV3106	PC	206.6	-05.2	00	000	206.6	-05.2	07.0	400 - 550
GGB1DV3107	PC	197.1	04.9	00	000	197.1	04.9	04.8	000 - 700
GGB1DV3201	PC	200.6	03.3	00	000	200.6	03.3	05.2	000 - 620
GGB1DV3202	PC	197.9	-05.4	00	000	197.9	-05.4	05.5	000 - 680
GGB1DV3203	LT	099.5	-67.9	00	000	099.5	-67.9	43.7	000 - 300
GGB1DV3203	PC	191.2	-01.3	00	000	191.2	-01.3	03.7	350 - 600
GGB1DV3204	LT	107.8	61.1	00	000	107.8	61.1	24.1	000 - 250
GGB1DV3204	PC	197.5	-01.7	00	000	197.5	-01.7	03.6	300 - 600
GGB1DV3205	PC	210.2	-04.3	00	000	210.2	-04.3	09.0	000 - 600
GGB1DV3206	PC	208.2	-03.9	00	000	208.2	-03.9	08.0	000 - 600
GGB1DV3209	PC	184.7	-10.4	00	000	184.7	-10.4	09.6	000 - 680

GGB1DV3301	PC	207.5	-19.4	41	327	202.3	03.1	05.9	100 - 600
GGB1DV3302	PC	203.8	-18.6	41	327	199.8	05.7	09.2	000 - 600
GGB1DV3303	LT	228.4	41.9	41	327	262.7	35.3	13.8	000 - 200
GGB1DV3303	PC	208.9	-23.5	41	327	201.1	-01.0	08.4	250 - 580
GGB1DV3304	PC	212.9	-19.3	41	327	206.5	00.1	09.1	000 - 580
GGB1DV3305	PC	212.3	-11.1	41	327	211.0	07.1	12.3	000 - 580
GGB1DV3401	PC	208.1	-00.1	32	324	211.6	13.3	12.7	000 - 580
GGB1DV3402	PC	208.4	-08.7	32	324	207.6	05.7	10.4	000 - 580
GGB1DV3403	PC	206.6	-13.3	32	324	203.9	02.4	11.4	000 - 600
GGB1DV3404	LT	176.5	53.2	32	324	233.4	71.2	16.0	000 - 200
GGB1DV3404	PC	205.7	-16.5	32	324	201.6	00.0	08.8	250 - 600
GGB1DV3405	PC	214.1	-15.7	32	324	209.0	-03.2	10.6	000 - 600
GGB1DV3406	PC	207.5	-12.0	32	324	205.2	03.1	07.5	000 - 660
GGB1DV3407	PC	219.4	-25.3	32	324	208.4	-14.0	03.1	150 - 660
GGB1DV3408	PC	207.3	-13.8	32	324	204.2	01.7	05.3	000 - 700
GGB1DV3409	PC	213.7	-09.8	32	324	211.7	02.1	18.8	000 - 660
GGB1DV3501	PC	186.7	-01.4	04	130	186.8	-03.6	20.5	000 - 400
GGB1DV3501	HT	177.8	-32.2	04	130	179.8	-34.8	16.7	450 - 640
GGB1DV3502	PC	181.7	-08.4	04	130	182.3	-10.9	09.3	000 - 640
GGB1DV3503	LT	202.3	37.0	04	130	199.5	35.7	14.6	000 - 250
GGB1DV3503	PC	190.9	-03.6	04	130	191.2	-05.5	10.5	300 - 550
GGB1DV3503	HT	203.8	28.8	04	130	201.7	27.6	17.6	580 - 660
GGB1DV3504	PC	187.0	03.8	04	130	186.8	01.7	06.2	000 - 700
GGB1DV3505	PC	195.4	05.9	04	130	195.1	04.3	12.1	000 - 550
GGB1DV3505	HT	155.8	17.8	04	130	155.3	14.2	17.3	580 - 700
GGB1DV3506	PC	197.3	-05.5	04	130	197.7	-07.1	09.9	000 - 620
GGB1DV3506	HT	148.9	00.3	04	130	148.9	-03.5	23.0	640 - 700
GGB1DV3507	LT	145.6	45.4	04	130	144.6	41.5	20.4	000 - 200
GGB1DV3507	PC	181.3	05.6	04	130	181.0	03.1	13.8	250 - 580
GGB1DV3507	HT	252.3	31.1	04	130	250.2	33.2	17.5	600 - 700
GGB1DV3508	LT	279.2	54.7	04	130	276.0	58.0	36.8	100 - 300
GGB1DV3508	PC	194.8	15.2	04	130	193.9	13.4	10.9	350 - 700
GGB1DV3509	LT	219.9	56.5	04	130	213.9	56.3	30.0	000 - 300
GGB1DV3509	PC	185.3	-01.6	04	130	185.5	-03.9	06.8	350 - 580
GGB1DV3509	HT	233.6	24.8	04	130	231.8	25.6	11.5	600 - 680
GGB1DV3510	LT	038.5	-06.6	04	130	038.1	-06.4	23.5	000 - 200
GGB1DV3510	PC	188.2	-10.2	04	130	188.9	-12.3	12.3	250 - 680
GGB1DV3511	LT	023.7	33.4	04	130	026.3	34.5	37.2	000 - 250
GGB1DV3511	PC	184.6	-04.6	04	130	184.9	-06.9	12.2	300 - 580
GGB1DV3511	HT	220.5	-02.9	04	130	220.7	-02.9	12.4	600 - 700
GGB1DV3512	PC	182.5	06.9	04	130	182.2	04.4	28.8	000 - 500
GGB1DV3512	HT	166.7	08.7	04	130	166.4	05.5	08.7	550 - 700
GGB1DV3513	LT	220.3	33.6	04	130	217.7	33.6	27.2	000 - 350
GGB1DV3513	PC	184.8	15.2	04	130	184.0	12.9	10.3	400 - 700
GGB1DV3601	LT	304.9	37.0	04	130	304.6	40.9	28.3	000 - 250
GGB1DV3601	PC	178.4	-15.0	04	130	179.3	-17.6	15.2	300 - 500
GGB1DV3601	HT	202.1	19.1	04	130	200.8	17.9	06.9	550 - 680
GGB1DV3602	LT	252.7	41.7	04	130	249.5	43.8	24.2	000 - 300
GGB1DV3602	PC	188.5	-09.3	04	130	189.1	-11.3	09.8	350 - 660
GGB1DV3603	LT	018.5	-14.8	04	130	017.5	-13.3	14.1	000 - 250
GGB1DV3603	PC	201.5	10.4	04	130	200.9	09.1	11.9	300 - 640
GGB1DV3604	LT	339.8	12.5	04	130	340.3	15.9	31.0	000 - 200
GGB1DV3604	PC	189.1	-02.7	04	130	189.3	-04.7	09.7	250 - 600
GGB1DV3604	HT	183.8	42.4	04	130	181.0	40.0	30.3	620 - 700
GGB1DV3605	LT	299.1	44.5	04	130	298.3	48.4	18.8	000 - 250
GGB1DV3605	PC	185.4	-11.8	04	130	186.1	-14.0	07.8	300 - 660
GGB1DV3606	LT	242.6	39.4	04	130	239.4	40.8	22.7	000 - 350
GGB1DV3606	PC	199.8	00.7	04	130	199.8	-00.7	05.1	400 - 700

GGB1DV3701	LT	255.6	64.9	40	140	180.9	54.2	16.4	000 - 300
GGB1DV3701	PC	199.9	21.3	40	140	193.7	-01.3	16.3	350 - 550
GGB1DV3701	HT	141.0	-22.7	40	140	142.0	-62.6	12.5	580 - 680
GGB1DV3702	PC	184.3	14.1	40	140	184.5	-15.1	10.4	000 - 700
GGB1DV3703	LT	358.0	62.6	40	140	096.0	65.9	11.8	000 - 200
GGB1DV3703	PC	190.7	17.1	40	140	188.6	-09.4	20.3	250 - 550
GGB1DV3703	HT	126.0	-05.0	40	140	120.7	-43.5	10.8	580 - 680
GGB1DV3704	PC	178.7	22.0	40	140	176.1	-10.3	10.8	000 - 700
GGB1DV3705	PC	199.8	23.1	40	140	192.6	00.2	18.5	000 - 550
GGB1DV3705	HT	145.4	05.4	40	140	146.5	-34.4	12.3	580 - 680
GGB1DV3706	PC	191.8	24.6	40	140	185.7	-02.4	17.9	150 - 550
GGB1DV3706	HT	160.6	-03.2	40	140	167.3	-40.1	14.7	580 - 700
GGB1DV3707	PC	188.7	18.9	40	140	186.0	-08.8	15.7	000 - 500
GGB1DV3707	HT	156.5	10.6	40	140	158.3	-27.7	19.7	550 - 700
GGB1DV3708	PC	184.5	-08.2	40	140	197.1	-34.3	16.9	000 - 500
GGB1DV3708	HT	167.5	-17.0	40	140	183.7	-50.3	29.7	550 - 700
GGB1DV3709	LT	308.1	65.0	40	140	158.1	73.7	14.5	000 - 200
GGB1DV3709	PC	185.7	13.3	40	140	186.2	-15.1	13.2	250 - 550
GGB1DV3709	HT	110.3	-12.6	40	140	096.5	-45.4	11.5	580 - 700
GGB1DV3710	LT	302.2	39.3	40	140	263.6	73.5	26.2	000 - 300
GGB1DV3710	PC	184.9	16.2	40	140	184.1	-12.9	12.6	350 - 550
GGB1DV3710	HT	149.4	-01.0	40	140	152.3	-40.3	14.7	580 - 700
GGB1DV3711	PC	202.2	10.1	40	140	201.9	-09.3	20.9	000 - 500
GGB1DV3711	HT	144.9	-43.7	40	140	169.9	-82.9	15.2	550 - 700
GGB1DV3712	LT	322.4	41.0	40	140	331.4	80.8	30.8	000 - 300
GGB1DV3712	PC	171.3	13.1	40	140	172.9	-21.2	11.6	350 - 700
GGB1DV3713	PC	198.6	33.9	40	140	185.8	08.6	22.6	000 - 550
GGB1DV3713	HT	147.6	-42.8	40	140	178.7	-81.1	21.1	580 - 700
GGB1DV3801	LT	226.5	80.7	40	140	154.1	48.6	21.2	000 - 300
GGB1DV3801	PC	194.0	13.8	40	140	193.0	-10.6	10.0	350 - 550
GGB1DV3801	HT	127.6	-13.0	40	140	120.2	-51.7	09.0	580 - 680
GGB1DV3802	LT	180.6	79.6	40	140	149.1	41.7	27.4	000 - 300
GGB1DV3802	PC	205.3	19.6	40	140	198.8	00.2	17.8	350 - 550
GGB1DV3802	HT	137.1	-24.0	40	140	133.9	-63.9	07.1	580 - 700
GGB1DV3803	LT	110.4	74.9	40	140	130.8	36.4	26.1	000 - 300
GGB1DV3803	PC	182.2	26.6	40	140	177.1	-04.8	09.4	350 - 580
GGB1DV3803	HT	178.8	-02.8	40	140	188.0	-32.6	04.0	600 - 700
GGB1DV3804	LT	293.2	81.5	40	140	147.1	57.4	22.4	000 - 300
GGB1DV3804	PC	186.6	08.2	40	140	189.6	-19.1	09.4	350 - 550
GGB1DV3804	HT	142.7	08.4	40	140	143.2	-31.6	15.4	580 - 680
GGB1DV3805	LT	196.7	35.0	40	140	183.8	08.7	43.7	000 - 250
GGB1DV3805	PC	190.2	02.6	40	140	195.9	-22.1	10.4	300 - 500
GGB1DV3805	HT	145.8	21.3	40	140	145.7	-18.5	19.5	550 - 700
GGB1DV3806	LT	152.4	72.8	40	140	144.4	33.1	37.2	000 - 350
GGB1DV3806	PC	181.4	-01.9	40	140	190.0	-30.5	10.2	400 - 600
GGB1DV3806	HT	137.0	-37.9	40	140	128.8	-77.7	06.9	620 - 680
GGB1DV3807	LT	349.2	67.1	40	140	110.1	67.5	29.8	000 - 250
GGB1DV3807	PC	189.6	-18.4	40	140	209.6	-39.6	12.0	300 - 700
GGB1DV3808	LT	216.3	59.6	40	140	177.3	35.7	27.4	000 - 250
GGB1DV3808	PC	183.2	20.7	40	140	180.5	-09.7	09.9	300 - 500
GGB1DV3808	HT	162.2	04.8	40	140	166.3	-32.0	07.2	550 - 700
GGB1DV3901	LT	077.3	36.7	02	275	076.8	38.6	29.5	000 - 300
GGB1DV3901	PC	190.0	-10.0	02	275	189.6	-10.2	11.2	350 - 620
GGB1DV3901	HT	192.3	34.8	02	275	193.6	34.5	14.3	640 - 700
GGB1DV3902	LT	228.3	38.5	02	275	229.4	37.1	40.6	100 - 350
GGB1DV3902	PC	195.1	-08.0	02	275	194.8	-08.3	10.1	400 - 620
GGB1DV3902	HT	190.5	32.2	02	275	191.7	32.0	08.6	640 - 700
GGB1DV3903	LT	213.5	38.7	02	275	214.9	37.7	13.1	150 - 300
GGB1DV3903	PC	197.2	-00.8	02	275	197.2	-01.3	06.3	350 - 640

GGB1DV3904	LT	209.8	53.3	02	275	212.2	52.4	12.5	150 - 300
GGB1DV3904	PC	198.5	01.2	02	275	198.5	00.8	09.7	350 - 700
GGB1DV3905	LT	221.2	-61.0	02	275	218.1	-62.1	37.8	000 - 300
GGB1DV3905	PC	190.1	-14.5	02	275	189.6	-14.7	18.8	350 - 550
GGB1DV3905	HT	214.0	36.5	02	275	215.2	35.5	23.8	580 - 700
GGB1DV3906	LT	079.9	56.8	02	275	079.0	58.7	30.4	000 - 250
GGB1DV3906	PC	187.9	-10.7	02	275	187.5	-10.8	13.2	300 - 600
GGB1DV3906	HT	220.8	22.4	02	275	221.4	21.2	15.4	620 - 700
GGB1DV3907	LT	070.1	21.2	02	275	069.8	23.1	27.2	100 - 250
GGB1DV3907	PC	184.8	-01.7	02	275	184.7	-01.7	12.8	300 - 580
GGB1DV3907	HT	252.5	38.1	02	275	253.1	36.3	12.4	600 - 700
GGB1DV3908	LT	331.1	36.4	02	275	329.9	35.3	39.3	000 - 300
GGB1DV3908	PC	185.8	-07.2	02	275	185.5	-07.2	13.0	350 - 550
GGB1DV3908	HT	222.6	12.4	02	275	222.9	11.1	14.3	580 - 700
GGB1DV3909	LT	095.3	28.0	02	275	095.3	30.0	31.5	100 - 250
GGB1DV3909	PC	198.2	-13.1	02	275	197.7	-13.5	19.2	300 - 580
GGB1DV3909	HT	238.4	29.5	02	275	239.0	27.9	27.0	600 - 700
GGB1DV3910	LT	222.4	44.6	02	275	223.9	43.4	26.5	100 - 250
GGB1DV3910	PC	191.9	-12.7	02	275	191.5	-13.0	21.2	300 - 550
GGB1DV3910	HT	212.9	59.0	02	275	215.7	58.0	11.6	580 - 700
GGB1DV3911	LT	226.6	15.4	02	275	227.0	14.0	23.5	000 - 200
GGB1DV3911	PC	189.9	03.6	02	275	190.1	03.4	11.6	250 - 600
GGB1DV3911	HT	298.1	15.4	02	275	297.9	13.6	25.5	620 - 700
GGB1DV3912	LT	200.5	28.3	02	275	201.5	27.7	03.2	150 - 250
GGB1DV3912	PC	186.8	-25.2	02	275	185.9	-25.2	18.5	300 - 550
GGB1DV3913	LT	091.6	-67.4	02	275	091.8	-65.4	29.3	000 - 300
GGB1DV3913	PC	192.9	-17.7	02	275	192.2	-18.0	07.5	350 - 580
GGB1DV3913	HT	198.1	08.7	02	275	198.4	08.2	25.0	600 - 700
GGB1DV3914	LT	003.1	02.7	02	275	003.0	02.6	32.2	000 - 200
GGB1DV3914	PC	188.1	02.3	02	275	188.2	02.2	14.4	250 - 700
GGB1DV3915	PC	195.5	06.4	02	275	195.7	06.0	18.4	000 - 550
GGB1DV3916	PC	190.0	05.7	02	275	190.2	05.6	11.3	000 - 700
GGB1DV3918	LT	027.4	08.1	02	275	027.1	08.8	26.9	000 - 300
GGB1DV3918	PC	192.3	-08.3	02	275	192.1	-08.5	22.8	350 - 680
GGB1DV3919	LT	049.7	-06.9	02	275	049.9	-05.5	10.4	100 - 250
GGB1DV3919	PC	175.4	-02.1	02	275	175.3	-01.8	09.8	300 - 550
GGB1DV3919	HT	261.8	16.5	02	275	261.9	14.5	22.0	600 - 700
GGB1DV3920	LT	013.0	08.9	02	275	012.7	09.2	08.7	000 - 200
GGB1DV3920	PC	188.7	-03.3	02	275	188.5	-03.5	13.5	250 - 700
GGB1DV3921	LT	215.3	38.4	02	275	216.6	37.3	04.5	000 - 150
GGB1DV3921	PC	186.0	05.2	02	275	186.2	05.1	08.4	200 - 550
GGB1DV3921	HT	245.2	24.8	02	275	245.6	23.1	21.4	580 - 700
GGB1DV4001	LT	226.2	-73.3	06	130	244.6	-71.7	16.7	000 - 200
GGB1DV4001	PC	186.0	04.2	06	130	185.8	00.8	13.0	250 - 550
GGB1DV4001	HT	220.1	-11.5	06	130	221.3	-11.4	09.8	580 - 640
GGB1DV4002	LT	221.8	-77.7	06	130	247.1	-76.2	22.1	000 - 200
GGB1DV4002	PC	184.2	-05.5	06	130	184.9	-09.0	17.4	250 - 500
GGB1DV4002	HT	217.7	-29.0	06	130	221.1	-29.1	09.6	580 - 620
GGB1DV4003	PC	192.0	-03.3	06	130	192.4	-06.1	06.4	000 - 640
GGB1DV4004	LT	225.2	-78.4	06	130	251.0	-76.4	45.8	000 - 200
GGB1DV4004	PC	197.0	04.9	06	130	196.6	02.6	05.1	250 - 550
GGB1DV4004	HT	211.6	-13.9	06	130	213.1	-14.7	05.0	580 - 680
GGB1DV4005	PC	194.4	-19.1	06	130	196.4	-21.6	06.0	000 - 700
GGB1DV4006	PC	196.3	12.9	06	130	195.2	10.5	10.7	000 - 700
GGB1DV4007	PC	184.9	22.4	06	130	183.0	18.9	37.4	000 - 450
GGB1DV4007	HT	224.3	-47.3	06	130	230.7	-46.6	27.6	500 - 640
GGB1DV4101	PC	190.2	-05.6	06	130	190.8	-08.6	18.3	000 - 500
GGB1DV4101	HT	206.2	-55.5	06	130	214.9	-56.4	11.3	550 - 700
GGB1DV4102	PC	181.9	-09.6	06	130	182.9	-13.3	19.2	000 - 500
GGB1DV4102	HT	196.5	-59.9	06	130	206.7	-61.8	11.2	550 - 700

GGB1DV4103	LT	020.3	64.1	06	130	032.8	65.5	39.8	000 - 200
GGB1DV4103	PC	179.4	-15.6	06	130	180.9	-19.5	14.3	250 - 500
GGB1DV4103	HT	191.6	-34.2	06	130	195.5	-36.9	10.2	550 - 700
GGB1DV4104	LT	049.6	35.3	06	130	053.7	34.1	22.0	000 - 300
GGB1DV4104	PC	188.4	-13.4	06	130	189.8	-16.5	08.9	350 - 580
GGB1DV4104	HT	211.0	-51.2	06	130	218.5	-51.8	07.8	600 - 700
GGB1DV4105	LT	007.5	13.2	06	130	008.9	16.4	38.0	000 - 300
GGB1DV4105	PC	187.2	-03.8	06	130	187.7	-07.1	02.8	350 - 580
GGB1DV4105	HT	165.5	-30.1	06	130	167.8	-34.9	14.8	600 - 700
GGB1DV4106	PC	197.2	-20.9	06	130	199.5	-23.2	15.6	000 - 580
GGB1DV4107	LT	235.1	76.8	06	130	208.9	77.1	24.4	000 - 200
GGB1DV4107	PC	194.2	-14.6	06	130	195.7	-17.1	25.1	300 - 580
GGB1DV4107	HT	250.8	-52.5	06	130	256.9	-49.1	14.4	600 - 660
GGB1DV4108	LT	353.9	02.4	06	130	354.3	06.7	33.7	000 - 150
GGB1DV4108	PC	202.4	-08.2	06	130	203.3	-10.0	26.7	200 - 580
GGB1DV4108	HT	199.7	-56.8	06	130	208.8	-58.5	25.6	600 - 680
GGB1DV4109	LT	335.6	09.8	06	130	336.2	15.2	16.3	000 - 200
GGB1DV4109	PC	189.8	-01.1	06	130	190.0	-04.1	19.7	250 - 400
GGB1DV4109	HT	251.2	-38.8	06	130	255.0	-35.6	24.6	450 - 680
GGB1DV4110	LT	013.0	33.0	06	130	016.7	35.6	24.8	000 - 200
GGB1DV4110	PC	166.4	-15.4	06	130	167.6	-20.2	19.5	250 - 450
GGB1DV4111	LT	007.4	33.4	06	130	011.0	36.5	17.7	000 - 150
GGB1DV4111	PC	176.6	-16.8	06	130	178.1	-20.9	15.2	200 - 450
GGB1DV4112	LT	045.7	31.7	06	130	049.4	30.9	27.0	000 - 200
GGB1DV4112	PC	198.1	-07.9	06	130	199.0	-10.1	22.7	250 - 550
GGB1DV4201	LT	005.0	22.9	06	130	007.2	26.3	25.0	000 - 150
GGB1DV4201	PC	175.9	-10.3	06	130	176.9	-14.4	13.1	200 - 500
GGB1DV4201	HT	176.9	-45.2	06	130	181.8	-49.1	08.0	550 - 680
GGB1DV4202	LT	016.2	37.5	06	130	020.7	39.7	12.3	000 - 150
GGB1DV4202	PC	188.1	-10.2	06	130	189.1	-13.3	05.2	200 - 550
GGB1DV4202	HT	220.2	-35.1	06	130	224.4	-34.9	05.2	580 - 680
GGB1DV4203	LT	030.9	48.1	06	130	037.7	48.7	06.8	000 - 150
GGB1DV4203	PC	176.6	-27.6	06	130	179.1	-31.6	23.4	200 - 500
GGB1DV4203	HT	211.7	-46.1	06	130	218.0	-46.7	09.2	550 - 660
GGB1DV4204	LT	009.4	30.5	06	130	012.7	33.4	08.8	000 - 150
GGB1DV4204	PC	186.4	-17.4	06	130	188.1	-20.6	05.1	200 - 600
GGB1DV4205	XX	054.9	-22.5	06	130	052.4	-23.9	19.8	000 - 640
GGB1DV4205	HT	142.5	14.5	06	130	142.3	08.6	02.9	660 - 700
GGB1DV4206	LT	358.6	02.6	06	130	359.0	06.6	21.9	000 - 350
GGB1DV4206	PC	229.?	-17.0	06	130	231.0	-15.9	16.0	400 - 550
GGB1DV4207	LT	267.4	-29.3	06	130	269.4	-24.9	23.5	000 - 150
GGB1DV4207	PC	189.9	-08.4	06	130	190.8	-11.4	10.4	200 - 450
GGB1DV4207	HT	195.5	-40.3	06	130	200.4	-42.6	02.6	500 - 580
GGB1DV4208	LT	028.4	53.9	06	130	036.7	54.7	21.0	000 - 150
GGB1DV4208	PC	192.6	-09.5	06	130	193.7	-12.2	08.9	200 - 500
GGB1DV4209	LT	031.9	50.0	06	130	039.1	50.5	29.0	000 - 150
GGB1DV4209	PC	195.9	-07.9	06	130	196.7	-10.3	06.2	200 - 500
GGB1DV4209	HT	159.6	-13.1	06	130	160.4	-18.3	37.2	550 - 700
GGB1DV4301	PC	210.9	05.7	39	172	215.3	-24.2	21.2	000 - 620
GGB1DV4302	PC	205.6	07.1	39	172	209.3	-25.1	13.4	000 - 620
GGB1DV4303	PC	202.2	02.0	39	172	208.0	-31.1	11.7	000 - 620
GGB1DV4304	PC	201.2	02.8	39	172	206.5	-30.7	08.2	000 - 620
GGB1DV4305	PC	213.1	-03.7	39	172	222.4	-31.6	09.2	000 - 550
GGB1DV4306	PC	201.8	09.5	39	172	204.6	-24.2	14.3	000 - 620
GGB1DV4307	PC	207.6	-08.3	39	172	219.1	-38.3	16.4	000 - 550
GGB1DV4308	PC	213.0	06.0	39	172	217.1	-23.1	15.4	000 - 600
GGB1DV4309	LT	286.8	25.4	39	172	263.7	34.9	16.8	000 - 200
GGB1DV4309	PC	227.6	-18.3	39	172	246.4	-35.6	15.3	250 - 600
GGB1DV4310	XX	283.0	-09.2	39	172	284.2	05.7	12.1	000 - 600
GGB1DV4311	PC	215.4	02.4	39	172	221.2	-25.1	12.9	000 - 550

GGB1DV4312	LT	256.4	-51.1	39	172	297.2	-40.1	11.8	000 - 250
GGB1DV4312	PC	220.1	-05.1	39	172	230.1	-29.2	03.7	300 - 550
GGB1DV4313	LT	290.4	-05.6	39	172	288.2	12.9	39.9	000 - 200
GGB1DV4313	PC	217.0	-03.3	39	172	226.0	-29.3	09.4	250 - 550
GGB1DV4314	PC	213.6	00.8	39	172	220.4	-27.3	11.1	000 - 500
GGB1DV4315	LT	332.1	17.6	39	172	319.4	53.0	27.9	000 - 300
GGB1DV4315	PC	233.4	16.5	39	172	229.6	-03.9	05.3	350 - 580
GGB1DV4316	LT	206.1	29.8	39	172	201.2	-03.8	34.2	000 - 400
GGB1DV4316	PC	237.3	12.6	39	172	234.9	-05.0	07.0	450 - 600
GGB1DV4317	PC	209.0	06.3	39	172	213.1	-24.4	14.5	000 - 580
GGB1DV4318	LT	101.9	86.0	39	172	166.2	49.5	31.7	000 - 350
GGB1DV4318	PC	206.7	10.1	39	172	209.2	-21.9	09.1	400 - 580
GGB1DV4319	LT	286.8	36.7	39	172	253.0	42.6	34.3	000 - 350
GGB1DV4319	PC	219.0	03.8	39	172	224.0	-22.1	06.5	400 - 600
GGB1DV4401	LT	247.4	-06.9	39	172	255.0	-14.6	13.9	000 - 250
GGB1DV4401	PC	209.7	12.2	39	172	211.2	-18.8	09.9	300 - 500
GGB1DV4402	LT	233.9	04.5	39	172	236.7	-13.6	23.2	000 - 250
GGB1DV4402	PC	210.4	00.1	39	172	217.5	-29.4	08.7	300 - 620
GGB1DV4402	HT	276.8	-11.1	39	172	280.5	00.5	20.0	600 - 700
GGB1DV4403	LT	297.0	-83.5	39	172	344.2	-47.0	42.7	000 - 250
GGB1DV4403	PC	205.4	04.8	39	172	210.1	-27.3	10.4	300 - 620
GGB1DV4403	HT	264.0	-17.6	39	172	274.7	-12.4	17.2	660 - 700
GGB1DV4404	LT	257.1	-19.5	39	172	270.9	-18.1	20.0	000 - 250
GGB1DV4404	PC	200.5	05.6	39	172	204.6	-28.4	10.0	300 - 680
GGB1DV4405	PC	205.1	-01.2	39	172	212.6	-32.9	11.4	000 - 580
GGB1DV4406	LT	222.1	-02.3	39	172	230.3	-25.7	22.7	000 - 250
GGB1DV4406	PC	208.7	10.7	39	172	210.9	-20.6	08.2	300 - 680
GGB1DV4501	LT	242.0	-41.0	38	192	284.2	-54.7	31.7	000 - 300
GGB1DV4501	PC	192.9	-04.2	38	192	193.3	-42.2	08.5	350 - 680
GGB1DV4502	LT	340.0	-56.0	38	192	353.5	-21.2	24.7	000 - 250
GGB1DV4502	PC	206.1	-13.8	38	192	213.7	-50.2	04.9	300 - 620
GGB1DV4503	PC	197.6	-04.8	38	192	199.6	-42.6	04.3	000 - 620
GGB1DV4504	PC	204.3	-08.9	38	192	209.5	-45.7	06.2	000 - 620
GGB1DV4505	PC	206.8	-05.1	38	192	211.8	-41.5	09.9	000 - 640
GGB1DV4601	PC	199.7	-03.7	38	192	202.3	-41.3	08.9	150 - 680
GGB1DV4602	LT	215.4	-29.5	38	192	238.6	-61.6	37.2	000 - 150
GGB1DV4602	PC	194.7	06.0	38	192	195.2	-32.0	09.0	200 - 680
GGB1DV4603	PC	198.8	-03.0	38	192	201.0	-40.6	09.2	000 - 680
GGB1DV4604	PC	201.4	-01.2	38	192	204.1	-38.6	12.1	150 - 660
GGB1DV4605	LT	268.4	-48.7	38	192	309.9	-43.4	29.5	000 - 150
GGB1DV4605	PC	196.3	-04.2	38	192	197.8	-42.0	07.7	200 - 660
GGB1DV4606	PC	193.9	-09.0	38	192	194.7	-47.0	11.1	000 - 580
GGB1DV4607	PC	200.3	-07.1	38	192	203.5	-44.6	08.1	000 - 580
GGB1DV4608	PC	193.0	01.5	38	192	193.3	-36.5	09.8	150 - 580
GGB1DV4609	PC	199.2	-12.9	38	192	203.1	-50.5	06.1	150 - 580
GGB1DV4701	PC	199.9	-17.7	38	170	215.7	-48.4	05.2	000 - 680
GGB1DV4702	PC	207.4	-16.0	38	170	223.5	-43.4	01.6	000 - 250
GGB1DV4703	PC	200.0	-11.9	38	170	212.1	-43.1	01.0	000 - 250
GGB1DV4704	PC	197.2	-13.3	38	170	209.5	-45.6	05.1	000 - 680
GGB1DV4705	PC	180.8	-28.0	38	170	192.8	-64.7	09.9	000 - 680
GGB1DV4706	PC	204.7	-15.2	38	170	219.8	-44.0	08.3	150 - 580
GGB1DV4707	PC	200.5	-16.6	38	170	215.6	-47.2	06.3	150 - 580
GGB1DV4708	PC	201.8	-14.8	38	170	216.1	-45.1	05.2	000 - 680
GGB1DV4709	PC	200.8	-06.2	38	170	210.1	-37.7	13.7	000 - 680
GGB1DV4710	LT	207.4	64.2	38	170	187.7	29.8	20.9	000 - 200
GGB1DV4710	PC	204.7	-20.8	38	170	223.9	-48.9	06.8	250 - 550
GGB1DV4711	LT	091.4	-79.2	38	170	007.7	-52.8	12.0	000 - 150
GGB1DV4711	PC	205.5	-00.1	38	170	212.2	-30.2	07.1	200 - 680

GGB1DV4712	LT	130.6	35.9	38	170	139.0	04.4	33.3	000 - 150
GGB1DV4712	PC	205.9	-11.3	38	170	218.7	-40.1	04.3	200 - 620
GGB1DV4713	LT	009.6	11.8	38	170	018.6	46.8	37.7	000 - 200
GGB1DV4713	PC	199.6	-11.0	38	170	211.1	-42.5	06.9	250 - 660
GGB1DV4714	LT	228.2	63.4	38	170	197.3	34.0	06.4	000 - 200
GGB1DV4714	PC	191.3	-12.3	38	170	201.2	-46.8	07.3	250 - 500
GGB1DV4716	PC	200.4	-02.5	38	170	207.8	-34.4	01.5	000 - 400
GGB1DV4801	LT	238.9	-14.9	90	004	256.0	33.7	21.6	100 - 250
GGB1DV4801	PC	201.0	-23.0	90	004	218.6	61.7	22.2	300 - 680
GGB1DV4802	LT	189.8	-01.2	90	004	262.3	84.1	19.9	100 - 400
GGB1DV4802	PC	181.2	-26.1	90	004	178.4	63.8	11.6	450 - 680
GGB1DV4803	LT	238.3	11.3	90	004	287.8	34.9	20.5	000 - 300
GGB1DV4803	PC	203.1	-33.0	90	004	210.8	52.4	11.9	350 - 640
GGB1DV4804	LT	249.2	07.7	90	004	282.4	24.6	22.9	000 - 300
GGB1DV4804	PC	210.5	-37.2	90	004	214.4	45.5	08.3	350 - 640
GGB1DV4805	LT	183.5	02.4	90	004	016.1	87.5	21.5	100 - 300
GGB1DV4805	PC	196.8	-35.5	90	004	201.3	52.5	13.2	350 - 640
GGB1DV4806	LT	206.5	63.1	90	004	353.0	24.7	33.1	000 - 350
GGB1DV4806	PC	198.0	-23.9	90	004	212.6	62.5	09.4	400 - 640
GGB1DV4807	PC	197.8	-44.2	90	004	197.7	44.1	11.8	000 - 680
GGB1DV4808	PC	204.1	-23.9	90	004	221.8	59.1	07.4	000 - 700
GGB1DV4809	PC	186.5	-67.9	90	004	185.0	22.1	10.3	000 - 680
GGB1DV4810	LT	299.0	19.9	90	004	295.7	-23.4	16.8	100 - 300
GGB1DV4810	PC	226.5	-75.4	90	004	194.0	10.7	05.4	350 - 660
GGB1DV4811	LT	238.9	45.9	90	004	325.6	23.6	10.6	000 - 300
GGB1DV4811	PC	229.5	-71.0	90	004	197.8	13.2	06.1	350 - 640
GGB1DV4812	LT	307.7	26.5	90	004	304.9	-29.8	35.1	000 - 350
GGB1DV4812	PC	211.0	-63.4	90	004	196.8	23.5	12.8	400 - 700
GGB1DV4813	LT	222.4	53.8	90	004	339.6	27.6	06.6	000 - 300
GGB1DV4813	PC	189.0	-54.1	90	004	187.6	35.8	13.7	350 - 640
GGB1DV4814	LT	070.4	80.1	90	004	013.1	-03.9	02.9	000 - 150
GGB1DV4814	PC	188.4	-77.0	90	004	185.0	13.0	17.1	200 - 640
GGB1DV4815	LT	260.3	-20.3	90	004	253.1	12.8	10.7	100 - 300
GGB1DV4815	PC	224.0	-79.8	90	004	190.6	07.8	26.8	350 - 640
GGB1DV4816	LT	267.6	34.8	90	004	308.9	05.2	10.4	000 - 200
GGB1DV4816	PC	225.7	-74.5	90	004	194.4	11.5	13.1	250 - 660
GGB1DV4817	LT	151.8	09.7	90	004	076.2	56.5	30.0	100 - 350
GGB1DV4817	PC	199.1	-38.2	90	004	202.3	49.4	08.2	450 - 660
GGB1DV4818	LT	290.4	19.4	90	004	294.2	-15.4	27.5	000 - 300
GGB1DV4818	PC	196.9	-47.9	90	004	195.4	40.8	05.5	350 - 660
GGB1DV4819	LT	001.5	-76.0	90	004	184.6	-14.0	24.4	000 - 200
GGB1DV4819	PC	195.2	-47.7	90	004	194.0	41.3	07.3	350 - 660
GGB1DV4820	LT	241.2	24.7	90	004	302.7	29.5	29.3	000 - 300
GGB1DV4820	PC	207.7	-48.8	90	004	203.4	37.1	05.1	350 - 660
GGB1DV4821	LT	010.1	-34.6	90	004	175.3	-55.0	34.0	000 - 300
GGB1DV4821	PC	200.2	-56.1	90	004	194.6	32.4	07.0	350 - 680
GGB1DV4822	LT	316.8	05.5	90	004	281.4	-42.5	28.2	000 - 400
GGB1DV4822	PC	190.6	-69.6	90	004	186.4	20.2	05.9	450 - 660
GGB1DV4823	LT	127.9	81.3	90	004	011.3	04.9	31.6	000 - 400
GGB1DV4823	PC	195.1	-62.4	90	004	189.7	27.0	06.7	450 - 660
GGB1DV4824	PC	199.3	-60.9	90	004	192.3	28.0	09.1	000 - 660
GGB1DV4901	LT	027.3	-48.0	82	006	165.5	-46.1	35.1	000 - 250
GGB1DV4901	PC	207.3	-44.0	82	006	204.5	34.6	08.8	300 - 620
GGB1DV4902	LT	186.8	28.5	82	006	003.9	69.5	17.6	150 - 300
GGB1DV4902	PC	208.5	-33.6	82	006	211.9	43.3	10.7	350 - 660
GGB1DV4903	LT	274.7	-74.9	82	006	201.2	-07.4	24.0	000 - 250
GGB1DV4903	PC	212.2	-36.8	82	006	213.0	38.9	08.0	300 - 660
GGB1DV4904	LT	108.1	43.5	82	006	053.0	14.3	43.2	000 - 250
GGB1DV4904	PC	221.9	-42.3	82	006	216.0	30.0	08.4	300 - 660
GGB1DV4905	LT	181.7	63.7	82	006	008.3	34.2	32.8	000 - 350

GGB1DV4905	PC	205.0	-39.9	82	006	204.7	38.9	07.8	400 - 660
GGB1DV4906	LT	229.3	38.2	82	006	320.7	40.7	31.7	000 - 350
GGB1DV4906	PC	211.6	-48.8	82	006	205.0	28.9	05.4	400 - 660
GGB1DV4907	LT	230.5	63.4	82	006	345.6	26.1	30.3	000 - 250
GGB1DV4907	PC	204.3	-39.0	82	006	204.6	40.1	09.4	300 - 680
GGB1DV4908	LT	357.5	19.8	82	006	349.4	-60.9	33.0	000 - 300
GGB1DV4908	PC	203.3	-28.4	82	006	210.0	50.0	18.3	350 - 580
GGB1DV4909	LT	350.2	54.4	82	006	355.8	-26.2	13.6	100 - 250
GGB1DV4909	PC	217.7	-36.3	82	006	217.8	36.6	09.1	300 - 500
GGB1DV4909	HT	203.5	-83.0	82	006	188.1	-01.3	08.6	550 - 600
GGB1DV4910	LT	134.7	43.0	82	006	049.0	33.2	38.2	000 - 400
GGB1DV4910	PC	203.6	-51.4	82	006	198.4	28.7	16.3	450 - 640
GGB1DV4911	LT	330.2	-31.2	82	006	236.3	-49.4	46.3	000 - 400
GGB1DV4911	PC	232.2	-45.0	82	006	219.6	22.7	08.4	450 - 640
GGB1DV4912	LT	171.4	-25.4	82	006	163.4	53.7	33.9	000 - 400
GGB1DV4912	PC	200.3	-49.6	82	006	196.7	31.0	16.0	450 - 600
GGB1DV4913	LT	183.7	-17.6	82	006	181.0	64.3	37.6	000 - 400
GGB1DV4913	PC	210.0	-36.5	82	006	211.3	40.1	22.9	450 - 600
GGB1DV4914	PC	200.6	-27.1	82	006	207.4	52.2	11.5	150 - 600
GGB1DV4915	LT	066.4	49.7	82	006	041.1	-12.2	13.6	100 - 250
GGB1DV4915	PC	207.9	-33.6	82	006	211.4	43.5	06.9	300 - 580
GGB1DV4916	LT	122.0	52.3	82	006	042.4	22.0	10.1	100 - 250
GGB1DV4916	PC	205.5	-31.2	82	006	210.5	46.6	10.2	300 - 600
GGB1DV4917	LT	191.4	30.7	82	006	354.2	66.8	28.5	000 - 350
GGB1DV4917	PC	200.5	-40.2	82	006	200.5	40.0	11.7	400 - 640
GGB1DV4918	PC	198.3	-29.1	82	006	203.2	51.0	11.5	000 - 550
GGB1DV4919	PC	219.5	-34.9	82	006	220.4	36.7	14.6	000 - 450
GGB1DV5001	LT	249.5	69.9	42	184	207.1	37.0	18.2	000 - 250
GGB1DV5001	PC	213.2	-06.4	42	184	224.4	-41.5	07.7	300 - 640
GGB1DV5002	LT	195.6	56.9	42	184	190.5	15.4	20.1	000 - 250
GGB1DV5002	PC	213.5	-10.5	42	184	227.3	-45.1	09.3	300 - 640
GGB1DV5003	PC	213.1	-07.3	42	184	224.8	-42.4	08.4	000 - 640
GGB1DV5004	LT	000.1	-37.0	42	184	000.9	04.9	19.1	100 - 200
GGB1DV5004	PC	216.6	-04.7	42	184	227.3	-38.5	06.5	250 - 600
GGB1DV5005	PC	225.1	-08.1	42	184	238.7	-37.1	09.7	000 - 600
GGB1DV5006	PC	213.3	-07.2	42	184	225.0	-42.3	07.4	000 - 640
GGB1DV5007	LT	343.5	-30.8	42	184	346.2	09.1	25.3	100 - 200
GGB1DV5007	PC	226.6	-09.0	42	184	240.9	-37.1	09.8	250 - 580
GGB1DV5008	LT	041.1	-40.4	42	184	031.4	-04.3	21.8	000 - 400
GGB1DV5008	PC	222.4	05.2	42	184	228.0	-27.0	13.3	500 - 580
GGB1DV5009	LT	004.6	-65.8	42	184	004.3	-23.8	38.7	000 - 200
GGB1DV5009	PC	211.2	-02.3	42	184	219.8	-38.6	06.9	250 - 600
GGB1DV5010	LT	136.8	48.6	42	184	153.9	14.9	16.9	100 - 200
GGB1DV5010	PC	192.6	-12.4	42	184	198.2	-53.7	07.9	250 - 550
GGB1DV5011	LT	151.8	35.2	42	184	158.1	-02.0	06.2	100 - 250
GGB1DV5011	PC	226.7	-02.4	42	184	236.6	-31.5	07.8	300 - 550
GGB1DV5012	LT	182.0	40.8	42	184	182.5	-01.1	30.8	000 - 300
GGB1DV5012	PC	218.4	-16.4	42	184	237.7	-47.7	14.2	350 - 550
GGB1DV5013	LT	186.8	77.6	42	184	184.7	35.6	18.8	000 - 250
GGB1DV5013	PC	222.7	00.7	42	184	230.8	-30.9	08.9	300 - 550
GGB1DV5101	PC	246.9	43.4	96	184	228.9	-23.6	09.6	000 - 640
GGB1DV5102	LT	229.2	10.8	96	184	264.7	-45.1	16.2	000 - 350
GGB1DV5102	PC	232.1	49.4	96	184	218.3	-30.8	06.5	400 - 640
GGB1DV5103	LT	224.2	19.1	96	184	251.8	-48.7	20.3	000 - 250
GGB1DV5103	PC	227.7	47.8	96	184	218.1	-34.1	06.0	300 - 640
GGB1DV5104	LT	024.2	-04.7	96	184	096.6	69.8	36.6	150 - 350
GGB1DV5104	PC	228.0	48.7	96	184	217.4	-33.4	06.8	400 - 640
GGB1DV5105	PC	228.7	48.3	96	184	218.0	-33.2	07.1	150 - 600
GGB1DV5106	PC	234.3	41.1	96	184	227.8	-33.2	08.4	150 - 600
GGB1DV5107	PC	231.2	40.4	96	184	227.4	-35.6	10.6	000 - 640

GGB1DV5108	PC	226.1	46.5	96	184	218.6	-35.7	09.9	000 - 640
GGB1DV5109	PC	234.1	43.6	96	184	225.1	-32.3	07.4	000 - 640
GGB1DV5110	PC	233.7	46.3	96	184	222.1	-31.3	08.4	000 - 640
GGB1DV5111	LT	014.7	-39.9	96	184	018.3	54.8	19.1	100 - 200
GGB1DV5111	PC	221.9	39.6	96	184	223.6	-42.2	16.7	250 - 550
GGB1DV5112	PC	214.4	36.2	96	184	222.4	-48.9	22.4	000 - 550
GGB1DV5113	LT	216.6	-82.3	96	184	359.9	-00.5	27.3	100 - 300
GGB1DV5113	PC	232.4	54.8	96	184	213.2	-27.8	24.3	350 - 660
GGB1DV5114	LT	065.0	12.5	96	184	111.3	26.6	10.9	100 - 200
GGB1DV5114	PC	229.5	41.2	96	184	225.8	-36.4	10.9	250 - 700
GGB1DV5115	LT	224.6	14.6	96	184	258.6	-49.2	10.0	150 - 300
GGB1DV5115	PC	242.3	51.8	96	184	219.1	-23.9	10.7	350 - 660
GGB1DV5116	LT	216.5	79.6	96	184	189.7	-14.7	17.6	000 - 300
GGB1DV5116	PC	232.6	46.4	96	184	221.5	-32.0	07.7	350 - 660
GGB1DV5117	PC	226.9	44.9	96	184	220.6	-36.1	13.4	150 - 660
GGB1DV5118	LT	293.0	44.8	96	184	226.8	09.0	21.4	000 - 250
GGB1DV5118	PC	224.4	39.8	96	184	224.9	-40.5	10.2	300 - 640
GGB1DV5201	LT	318.3	26.3	52	022	328.4	-02.3	15.6	000 - 200
GGB1DV5201	PC	263.2	-30.6	52	022	250.9	00.8	08.9	250 - 660
GGB1DV5202	LT	140.5	-39.9	52	022	159.4	-06.1	06.9	100 - 200
GGB1DV5202	PC	259.7	-30.0	52	022	249.1	03.2	09.5	300 - 600
GGB1DV5202	HT	298.9	-24.9	52	022	275.6	-20.2	04.7	640 - 680
GGB1DV5203	PC	255.2	-28.5	52	022	247.2	07.0	05.1	150 - 660
GGB1DV5204	PC	250.4	-28.0	52	022	244.1	09.9	07.1	150 - 600
GGB1DV5205	LT	085.6	-45.2	52	022	142.2	-43.1	36.6	000 - 250
GGB1DV5205	PC	244.5	-16.4	52	022	246.6	22.5	09.6	300 - 620
GGB1DV5206	LT	090.6	-52.8	52	022	153.1	-41.6	15.3	150 - 300
GGB1DV5206	XX	035.6	-25.6	52	022	068.9	-73.1	07.3	350 - 620
GGB1DV5207	PC	246.2	-17.4	52	022	247.4	20.8	05.8	150 - 660
GGB1DV5208	LT	084.0	27.9	52	022	073.4	-02.2	36.1	000 - 350
GGB1DV5208	PC	235.9	-20.0	52	022	237.0	23.8	11.8	400 - 660
GGB1DV5209	LT	292.6	-70.9	52	022	225.8	-35.8	41.8	000 - 350
GGB1DV5209	PC	238.6	-09.3	52	022	245.7	31.7	07.6	400 - 640
GGB1DV5210	LT	351.8	-73.1	52	022	215.7	-51.9	39.5	000 - 250
GGB1DV5210	PC	227.6	06.4	52	022	244.8	50.9	06.9	300 - 640
GGB1DV5211	PC	250.0	-15.0	52	022	252.0	20.5	05.1	000 - 660
GGB1DV5212	PC	245.2	-15.2	52	022	247.9	23.1	18.6	000 - 600
GGB1DV5213	LT	205.2	50.0	52	022	012.3	77.8	10.1	150 - 300
GGB1DV5213	PC	241.1	-22.4	52	022	240.1	19.3	14.9	350 - 600
GGB1DV5214	LT	003.4	-65.3	52	022	217.8	-60.7	26.4	000 - 350
GGB1DV5214	PC	241.9	-00.6	52	022	255.1	36.8	11.6	400 - 620
GGB1DV5215	PC	247.1	-16.9	52	022	248.4	20.7	25.0	000 - 580
GGB1DV5216	LT	293.1	53.3	52	022	338.9	28.9	30.2	000 - 300
GGB1DV5216	PC	234.8	-19.1	52	022	236.4	25.1	10.7	350 - 620
GGB1DV5217	LT	301.5	77.6	52	022	007.0	35.0	33.2	000 - 300
GGB1DV5217	PC	240.2	-08.2	52	022	247.9	31.7	06.2	350 - 620

Table A-1b Palaeomagnetic results grouped into components.
See caption Table A-1a for more information.

SPECIMEN	Comp	Dec	Inc	Tilt	Dir	CDec	CInc	a95	Temp. range
GGB1DV0101	LT	321.0	52.0	15	165	308.5	65.1	11.1	000 - 150
GGB1DV0102	LT	228.2	78.4	15	165	192.7	67.3	16.6	000 - 150
GGB1DV0103	LT	266.5	52.5	15	165	246.5	52.9	25.4	000 - 150
GGB1DV0105	LT	119.2	-52.9	15	165	099.8	-61.6	23.8	000 - 150
GGB1DV0201	LT	211.2	37.3	15	177	206.4	24.5	20.1	000 - 300
GGB1DV0202	LT	290.5	78.9	15	177	221.6	75.4	27.3	000 - 350
GGB1DV0203	LT	016.2	83.2	15	177	162.4	81.1	40.0	000 - 350
GGB1DV0204	LT	298.3	72.1	15	177	247.6	73.8	31.3	000 - 350
GGB1DV0205	LT	198.5	64.0	15	177	191.4	49.7	33.0	000 - 350
GGB1DV0304	LT	025.7	-05.3	17	136	025.0	00.8	04.7	100 - 200
GGB1DV0305	LT	035.5	-30.8	17	136	026.4	-26.4	02.7	100 - 200
GGB1DV0401	LT	044.7	08.5	19	160	048.6	16.1	41.0	000 - 300
GGB1DV0701	LT	019.0	71.4	48	168	150.5	56.9	28.5	000 - 250
GGB1DV0702	LT	106.7	-74.1	48	168	009.0	-47.8	24.7	000 - 200
GGB1DV0703	LT	310.0	75.8	48	168	182.4	52.4	06.8	000 - 200
GGB1DV0704	LT	224.8	33.3	48	168	212.4	01.5	25.8	000 - 250
GGB1DV0705	LT	287.2	45.0	48	168	232.5	46.8	20.3	000 - 200
GGB1DV1402	LT	186.1	71.1	15	165	177.2	56.6	10.2	000 - 200
GGB1DV1403	LT	201.4	60.6	15	165	190.6	47.7	18.8	000 - 250
GGB1DV1404	LT	237.0	86.2	15	165	177.8	73.4	21.2	000 - 250
GGB1DV1405	LT	247.1	74.6	15	165	207.7	67.2	15.0	000 - 250
GGB1DV1505	LT	167.9	19.5	15	165	167.7	04.5	36.5	000 - 350
GGB1DV1604	LT	312.3	76.6	15	165	228.2	81.9	05.8	000 - 150
GGB1DV1605	LT	334.2	67.8	15	165	314.3	82.0	07.3	000 - 150
GGB1DV1701	LT	162.5	72.1	15	165	163.6	57.1	09.8	000 - 150
GGB1DV1704	LT	215.4	73.2	15	165	192.6	61.3	10.6	000 - 150
GGB1DV1801	LT	241.2	86.9	15	165	176.1	74.0	17.8	000 - 250
GGB1DV1802	LT	321.2	73.1	15	165	259.7	83.2	04.4	000 - 150
GGB1DV1803	LT	332.9	73.8	15	165	269.7	86.5	11.1	000 - 100
GGB1DV1804	LT	337.1	75.1	15	165	249.1	88.0	14.2	000 - 250
GGB1DV1805	LT	315.6	81.3	15	165	195.0	81.5	19.3	000 - 250
GGB1DV1903	LT	277.7	67.0	15	165	240.6	68.1	22.6	000 - 200
GGB1DV2001	LT	040.5	66.3	15	165	078.1	70.6	10.6	000 - 200
GGB1DV2002	LT	060.2	72.8	15	165	106.3	70.4	16.4	000 - 200
GGB1DV2301	LT	278.8	-79.2	14	140	301.7	-66.7	17.5	000 - 200
GGB1DV2401	LT	007.2	-12.5	55	160	013.5	36.0	31.3	000 - 300
GGB1DV2402	LT	219.0	52.4	57	168	196.5	06.3	41.1	000 - 300
GGB1DV2403	LT	008.7	42.9	57	168	115.4	70.9	14.0	000 - 250
GGB1DV2406	LT	203.9	19.8	57	168	206.3	-27.1	21.4	000 - 300
GGB1DV2407	LT	229.5	-33.3	57	168	276.3	-39.3	16.1	000 - 200
GGB1DV2410	LT	356.7	23.6	62	162	057.1	76.0	46.5	000 - 200
GGB1DV2411	LT	192.9	39.8	62	162	186.2	-16.4	16.0	000 - 300
GGB1DV2412	LT	198.7	12.4	62	162	208.3	-36.2	33.4	000 - 300
GGB1DV2413	LT	180.7	50.5	62	162	174.0	-09.8	33.9	000 - 300
GGB1DV2414	LT	192.8	17.2	62	162	199.1	-35.9	20.7	000 - 300
GGB1DV2415	LT	173.3	49.4	62	162	169.5	-11.9	30.5	000 - 300
GGB1DV2416	LT	030.2	59.2	62	162	129.5	44.8	40.1	000 - 200
GGB1DV2417	LT	045.5	53.4	62	162	119.6	37.7	35.9	000 - 250
GGB1DV2501	LT	339.8	19.9	62	162	327.9	81.6	24.4	000 - 250
GGB1DV2502	LT	024.5	52.2	62	162	121.6	50.3	21.3	000 - 250
GGB1DV2503	LT	020.7	-02.0	62	162	039.6	42.2	20.2	000 - 300
GGB1DV2504	LT	003.1	69.0	62	162	151.1	47.1	30.0	000 - 300
GGB1DV2505	LT	020.4	68.3	62	162	143.4	43.8	42.7	000 - 200
GGB1DV2506	LT	027.2	57.1	62	162	127.5	47.1	31.7	000 - 250
GGB1DV2507	LT	016.5	-04.3	62	162	033.3	43.7	05.6	000 - 200
GGB1DV2509	LT	016.3	-08.9	62	162	029.0	40.4	07.4	000 - 200

GGB1DV2601	LT	175.6	-81.6	54	330	154.1	-28.4	21.7	000 - 200
GGB1DV2602	LT	087.0	-25.4	54	330	096.2	04.6	20.5	000 - 200
GGB1DV2603	LT	007.2	73.4	54	330	340.8	22.3	22.2	000 - 200
GGB1DV2604	LT	344.6	72.1	54	330	334.7	18.6	16.0	000 - 200
GGB1DV2606	LT	323.2	59.0	54	330	326.5	05.2	13.0	000 - 150
GGB1DV2609	LT	303.8	-31.9	54	330	243.0	-67.9	25.0	000 - 200
GGB1DV2611	LT	048.2	04.9	54	330	049.0	-06.6	13.3	000 - 250
GGB1DV2612	LT	294.9	-22.0	54	330	254.9	-56.5	28.9	000 - 200
GGB1DV2613	LT	168.6	07.6	54	330	185.3	56.9	33.8	000 - 250
GGB1DV2615	LT	300.3	-26.9	54	330	251.4	-63.2	35.7	000 - 200
GGB1DV2714	LT	228.2	82.7	25	166	179.4	60.9	26.5	000 - 200
GGB1DV2715	LT	121.4	39.7	25	166	130.8	20.4	29.6	000 - 200
GGB1DV2716	LT	121.7	-04.5	25	166	117.4	-21.8	33.0	000 - 250
GGB1DV2717	LT	164.0	60.4	25	166	164.8	35.4	17.2	000 - 200
GGB1DV2718	LT	276.0	27.7	25	166	261.3	33.3	35.3	000 - 200
GGB1DV2719	LT	027.8	-69.8	25	166	006.1	-47.9	21.9	000 - 200
GGB1DV2720	LT	012.0	29.3	25	166	023.2	50.8	21.4	000 - 200
GGB1DV2721	LT	121.4	37.0	25	166	129.9	17.7	01.8	000 - 150
GGB1DV2722	LT	020.7	06.1	25	166	025.1	26.2	09.7	000 - 150
GGB1DV2801	LT	148.2	74.5	14	180	162.8	61.7	25.7	000 - 250
GGB1DV2802	LT	038.6	57.5	14	180	058.8	67.0	25.6	000 - 150
GGB1DV2803	LT	185.5	-33.4	14	180	186.8	-47.3	26.3	000 - 200
GGB1DV2901	LT	231.3	09.1	00	000	231.3	09.1	30.9	000 - 350
GGB1DV2902	LT	134.5	06.9	00	000	134.5	06.9	20.1	000 - 150
GGB1DV2903	LT	326.4	-13.7	00	000	326.4	-13.7	32.8	000 - 150
GGB1DV2904	LT	127.3	02.4	00	000	127.3	02.4	23.4	000 - 150
GGB1DV2906	LT	192.2	10.4	00	000	192.2	10.4	23.3	000 - 300
GGB1DV2907	LT	289.1	-45.5	00	000	289.1	-45.5	06.6	100 - 250
GGB1DV3001	LT	125.5	59.6	04	251	131.5	61.8	19.9	000 - 150
GGB1DV3002	LT	260.8	73.2	04	251	258.9	69.3	17.4	000 - 150
GGB1DV3003	LT	261.5	-60.5	04	251	263.0	-64.4	38.3	000 - 350
GGB1DV3004	LT	283.6	-67.7	04	251	289.9	-71.0	43.6	000 - 350
GGB1DV3005	LT	152.8	72.2	04	251	165.4	72.3	19.8	000 - 200
GGB1DV3101	LT	179.2	23.5	00	000	179.2	23.5	21.7	100 - 300
GGB1DV3103	LT	002.7	14.7	00	000	002.7	14.7	38.5	000 - 300
GGB1DV3105	LT	045.5	42.5	00	000	045.5	42.5	35.4	000 - 300
GGB1DV3106	LT	054.6	-11.0	00	000	054.6	-11.0	46.3	000 - 350
GGB1DV3203	LT	099.5	-67.9	00	000	099.5	-67.9	43.7	000 - 300
GGB1DV3204	LT	107.8	61.1	00	000	107.8	61.1	24.1	000 - 250
GGB1DV3303	LT	228.4	41.9	41	327	262.7	35.3	13.8	000 - 200
GGB1DV3404	LT	176.5	53.2	32	324	233.4	71.2	16.0	000 - 200
GGB1DV3503	LT	202.3	37.0	04	130	199.5	35.7	14.6	000 - 250
GGB1DV3507	LT	145.6	45.4	04	130	144.6	41.5	20.4	000 - 200
GGB1DV3508	LT	279.2	54.7	04	130	276.0	58.0	36.8	100 - 300
GGB1DV3509	LT	219.9	56.5	04	130	213.9	56.3	30.0	000 - 300
GGB1DV3510	LT	038.5	-06.6	04	130	038.1	-06.4	23.5	000 - 200
GGB1DV3511	LT	023.7	33.4	04	130	026.3	34.5	37.2	000 - 250
GGB1DV3513	LT	220.3	33.6	04	130	217.7	33.6	27.2	000 - 350
GGB1DV3601	LT	304.9	37.0	04	130	304.6	40.9	28.3	000 - 250
GGB1DV3602	LT	252.7	41.7	04	130	249.5	43.8	24.2	000 - 300
GGB1DV3603	LT	018.5	-14.8	04	130	017.5	-13.3	14.1	000 - 250
GGB1DV3604	LT	339.8	12.5	04	130	340.3	15.9	31.0	000 - 200
GGB1DV3605	LT	299.1	44.5	04	130	298.3	48.4	18.8	000 - 250
GGB1DV3606	LT	242.6	39.4	04	130	239.4	40.8	22.7	000 - 350
GGB1DV3701	LT	255.6	64.9	40	140	180.9	54.2	16.4	000 - 300
GGB1DV3703	LT	358.0	62.6	40	140	096.0	65.9	11.8	000 - 200
GGB1DV3709	LT	308.1	65.0	40	140	158.1	73.7	14.5	000 - 200
GGB1DV3710	LT	302.2	39.3	40	140	263.6	73.5	26.2	000 - 300
GGB1DV3712	LT	322.4	41.0	40	140	331.4	80.8	30.8	000 - 300
GGB1DV3801	LT	226.5	80.7	40	140	154.1	48.6	21.2	000 - 300
GGB1DV3802	LT	180.6	79.6	40	140	149.1	41.7	27.4	000 - 300
GGB1DV3803	LT	110.4	74.9	40	140	130.8	36.4	26.1	000 - 300

GGB1DV3804	LT	293.2	81.5	40	140	147.1	57.4	22.4	000 - 300
GGB1DV3805	LT	196.7	35.0	40	140	183.8	08.7	43.7	000 - 250
GGB1DV3806	LT	152.4	72.8	40	140	144.4	33.1	37.2	000 - 350
GGB1DV3807	LT	349.2	67.1	40	140	110.1	67.5	29.8	000 - 250
GGB1DV3808	LT	216.3	59.6	40	140	177.3	35.7	27.4	000 - 250
GGB1DV3901	LT	077.3	36.7	02	275	076.8	38.6	29.5	000 - 300
GGB1DV3902	LT	228.3	38.5	02	275	229.4	37.1	40.6	100 - 350
GGB1DV3903	LT	213.5	38.7	02	275	214.9	37.7	13.1	150 - 300
GGB1DV3904	LT	209.8	53.3	02	275	212.2	52.4	12.5	150 - 300
GGB1DV3905	LT	221.2	-61.0	02	275	218.1	-62.1	37.8	000 - 300
GGB1DV3906	LT	079.9	56.8	02	275	079.0	58.7	30.4	000 - 250
GGB1DV3907	LT	070.1	21.2	02	275	069.8	23.1	27.2	100 - 250
GGB1DV3908	LT	331.1	36.4	02	275	329.9	35.3	39.3	000 - 300
GGB1DV3909	LT	095.3	28.0	02	275	095.3	30.0	31.5	100 - 250
GGB1DV3910	LT	222.4	44.6	02	275	223.9	43.4	26.5	100 - 250
GGB1DV3911	LT	226.6	15.4	02	275	227.0	14.0	23.5	000 - 200
GGB1DV3912	LT	200.5	28.3	02	275	201.5	27.7	03.2	150 - 250
GGB1DV3913	LT	091.6	-67.4	02	275	091.8	-65.4	29.3	000 - 300
GGB1DV3914	LT	003.1	02.7	02	275	003.0	02.6	32.2	000 - 200
GGB1DV3918	LT	027.4	08.1	02	275	027.1	08.8	26.9	000 - 300
GGB1DV3919	LT	049.7	-06.9	02	275	049.9	-05.5	10.4	100 - 250
GGB1DV3920	LT	013.0	08.9	02	275	012.7	09.2	08.7	000 - 200
GGB1DV3921	LT	215.3	38.4	02	275	216.6	37.3	04.5	000 - 150
GGB1DV4001	LT	226.2	-73.3	06	130	244.6	-71.7	16.7	000 - 200
GGB1DV4002	LT	221.8	-77.7	06	130	247.1	-76.2	22.1	000 - 200
GGB1DV4004	LT	225.2	-78.4	06	130	251.0	-76.4	45.8	000 - 200
GGB1DV4103	LT	020.3	64.1	06	130	032.8	65.5	39.8	000 - 200
GGB1DV4104	LT	049.6	35.3	06	130	053.7	34.1	22.0	000 - 300
GGB1DV4105	LT	007.5	13.2	06	130	008.9	16.4	38.0	000 - 300
GGB1DV4107	LT	235.1	76.8	06	130	208.9	77.1	24.4	000 - 200
GGB1DV4108	LT	353.9	02.4	06	130	354.3	06.7	33.7	000 - 150
GGB1DV4109	LT	335.6	09.8	06	130	336.2	15.2	16.3	000 - 200
GGB1DV4110	LT	013.0	33.0	06	130	016.7	35.6	24.8	000 - 200
GGB1DV4111	LT	007.4	33.4	06	130	011.0	36.5	17.7	000 - 150
GGB1DV4112	LT	045.7	31.7	06	130	049.4	30.9	27.0	000 - 200
GGB1DV4201	LT	005.0	22.9	06	130	007.2	26.3	25.0	000 - 150
GGB1DV4202	LT	016.2	37.5	06	130	020.7	39.7	12.3	000 - 150
GGB1DV4203	LT	030.9	48.1	06	130	037.7	48.7	06.8	000 - 150
GGB1DV4204	LT	009.4	30.5	06	130	012.7	33.4	08.8	000 - 150
GGB1DV4206	LT	358.6	02.6	06	130	359.0	06.6	21.9	000 - 350
GGB1DV4207	LT	267.4	-29.3	06	130	269.4	-24.9	23.5	000 - 150
GGB1DV4208	LT	028.4	53.9	06	130	036.7	54.7	21.0	000 - 150
GGB1DV4209	LT	031.9	50.0	06	130	039.1	50.5	29.0	000 - 150
GGB1DV4309	LT	286.8	25.4	39	172	263.7	34.9	16.8	000 - 200
GGB1DV4312	LT	256.4	-51.1	39	172	297.2	-40.1	11.8	000 - 250
GGB1DV4313	LT	290.4	-05.6	39	172	288.2	12.9	39.9	000 - 200
GGB1DV4315	LT	332.1	17.6	39	172	319.4	53.0	27.9	000 - 300
GGB1DV4316	LT	206.1	29.8	39	172	201.2	-03.8	34.2	000 - 400
GGB1DV4318	LT	101.9	86.0	39	172	166.2	49.5	31.7	000 - 350
GGB1DV4319	LT	286.8	36.7	39	172	253.0	42.6	34.3	000 - 350
GGB1DV4401	LT	247.4	-06.9	39	172	255.0	-14.6	13.9	000 - 250
GGB1DV4402	LT	233.9	04.5	39	172	236.7	-13.6	23.2	000 - 250
GGB1DV4403	LT	297.0	-83.5	39	172	344.2	-47.0	42.7	000 - 250
GGB1DV4404	LT	257.1	-19.5	39	172	270.9	-18.1	20.0	000 - 250
GGB1DV4406	LT	222.1	-02.3	39	172	230.3	-25.7	22.7	000 - 250
GGB1DV4501	LT	242.0	-41.0	38	192	284.2	-54.7	31.7	000 - 300
GGB1DV4502	LT	340.0	-56.0	38	192	353.5	-21.2	24.7	000 - 250
GGB1DV4602	LT	215.4	-29.5	38	192	238.6	-61.6	37.2	000 - 150
GGB1DV4605	LT	268.4	-48.7	38	192	309.9	-43.4	29.5	000 - 150
GGB1DV4710	LT	207.4	64.2	38	170	187.7	29.8	20.9	000 - 200
GGB1DV4711	LT	091.4	-79.2	38	170	007.7	-52.8	12.0	000 - 150
GGB1DV4712	LT	130.6	35.9	38	170	139.0	04.4	33.3	000 - 150

GGB1DV4713	LT	009.6	11.8	38	170	018.6	46.8	37.7	000 - 200
GGB1DV4714	LT	228.2	63.4	38	170	197.3	34.0	06.4	000 - 200
GGB1DV4801	LT	238.9	-14.9	90	004	256.0	33.7	21.6	100 - 250
GGB1DV4802	LT	189.8	-01.2	90	004	262.3	84.1	19.9	100 - 400
GGB1DV4803	LT	238.3	11.3	90	004	287.8	34.9	20.5	000 - 300
GGB1DV4804	LT	249.2	07.7	90	004	282.4	24.6	22.9	000 - 300
GGB1DV4805	LT	183.5	02.4	90	004	016.1	87.5	21.5	100 - 300
GGB1DV4806	LT	206.5	63.1	90	004	353.0	24.7	33.1	000 - 350
GGB1DV4810	LT	299.0	19.9	90	004	295.7	-23.4	16.8	100 - 300
GGB1DV4811	LT	238.9	45.9	90	004	325.6	23.6	10.6	000 - 300
GGB1DV4812	LT	307.7	26.5	90	004	304.9	-29.8	35.1	000 - 350
GGB1DV4813	LT	222.4	53.8	90	004	339.6	27.6	06.6	000 - 300
GGB1DV4814	LT	070.4	80.1	90	004	013.1	-03.9	02.9	000 - 150
GGB1DV4815	LT	260.3	-20.3	90	004	253.1	12.8	10.7	100 - 300
GGB1DV4816	LT	267.6	34.8	90	004	308.9	05.2	10.4	000 - 200
GGB1DV4817	LT	151.8	09.7	90	004	076.2	56.5	30.0	100 - 350
GGB1DV4818	LT	290.4	19.4	90	004	294.2	-15.4	27.5	000 - 300
GGB1DV4819	LT	001.5	-76.0	90	004	184.6	-14.0	24.4	000 - 200
GGB1DV4820	LT	241.2	24.7	90	004	302.7	29.5	29.3	000 - 300
GGB1DV4821	LT	010.1	-34.6	90	004	175.3	-55.0	34.0	000 - 300
GGB1DV4822	LT	316.8	05.5	90	004	281.4	-42.5	28.2	000 - 400
GGB1DV4823	LT	127.9	81.3	90	004	011.3	04.9	31.6	000 - 400
GGB1DV4901	LT	027.3	-48.0	82	006	165.5	-46.1	35.1	000 - 250
GGB1DV4902	LT	186.8	28.5	82	006	003.9	69.5	17.6	150 - 300
GGB1DV4903	LT	274.7	-74.9	82	006	201.2	-07.4	24.0	000 - 250
GGB1DV4904	LT	108.1	43.5	82	006	053.0	14.3	43.2	000 - 250
GGB1DV4905	LT	181.7	63.7	82	006	008.3	34.2	32.8	000 - 350
GGB1DV4906	LT	229.3	38.2	82	006	320.7	40.7	31.7	000 - 350
GGB1DV4907	LT	230.5	63.4	82	006	345.6	26.1	30.3	000 - 250
GGB1DV4908	LT	357.5	19.8	82	006	349.4	-60.9	33.0	000 - 300
GGB1DV4909	LT	350.2	54.4	82	006	355.8	-26.2	13.6	100 - 250
GGB1DV4910	LT	134.7	43.0	82	006	049.0	33.2	38.2	000 - 400
GGB1DV4911	LT	330.2	-31.2	82	006	236.3	-49.4	46.3	000 - 400
GGB1DV4912	LT	171.4	-25.4	82	006	163.4	53.7	33.9	000 - 400
GGB1DV4913	LT	183.7	-17.6	82	006	181.0	64.3	37.6	000 - 400
GGB1DV4915	LT	066.4	49.7	82	006	041.1	-12.2	13.6	100 - 250
GGB1DV4916	LT	122.0	52.3	82	006	042.4	22.0	10.1	100 - 250
GGB1DV4917	LT	191.4	30.7	82	006	354.2	66.8	28.5	000 - 350
GGB1DV5001	LT	249.5	69.9	42	184	207.1	37.0	18.2	000 - 250
GGB1DV5002	LT	195.6	56.9	42	184	190.5	15.4	20.1	000 - 250
GGB1DV5004	LT	000.1	-37.0	42	184	000.9	04.9	19.1	100 - 200
GGB1DV5007	LT	343.5	-30.8	42	184	346.2	09.1	25.3	100 - 200
GGB1DV5008	LT	041.1	-40.4	42	184	031.4	-04.3	21.8	000 - 400
GGB1DV5009	LT	004.6	-65.8	42	184	004.3	-23.8	38.7	000 - 200
GGB1DV5010	LT	136.8	48.6	42	184	153.9	14.9	16.9	100 - 200
GGB1DV5011	LT	151.8	35.2	42	184	158.1	-02.0	06.2	100 - 250
GGB1DV5012	LT	182.0	40.8	42	184	182.5	-01.1	30.8	000 - 300
GGB1DV5013	LT	186.8	77.6	42	184	184.7	35.6	18.8	000 - 250
GGB1DV5102	LT	229.2	10.8	96	184	264.7	-45.1	16.2	000 - 350
GGB1DV5103	LT	224.2	19.1	96	184	251.8	-48.7	20.3	000 - 250
GGB1DV5104	LT	024.2	-04.7	96	184	096.6	69.8	36.6	150 - 350
GGB1DV5111	LT	014.7	-39.9	96	184	018.3	54.8	19.1	100 - 200
GGB1DV5113	LT	216.6	-82.3	96	184	359.9	-00.5	27.3	100 - 300
GGB1DV5114	LT	065.0	12.5	96	184	111.3	26.6	10.9	100 - 200
GGB1DV5115	LT	224.6	14.6	96	184	258.6	-49.2	10.0	150 - 300
GGB1DV5116	LT	216.5	79.6	96	184	189.7	-14.7	17.6	000 - 300
GGB1DV5118	LT	293.0	44.8	96	184	226.8	09.0	21.4	000 - 250
GGB1DV5201	LT	318.3	26.3	52	022	328.4	-02.3	15.6	000 - 200
GGB1DV5202	LT	140.5	-39.9	52	022	159.4	-06.1	06.9	100 - 200
GGB1DV5205	LT	085.6	-45.2	52	022	142.2	-43.1	36.6	000 - 250
GGB1DV5206	LT	090.6	-52.8	52	022	153.1	-41.6	15.3	150 - 300
GGB1DV5208	LT	084.0	27.9	52	022	073.4	-02.2	36.1	000 - 350

GGB1DV5209	LT	292.6	-70.9	52	022	225.8	-35.8	41.8	000 - 350
GGB1DV5210	LT	351.8	-73.1	52	022	215.7	-51.9	39.5	000 - 250
GGB1DV5213	LT	205.2	50.0	52	022	012.3	77.8	10.1	150 - 300
GGB1DV5214	LT	003.4	-65.3	52	022	217.8	-60.7	26.4	000 - 350
GGB1DV5216	LT	293.1	53.3	52	022	338.9	28.9	30.2	000 - 300
GGB1DV5217	LT	301.5	77.6	52	022	007.0	35.0	33.2	000 - 300
GGB1DV0101	PC	204.4	00.3	15	165	205.3	-11.3	04.9	200 - 625
GGB1DV0102	PC	201.0	-00.4	15	165	202.0	-12.5	05.6	200 - 625
GGB1DV0103	PC	192.5	09.6	15	165	192.1	-03.7	07.2	200 - 720
GGB1DV0104	PC	184.9	-09.0	15	165	186.4	-23.1	07.3	000 - 400
GGB1DV0105	PC	183.1	-01.0	15	165	183.8	-15.2	07.6	200 - 720
GGB1DV0201	PC	191.5	11.2	15	177	191.3	-03.3	06.5	350 - 600
GGB1DV0202	PC	197.7	15.6	15	177	197.0	01.5	07.5	400 - 600
GGB1DV0203	PC	211.0	-04.4	15	177	212.6	-16.7	06.2	400 - 600
GGB1DV0204	PC	187.4	10.3	15	177	187.3	-04.4	09.8	400 - 720
GGB1DV0205	PC	175.7	20.0	15	177	175.7	05.0	02.9	400 - 500
GGB1DV0301	PC	210.3	10.1	17	136	208.1	05.1	10.3	100 - 550
GGB1DV0302	PC	192.4	23.5	17	136	187.7	13.4	28.7	000 - 500
GGB1DV0303	PC	219.1	-04.4	17	136	220.7	-06.2	14.4	000 - 550
GGB1DV0304	PC	208.5	05.9	17	136	207.5	00.7	03.5	250 - 700
GGB1DV0305	PC	226.7	06.8	17	136	224.7	06.7	05.8	250 - 675
GGB1DV0401	PC	006.4	11.6	19	160	009.7	28.4	07.9	350 - 700
GGB1DV0402	PC	020.5	-16.3	19	160	018.6	-01.6	13.9	000 - 550
GGB1DV0403	PC	012.7	02.7	19	160	014.7	18.6	16.6	000 - 600
GGB1DV0404	PC	006.3	-14.5	19	160	005.4	02.6	13.6	000 - 550
GGB1DV0405	PC	024.5	-02.6	19	160	025.5	10.9	13.6	000 - 500
GGB1DV0501	PC	211.2	-00.5	18	167	212.7	-13.3	02.7	000 - 720
GGB1DV0502	PC	209.2	00.4	18	167	210.5	-12.9	02.0	000 - 720
GGB1DV0503	PC	212.9	-02.2	18	167	214.9	-14.5	02.4	000 - 720
GGB1DV0504	PC	211.9	-01.5	18	167	213.7	-14.1	05.5	000 - 550
GGB1DV0505	PC	206.9	-03.2	18	167	209.0	-16.9	03.8	000 - 550
GGB1DV0601	PC	208.6	03.5	10	190	208.7	-05.9	04.6	000 - 700
GGB1DV0602	PC	208.5	-01.3	10	190	208.8	-10.8	04.5	000 - 700
GGB1DV0603	PC	204.0	01.4	10	190	204.2	-08.3	03.0	000 - 700
GGB1DV0604	PC	208.4	02.1	10	190	208.5	-07.4	03.9	000 - 700
GGB1DV0605	PC	214.6	00.3	10	190	214.9	-08.8	03.3	000 - 700
GGB1DV0701	PC	209.1	00.9	48	168	219.8	-33.3	03.3	300 - 720
GGB1DV0702	PC	208.7	00.7	48	168	219.7	-33.7	03.8	250 - 720
GGB1DV0703	PC	206.4	-02.1	48	168	219.3	-37.3	03.2	250 - 720
GGB1DV0704	PC	210.0	15.1	48	168	211.9	-21.0	03.0	300 - 700
GGB1DV0705	PC	212.6	03.6	48	168	221.3	-29.1	04.7	250 - 700
GGB1DV0801	PC	209.8	-11.6	40	340	210.6	14.6	02.4	000 - 720
GGB1DV0802	PC	201.2	-14.9	40	340	201.4	15.7	02.1	000 - 720
GGB1DV0803	PC	210.5	-11.3	40	340	211.4	14.6	03.0	000 - 720
GGB1DV0804	PC	205.4	-12.2	40	340	206.5	16.2	03.7	000 - 700
GGB1DV0805	PC	206.8	-13.7	40	340	206.9	14.2	02.6	000 - 675
GGB1DV0901	PC	200.1	-04.4	64	333	216.4	35.2	03.3	000 - 720
GGB1DV0902	PC	206.8	-05.7	64	333	219.6	29.0	04.8	000 - 720
GGB1DV0903	PC	202.5	-04.8	64	333	217.7	33.0	03.8	000 - 720
GGB1DV1001	PC	213.5	-00.3	45	349	223.1	30.1	02.8	000 - 700
GGB1DV1002	PC	207.1	-04.4	45	349	214.3	30.1	02.6	000 - 700
GGB1DV1003	PC	207.8	-03.4	45	349	215.5	30.5	02.8	000 - 675
GGB1DV1004	PC	207.8	-03.9	45	349	215.2	30.1	03.3	000 - 700
GGB1DV1005	PC	206.8	-05.2	45	349	213.5	29.5	02.5	000 - 675
GGB1DV1201	PC	199.0	-03.9	65	342	218.4	43.9	04.6	000 - 720
GGB1DV1202	PC	199.9	-01.5	65	342	221.9	44.8	03.8	000 - 700
GGB1DV1203	PC	195.7	-04.9	65	342	214.3	45.6	04.9	000 - 675
GGB1DV1204	PC	194.5	-06.5	65	342	211.4	45.3	05.9	000 - 700
GGB1DV1205	PC	199.6	02.5	65	342	226.2	47.3	07.0	000 - 700
GGB1DV1401	PC	197.3	-09.2	15	165	199.6	-21.8	05.5	100 - 700
GGB1DV1403	PC	189.9	-06.1	15	165	191.4	-19.6	04.3	300 - 700

GGB1DV1404	PC	194.1	01.9	15	165	194.7	-11.2	04.8	300 - 700
GGB1DV1405	PC	180.6	02.6	15	165	180.9	-11.8	07.0	300 - 700
GGB1DV1501	PC	181.6	04.4	15	165	181.8	-10.0	05.9	100 - 625
GGB1DV1502	PC	194.6	-02.1	15	165	195.7	-15.1	09.8	150 - 700
GGB1DV1503	PC	186.9	09.9	15	165	186.6	-04.0	13.5	100 - 500
GGB1DV1504	PC	192.0	-01.0	15	165	193.0	-14.3	09.3	100 - 700
GGB1DV1505	PC	199.8	22.0	15	165	197.4	09.5	05.8	400 - 700
GGB1DV1601	PC	183.6	03.8	15	165	183.9	-10.4	09.9	100 - 550
GGB1DV1602	PC	173.8	03.0	15	165	174.0	-11.8	12.0	100 - 700
GGB1DV1603	PC	189.9	-00.5	15	165	190.7	-14.0	02.6	150 - 350
GGB1DV1604	PC	189.5	-08.8	15	165	191.3	-22.4	07.5	200 - 400
GGB1DV1605	PC	179.3	-13.3	15	165	180.7	-27.8	11.6	200 - 400
GGB1DV1701	PC	182.3	02.9	15	165	182.6	-11.4	06.8	200 - 700
GGB1DV1702	PC	186.2	06.2	15	165	186.2	-07.8	09.4	100 - 500
GGB1DV1703	PC	188.3	05.6	15	165	188.5	-08.2	06.7	100 - 700
GGB1DV1704	PC	180.4	-05.9	15	165	181.3	-20.3	06.0	200 - 600
GGB1DV1705	PC	183.9	03.7	15	165	184.2	-10.5	07.8	100 - 550
GGB1DV1801	PC	197.8	-13.4	15	165	200.9	-25.8	08.2	300 - 600
GGB1DV1802	PC	189.9	-07.6	15	165	191.5	-21.2	09.7	200 - 500
GGB1DV1803	PC	165.3	02.8	15	165	165.3	-12.2	07.1	250 - 675
GGB1DV1804	PC	200.9	16.8	15	165	199.3	04.5	15.1	300 - 650
GGB1DV1805	PC	178.6	00.1	15	165	179.0	-14.4	10.8	300 - 700
GGB1DV1901	PC	178.0	-00.7	15	165	178.5	-15.3	06.8	150 - 700
GGB1DV1902	PC	191.2	03.0	15	165	191.6	-10.4	09.4	150 - 550
GGB1DV1903	PC	189.1	-05.3	15	165	190.4	-18.9	01.9	250 - 400
GGB1DV1904	PC	196.4	-01.6	15	165	197.6	-14.4	05.6	100 - 500
GGB1DV1905	PC	181.2	-13.4	15	165	182.8	-27.8	02.9	100 - 450
GGB1DV2001	PC	193.8	-11.9	15	165	196.3	-24.9	11.2	250 - 625
GGB1DV2002	PC	196.0	-06.3	15	165	197.8	-19.1	11.2	250 - 700
GGB1DV2003	PC	187.6	-10.4	15	165	189.4	-24.2	05.1	100 - 700
GGB1DV2004	PC	184.3	-07.6	15	165	185.6	-21.7	11.4	100 - 650
GGB1DV2101	PC	185.5	-15.0	19	132	191.4	-25.6	03.2	000 - 660
GGB1DV2102	PC	188.0	-04.5	19	132	190.7	-14.9	09.0	000 - 620
GGB1DV2103	PC	184.5	-07.6	19	132	188.2	-18.8	03.9	000 - 620
GGB1DV2104	PC	187.5	-09.8	19	132	191.8	-20.0	03.0	000 - 620
GGB1DV2105	PC	187.7	-04.7	19	132	190.5	-15.1	03.0	000 - 640
GGB1DV2106	PC	186.5	-08.6	19	132	190.4	-19.2	03.8	000 - 640
GGB1DV2107	PC	196.6	12.2	19	132	194.2	03.6	14.5	000 - 580
GGB1DV2108	PC	183.5	-00.8	19	132	185.3	-12.5	08.5	000 - 700
GGB1DV2109	PC	182.6	-11.1	19	132	187.2	-22.6	10.8	000 - 580
GGB1DV2110	PC	181.3	-09.0	19	132	185.3	-21.0	08.2	000 - 580
GGB1DV2111	PC	186.4	-11.8	19	132	191.3	-22.3	10.3	000 - 680
GGB1DV2201	PC	184.8	-17.2	24	123	193.9	-27.0	18.9	000 - 580
GGB1DV2202	PC	192.0	-04.1	24	123	195.3	-12.2	05.2	000 - 640
GGB1DV2203	PC	189.8	-09.9	24	123	195.6	-18.3	03.5	000 - 660
GGB1DV2204	PC	186.4	-10.8	24	123	192.6	-20.5	05.2	000 - 680
GGB1DV2205	PC	185.9	-19.6	24	123	196.1	-28.8	05.8	000 - 640
GGB1DV2206	PC	193.3	-02.7	24	123	195.9	-10.4	08.2	000 - 620
GGB1DV2207	PC	189.1	-02.7	24	123	192.1	-12.0	03.8	000 - 660
GGB1DV2208	PC	188.6	-02.5	24	123	191.4	-11.9	05.6	000 - 680
GGB1DV2209	PC	186.3	-03.7	24	123	189.7	-14.0	04.1	000 - 640
GGB1DV2301	PC	195.4	-18.6	14	140	200.2	-26.1	08.2	250 - 700
GGB1DV2302	PC	194.3	-19.1	14	140	199.3	-26.8	03.4	000 - 640
GGB1DV2303	PC	189.1	-16.7	14	140	193.3	-25.5	03.1	000 - 640
GGB1DV2304	PC	188.8	-14.7	14	140	192.6	-23.6	04.5	000 - 640
GGB1DV2305	PC	194.7	-10.0	14	140	197.6	-17.8	03.4	000 - 640
GGB1DV2306	PC	190.3	-15.8	14	140	194.4	-24.4	02.9	000 - 640
GGB1DV2307	PC	192.3	-13.8	14	140	195.9	-22.0	09.5	000 - 700
GGB1DV2401	PC	201.6	03.3	55	160	214.4	-35.4	02.1	350 - 640
GGB1DV2402	PC	200.4	02.5	57	168	215.2	-43.1	02.2	350 - 620
GGB1DV2403	PC	201.2	14.9	57	168	206.9	-32.5	06.3	300 - 580
GGB1DV2404	PC	192.6	08.1	57	168	202.1	-42.7	05.0	100 - 640

GGB1DV2405	PC	196.3	03.0	57	168	210.1	-45.1	04.6	000 - 680
GGB1DV2406	PC	193.2	08.1	57	168	202.9	-42.4	03.2	350 - 660
GGB1DV2407	PC	186.2	10.7	57	168	192.8	-42.9	04.4	250 - 700
GGB1DV2408	PC	205.9	16.3	62	162	211.3	-28.7	16.3	100 - 700
GGB1DV2409	PC	197.9	27.0	62	162	197.2	-25.1	08.7	100 - 680
GGB1DV2410	PC	202.3	16.3	62	162	208.4	-31.0	04.1	250 - 620
GGB1DV2411	PC	201.5	13.5	62	162	209.9	-33.6	02.2	350 - 620
GGB1DV2412	PC	191.9	13.1	62	162	201.1	-39.7	05.3	350 - 620
GGB1DV2413	PC	190.4	20.1	62	162	194.9	-34.6	04.1	350 - 620
GGB1DV2414	PC	187.1	17.6	62	162	193.0	-38.3	06.0	350 - 600
GGB1DV2415	PC	187.3	18.2	62	162	192.8	-37.7	03.6	350 - 600
GGB1DV2416	PC	190.0	08.6	62	162	202.6	-44.4	06.9	350 - 620
GGB1DV2417	PC	186.9	13.9	62	162	195.2	-41.7	05.8	300 - 600
GGB1DV2501	PC	194.1	10.2	62	162	205.7	-40.8	03.2	300 - 660
GGB1DV2502	PC	194.0	03.4	62	162	211.6	-46.0	04.0	300 - 660
GGB1DV2503	PC	198.0	09.2	62	162	210.3	-39.0	13.6	350 - 700
GGB1DV2504	PC	189.1	12.3	62	162	198.7	-41.9	04.8	350 - 680
GGB1DV2505	PC	194.6	18.1	62	162	200.2	-34.1	05.7	250 - 680
GGB1DV2506	PC	192.2	05.7	62	162	207.5	-45.4	05.2	300 - 660
GGB1DV2507	PC	195.7	08.2	62	162	209.0	-41.3	05.5	250 - 700
GGB1DV2508	PC	208.3	03.6	62	162	224.3	-35.4	04.1	000 - 700
GGB1DV2509	PC	200.1	10.8	62	162	210.9	-36.5	05.0	250 - 700
GGB1DV2510	PC	195.4	20.0	62	162	199.7	-32.2	05.8	000 - 700
GGB1DV2601	PC	200.6	-11.1	54	330	205.4	23.0	23.0	250 - 640
GGB1DV2602	PC	205.1	-11.9	54	330	208.3	19.4	05.0	250 - 600
GGB1DV2605	PC	207.8	-13.3	54	330	209.2	16.5	05.7	000 - 640
GGB1DV2606	PC	211.1	-12.4	54	330	212.2	14.8	05.8	200 - 640
GGB1DV2607	PC	216.1	-09.9	54	330	217.5	12.8	04.0	000 - 700
GGB1DV2612	PC	205.5	-16.6	54	330	205.1	15.7	04.7	250 - 700
GGB1DV2614	PC	202.6	-15.2	54	330	204.0	18.7	06.0	100 - 640
GGB1DV2615	PC	206.4	-17.0	54	330	205.5	14.9	04.7	250 - 700
GGB1DV2704	PC	208.1	-02.0	25	166	211.6	-20.2	03.4	000 - 700
GGB1DV2706	PC	207.3	-11.9	25	166	214.1	-29.8	02.6	000 - 700
GGB1DV2707	PC	207.1	-05.1	25	166	211.5	-23.5	04.7	000 - 700
GGB1DV2708	PC	208.0	-06.8	25	166	213.0	-24.8	06.0	000 - 700
GGB1DV2709	PC	205.5	-02.8	25	166	209.1	-21.7	03.9	000 - 700
GGB1DV2710	PC	213.0	-09.5	25	166	219.2	-25.7	04.1	000 - 700
GGB1DV2711	PC	208.1	-01.3	25	166	211.3	-19.5	03.4	000 - 640
GGB1DV2712	PC	216.8	-10.0	25	166	223.2	-24.9	03.6	000 - 700
GGB1DV2713	PC	209.8	-06.6	25	166	214.9	-24.0	02.8	000 - 700
GGB1DV2714	PC	211.2	-03.6	25	166	215.2	-20.7	05.0	250 - 640
GGB1DV2715	PC	209.8	-09.6	25	166	215.9	-26.9	03.6	250 - 660
GGB1DV2716	PC	210.5	-10.7	25	166	217.0	-27.7	04.6	300 - 700
GGB1DV2717	PC	200.7	-04.3	25	166	204.6	-24.5	02.3	250 - 700
GGB1DV2718	PC	207.1	-07.9	25	166	212.5	-26.1	02.7	250 - 700
GGB1DV2719	PC	210.4	-08.0	25	166	216.0	-25.2	04.0	250 - 700
GGB1DV2720	PC	206.2	-04.2	25	166	210.3	-22.9	03.9	250 - 700
GGB1DV2721	PC	202.7	-05.7	25	166	207.1	-25.3	03.8	200 - 700
GGB1DV2722	PC	202.2	-03.5	25	166	206.0	-23.3	03.9	200 - 700
GGB1DV2802	PC	220.5	-03.3	14	180	221.9	-13.8	07.3	200 - 700
GGB1DV2803	PC	210.5	-06.3	14	180	212.1	-18.3	05.3	250 - 700
GGB1DV2901	PC	206.9	-18.4	00	000	206.9	-18.4	04.8	400 - 580
GGB1DV2902	PC	206.2	-11.5	00	000	206.2	-11.5	03.0	200 - 580
GGB1DV2903	PC	190.4	-10.1	00	000	190.4	-10.1	05.6	200 - 550
GGB1DV2904	PC	197.9	06.2	00	000	197.9	06.2	09.3	200 - 550
GGB1DV2905	PC	210.1	-14.9	00	000	210.1	-14.9	06.3	000 - 700
GGB1DV2906	PC	200.4	-13.3	00	000	200.4	-13.3	05.2	350 - 550
GGB1DV2907	PC	217.4	-10.2	00	000	217.4	-10.2	06.4	300 - 700
GGB1DV3001	PC	203.0	-05.5	04	251	202.6	-08.2	07.4	200 - 600
GGB1DV3002	PC	199.6	-07.5	04	251	199.1	-10.0	08.3	200 - 600
GGB1DV3003	PC	206.7	00.4	04	251	206.6	-02.4	14.3	400 - 620
GGB1DV3004	PC	199.0	-00.7	04	251	198.9	-03.2	14.9	400 - 620

GGB1DV3005	PC	200.0	-02.1	04	251	199.8	-04.6	05.3	250 - 580
GGB1DV3006	PC	199.4	-03.5	04	251	199.2	-05.9	05.6	000 - 700
GGB1DV3007	PC	205.2	-03.3	04	251	204.9	-06.1	05.2	000 - 680
GGB1DV3008	PC	208.7	-01.7	04	251	208.6	-04.6	04.2	000 - 700
GGB1DV3101	PC	204.9	01.9	00	000	204.9	01.9	07.6	350 - 580
GGB1DV3102	PC	204.0	01.0	00	000	204.0	01.0	06.4	000 - 550
GGB1DV3103	PC	208.8	-07.7	00	000	208.8	-07.7	04.1	350 - 550
GGB1DV3104	PC	207.2	-08.1	00	000	207.2	-08.1	02.9	000 - 350
GGB1DV3105	PC	195.7	-06.9	00	000	195.7	-06.9	04.3	350 - 550
GGB1DV3106	PC	206.6	-05.2	00	000	206.6	-05.2	07.0	400 - 550
GGB1DV3107	PC	197.1	04.9	00	000	197.1	04.9	04.8	000 - 700
GGB1DV3201	PC	200.6	03.3	00	000	200.6	03.3	05.2	000 - 620
GGB1DV3202	PC	197.9	-05.4	00	000	197.9	-05.4	05.5	000 - 680
GGB1DV3203	PC	191.2	-01.3	00	000	191.2	-01.3	03.7	350 - 600
GGB1DV3204	PC	197.5	-01.7	00	000	197.5	-01.7	03.6	300 - 600
GGB1DV3205	PC	210.2	-04.3	00	000	210.2	-04.3	09.0	000 - 600
GGB1DV3206	PC	208.2	-03.9	00	000-	208.2	-03.9	08.0	000 - 600
GGB1DV3209	PC	184.7	-10.4	00	000	184.7	-10.4	09.6	000 - 680
GGB1DV3301	PC	207.5	-19.4	41	327	202.3	03.1	05.9	100 - 600
GGB1DV3302	PC	203.8	-18.6	41	327	199.8	05.7	09.2	000 - 600
GGB1DV3303	PC	208.9	-23.5	41	327	201.1	-01.0	08.4	250 - 580
GGB1DV3304	PC	212.9	-19.3	41	327	206.5	00.1	09.1	000 - 580
GGB1DV3305	PC	212.3	-11.1	41	327	211.0	07.1	12.3	000 - 580
GGB1DV3401	PC	208.1	-00.1	32	324	211.6	13.3	12.7	000 - 580
GGB1DV3402	PC	208.4	-08.7	32	324	207.6	05.7	10.4	000 - 580
GGB1DV3403	PC	206.6	-13.3	32	324	203.9	02.4	11.4	000 - 600
GGB1DV3404	PC	205.7	-16.5	32	324	201.6	00.0	08.8	250 - 600
GGB1DV3405	PC	214.1	-15.7	32	324	209.0	-03.2	10.6	000 - 600
GGB1DV3406	PC	207.5	-12.0	32	324	205.2	03.1	07.5	000 - 660
GGB1DV3407	PC	219.4	-25.3	32	324	208.4	-14.0	03.1	150 - 660
GGB1DV3408	PC	207.3	-13.8	32	324	204.2	01.7	05.3	000 - 700
GGB1DV3409	PC	213.7	-09.8	32	324	211.7	02.1	18.8	000 - 660
GGB1DV3501	PC	186.7	-01.4	04	130	186.8	-03.6	20.5	000 - 400
GGB1DV3502	PC	181.7	-08.4	04	130	182.3	-10.9	09.3	000 - 640
GGB1DV3503	PC	190.9	-03.6	04	130	191.2	-05.5	10.5	300 - 550
GGB1DV3504	PC	187.0	03.8	04	130	186.8	01.7	06.2	000 - 700
GGB1DV3505	PC	195.4	05.9	04	130	195.1	04.3	12.1	000 - 550
GGB1DV3506	PC	197.3	-05.5	04	130	197.7	-07.1	09.9	000 - 620
GGB1DV3507	PC	181.3	05.6	04	130	181.0	03.1	13.8	250 - 580
GGB1DV3508	PC	194.8	15.2	04	130	193.9	13.4	10.9	350 - 700
GGB1DV3509	PC	185.3	-01.6	04	130	185.5	-03.9	06.8	350 - 580
GGB1DV3510	PC	188.2	-10.2	04	130	188.9	-12.3	12.3	250 - 680
GGB1DV3511	PC	184.6	-04.6	04	130	184.9	-06.9	12.2	300 - 580
GGB1DV3512	PC	182.5	06.9	04	130	182.2	04.4	28.8	000 - 500
GGB1DV3513	PC	184.8	15.2	04	130	184.0	12.9	10.3	400 - 700
GGB1DV3601	PC	178.4	-15.0	04	130	179.3	-17.6	15.2	300 - 500
GGB1DV3602	PC	188.5	-09.3	04	130	189.1	-11.3	09.8	350 - 660
GGB1DV3603	PC	201.5	10.4	04	130	200.9	09.1	11.9	300 - 640
GGB1DV3604	PC	189.1	-02.7	04	130	189.3	-04.7	09.7	250 - 600
GGB1DV3605	PC	185.4	-11.8	04	130	186.1	-14.0	07.8	300 - 660
GGB1DV3606	PC	199.8	00.7	04	130	199.8	-00.7	05.1	400 - 700
GGB1DV3701	PC	199.9	21.3	40	140	193.7	-01.3	16.3	350 - 550
GGB1DV3702	PC	184.3	14.1	40	140	184.5	-15.1	10.4	000 - 700
GGB1DV3703	PC	190.7	17.1	40	140	188.6	-09.4	20.3	250 - 550
GGB1DV3704	PC	178.7	22.0	40	140	176.1	-10.3	10.8	000 - 700
GGB1DV3705	PC	199.8	23.1	40	140	192.6	00.2	18.5	000 - 550
GGB1DV3706	PC	191.8	24.6	40	140	185.7	-02.4	17.9	150 - 550
GGB1DV3707	PC	188.7	18.9	40	140	186.0	-08.8	15.7	000 - 500
GGB1DV3708	PC	184.5	-08.2	40	140	197.1	-34.3	16.9	000 - 500
GGB1DV3709	PC	185.7	13.3	40	140	186.2	-15.1	13.2	250 - 550
GGB1DV3710	PC	184.9	16.2	40	140	184.1	-12.9	12.6	350 - 550
GGB1DV3711	PC	202.2	10.1	40	140	201.9	-09.3	20.9	000 - 500

GGB1DV3712	PC	171.3	13.1	40	140	172.9	-21.2	11.6	350 - 700
GGB1DV3713	PC	198.6	33.9	40	140	185.8	08.6	22.6	000 - 550
GGB1DV3801	PC	194.0	13.8	40	140	193.0	-10.6	10.0	350 - 550
GGB1DV3802	PC	205.3	19.6	40	140	198.8	00.2	17.8	350 - 550
GGB1DV3803	PC	182.2	26.6	40	140	177.1	-04.8	09.4	350 - 580
GGB1DV3804	PC	186.6	08.2	40	140	189.6	-19.1	09.4	350 - 550
GGB1DV3805	PC	190.2	02.6	40	140	195.9	-22.1	10.4	300 - 500
GGB1DV3806	PC	181.4	-01.9	40	140	190.0	-30.5	10.2	400 - 600
GGB1DV3807	PC	189.6	-18.4	40	140	209.6	-39.6	12.0	300 - 700
GGB1DV3808	PC	183.2	20.7	40	140	180.5	-09.7	09.9	300 - 500
GGB1DV3901	PC	190.0	-10.0	02	275	189.6	-10.2	11.2	350 - 620
GGB1DV3902	PC	195.1	-08.0	02	275	194.8	-08.3	10.1	400 - 620
GGB1DV3903	PC	197.2	-00.8	02	275	197.2	-01.3	06.3	350 - 640
GGB1DV3904	PC	198.5	01.2	02	275	198.5	00.8	09.7	350 - 700
GGB1DV3905	PC	190.1	-14.5	02	275	189.6	-14.7	18.8	350 - 550
GGB1DV3906	PC	187.9	-10.7	02	275	187.5	-10.8	13.2	300 - 600
GGB1DV3907	PC	184.8	-01.7	02	275	184.7	-01.7	12.8	300 - 580
GGB1DV3908	PC	185.8	-07.2	02	275	185.5	-07.2	13.0	350 - 550
GGB1DV3909	PC	198.2	-13.1	02	275	197.7	-13.5	19.2	300 - 580
GGB1DV3910	PC	191.9	-12.7	02	275	191.5	-13.0	21.2	300 - 550
GGB1DV3911	PC	189.9	03.6	02	275	190.1	03.4	11.6	250 - 600
GGB1DV3912	PC	186.8	-25.2	02	275	185.9	-25.2	18.5	300 - 550
GGB1DV3913	PC	192.9	-17.7	02	275	192.2	-18.0	07.5	350 - 580
GGB1DV3914	PC	188.1	02.3	02	275	188.2	02.2	14.4	250 - 700
GGB1DV3915	PC	195.5	06.4	02	275	195.7	06.0	18.4	000 - 550
GGB1DV3916	PC	190.0	05.7	02	275	190.2	05.6	11.3	000 - 700
GGB1DV3918	PC	192.3	-08.3	02	275	192.1	-08.5	22.8	350 - 680
GGB1DV3919	PC	175.4	-02.1	02	275	175.3	-01.8	09.8	300 - 550
GGB1DV3920	PC	188.7	-03.3	02	275	188.5	-03.5	13.5	250 - 700
GGB1DV3921	PC	186.0	05.2	02	275	186.2	05.1	08.4	200 - 550
GGB1DV4001	PC	186.0	04.2	06	130	185.8	00.8	13.0	250 - 550
GGB1DV4002	PC	184.2	-05.5	06	130	184.9	-09.0	17.4	250 - 500
GGB1DV4003	PC	192.0	-03.3	06	130	192.4	-06.1	06.4	000 - 640
GGB1DV4004	PC	197.0	04.9	06	130	196.6	02.6	05.1	250 - 550
GGB1DV4005	PC	194.4	-19.1	06	130	196.4	-21.6	06.0	000 - 700
GGB1DV4006	PC	196.3	12.9	06	130	195.2	10.5	10.7	000 - 700
GGB1DV4007	PC	184.9	22.4	06	130	183.0	18.9	37.4	000 - 450
GGB1DV4101	PC	190.2	-05.6	06	130	190.8	-08.6	18.3	000 - 500
GGB1DV4102	PC	181.9	-09.6	06	130	182.9	-13.3	19.2	000 - 500
GGB1DV4103	PC	179.4	-15.6	06	130	180.9	-19.5	14.3	250 - 500
GGB1DV4104	PC	188.4	-13.4	06	130	189.8	-16.5	08.9	350 - 580
GGB1DV4105	PC	187.2	-03.8	06	130	187.7	-07.1	02.8	350 - 580
GGB1DV4106	PC	197.2	-20.9	06	130	199.5	-23.2	15.6	000 - 580
GGB1DV4107	PC	194.2	-14.6	06	130	195.7	-17.1	25.1	300 - 580
GGB1DV4108	PC	202.4	-08.2	06	130	203.3	-10.0	26.7	200 - 580
GGB1DV4109	PC	189.8	-01.1	06	130	190.0	-04.1	19.7	250 - 400
GGB1DV4110	PC	166.4	-15.4	06	130	167.6	-20.2	19.5	250 - 450
GGB1DV4111	PC	176.6	-16.8	06	130	178.1	-20.9	15.2	200 - 450
GGB1DV4112	PC	198.1	-07.9	06	130	199.0	-10.1	22.7	250 - 550
GGB1DV4201	PC	175.9	-10.3	06	130	176.9	-14.4	13.1	200 - 500
GGB1DV4202	PC	188.1	-10.2	06	130	189.1	-13.3	05.2	200 - 550
GGB1DV4203	PC	176.6	-27.6	06	130	179.1	-31.6	23.4	200 - 500
GGB1DV4204	PC	186.4	-17.4	06	130	188.1	-20.6	05.1	200 - 600
GGB1DV4206	PC	229.2	-17.0	06	130	231.0	-15.9	16.0	400 - 550
GGB1DV4207	PC	189.9	-08.4	06	130	190.8	-11.4	10.4	200 - 450
GGB1DV4208	PC	192.6	-09.5	06	130	193.7	-12.2	08.9	200 - 500
GGB1DV4209	PC	195.9	-07.9	06	130	196.7	-10.3	06.2	200 - 500
GGB1DV4301	PC	210.9	05.7	39	172	215.3	-24.2	21.2	000 - 620
GGB1DV4302	PC	205.6	07.1	39	172	209.3	-25.1	13.4	000 - 620
GGB1DV4303	PC	202.2	02.0	39	172	208.0	-31.1	11.7	000 - 620
GGB1DV4304	PC	201.2	02.8	39	172	206.5	-30.7	08.2	000 - 620
GGB1DV4305	PC	213.1	-03.7	39	172	222.4	-31.6	09.2	000 - 550

GGB1DV4306	PC	201.8	09.5	39	172	204.6	-24.2	14.3	000 - 620
GGB1DV4307	PC	207.6	-08.3	39	172	219.1	-38.3	16.4	000 - 550
GGB1DV4308	PC	213.0	06.0	39	172	217.1	-23.1	15.4	000 - 600
GGB1DV4309	PC	227.6	-18.3	39	172	246.4	-35.6	15.3	250 - 600
GGB1DV4311	PC	215.4	02.4	39	172	221.2	-25.1	12.9	000 - 550
GGB1DV4312	PC	220.1	-05.1	39	172	230.1	-29.2	03.7	300 - 550
GGB1DV4313	PC	217.0	-03.3	39	172	226.0	-29.3	09.4	250 - 550
GGB1DV4314	PC	213.6	00.8	39	172	220.4	-27.3	11.1	000 - 500
GGB1DV4315	PC	233.4	16.5	39	172	229.6	-03.9	05.3	350 - 580
GGB1DV4316	PC	237.3	12.6	39	172	234.9	-05.0	07.0	450 - 600
GGB1DV4317	PC	209.0	06.3	39	172	213.1	-24.4	14.5	000 - 580
GGB1DV4318	PC	206.7	10.1	39	172	209.2	-21.9	09.1	400 - 580
GGB1DV4319	PC	219.0	03.8	39	172	224.0	-22.1	06.5	400 - 600
GGB1DV4401	PC	209.7	12.2	39	172	211.2	-18.8	09.9	300 - 500
GGB1DV4402	PC	210.4	00.1	39	172	217.5	-29.4	08.7	300 - 620
GGB1DV4403	PC	205.4	04.8	39	172	210.1	-27.3	10.4	300 - 620
GGB1DV4404	PC	200.5	05.6	39	172	204.6	-28.4	10.0	300 - 680
GGB1DV4405	PC	205.1	-01.2	39	172	212.6	-32.9	11.4	000 - 580
GGB1DV4406	PC	208.7	10.7	39	172	210.9	-20.6	08.2	300 - 680
GGB1DV4501	PC	192.9	-04.2	38	192	193.3	-42.2	08.5	350 - 680
GGB1DV4502	PC	206.1	-13.8	38	192	213.7	-50.2	04.9	300 - 620
GGB1DV4503	PC	197.6	-04.8	38	192	199.6	-42.6	04.3	000 - 620
GGB1DV4504	PC	204.3	-08.9	38	192	209.5	-45.7	06.2	000 - 620
GGB1DV4505	PC	206.8	-05.1	38	192	211.8	-41.5	09.9	000 - 640
GGB1DV4601	PC	199.7	-03.7	38	192	202.3	-41.3	08.9	150 - 680
GGB1DV4602	PC	194.7	06.0	38	192	195.2	-32.0	09.0	200 - 680
GGB1DV4603	PC	198.8	-03.0	38	192	201.0	-40.6	09.2	000 - 680
GGB1DV4604	PC	201.4	-01.2	38	192	204.1	-38.6	12.1	150 - 660
GGB1DV4605	PC	196.3	-04.2	38	192	197.8	-42.0	07.7	200 - 660
GGB1DV4606	PC	193.9	-09.0	38	192	194.7	-47.0	11.1	000 - 580
GGB1DV4607	PC	200.3	-07.1	38	192	203.5	-44.6	08.1	000 - 580
GGB1DV4608	PC	193.0	01.5	38	192	193.3	-36.5	09.8	150 - 580
GGB1DV4609	PC	199.2	-12.9	38	192	203.1	-50.5	06.1	150 - 580
GGB1DV4701	PC	199.9	-17.7	38	170	215.7	-48.4	05.2	000 - 680
GGB1DV4702	PC	207.4	-16.0	38	170	223.5	-43.4	01.6	000 - 250
GGB1DV4703	PC	200.0	-11.9	38	170	212.1	-43.1	01.0	000 - 250
GGB1DV4704	PC	197.2	-13.3	38	170	209.5	-45.6	05.1	000 - 680
GGB1DV4705	PC	180.8	-28.0	38	170	192.8	-64.7	09.9	000 - 680
GGB1DV4706	PC	204.7	-15.2	38	170	219.8	-44.0	08.3	150 - 580
GGB1DV4707	PC	200.5	-16.6	38	170	215.6	-47.2	06.3	150 - 580
GGB1DV4708	PC	201.8	-14.8	38	170	216.1	-45.1	05.2	000 - 680
GGB1DV4709	PC	200.8	-06.2	38	170	210.1	-37.7	13.7	000 - 680
GGB1DV4710	PC	204.7	-20.8	38	170	223.9	-48.9	06.8	250 - 550
GGB1DV4711	PC	205.5	-00.1	38	170	212.2	-30.2	07.1	200 - 680
GGB1DV4712	PC	205.9	-11.3	38	170	218.7	-40.1	04.3	200 - 620
GGB1DV4713	PC	199.6	-11.0	38	170	211.1	-42.5	06.9	250 - 660
GGB1DV4714	PC	191.3	-12.3	38	170	201.2	-46.8	07.3	250 - 500
GGB1DV4716	PC	200.4	-02.5	38	170	207.8	-34.4	01.5	000 - 400
GGB1DV4801	PC	201.0	-23.0	90	004	218.6	61.7	22.2	300 - 680
GGB1DV4802	PC	181.2	-26.1	90	004	178.4	63.8	11.6	450 - 680
GGB1DV4803	PC	203.1	-33.0	90	004	210.8	52.4	11.9	350 - 640
GGB1DV4804	PC	210.5	-37.2	90	004	214.4	45.5	08.3	350 - 640
GGB1DV4805	PC	196.8	-35.5	90	004	201.3	52.5	13.2	350 - 640
GGB1DV4806	PC	198.0	-23.9	90	004	212.6	62.5	09.4	400 - 640
GGB1DV4807	PC	197.8	-44.2	90	004	197.7	44.1	11.8	000 - 680
GGB1DV4808	PC	204.1	-23.9	90	004	221.8	59.1	07.4	000 - 700
GGB1DV4809	PC	186.5	-67.9	90	004	185.0	22.1	10.3	000 - 680
GGB1DV4810	PC	226.5	-75.4	90	004	194.0	10.7	05.4	350 - 660
GGB1DV4811	PC	229.5	-71.0	90	004	197.8	13.2	06.1	350 - 640
GGB1DV4812	PC	211.0	-63.4	90	004	196.8	23.5	12.8	400 - 700
GGB1DV4813	PC	189.0	-54.1	90	004	187.6	35.8	13.7	350 - 640
GGB1DV4814	PC	188.4	-77.0	90	004	185.0	13.0	17.1	200 - 640

GGB1DV4815	PC	224.0	-79.8	90	004	190.6	07.8	26.8	350 - 640
GGB1DV4816	PC	225.7	-74.5	90	004	194.4	11.5	13.1	250 - 660
GGB1DV4817	PC	199.1	-38.2	90	004	202.3	49.4	08.2	450 - 660
GGB1DV4818	PC	196.9	-47.9	90	004	195.4	40.8	05.5	350 - 660
GGB1DV4819	PC	195.2	-47.7	90	004	194.0	41.3	07.3	350 - 660
GGB1DV4820	PC	207.7	-48.8	90	004	203.4	37.1	05.1	350 - 660
GGB1DV4821	PC	200.2	-56.1	90	004	194.6	32.4	07.0	350 - 680
GGB1DV4822	PC	190.6	-69.6	90	004	186.4	20.2	05.9	450 - 660
GGB1DV4823	PC	195.1	-62.4	90	004	189.7	27.0	06.7	450 - 660
GGB1DV4824	PC	199.3	-60.9	90	004	192.3	28.0	09.1	000 - 660
GGB1DV4901	PC	207.3	-44.0	82	006	204.5	34.6	08.8	300 - 620
GGB1DV4902	PC	208.5	-33.6	82	006	211.9	43.3	10.7	350 - 660
GGB1DV4903	PC	212.2	-36.8	82	006	213.0	38.9	08.0	300 - 660
GGB1DV4904	PC	221.9	-42.3	82	006	216.0	30.0	08.4	300 - 660
GGB1DV4905	PC	205.0	-39.9	82	006	204.7	38.9	07.8	400 - 660
GGB1DV4906	PC	211.6	-48.8	82	006	205.0	28.9	05.4	400 - 660
GGB1DV4907	PC	204.3	-39.0	82	006	204.6	40.1	09.4	300 - 680
GGB1DV4908	PC	203.3	-28.4	82	006	210.0	50.0	18.3	350 - 580
GGB1DV4909	PC	217.7	-36.3	82	006	217.8	36.6	09.1	300 - 500
GGB1DV4910	PC	203.6	-51.4	82	006	198.4	28.7	16.3	450 - 640
GGB1DV4911	PC	232.2	-45.0	82	006	219.6	22.7	08.4	450 - 640
GGB1DV4912	PC	200.3	-49.6	82	006	196.7	31.0	16.0	450 - 600
GGB1DV4913	PC	210.0	-36.5	82	006	211.3	40.1	22.9	450 - 600
GGB1DV4914	PC	200.6	-27.1	82	006	207.4	52.2	11.5	150 - 600
GGB1DV4915	PC	207.9	-33.6	82	006	211.4	43.5	06.9	300 - 580
GGB1DV4916	PC	205.5	-31.2	82	006	210.5	46.6	10.2	300 - 600
GGB1DV4917	PC	200.5	-40.2	82	006	200.5	40.0	11.7	400 - 640
GGB1DV4918	PC	198.3	-29.1	82	006	203.2	51.0	11.5	000 - 550
GGB1DV4919	PC	219.5	-34.9	82	006	220.4	36.7	14.6	000 - 450
GGB1DV5001	PC	213.2	-06.4	42	184	224.4	-41.5	07.7	300 - 640
GGB1DV5002	PC	213.5	-10.5	42	184	227.3	-45.1	09.3	300 - 640
GGB1DV5003	PC	213.1	-07.3	42	184	224.8	-42.4	08.4	000 - 640
GGB1DV5004	PC	216.6	-04.7	42	184	227.3	-38.5	06.5	250 - 600
GGB1DV5005	PC	225.1	-08.1	42	184	238.7	-37.1	09.7	000 - 600
GGB1DV5006	PC	213.3	-07.2	42	184	225.0	-42.3	07.4	000 - 640
GGB1DV5007	PC	226.6	-09.0	42	184	240.9	-37.1	09.8	250 - 580
GGB1DV5008	PC	222.4	05.2	42	184	228.0	-27.0	13.3	500 - 580
GGB1DV5009	PC	211.2	-02.3	42	184	219.8	-38.6	06.9	250 - 600
GGB1DV5010	PC	192.6	-12.4	42	184	198.2	-53.7	07.9	250 - 550
GGB1DV5011	PC	226.7	-02.4	42	184	236.6	-31.5	07.8	300 - 550
GGB1DV5012	PC	218.4	-16.4	42	184	237.7	-47.7	14.2	350 - 550
GGB1DV5013	PC	222.7	00.7	42	184	230.8	-30.9	08.9	300 - 550
GGB1DV5101	PC	246.9	43.4	96	184	228.9	-23.6	09.6	000 - 640
GGB1DV5102	PC	232.1	49.4	96	184	218.3	-30.8	06.5	400 - 640
GGB1DV5103	PC	227.7	47.8	96	184	218.1	-34.1	06.0	300 - 640
GGB1DV5104	PC	228.0	48.7	96	184	217.4	-33.4	06.8	400 - 640
GGB1DV5105	PC	228.7	48.3	96	184	218.0	-33.2	07.1	150 - 600
GGB1DV5106	PC	234.3	41.1	96	184	227.8	-33.2	08.4	150 - 600
GGB1DV5107	PC	231.2	40.4	96	184	227.4	-35.6	10.6	000 - 640
GGB1DV5108	PC	226.1	46.5	96	184	218.6	-35.7	09.9	000 - 640
GGB1DV5109	PC	234.1	43.6	96	184	225.1	-32.3	07.4	000 - 640
GGB1DV5110	PC	233.7	46.3	96	184	222.1	-31.3	08.4	000 - 640
GGB1DV5111	PC	221.9	39.6	96	184	223.6	-42.2	16.7	250 - 550
GGB1DV5112	PC	214.4	36.2	96	184	222.4	-48.9	22.4	000 - 550
GGB1DV5113	PC	232.4	54.8	96	184	213.2	-27.8	24.3	350 - 660
GGB1DV5114	PC	229.5	41.2	96	184	225.8	-36.4	10.9	250 - 700
GGB1DV5115	PC	242.3	51.8	96	184	219.1	-23.9	10.7	350 - 660
GGB1DV5116	PC	232.6	46.4	96	184	221.5	-32.0	07.7	350 - 660
GGB1DV5117	PC	226.9	44.9	96	184	220.6	-36.1	13.4	150 - 660
GGB1DV5118	PC	224.4	39.8	96	184	224.9	-40.5	10.2	300 - 640
GGB1DV5201	PC	263.2	-30.6	52	022	250.9	00.8	08.9	250 - 660
GGB1DV5202	PC	259.7	-30.0	52	022	249.1	03.2	09.5	300 - 600

GGB1DV5203	PC	255.2	-28.5	52	022	247.2	07.0	05.1	150 - 660
GGB1DV5204	PC	250.4	-28.0	52	022	244.1	09.9	07.1	150 - 600
GGB1DV5205	PC	244.5	-16.4	52	022	246.6	22.5	09.6	300 - 620
GGB1DV5207	PC	246.2	-17.4	52	022	247.4	20.8	05.8	150 - 660
GGB1DV5208	PC	235.9	-20.0	52	022	237.0	23.8	11.8	400 - 660
GGB1DV5209	PC	238.6	-09.3	52	022	245.7	31.7	07.6	400 - 640
GGB1DV5210	PC	227.6	06.4	52	022	244.8	50.9	06.9	300 - 640
GGB1DV5211	PC	250.0	-15.0	52	022	252.0	20.5	05.1	000 - 660
GGB1DV5212	PC	245.2	-15.2	52	022	247.9	23.1	18.6	000 - 600
GGB1DV5213	PC	241.1	-22.4	52	022	240.1	19.3	14.9	350 - 600
GGB1DV5214	PC	241.9	-00.6	52	022	255.1	36.8	11.6	400 - 620
GGB1DV5215	PC	247.1	-16.9	52	022	248.4	20.7	25.0	000 - 580
GGB1DV5216	PC	234.8	-19.1	52	022	236.4	25.1	10.7	350 - 620
GGB1DV5217	PC	240.2	-08.2	52	022	247.9	31.7	06.2	350 - 620
GGB1DV1402	XX	187.2	-40.3	15	165	194.2	-53.9	09.3	250 - 700
GGB1DV2603	XX	035.4	-05.8	54	330	049.9	-23.2	05.3	250 - 640
GGB1DV2604	XX	065.6	-12.3	54	330	073.2	-02.8	03.9	250 - 640
GGB1DV2608	XX	116.9	-17.6	54	330	114.0	27.9	03.6	000 - 700
GGB1DV2609	XX	295.4	-03.5	54	330	277.4	-44.5	05.2	250 - 700
GGB1DV2610	XX	359.8	09.0	54	330	007.9	-37.0	05.7	000 - 700
GGB1DV2611	XX	337.3	-07.4	54	330	345.0	-60.7	04.3	300 - 700
GGB1DV2613	XX	355.1	-01.7	54	330	009.9	-48.5	04.3	300 - 700
GGB1DV2801	XX	133.5	19.1	14	180	136.0	09.3	03.1	300 - 700
GGB1DV4205	XX	054.9	-22.5	06	130	052.4	-23.9	19.8	000 - 640
GGB1DV4310	XX	283.0	-09.2	39	172	284.2	05.7	12.1	000 - 600
GGB1DV5206	XX	035.6	-25.6	52	022	068.9	-73.1	07.3	350 - 620
GGB1DV0104	HT	196.9	43.3	15	165	191.4	30.1	12.4	450 - 720
GGB1DV0202	HT	203.7	37.5	15	177	199.9	23.9	05.7	625 - 720
GGB1DV0203	HT	186.1	09.1	15	177	186.0	-05.8	06.2	625 - 720
GGB1DV0205	HT	160.6	26.4	15	177	162.0	11.9	19.4	550 - 720
GGB1DV0301	HT	122.3	-24.0	17	136	119.5	-40.4	21.1	600 - 700
GGB1DV0302	HT	228.9	20.5	17	136	222.5	20.4	20.4	550 - 700
GGB1DV0303	HT	171.5	-17.3	17	136	176.1	-30.7	13.5	600 - 700
GGB1DV0402	HT	017.1	-03.3	19	160	018.0	11.8	08.9	600 - 675
GGB1DV0403	HT	315.3	-06.9	19	160	315.1	10.4	08.2	625 - 700
GGB1DV0404	HT	004.5	-43.0	19	160	359.6	-25.3	17.1	600 - 700
GGB1DV0405	HT	249.5	17.0	19	160	243.9	15.9	36.7	550 - 700
GGB1DV1501	HT	272.7	-86.4	15	165	332.9	-73.6	08.0	650 - 700
GGB1DV1503	HT	225.3	31.9	15	165	218.6	23.7	04.8	550 - 700
GGB1DV1601	HT	196.8	29.3	15	165	193.6	16.3	20.2	600 - 700
GGB1DV1603	HT	349.1	-09.8	15	165	349.1	05.1	28.1	400 - 675
GGB1DV1604	HT	124.8	-19.3	15	165	120.1	-30.4	43.3	450 - 700
GGB1DV1605	HT	346.7	55.2	15	165	347.9	70.2	19.8	450 - 700
GGB1DV1702	HT	236.6	-66.6	15	165	272.1	-66.7	17.6	550 - 700
GGB1DV1704	HT	244.9	41.6	15	165	232.9	37.4	08.8	625 - 700
GGB1DV1705	HT	294.0	04.0	15	165	292.2	13.3	23.7	600 - 700
GGB1DV1801	HT	118.8	-61.3	15	165	090.2	-68.9	13.9	625 - 700
GGB1DV1802	HT	127.0	22.0	15	165	129.6	10.0	41.3	550 - 700
GGB1DV1902	HT	241.5	06.5	15	165	240.3	02.8	08.3	600 - 700
GGB1DV1903	HT	144.3	02.3	15	165	143.9	-11.7	10.2	450 - 700
GGB1DV1904	HT	147.6	03.4	15	165	147.3	-10.9	08.6	550 - 700
GGB1DV1905	HT	209.2	35.5	15	165	203.5	24.2	28.5	500 - 700
GGB1DV3501	HT	177.8	-32.2	04	130	179.8	-34.8	16.7	450 - 640
GGB1DV3503	HT	203.8	28.8	04	130	201.7	27.6	17.6	580 - 660
GGB1DV3505	HT	155.8	17.8	04	130	155.3	14.2	17.3	580 - 700
GGB1DV3506	HT	148.9	00.3	04	130	148.9	-03.5	23.0	640 - 700
GGB1DV3507	HT	252.3	31.1	04	130	250.2	33.2	17.5	600 - 700
GGB1DV3509	HT	233.6	24.8	04	130	231.8	25.6	11.5	600 - 680
GGB1DV3511	HT	220.5	-02.9	04	130	220.7	-02.9	12.4	600 - 700
GGB1DV3512	HT	166.7	08.7	04	130	166.4	05.5	08.7	550 - 700

GGB1DV3601	HT	202.1	19.1	04	130	200.8	17.9	06.9	550 - 680
GGB1DV3604	HT	183.8	42.4	04	130	181.0	40.0	30.3	620 - 700
GGB1DV3701	HT	141.0	-22.7	40	140	142.0	-62.6	12.5	580 - 680
GGB1DV3703	HT	126.0	-05.0	40	140	120.7	-43.5	10.8	580 - 680
GGB1DV3705	HT	145.4	05.4	40	140	146.5	-34.4	12.3	580 - 680
GGB1DV3706	HT	160.6	-03.2	40	140	167.3	-40.1	14.7	580 - 700
GGB1DV3707	HT	156.5	10.6	40	140	158.3	-27.7	19.7	550 - 700
GGB1DV3708	HT	167.5	-17.0	40	140	183.7	-50.3	29.7	550 - 700
GGB1DV3709	HT	110.3	-12.6	40	140	096.5	-45.4	11.5	580 - 700
GGB1DV3710	HT	149.4	-01.0	40	140	152.3	-40.3	14.7	580 - 700
GGB1DV3711	HT	144.9	-43.7	40	140	169.9	-82.9	15.2	550 - 700
GGB1DV3713	HT	147.6	-42.8	40	140	178.7	-81.1	21.1	580 - 700
GGB1DV3801	HT	127.6	-13.0	40	140	120.2	-51.7	09.0	580 - 680
GGB1DV3802	HT	137.1	-24.0	40	140	133.9	-63.9	07.1	580 - 700
GGB1DV3803	HT	178.8	-02.8	40	140	188.0	-32.6	04.0	600 - 700
GGB1DV3804	HT	142.7	08.4	40	140	143.2	-31.6	15.4	580 - 680
GGB1DV3805	HT	145.8	21.3	40	140	145.7	-18.5	19.5	550 - 700
GGB1DV3806	HT	137.0	-37.9	40	140	128.8	-77.7	06.9	620 - 680
GGB1DV3808	HT	162.2	04.8	40	140	166.3	-32.0	07.2	550 - 700
GGB1DV3901	HT	192.3	34.8	02	275	193.6	34.5	14.3	640 - 700
GGB1DV3902	HT	190.5	32.2	02	275	191.7	32.0	08.6	640 - 700
GGB1DV3905	HT	214.0	36.5	02	275	215.2	35.5	23.8	580 - 700
GGB1DV3906	HT	220.8	22.4	02	275	221.4	21.2	15.4	620 - 700
GGB1DV3907	HT	252.5	38.1	02	275	253.1	36.3	12.4	600 - 700
GGB1DV3908	HT	222.6	12.4	02	275	222.9	11.1	14.3	580 - 700
GGB1DV3909	HT	238.4	29.5	02	275	239.0	27.9	27.0	600 - 700
GGB1DV3910	HT	212.9	59.0	02	275	215.7	58.0	11.6	580 - 700
GGB1DV3911	HT	298.1	15.4	02	275	297.9	13.6	25.5	620 - 700
GGB1DV3913	HT	198.1	08.7	02	275	198.4	08.2	25.0	600 - 700
GGB1DV3919	HT	261.8	16.5	02	275	261.9	14.5	22.0	600 - 700
GGB1DV3921	HT	245.2	24.8	02	275	245.6	23.1	21.4	580 - 700
GGB1DV4001	HT	220.1	-11.5	06	130	221.3	-11.4	09.8	580 - 640
GGB1DV4002	HT	217.7	-29.0	06	130	221.1	-29.1	09.6	580 - 620
GGB1DV4004	HT	211.6	-13.9	06	130	213.1	-14.7	05.0	580 - 680
GGB1DV4007	HT	224.3	-47.3	06	130	230.7	-46.6	27.6	500 - 640
GGB1DV4101	HT	206.2	-55.5	06	130	214.9	-56.4	11.3	550 - 700
GGB1DV4102	HT	196.5	-59.9	06	130	206.7	-61.8	11.2	550 - 700
GGB1DV4103	HT	191.6	-34.2	06	130	195.5	-36.9	10.2	550 - 700
GGB1DV4104	HT	211.0	-51.2	06	130	218.5	-51.8	07.8	600 - 700
GGB1DV4105	HT	165.5	-30.1	06	130	167.8	-34.9	14.8	600 - 700
GGB1DV4107	HT	250.8	-52.5	06	130	256.9	-49.1	14.4	600 - 660
GGB1DV4108	HT	199.7	-56.8	06	130	208.8	-58.5	25.6	600 - 680
GGB1DV4109	HT	251.2	-38.8	06	130	255.0	-35.6	24.6	450 - 680
GGB1DV4201	HT	176.9	-45.2	06	130	181.8	-49.1	08.0	550 - 680
GGB1DV4202	HT	220.2	-35.1	06	130	224.4	-34.9	05.2	580 - 680
GGB1DV4203	HT	211.7	-46.1	06	130	218.0	-46.7	09.2	550 - 660
GGB1DV4205	HT	142.5	14.5	06	130	142.3	08.6	02.9	660 - 700
GGB1DV4207	HT	195.5	-40.3	06	130	200.4	-42.6	02.6	500 - 580
GGB1DV4209	HT	159.6	-13.1	06	130	160.4	-18.3	37.2	550 - 700
GGB1DV4402	HT	276.8	-11.1	39	172	280.5	00.5	20.0	600 - 700
GGB1DV4403	HT	264.0	-17.6	39	172	274.7	-12.4	17.2	660 - 700
GGB1DV4909	HT	203.5	-83.0	82	006	188.1	-01.3	08.6	550 - 600
GGB1DV5202	HT	298.9	-24.9	52	022	275.6	-20.2	04.7	640 - 680

Table A-2 Palaeomagnetic results from Namurian and Westphalian A sediments from South Wales.
Dec/CDec = in situ/tilt-corrected declination.
Inc/CInc = in situ/tilt-corrected inclination.
Tilt/Dir = bedding correction where Dir = direction of the tilt.
a95 = there is a probability of 95% that the true mean is within α° from the calculated mean (using Fisher statistics).
The unit of the temperature is °C (except 0 denotes before the treatment).
Specimens measured with a SQUID are given symbol +.
Specimens excluded in calculating the site means are given symbol *.

SPECIMEN	Dec	Inc	Tilt	Dir	CDec	CInc	a95	Temp. used
FGB1SW0201	278.16	75.94	08	173	245.91	75.80	05.37	0 - 350 *
FGB1SW0202	195.25	05.51	08	173	195.15	-01.90	12.74	0 - 450
FGB1SW0203	335.59	51.30	08	173	331.79	58.86	12.64	0 - 350 *
FGB1SW0204	281.91	-01.69	08	173	281.96	00.91	19.24	100 - 250 *
FGB1SW0205	257.58	28.65	08	173	253.33	27.60	14.70	0 - 400 *
FGB1SW0206	211.52	15.24	08	173	210.46	08.93	11.88	200 - 400
FGB1SW0207	145.91	27.44	08	173	147.48	20.27	03.41	0 - 500 *
FGB1SW0208	228.89	25.61	08	173	226.08	20.96	05.83	0 - 550 *
FGB1SW0209	224.49	-39.72	08	173	230.37	-44.38	07.45	0 - 450 *
FGB1SW0210	228.30	72.81	08	173	212.05	67.31	19.04	0 - 400 *
FGB1SW0211	141.40	-28.61	08	173	138.68	-35.33	10.67	0 - 350 *
FGB1SW0212	239.08	-27.93	08	173	243.28	-30.91	10.14	0 - 300 *
FGB1SW0213	293.43	35.56	08	173	288.00	39.29	15.33	0 - 500 *
FGB1SW0214	147.87	-43.65	08	173	143.92	-50.78	05.24	0 - 550 *
FGB1SW0215	183.44	72.22	08	173	180.33	64.31	10.20	0 - 450 *
FGB1SW0216	208.16	-03.52	08	173	208.71	-10.04	22.70	200 - 450
FGB1SW0217	021.48	21.11	08	173	023.28	28.08	26.44	0 - 250
FGB1SW0218	318.06	66.40	08	173	303.73	72.39	18.53	0 - 550 *
FGB1SW0219	329.93	47.47	08	173	325.70	54.72	04.00	0 - 550 *
FGB1SW0220	197.50	06.93	08	173	197.31	-00.36	11.45	0 - 400
FGB1SW0221	138.51	-16.84	08	173	136.81	-23.37	13.24	0 - 350 *
FGB1SW0222	215.68	-11.29	08	173	217.07	-17.11	11.21	200 - 400
FGB1SW0301	210.17	-05.50	08	173	210.92	-11.85	08.74	0 - 350
FGB1SW0302	240.19	12.74	08	173	238.74	09.54	09.13	0 - 350 *
FGB1SW0303	225.65	-21.86	08	173	228.57	-26.56	08.22	0 - 350
FGB1SW0304	216.20	-09.32	08	173	217.40	-15.10	15.40	0 - 350
FGB1SW0305	200.38	-10.56	08	173	201.32	-17.64	23.75	100 - 350
FGB1SW0306	217.85	-05.90	08	173	218.72	-11.53	17.52	0 - 350
FGB1SW0307	275.75	53.23	08	173	264.90	54.26	30.95	0 - 350 *
FGB1SW0308	198.20	06.11	08	173	198.05	-01.14	30.97	0 - 350 *
FGB1SW0309	211.34	19.73	08	173	209.89	13.39	14.44	0 - 550
FGB1SW0310	204.53	20.36	08	173	203.28	13.49	33.53	0 - 350 *
FGB1SW0311	164.83	01.53	08	173	164.78	-06.39	14.77	0 - 550
FGB1SW0312	227.16	18.55	08	173	225.30	13.76	17.17	0 - 350
FGB1SW0313	214.55	66.64	08	173	204.95	60.20	20.85	0 - 550 *
FGB1SW0314	046.05	65.32	08	173	062.90	69.19	33.36	0 - 350 *
FGB1SW0315	181.82	-59.15	08	173	184.62	-67.03	06.77	0 - 350 *
FGB1SW0316	216.30	20.65	08	173	214.57	14.74	17.11	100 - 350
FGB1SW0317	205.97	17.36	08	173	204.90	10.60	14.19	100 - 350
FGB1SW0318	061.85	75.31	08	173	093.54	76.08	34.56	0 - 350 *
FGB1SW0319	251.23	36.37	08	173	245.72	34.36	63.93	0 - 350 *
FGB1SW0320	201.32	-24.50	08	173	203.41	-31.48	26.33	0 - 350
FGB1SW0321	175.16	-29.61	08	173	175.37	-37.60	10.62	0 - 350
FGB1SW0322	195.78	53.36	08	173	192.39	45.89	47.85	0 - 350 *
FGB1SW0401	136.09	54.09	07	175	141.27	48.44	04.04	0 - 300 *
FGB1SW0402	211.45	72.04	07	175	201.84	66.06	10.76	0 - 400 *

FGB1SW0403	210.70	33.56	07	175	208.34	27.79	08.72	0 - 300	
FGB1SW0404	053.31	62.98	07	175	066.64	65.96	23.73	0 - 350	*
FGB1SW0405	003.68	66.58	07	175	007.17	73.47	08.81	0 - 350	*
FGB1SW0406	148.86	48.58	07	175	151.83	42.21	08.94	0 - 350	*
FGB1SW0407	086.16	83.25	07	175	131.40	80.19	18.25	0 - 200	*
FGB1SW0408	094.18	43.17	07	175	100.44	41.67	08.02	0 - 300	*
FGB1SW0409	122.41	28.94	07	175	125.16	24.55	04.39	0 - 500	*
FGB1SW0410	194.55	05.83	07	175	194.45	-00.77	19.70	0 - 300	
FGB1SW0411	177.01	15.45	07	175	176.96	08.45	13.61	100 - 300	
FGB1SW0412	248.11	36.50	07	175	243.42	34.19	23.69	0 - 400	*
FGB1SW0501	161.81	10.08	07	175	162.00	03.26	02.68	0 - 350	
FGB1SW0502	182.18	44.43	07	175	181.46	37.48	10.88	0 - 450	*
FGB1SW0503	174.58	07.92	07	175	174.58	00.92	08.12	0 - 550	
FGB1SW0504	138.30	37.98	07	175	141.15	32.26	02.04	0 - 550	*
FGB1SW0505	106.70	54.19	07	175	114.98	51.13	02.31	0 - 500	*
FGB1SW0506	207.90	44.71	07	175	204.66	38.72	05.72	0 - 500	*
FGB1SW0507	215.15	-02.73	07	175	215.58	-08.07	14.20	0 - 300	
FGB1SW0508	207.12	-00.56	07	175	207.35	-06.48	18.02	0 - 300	
FGB1SW0601	143.98	11.91	07	175	144.54	05.89	09.31	0 - 300	*
FGB1SW0602	185.80	05.01	07	175	185.76	-01.87	15.21	150 - 300	
FGB1SW0603	115.26	15.72	07	175	116.75	12.11	08.27	150 - 300	*
FGB1SW0701	192.04	-08.72	07	175	192.48	-15.41	16.47	0 - 250	
FGB1SW0702	194.75	20.25	07	175	194.04	13.65	32.83	150 - 300	*
FGB1SW0703	215.53	05.21	07	175	215.33	-00.12	17.61	150 - 350	
FGB1SW0704	204.09	-09.68	07	175	204.87	-15.78	09.22	0 - 350	
FGB1SW0705	186.40	08.60	07	175	186.28	01.74	15.13	150 - 300	
FGB1SW0706	186.65	07.06	07	175	186.56	00.20	15.25	0 - 350	
FGB1SW0707	213.43	08.74	07	175	212.98	03.24	14.66	0 - 350	
FGB1SW0708	142.02	23.94	07	175	143.45	18.02	15.38	0 - 400	*
FGB1SW0709	234.55	42.21	07	175	229.56	38.40	36.70	0 - 350	*
FGB1SW0801	176.87	-01.24	07	175	176.89	-08.24	11.53	150 - 400	
FGB1SW0802	180.96	09.59	07	175	180.88	02.63	12.95	200 - 400	
FGB1SW0803	114.98	44.99	07	175	120.50	41.20	39.29	0 - 200	*
FGB1SW0804	293.33	19.75	07	175	290.89	22.94	10.48	0 - 500	*
FGB1SW0805	291.77	-02.56	07	175	291.88	00.60	15.48	0 - 450	*
FGB1SW0806	216.76	-11.81	07	175	217.97	-16.99	20.26	0 - 400	
FGB1SW0807	192.43	02.98	07	175	192.44	-03.70	20.38	150 - 500	
FGB1SW0808	204.98	-12.29	07	175	205.95	-18.33	25.03	150 - 500	
FGB1SW0809	197.14	01.56	07	175	197.22	-04.92	24.33	250 - 400	
FGB1SW0901	146.87	-12.41	07	175	145.94	-18.56	11.10	0 - 450	*
FGB1SW0903	041.56	50.04	07	175	048.51	54.55	07.03	0 - 625	*
FGB1SW0906	191.69	24.17	07	175	190.94	17.45	12.32	150 - 500	
FGB1SW0907	157.92	61.08	07	175	160.90	54.33	17.54	0 - 550	*
FGB1SW1001	201.46	19.17	07	175	200.58	12.88	13.60	150 - 350	
FGB1SW1002	010.84	75.75	07	175	024.88	82.25	10.01	0 - 350	*
FGB1SW1003	204.39	06.02	07	175	204.21	-00.09	21.75	0 - 350	
FGB1SW1004	197.79	01.23	07	175	197.88	-05.22	05.78	0 - 450	
FGB1SW1005	194.23	10.74	07	175	193.93	04.12	05.09	0 - 500	
FGB1SW1006	194.80	13.83	07	175	194.36	07.23	05.26	0 - 500	
FGB1SW1007	203.23	06.81	07	175	203.02	00.63	10.76	0 - 350	
FGB1SW1009	196.85	02.63	07	175	196.88	-03.87	05.53	0 - 500	
FGB1SW1010	207.83	-00.40	07	175	208.05	-06.28	07.10	0 - 500	
FGB1SW1012	194.48	00.47	07	175	194.60	-06.13	06.48	0 - 550	
FGB1SW1101	203.04	09.61	07	175	202.67	03.42	09.12	0 - 250	
FGB1SW1102	171.25	88.77	07	175	164.88	83.19	05.88	0 - 350	*

FGB1SW1104	198.31	-01.66	07	175	198.55	-08.08	12.45	0 - 300
FGB1SW1105	215.96	-08.34	07	175	216.86	-13.59	16.63	0 - 300
FGB1SW113A	312.85	81.93	07	175	254.56	84.50	06.17	0 - 350 *
FGB1SW113B	188.85	07.81	07	175	188.72	01.01	15.55	0 - 250
FGB1SW1201	149.71	80.48	07	175	160.26	73.87	06.42	0 - 450 *
FGB1SW1202	355.30	81.23	07	175	356.48	88.23	15.01	0 - 450 *
FGB1SW1203	187.99	23.76	07	175	187.42	16.93	10.70	0 - 350
FGB1SW1204	186.13	22.51	07	175	185.67	15.64	07.72	0 - 300
FGB1SW1205	190.95	-02.77	07	175	191.16	-09.50	05.02	0 - 450
FGB1SW1206	026.90	72.65	07	175	044.42	78.03	09.46	0 - 450 *
FGB1SW1208	199.25	-06.04	07	175	199.72	-12.41	08.38	0 - 300
FGB1SW1209	176.54	16.18	07	175	176.50	09.18	07.27	0 - 300
FGB1SW1301	128.32	47.75	07	175	133.25	42.73	02.20	0 - 600 *
FGB1SW1302	196.10	-01.44	07	175	196.31	-07.97	03.56	0 - 350
FGB1SW1303	215.39	-10.71	07	175	216.48	-16.00	14.97	0 - 350
FGB1SW1304	151.59	35.90	07	175	153.31	29.43	02.89	0 - 600 *
FGB1SW1305	174.93	-21.67	07	175	174.93	-28.67	15.59	0 - 450
FGB1SW1306	154.91	27.00	07	175	155.94	20.40	06.53	0 - 450 *
FGB1SW1401	178.63	27.95	07	175	178.43	20.96	10.16	0 - 350
FGB1SW1402	207.53	-10.21	07	175	208.42	-16.08	16.02	0 - 450
FGB1SW1403	207.36	01.42	07	175	207.46	-04.49	05.74	0 - 350
FGB1SW1404	205.31	-08.73	07	175	206.05	-14.75	11.61	0 - 450
FGB1SW1405	191.28	-06.26	07	175	191.62	-12.97	15.99	0 - 450
FGB1SW1406	196.49	02.92	07	175	196.51	-03.59	07.45	0 - 350
FGB1SW1407	100.17	08.16	07	175	101.02	06.28	16.66	0 - 250 *
FGB1SW1501	008.56	-57.17	110	359	173.71	-12.41	23.03	0 - 450
FGB1SW1502	006.58	-55.05	110	359	174.52	-14.67	05.10	0 - 450
FGB1SW1503	345.92	-59.52	110	359	185.69	-09.76	07.00	0 - 450
FGB1SW1504	359.84	-54.72	110	359	178.50	-15.28	03.91	0 - 400
FGB1SW1505	348.35	-48.45	110	359	186.54	-20.89	31.33	0 - 550
FGB1SW1701	004.48	-64.57	104	004	183.79	-11.43	04.44	0 - 400
FGB1SW1702	015.73	-49.63	104	004	175.61	-25.53	04.26	0 - 450
FGB1SW1703	042.73	-71.53	104	004	172.57	-00.59	09.32	0 - 450
FGB1SW1704	046.66	-47.26	104	004	155.11	-17.85	07.36	0 - 400
FGB1SW1705	055.59	-40.99	104	004	145.74	-17.24	12.81	0 - 400
FGB1SW1901	221.29	09.63	38	017	230.83	43.24	08.40	0 - 450
FGB1SW1902	198.78	-15.45	38	017	198.86	22.53	08.17	0 - 500
FGB1SW1903	197.83	-10.90	38	017	197.92	27.10	05.17	0 - 450
FGB1SW1904	215.31	-28.13	38	017	213.26	08.27	14.20	0 - 500
FGB1SW1905	205.54	-02.11	38	017	207.49	35.41	23.01	0 - 450
FGB1SW2101	289.52	62.79	15	078	316.53	73.72	29.34	0 - 400 *
FGB1SW2102	310.99	67.46	15	078	351.02	72.15	27.03	0 - 400 *
FGB1SW2103	230.49	68.17	15	078	192.51	79.12	33.90	0 - 400 *
FGB1SW2104	310.64	56.85	15	078	334.56	63.46	23.95	0 - 400 *
FGB1SW2105	305.62	55.34	15	078	327.46	63.35	24.16	0 - 400 *
FGB1SW2201	203.63	13.86	10	079	201.13	19.37	15.18	0 - 500
FGB1SW2202	185.93	17.96	10	079	182.55	20.60	27.64	0 - 500
FGB1SW2203	155.36	14.33	10	079	153.11	11.78	33.17	0 - 500 *
FGB1SW2204	192.39	44.87	10	079	182.37	48.04	35.97	0 - 500 *
FGB1SW2205	168.62	-25.48	10	079	173.36	-25.13	36.60	0 - 500 *
FGB1SW2401	155.29	06.86	15	154	155.29	-08.14	36.94	0 - 200 *
FGB1SW2402	209.71	21.35	15	154	206.01	12.47	18.31	0 - 150
FGB1SW2403	199.36	-22.76	15	154	205.30	-32.78	42.98	0 - 150 *

FGB1SW2404	203.79	-05.82	15	154	205.97	-15.32	83.73	0 - 150 *
FGB1SW2405	208.68	-15.21	15	154	213.11	-23.44	-	0 - 150 *
FGB1SW2501	207.51	05.21	07	214	207.53	-01.75	57.04	0 - 400 *
FGB1SW2502	197.43	-35.16	07	214	195.76	-41.84	59.43	0 - 400 *
FGB1SW2503	213.63	-09.55	07	214	213.62	-16.55	49.00	0 - 400 *
FGB1SW2504	211.92	-20.85	07	214	211.80	-27.85	42.83	0 - 400 *
FGB1SW2505	198.56	-16.92	07	214	197.85	-23.66	41.45	0 - 400 *
FGB1SW2601	245.42	-26.39	10	274	242.43	-35.05	50.84	0 - 400 *
FGB1SW2602	197.44	-10.86	10	274	195.37	-13.01	50.29	0 - 400 *
FGB1SW2603	218.43	-29.05	10	274	213.17	-34.33	48.41	0 - 400 *
FGB1SW2604	229.87	-03.73	10	274	228.97	-10.86	73.90	0 - 400 *
FGB1SW2605	223.26	-31.02	10	274	217.82	-36.99	56.10	0 - 400 *
FGB1SW2801	180.50	-07.07	08	155	181.16	-14.27	07.64	0 - 400
FGB1SW2802	201.84	-11.34	08	155	203.32	-16.74	11.32	0 - 400
FGB1SW2803	189.08	-5.85	08	155	189.81	-12.45	07.24	0 - 400
FGB1SW2804	188.70	03.64	08	155	188.68	-03.02	08.65	0 - 400
FGB1SW2805	187.43	-9.78	08	155	188.45	-16.50	05.71	0 - 400
FGB1SW2901	198.49	-6.18	07	200	198.46	-13.18	12.68	0 - 400
FGB1SW2902	192.64	00.03	07	200	192.59	-06.91	11.02	0 - 400
FGB1SW2903	190.77	12.64	07	200	190.95	05.73	14.33	0 - 400
FGB1SW2904	197.28	-2.15	07	200	197.25	-09.14	09.23	0 - 400
FGB1SW2905	187.46	03.54	07	200	187.46	-03.29	16.43	0 - 350
FGB1SW3001	188.82	05.88	10	183	188.80	-04.07	12.27	0 - 300
FGB1SW3002	200.30	03.35	10	183	200.37	-06.20	14.97	0 - 300
FGB1SW3003	213.89	-05.56	10	183	214.79	-14.11	13.38	0 - 300
FGB1SW3004	194.44	07.25	10	183	194.36	-02.55	16.43	0 - 300
FGB1SW3005	172.12	-15.77	10	183	171.38	-25.58	23.78	0 - 300
FGB1SW3101	214.23	09.46	06	172	213.72	05.00	11.50	0 - 300
FGB1SW3102	206.57	-4.74	06	172	207.00	-09.67	15.55	0 - 300
FGB1SW3103	207.18	13.13	06	172	206.53	08.20	08.03	0 - 300
FGB1SW3104	202.63	-08.13	06	172	203.21	-13.28	08.50	0 - 300
FGB1SW3105	188.20	-52.21	06	172	190.79	-57.93	04.09	0 - 300 *
FGB1SW3201	171.81	-28.14	12	161	173.45	-39.90	08.72	0 - 300
FGB1SW3202	175.24	-13.13	12	161	176.62	-29.73	10.70	0 - 300
FGB1SW3203	184.47	-55.18	12	161	194.65	-65.77	02.85	0 - 300 *
FGB1SW3204	212.43	-32.83	12	161	219.68	-39.73	09.45	0 - 300 *
FGB1SW3303	303.68	59.76	38	180	233.35	58.51	13.93	0 - 300 *
FGB1SW3305	223.61	27.21	38	180	217.87	-02.07	06.42	0 - 200 +
FGB1SW3306	261.49	77.48	38	180	198.89	48.55	03.50	0 - 350 *
FGB1SW3308	234.05	11.45	38	180	234.04	-11.41	05.63	0 - 300 +
FGB1SW3309	185.31	38.03	38	180	184.18	00.15	06.99	0 - 300 +
FGB1SW3310	209.71	04.69	38	180	218.02	-36.68	04.70	0 - 300 +
FGB1SW3311	196.24	-06.43	38	180	202.14	-42.50	07.45	0 - 400 +
FGB1SW3403	211.93	24.18	47	178	209.97	-15.92	05.04	0 - 300 +
FGB1SW3406	223.34	60.99	47	178	199.58	20.31	13.30	0 - 400 +
FGB1SW3407	203.41	31.34	47	178	200.01	-12.09	02.94	0 - 250 +
FGB1SW3408	196.15	33.24	47	178	193.45	-11.97	11.02	0 - 350 +
FGB1SW3409	206.18	24.52	47	178	204.80	-17.67	03.47	0 - 300 +
FGB1SW3501	338.55	74.66	71	018	008.25	06.94	06.40	0 - 400 *
FGB1SW3502	348.83	68.69	71	018	007.80	00.19	03.83	0 - 300 *
FGB1SW3503	348.70	71.47	71	018	009.04	02.67	02.20	0 - 400 *
FGB1SW3505	193.55	07.16	71	018	177.34	77.39	09.43	0 - 350 +

FGB1SW3506	146.21	-32.10	71	018	153.32	18.81	08.85	0 - 400 + *
FGB1SW3507	189.86	-04.88	71	018	178.64	64.81	06.41	0 - 300 +
FGB1SW3508	234.08	-12.69	71	018	249.05	42.37	07.09	0 - 300 +
FGB1SW3509	184.10	33.16	71	018	056.52	71.16	14.57	0 - 300 +
FGB1SW3510	007.74	73.51	71	018	015.10	02.76	08.07	0 - 400 *
FGB1SW3601	005.70	68.53	82	018	013.41	-12.98	04.40	0 - 400 *
FGB1SW3602	351.22	67.75	82	018	007.96	-11.88	02.22	0 - 400 *
FGB1SW3604	205.06	-08.97	82	018	220.66	71.63	04.25	0 - 300 +
FGB1SW3605	216.59	-28.68	82	018	223.32	49.17	07.23	0 - 300 +
FGB1SW3608	206.57	-38.10	82	018	207.26	43.21	06.01	0 - 300 +
FGB1SW3610	167.82	-18.28	82	018	149.67	50.28	10.63	0 - 400 +
FGB1SW3611	186.56	-25.64	82	018	180.03	54.57	07.30	0 - 300 +
FGB1SW4106	318.02	74.48	32	325	322.47	42.56	08.69	0 - 300 *
FGB1SW4109	343.58	65.55	32	325	334.19	34.34	04.36	0 - 350 *
FGB1SW4110	353.01	66.02	32	325	338.61	35.78	05.60	0 - 350 *
FGB1SW4111	348.94	71.10	32	325	334.91	40.20	02.80	0 - 300 *
FGB1SW4113	341.70	70.03	32	325	332.21	38.59	03.09	0 - 250 *
FGB1SW4114	345.15	68.59	32	325	334.11	37.44	08.09	0 - 300 *
FGB1SW4115	342.99	66.74	32	325	333.61	35.46	01.33	0 - 250 *
FGB1SW4116	342.25	69.64	32	325	332.55	38.24	01.79	0 - 350 *
FGB1SW4117	333.17	71.22	32	325	328.39	39.35	01.44	0 - 300 *
FGB1SW4118	007.24	41.18	32	325	356.63	15.25	07.47	0 - 300 *
FGB1SW4119	326.19	35.17	57	304	323.03	-18.73	07.49	0 - 350 *
FGB1SW4120	317.14	75.72	57	304	307.40	19.05	04.82	0 - 250 *
FGB1SW4201	087.25	-28.35	47	188	070.03	-11.76	10.82	0 - 250 *
FGB1SW4202	186.48	-5.45	47	188	185.52	-52.43	15.02	0 - 250
FGB1SW4204	107.48	86.33	47	188	183.10	42.29	04.60	0 - 250 *
FGB1SW4214	075.65	89.04	30	186	184.19	60.32	04.07	0 - 250 *
FGB1SW4303	308.30	67.52	71	336	325.76	-01.10	02.58	0 - 350 *
FGB1SW4309	321.03	74.65	71	336	332.07	04.14	02.98	0 - 300 *
FGB1SW4310	325.83	66.98	71	336	332.03	-03.69	03.36	0 - 250 *
FGB1SW4409	344.77	57.66	48	179	204.09	71.93	04.41	0 - 200 *
FGB1SW4411	339.00	61.13	48	179	204.43	67.39	04.53	0 - 250 *

APPENDIX B

Table B-1 Results from the FOLDCONT program (ORS).

LLANTHONY (SOUTH WALES)

	DEC	INC	TILT	DIR
S-E LIMB				
	189.2	17.1	40.0	140.0
	189.0	09.1	40.0	140.0
W LIMB				
	190.3	-05.6	02.0	275.0

********** k MAXIMUM **********

S-E LIMB 72.0 % UNFOLDED W LIMB 100.0 % UNFOLDED
Mean Dec.= 188.6 Mean Inc.= -6.1 A95 = 2.2
Data = 3 R value = 2.994561 k max = 367.7

> > > > > > > > > EXPECTED(INC.= -6.0 +/- 2.0)< < < < < < < < <

MEAN DEC.= 188.6 MEAN INC.= -6.1
S-E LIMB 72.0 % unfolded W LIMB 100.0 % unfolded
A95 = 2.2 R value = 2.994561 k max = 367.7

********** USUAL FOLD TEST **********

S-E LIMB 72.0 % UNFOLDED W LIMB 72.0 % UNFOLDED
Mean Dec.= 188.6 Mean Inc.= -6.1 A95 = 2.2
Data = 3 R value = 2.994530 k max = 365.6

McELHINNY TEST (95% CONFIDENCE LIMIT)

Variance ratio (F) = 6.38
k1 (k-parameter for in situ) = 49.5
k2 (k-parameter at 95% limit; = k1 * F) = 315.8
k3 (k-parameter for fully unfolded) = 177.7

LLANSTEPHAN (SOUTH WALES)

	DEC	INC	TILT	DIR
NORTH LIMB				
	206.9	-13.5	54.0	330.0
	209.1	-18.4	41.0	327.0
	210.0	-12.8	32.0	324.0
	197.7	-02.9	65.0	342.0
	208.6	-03.4	45.0	349.0
	203.1	-05.0	64.0	333.0
	206.8	-12.8	40.0	340.0
SOUTH LIMB				
	208.0	-06.3	25.0	166.0
	209.4	03.6	48.0	168.0
	208.8	01.2	10.0	190.0
	210.4	-01.4	18.0	167.0

********** k MAXIMUM **********

NORTH LIMB 0.0 % UNFOLDED SOUTH LIMB 36.0 % UNFOLDED
Mean Dec.= 207.3 Mean Inc.= -9.1 A95 = 1.7
Data = 11 R value = 10.933667 k max = 150.8

> > > > > > > > > EXPECTED(INC.= -6.0 +/- 5.0) < < < < < < < < <

MEAN DEC.= 207.3 MEAN INC.= -9.1
NORTH LIMB 0.0 % unfolded SOUTH LIMB 36.0 % unfolded
A95 = 1.7 R value = 10.933667 k max = 150.8

********** USUAL FOLD TEST **********

NORTH LIMB 10.0 % UNFOLDED SOUTH LIMB 10.0 % UNFOLDED
Mean Dec.= 206.8 Mean Inc.= -5.2 A95 = 1.9
Data = 11 R value = 10.919617 k max = 124.4

McELHINNY TEST (95% CONFIDENCE LIMIT)

Variance ratio (F) = 2.12
k1 (k-parameter for in situ) = 106.1
k2 (k-parameter at 95% limit; = k1 * F) = 224.9
k3 (k-parameter for fully unfolded) = 10.8

LLANSTEPHAN (SOUTH WALES)

	DEC	INC	TILT	DIR
NORTH LIMB				
	206.9	-13.5	54.0	330.0
	209.1	-18.4	41.0	327.0
	210.0	-12.8	32.0	324.0
	197.7	-02.9	65.0	342.0
	208.6	-03.4	45.0	349.0
	203.1	-05.0	64.0	333.0
	206.8	-12.8	40.0	340.0
SOUTH LIMB				
	208.0	-06.3	25.0	166.0
	209.4	03.6	48.0	168.0
	208.8	01.2	10.0	190.0
	210.4	-01.4	18.0	167.0

PLUNGE CORRECTED : amount/dir = 05.0/ 250.0

NORTH LIMB				
	206.0	-17.1	53.3	333.6
	207.9	-22.1	40.1	332.8
	209.1	-16.6	31.0	332.0
	197.4	-05.9	65.3	344.3
	208.3	-07.1	46.0	353.8
	202.7	-08.4	63.5	335.5
	205.9	-16.4	40.3	345.9
SOUTH LIMB				
	207.5	-10.0	24.9	155.2
	209.5	-00.2	47.5	163.5
	208.8	-02.6	08.6	160.3
	210.2	-05.2	18.1	151.6

********** k MAXIMUM **********

NORTH LIMB 0.0 % UNFOLDED SOUTH LIMB 36.0 % UNFOLDED
Mean Dec.= 207.0 Mean Inc.=-12.2 A95 = 1.8
Data = 11 R value = 10.928006 k max = 138.9

> > > > > > > > > EXPECTED(INC.= -6.0 +/- 5.0)< < < < < < < < <

MEAN DEC.= 206.7 MEAN INC.=-10.9
NORTH LIMB 4.0 % unfolded SOUTH LIMB 28.0 % unfolded
A95 = 1.8 R value = 10.925462 k max = 134.2

********** USUAL FOLD TEST **********

NORTH LIMB 10.0 % UNFO'.DED SOUTH LIMB 10.0 % UNFOLDED
Mean Dec.= 206.3 Mean Inc.= -8.6 A95 = 1.9
Data = 11 R value = 10.917131 k max = 120.7

McELHINNY TEST (95% CONFIDENCE LIMIT)

Variance ratio (F) = 2.12
k1 (k-parameter for in situ) = 106.1
k2 (k-parameter at 95% limit; = k1 * F) = 224.9
k3 (k-parameter for fully unfolded) = 10.8

FRESHWATER EAST (SOUTH WALES)

	DEC	INC	TILT	DIR
NORTH LIMB				
	200.3	-52.2	90.0	004.0
	208.8	-38.6	82.0	006.0
SOUTH LIMB				
	216.6	-06.3	42.0	184.0

********** k MAXIMUM **********

NORTH LIMB 46.0 % UNFOLDED SOUTH LIMB 0.0 % UNFOLDED
Mean Dec.= 204.8 Mean Inc.= -7.1 A95 = 6.4
Data = 3 R value = 2.956203 k max = 45.7

> > > > > > > > > EXPECTED(INC.= -6.0 +/- 5.0)< < < < < < < < <

MEAN DEC.= 204.8 MEAN INC.= -7.1
NORTH LIMB 46.0 % unfolded SOUTH LIMB 0.0 % unfolded
A95 = 6.4 R value = 2.956203 k max = 45.7

********** USUAL FOLD TEST **********

NORTH LIMB 32.0 % UNFOLDED SOUTH LIMB 32.0 % UNFOLDED
Mean Dec.= 205.9 Mean Inc.=-18.8 A95 = 6.5
Data = 3 R value = 2.954834 k max = 44.3

McELHINNY TEST (95% CONFIDENCE LIMIT)

Variance ratio (F) = 6.38
k1 (k-parameter for in situ) = 11.1
k2 (k-parameter at 95% limit; = k1 * F) = 70.8
k3 (k-parameter for fully unfolded) = 3.1

FRESHWATER EAST (SOUTH WALES)

The plunge correction (see text) :
North limb : 08/297
South limb : 14/095

	DEC	INC	TILT	DIR
NORTH LIMB				
	190.5	-50.6	86.9	004.2
	202.4	-38.4	79.2	007.2
SOUTH LIMB				
	217.1	01.1	43.6	199.1

********** k MAXIMUM **********

NORTH LIMB 0.0 % UNFOLDED SOUTH LIMB 100.0 % UNFOLDED
Mean Dec.= 206.1 Mean Inc.=-43.7 A95 = 7.2
Data = 3 R value = 2.944681 k max = 36.2

> > > > > > > > > EXPECTED(INC.= -6.0 +/- 5.0)< < < < < < < < <

MEAN DEC.= 201.6 MEAN INC.=-10.2
NORTH LIMB 42.0 % unfolded SOUTH LIMB 26.0 % unfolded
A95 = 8.0 R value = 2.931876 k max = 29.4

********** USUAL FOLD TEST **********

NORTH LIMB 36.0 % UNFOLDED SOUTH LIMB 36.0 % UNFOLDED
Mean Dec.= 201.9 Mean Inc.=-14.9 A95 = 7.9
Data = 3 R value = 2.932647 k max = 29.7

McELHINNY TEST (95% CONFIDENCE LIMIT)

Variance ratio (F) = 6.38
k1 (k-parameter for in situ) = 7.8
k2 (k-parameter at 95% limit; = k1 * F) = 49.8
k3 (k-parameter for fully unfolded) = 3.1

FRESHWATER EAST (SOUTH WALES)

	DEC	INC	TILT	DIR
NORTH LIMB				
	200.3	-52.2	90.0	004.0
	208.8	-38.6	82.0	006.0
SOUTH LIMB				
	216.6	-06.3	42.0	184.0

PLUNGE CORRECTED : amount/dir = 14.0/ 95.0

NORTH LIMB				
	215.5	-46.7	90.2	004.0
	217.6	-31.9	82.0	004.0
SOUTH LIMB				
	217.1	01.1	43.6	199.1

********** k MAXIMUM **********

NORTH LIMB 54.0 % UNFOLDED SOUTH LIMB 0.0 % UNFOLDED
Mean Dec.= 211.5 Mean Inc.= 1.8 A95 = 4.0
Data = 3 R value = 2.982592 k max = 114.9

> > > > > > > > > EXPECTED(INC.= -6.0 +/- 5.0)< < < < < < < < <

MEAN DEC.= 211.5 MEAN INC.= -1.1
NORTH LIMB 50.0 % unfolded SOUTH LIMB 6.0 % unfolded
A95 = 4.0 R value = 2.982245 k max = 112.6

********** USUAL FOLD TEST **********

NORTH LIMB 34.0 % UNFOLDED SOUTH LIMB 34.0 % UNFOLDED
Mean Dec.= 212.1 Mean Inc.=-13.4 A95 = 4.1
Data = 3 R value = 2.981267 k max = 106.8

McELHINNY TEST (95% CONFIDENCE LIMIT)

Variance ratio (F) = 6.38
k1 (k-parameter for in situ) = 11.1
k2 (k-parameter at 95% limit; = k1 * F) = 70.8
k3 (k-parameter for fully unfolded) = 3.4

FRESHWATER WEST (SOUTH WALES)

	DEC	INC	TILT	DIR
NORTH LIMB				
	244.8	-17.2	52.0	022.0
SOUTH LIMB				
	230.2	45.2	96.0	184.0

********** k MAXIMUM **********

NORTH LIMB 100.0 % UNFOLDED SOUTH LIMB 16.0 % UNFOLDED
Mean Dec.= 234.7 Mean Inc.= 28.3 A95 = 12.5
Data = 2 R value = 1.953403 k max = 21.5

> > > > > > > > > EXPECTED(INC.= -6.0 +/- 5.0)< < < < < < < < <

MEAN DEC.= 229.3 MEAN INC.=-10.9
NORTH LIMB 20.0 % unfolded SOUTH LIMB 72.0 % unfolded
A95 = 13.9 R value = 1.942830 k max = 17.5

********** USUAL FOLD TEST **********

NORTH LIMB 52.0 % UNFOLDED SOUTH LIMB 52.0 % UNFOLDED
Mean Dec.= 228.6 Mean Inc.= 4.1 A95 = 14.1
Data = 2 R value = 1.941283 k max = 17.0

McELHINNY TEST (95% CONFIDENCE LIMIT)

Variance ratio (F) = 18.99
k1 (k-parameter for in situ) = 3.3
k2 (k-parameter at 95% limit; = k1 * F) = 62.7
k3 (k-parameter for fully unfolded) = 3.7

FRESHWATER WEST (SOUTH WALES)

The plunge correction (see text) :
North limb : 07/275
South limb : 15/310

	DEC	INC	TILT	DIR
NORTH LIMB				
	243.5	-23.2	54.3	027.0
SOUTH LIMB				
	243.7	40.8	104.6	186.3

********** k MAXIMUM **********

NORTH LIMB 0.0 % UNFOLDED SOUTH LIMB 92.0 % UNFOLDED
Mean Dec.= 238.3 Mean Inc.=-25.9 A95 = 5.5
Data = 2 R value = 1.990850 k max = 109.3

> > > > > > > > > EXPECTED(INC.= -6.0 +/- 5.0)< < < < < < < < <

MEAN DEC.= 233.8 MEAN INC.=-10.8
NORTH LIMB 30.0 % unfolded SOUTH LIMB 70.0 % unfolded
A95 = 6.9 R value = 1.985822 k max = 70.5

********** USUAL FOLD TEST **********

NORTH LIMB 54.0 % UNFOLDED SOUTH LIMB 54.0 % UNFOLDED
Mean Dec.= 233.0 Mean Inc.= 1.1 A95 = 7.1
Data = 2 R value = 1.984633 k max = 65.1

McELHINNY TEST (95% CONFIDENCE LIMIT)

Variance ratio (F) = 18.99
k1 (k-parameter for in situ) = 3.2
k2 (k-parameter at 95% limit; = k1 * F) = 60.8
k3 (k-parameter for fully unfolded) = 4.3

ORIELTON ANTICLINE

	DEC	INC	TILT	DIR
NORTH LIMB				
	200.3	-52.2	90.0	004.0
	208.8	-38.6	82.0	006.0
SOUTH LIMB				
	230.2	45.2	96.0	184.0

********** k MAXIMUM **********

NORTH LIMB 100.0 % UNFOLDED SOUTH LIMB 18.0 % UNFOLDED
Mean Dec.= 208.9 Mean Inc.= 36.1 A95 = 5.6
Data = 3 R value = 2.965741 k max = 58.4

> > > > > > > > > EXPECTED(INC.= -6.0 +/- 5.0)< < < < < < < < <

MEAN DEC.= 204.1 MEAN INC.= -1.1
NORTH LIMB 54.0 % unfolded SOUTH LIMB 60.0 % unfolded
A95 = 5.8 R value = 2.962788 k max = 53.7

********** USUAL FOLD TEST **********

NORTH LIMB 56.0 % UNFOLDED SOUTH LIMB 56.0 % UNFOLDED
Mean Dec.= 204.1 Mean Inc.= 1.1 A95 = 5.8
Data = 3 R value = 2.963054 k max = 54.1

McELHINNY TEST (95% CONFIDENCE LIMIT)

Variance ratio (F) = 6.38
k1 (k-parameter for in situ) = 2.4
k2 (k-parameter at 95% limit; = k1 * F) = 15.3
k3 (k-parameter for fully unfolded) = 3.7

ORIELTON ANTICLINE
The plunge correction (see text) :
North limb : 08/297
South limb : 15/310

	DEC	INC	TILT	DIR
NORTH LIMB				
	190.5	-50.6	86.9	004.2
	202.4	-38.4	79.2	007.2
SOUTH LIMB				
	243.7	40.8	104.6	186.3

********** k MAXIMUM **********

NORTH LIMB 100.0 % UNFOLDED SOUTH LIMB 20.0 % UNFOLDED
Mean Dec.= 208.7 Mean Inc.= 35.6 A95 = 10.3
Data = 3 R value = 2.886654 k max = 17.6

> > > > > > > > > EXPECTED(INC.= -6.0 +/- 5.0)< < < < < < < < <

MEAN DEC.= 204.3 MEAN INC.= -2.0
NORTH LIMB 52.0 % unfolded SOUTH LIMB 58.0 % unfolded
A95 = 10.6 R value = 2.882324 k max = 17.0

********** USUAL FOLD TEST **********

NORTH LIMB 56.0 % UNFOLDED SOUTH LIMB 56.0 % UNFOLDED
Mean Dec.= 204.3 Mean Inc.= 0.8 A95 = 10.6
Data = 3 R value = 2.882317 k max = 17.0

McELHINNY TEST (95% CONFIDENCE LIMIT)

Variance ratio (F) = 6.38
k1 (k-parameter for in situ) = 2.3
k2 (k-parameter at 95% limit; = k1 * F) = 14.7
k3 (k-parameter for fully unfolded) = 3.1

ORIELTON ANTICLINE

The plunge correction (see text) :
North limb : 14/095
South limb : 15/310

	DEC	INC	TILT	DIR
NORTH LIMB				
	215.5	-46.7	90.2	004.0
	217.6	-31.9	82.0	004.0
SOUTH LIMB				
	243.7	40.8	104.6	186.3

********** k MAXIMUM **********

NORTH LIMB 100.0 % UNFOLDED SOUTH LIMB 16.0 % UNFOLDED
Mean Dec.= 222.1 Mean Inc.= 35.5 A95 = 5.6
Data = 3 R value = 2.965233 k max = 57.5

> > > > > > > > > EXPECTED(INC.= -6.0 +/- 5.0)< < < < < < < < <

MEAN DEC.= 214.4 MEAN INC.= -1.4
NORTH LIMB 50.0 % unfolded SOUTH LIMB 58.0 % unfolded
A95 = 6.1 R value = 2.958994 k max = 48.8

********** USUAL FOLD TEST **********

NORTH LIMB 54.0 % UNFOLDED SOUTH LIMB 54.0 % UNFOLDED
Mean Dec.= 214.4 Mean Inc.= 1.8 A95 = 6.1
Data = 3 R value = 2.959533 k max = 49.4

McELHINNY TEST (95% CONFIDENCE LIMIT)

Variance ratio (F) = 6.38
k1 (k-parameter for in situ) = 2.9
k2 (k-parameter at 95% limit; = k1 * F) = 18.5
k3 (k-parameter for fully unfolded) = 3.7

ORIELTON SYNCLINE

	DEC	INC	TILT	DIR
NORTH LIMB	216.6	-06.3	42.0	184.0
SOUTH LIMB	244.8	-17.2	52.0	022.0

********** k MAXIMUM **********

NORTH LIMB 60.0 % UNFOLDED SOUTH LIMB 0.0 % UNFOLDED
Mean Dec.= 233.3 Mean Inc.=-22.6 A95 = 12.2
Data = 2 R value = 1.955853 k max = 22.7

> > > > > > > > > EXPECTED(INC.= -6.0 +/- 5.0)< < < < < < < < <

MEAN DEC.= 230.2 MEAN INC.=-10.9
NORTH LIMB 18.0 % unfolded SOUTH LIMB 22.0 % unfolded
A95 = 13.0 R value = 1.950282 k max = 20.1

********** USUAL FOLD TEST **********

NORTH LIMB 20.0 % UNFOLDED SOUTH LIMB 20.0 % UNFOLDED
Mean Dec.= 230.4 Mean Inc.=-11.7 A95 = 12.9
Data = 2 R value = 1.950569 k max = 20.2

McELHINNY TEST (95% CONFIDENCE LIMIT)

Variance ratio (F) = 18.99
k1 (k-parameter for in situ) = 15.0
k2 (k-parameter at 95% limit; = k1 * F) = 284.8
k3 (k-parameter for fully unfolded) = 3.3

ORIELTON SYNCLINE

The plunge correction (see text) :
North limb : 14/095
South limb : 07/275

	DEC	INC	TILT	DIR
NORTH LIMB	217.1	-01.1	43.6	199.1
SOUTH LIMB	243.5	-23.2	54.3	027.0

********** k MAXIMUM **********

NORTH LIMB 74.0 % UNFOLDED SOUTH LIMB 0.0 % UNFOLDED
Mean Dec.= 232.0 Mean Inc.=-26.8 A95 = 11.1
Data = 2 R value = 1.963166 k max = 27.1

> > > > > > > > > EXPECTED INC.= -6.0 +/- 5.0)< < < < < < < < <

MEAN DEC.= 229.1 MEAN INC.=-10.8
NORTH LIMB 30.0 % unfolded SOUTH LIMB 30.0 % unfolded
A95 = 11.6 R value = 1.960255 k max = 25.2

********** USUAL FOLD TEST **********

NORTH LIMB 30.0 % UNFOLDED SOUTH LIMB 30.0 % UNFOLDED
Mean Dec.= 229.1 Mean Inc.=-10.8 A95 = 11.6
Data = 2 R value = 1.960255 k max = 25.2

McELHINNY TEST (95% CONFIDENCE LIMIT)

Variance ratio (F) = 18.99
k1 (k-parameter for in situ) = 10.5
k2 (k-parameter at 95% limit; = k1 * F) = 199.4
k3 (k-parameter for fully unfolded) = 3.2

Table B-2 Results from the FOLDCONT program (Westphalian A).

Saundersfoot

	DEC	INC	TILT	DIR
NORTH LIMB				
	200.5	05.9	71.0	018.0
	196.2	-24.9	82.0	018.0
SOUTH LIMB				
	210.5	13.7	38.0	180.0
	206.9	35.0	47.0	178.0

********** k MAXIMUM **********

NORTH LIMB 24.0 % UNFOLDED SOUTH LIMB 46.0 % UNFOLDED
Mean Dec.= 202.2 Mean Inc.= 7.9 A95 = 6.5
Data = 4 R value = 3.903693 k max = 31.2

> > > > > > > > > EXPECTED(INC.=-10.0 +/- 10.0)< < < < < < < < <

MEAN DEC.= 202.1 MEAN INC.= -0.1
NORTH LIMB 14.0 % unfolded SOUTH LIMB 68.0 % unfolded
A95 = 6.5 R value = 3.902816 k max = 30.9

********** USUAL FOLD TEST **********

NORTH LIMB 32.0 % UNFOLDED SOUTH LIMB 32.0 % UNFOLDED
Mean Dec.= 202.5 Mean Inc.= 13.7 A95 = 6.5
Data = 4 R value = 3.903390 k max = 31.1

McELHINNY TEST (95% CONFIDENCE LIMIT)

Variance ratio (F) = 4.28
k1 (k-parameter for in situ) = 10.2
k2 (k-parameter at 95% limit; = k1 * F) = 43.7
k3 (k-parameter for fully unfolded) = 3.0

Saundersfoot

	DEC	INC	TILT	DIR
NORTH LIMB				
	200.5	05.9	71.0	018.0
	196.2	-24.9	82.0	018.0
SOUTH LIMB				
	210.5	13.7	38.0	180.0
	206.9	35.0	47.0	178.0

PLUNGE CORRECTED : amount/dir = 18.0/ 106.0

NORTH LIMB				
	198.5	06.9	71.3	011.8
	204.3	-23.6	81.8	015.4
SOUTH LIMB				
	205.6	17.4	36.7	203.9
	193.9	36.3	44.1	195.7

********** k MAXIMUM **********

NORTH LIMB 48.0 % UNFOLDED SOUTH LIMB 0.0 % UNFOLDED
Mean Dec.= 201.3 Mean Inc.= 27.6 A95 = 6.2
Data = 4 R value = 3.913350 k max = 34.6

> > > > > > > > > EXPECTED(INC.=-10.0 +/- 10.0)< < < < < < < < <

MEAN DEC.= 200.5 MEAN INC.= -0.3
NORTH LIMB 12.0 % unfolded SOUTH LIMB 70.0 % unfolded
A95 = 6.3 R value = 3.907787 k max = 32.5

********** USUAL FOLD TEST **********

NORTH LIMB 32.0 % UNFOLDED SOUTH LIMB 32.0 % UNFOLDED
Mean Dec.= 200.8 Mean Inc.= 15.0 A95 = 6.2
Data = 4 R value = 3.911283 k max = 33.8

McELHINNY TEST (95% CONFIDENCE LIMIT)

Variance ratio (F) = 4.28
k1 (k-parameter for in situ) = 10.2
k2 (k-parameter at 95% limit; = k1 * F) = 43.7
k3 (k-parameter for fully unfolded) = 3.0

APPENDIX C

PROGRAM FOLDCONT

The program calculates the values of k-parameter based on a formula

$$k = (N - 1) / (N - R)$$

where N = *the number of vectors involved in the process*
R = *the magnitude of the vector resultant*

```
      REAL FOLD1(51),FOLD2(51),DEC1(20),XINC1(20),DEC2(20),XINC2(20),
     *DIR1(20),DIR2(20),TILT1(20),TILT2(20),W(16000),Z(51,51),
     *ZINC(51,51)
      INTEGER N1,N2,NW,NTILT
      REAL XKREF,FREF1,FREF2,TEMP,FTEST,XKLIMIT
      COMMON XIREF,BIREF
      CHARACTER*4 HEAD(20),XTTL(3),YTTL(3)
      PARAMETER (P = 0.95)
      RAD = 180.0/3.141592654
  101 FORMAT(20A4)
  102 FORMAT(20A4,/)
  103 FORMAT(14X,'DEC',7X,'INC',7X,'TILT',6X,'DIR')
  104 FORMAT(3A4)
  105 FORMAT(11X,4(F7.1,3X))
      READ(2,101) (HEAD(I),I = 1,20)
      WRITE(3,102) (HEAD(I),I = 1,20)
      WRITE(3,103)
      READ(2,104) (XTTL(I),I = 1,3)
      WRITE(3,104) (XTTL(I),I = 1,3)
      READ(2,104) (YTTL(I),I = 1,3)
      DO 106,I = 1,20
      READ(2,*) DEC1(I),XINC1(I),TILT1(I),DIR1(I)
      IF(DEC1(I).EQ.-222.0.OR.XINC1(I).EQ.-222.0) GO TO 107
      WRITE(3,105) DEC1(I),XINC1(I),TILT1(I),DIR1(I)
  106 CONTINUE
  107 N1 = I -1
      WRITE(3,101) (YTTL(I),I = 1,3)
      DO 108,J = 1,20
      READ(2,*,END = 109) DEC2(J),XINC2(J),TILT2(J),DIR2(J)
      WRITE(3,105) DEC2(J),XINC2(J),TILT2(J),DIR2(J)
  108 CONTINUE
  109 N2 = J - 1
```

For a plunging fold,
the palaeomagnetic directions and the bedding (i.e. the pole)
are plunge-corrected first.

```
      WRITE(1,*) 'Enter the PLUNGE and the TREND'
      READ(1,*) PLUNGE,TREND
      IF(PLUNGE.NE.0.0) THEN
      WRITE(3,9990) PLUNGE,TREND
 9990 FORMAT(/,10X,'PLUNGE CORRECTED : Amount/Dir = ',F6.1,'/',F6.1,/)
      WRITE(3,104) (XTTL(I),I = 1,3)
      DO 9991,I = 1,N1
       CALL ROTATE(XINC1(I),DEC1(I),TREND,PLUNGE,DEC1(I),XINC1(I))
       X = 90.0-TILT1(I)
       IF(DIR1(I).GT.180.0) THEN
       Y = DIR1(I)-180.0
       ELSE
       Y = DIR1(I) + 180.0
       ENDIF
       CALL ROTATE(PINC,PDEC,TREND,PLUNGE,Y,X)
       TILT1(I) = 90.0-PINC
       IF(PDEC.GT.180.0) THEN
       DIR1(I) = PDEC-180.0
       ELSE
       DIR1(I) = PDEC + 180.0
       ENDIF
       WRITE(3,105) DEC1(I),XINC1(I),TILT1(I),DIR1(I)
 9991  CONTINUE
       WRITE(3,101) (YTTL(I),I = 1,3)
       DO 9992,J = 1,N2
        CALL ROTATE(XINC2(J),DEC2(J),TREND,PLUNGE,DEC2(J),XINC2(J))
        X = 90.0-TILT2(J)
        IF(DIR2(J).GT.180.0) THEN
        Y = DIR2(J)-180.0
        ELSE
        Y = DIR2(J) + 180.0
        ENDIF
```

```
      CALL ROTATE(PINC,PDEC,TREND,PLUNGE,Y,X)
      TILT2(J) = 90.0-PINC
      IF(PDEC.GT.180.0) THEN
      DIR2(J)=PDEC-180.0
      ELSE
      DIR2(J)=PDEC+180.0
      ENDIF
      WRITE(3,105) DEC2(J),XINC2(J),TILT2(J),DIR2(J)
9992   CONTINUE
      ENDIF

      Generate the F table by calling the function G01CBF from
                  the NAG Fortran Library

      IFAIL = 0
      NTEST = 2 * ((N1+N2)-1)
      FTEST = G01CBF(P,NTEST,NTEST,IFAIL)
      FTEST = REAL(INT(FTEST*100.0))/100.0
      IF(IFAIL.NE.0) THEN
      PRINT*,'Failed to generate the F table'
      STOP
      ENDIF

      XTEMP=2.0
      NTILT=INT(100.0/XTEMP)+1
      XIMAX=0.0
      XIMIN=0.0
      XKMAX=0.0
      XKMIN=0.0
      XKREF=0.0
      WRITE(1,*) 'Enter the EXPECTED inclination and its bandwidth'
      READ(1,*) XIREF,BIREF
      DO 111, I=1,NTILT
       FOLD1(I)=REAL(I-1)*XTEMP
       DO 110, M=1,NTILT
        FOLD2(M)=REAL(M-1)*XTEMP
        CALL MEANS(XINC1,DEC1,TILT1,DIR1,N1,FOLD1(I),XINC2,DEC2,TILT2,
     *   DIR2,N2,FOLD2(M),R,DECM,XINCM,A95,TEMP)
        Z(I,M)=(REAL(N1+N2-1))/(REAL(N1+N2)-R)
        XKMAX=AMAX1(XKMAX,Z(I,M))
        XKMIN=AMIN1(XKMIN,Z(I,M))
        IF(TEMP.EQ.1.0) XKREF=AMAX1(XKREF,Z(I,M))
        ZINC(I,M)=XINCM
        XIMAX=AMAX1(XIMAX,ZINC(I,M))
        XIMIN=AMIN1(XIMIN,ZINC(I,M))
  110 CONTINUE
  111 CONTINUE
      ZINST = REAL(INT(Z(1,1)*10.0))/10.0
      XKLIMIT = ZINST * FTEST
      DO 113,I=1,NTILT
       DO 112,J=1,NTILT
        IF(Z(I,J).EQ.XKMAX) THEN
        FMAX1=FOLD1(I)
        FMAX2=FOLD2(J)
        GO TO 114
        ENDIF
  112 CONTINUE
  113 CONTINUE
  114 CALL MEANS(XINC1,DEC1,TILT1,DIR1,N1,FMAX1,XINC2,DEC2,TILT2,DIR2,
     *N2,FMAX2,R,DECM,XINCM,A95,TEMP)
      WRITE(3,115)
  115 FORMAT(/,25('*'),' k  MAXIMUM ',25('*'))
      WRITE(3,116) XTTL,FMAX1,YTTL,FMAX2
  116 FORMAT(1X,/,2(3A4,2X,F5.1,1X,'% UNFOLDED',5X))
      WRITE(3,117) DECM,XINCM,A95
  117 FORMAT(1X,'Mean Dec.=',F6.1,3X,'Mean Inc.=',F5.1,3X,'A95 =',F5.1)
      WRITE(3,118) N1+N2,R,XKMAX
  118 FORMAT(1X,'Data =',I4,3X,'R value =',F10.6,3X,'k max =',F7.1)
      DO 120,I=1,NTILT
       DO 119,J=1,NTILT
        IF(Z(I,J).EQ.XKREF) THEN
        FREF1=FOLD1(I)
        FREF2=FOLD2(J)
        CALL MEANS(XINC1,DEC1,TILT1,DIR1,N1,FMAX1,XINC2,DEC2,TILT2,
     *   DIR2,N2,FMAX2,R,DECM,XINCM,A95,TEMP)
        IF(ABS(XINCM-XIREF).LT.BIREF) GO TO 121
        ENDIF
  119 CONTINUE
  120 CONTINUE
  121  WRITE(3,122) XIREF,BIREF
  122 FORMAT(/,17('>'),'EXPECTED',(INC.=',F5.1,' +/-',F5.1,')',17('<'))
```

```
      WRITE(3,123) DECM,XINCM
123 FORMAT(1X,'Mean Dec. =',F6.1,3X,'Mean Inc. =',F5.1)
      WRITE(3,124) XTTL,FREF1,YTTL,FREF2
124 FORMAT(1X,/,2(3A4,2X,F5.1,1X,'% unfolded',5X))
      WRITE(3,125) A95,R,XKREF
125 FORMAT(1X,'A95 =',F5.1,3X,'R value =',F10.6,3X,'k max  =',F7.1)
      ZMAX = 0.0
      DO 126,I = 1,NTILT
        FOLD2(I) = Z(I,I)
        ZMAX = AMAX1(ZMAX,FOLD2(I))
126 CONTINUE
      DO 127,I = 1,NTILT
        IF(FOLD2(I).EQ.ZMAX) THEN
        FMAX = FOLD1(I)
        GO TO 120
        ENDIF
127 CONTINUE
128 CALL MEANS(XINC1,DEC1,TILT1,DIR1,N1,FMAX,XINC2,DEC2,TILT2,DIR2,
     *N2,FMAX,R,DECM,XINCM,A95,TEMP)
      WRITE(3,129)
129 FORMAT(/,25('*'),' USUAL FOLD TEST ',25('*'))
      WRITE(3,130) XTTL,FMAX,YTTL,FMAX
130 FORMAT(1X,/,2(3A4,2X,F5.1,1X,'% UNFOLDED',5X))
      WRITE(3,131) DECM,XINCM,A95
131 FORMAT(1X,'Mean Dec. =',F6.1,3X,'Mean Inc. =',F5.1,3X,'A95 =',F5.1)
      WRITE(3,132) N1 + N2,R,ZMAX
132 FORMAT(1X,'Data =',I4,3X,'R value =',F10.6,3X,'k max =',F7.1)
      WRITE(3,133)
133 FORMAT(/,1X,'McELHINNY TEST (95% CONFIDENCE LIMIT)')
      WRITE(3,134) FTEST
134 FORMAT(/,1X,'Variance ratio (F) =',F7.2)
      WRITE(3,135) ZINST
135 FORMAT(1X,'k1 (k-parameter for in situ) =',F9.2)
      WRITE(3,136) XKLIMIT
136 FORMAT(1X,'k2 (k-parameter at 96% limit; = k1 * F) =',F7.1)
      WRITE(3,137) Z(NTILT,NTILT)
137 FORMAT(1X,'k3 (k-parameter for fully unfolded) =',F7.1)
      XLO = 0.0
      YLO = 0.0
      XHI = 100.0
      YHI = 100.0
      NW = 16000
```

The following is to draw the picture. The GINO-F graphic package is used.

```
      CALL GINO
      CALL SAVDRA
      CALL CHAENQ(ITYP,CHAWID,CHAHIG,NSIZE,AITAL,ANG)
```

The bottom picture.

```
      CALL WINDO2(0.0,150.0,0.0,150.0)
      CALL MOVTO2(11.0*CHAWID,150.0-3.0*CHAHIG)
      CALL WIDENQ(WIDTH)
      CALL LINWID(3.0*WIDTH)
      CALL CHASTR('CONTOUR OF k-PARAMETER')
      CALL LINWID(WIDTH)
      NCONT = 4
      XINT = (XKMAX-XKMIN)/REAL(NCONT + 1)
      XKMIN = XKMIN + XINT
      CALL TITLE(4,7,HEAD)
      CALL LABCON(0,0,60.0,1)
      CALL LEVELS(XKMIN,XKMAX)
      CALL DRACON(NTILT,XLO,XHI,NTILT,YLO,YHI,Z,NCONT,1,NW,W)
      CALL LINCOL(2)
      CALL ADDCON(XKMAX-XKMAX*0.05,1,NW,W)
      CALL SETFRA(2)
      CALL LABCON(0,1,40.0,0)
      CALL LEVELS(XIMIN,XIMAX)
      CALL DRACON(NTILT,XLO,XHI,NTILT,YLO,YHI,ZINC,0,0,NW,W)
      CALL LINCOL(2)
      CALL ADDCON(XIREF-BIREF,0,NW,W)
      CALL LINCOL(2)
      CALL ADDCON(XIREF,0,NW,W)
      CALL LINCOL(2)
      CALL ADDCON(XIREF + BIREF,0,NW,W)
      CALL MOVTO2(11.0*CHAWID,0.5*CHAHIG)
      CALL CHASIZ(CHAWID/1.5,CHAHIG/1.5)
      CALL LINCOL(1)
      CALL CHASTR(' X = ')
      CALL CHAARR(XTTL,3,4)
```

```
      CALL CHASTR(' Y = ')
      CALL CHAARR(YTTL,3,4)
      CALL CHASTR('  ( %  Unfolding ) ')
      CALL CHASIZ(CHAWID/1.3,CHAHIG/1.3)
```

The top picture.

```
      CALL WINDO2(0.0,150.0,150.0,200.0)
      XMIN = 11.0*CHAWID
      YMIN = 150.0  +  3.0*CHAHIG
      XMAX  =  150.0 - 8.0*CHAWID
      YMAX  =  200.0 - 3.0*CHAHIG
      CALL AXIPOS(1,XMIN,YMIN,XMAX-XMIN,1)
      CALL AXIPOS(1,XMIN,YMIN,YMAX-YMIN,2)
      CALL AXISCA(1,20,XLO,XHI,1)
      IF(XKLIMIT.GT.XKMAX) THEN
      CALL AXISCA(1,5,0.0,XKLIMIT,2)
      ELSE
      CALL AXISCA(1,5,0.0,XKMAX,2)
      ENDIF
      CALL AXIDRA(-1,-1,2)
      CALL AXIDRA(1,1,1)
      CALL LINCOL(2)
      CALL GRACUR(FOLD1,FOLD2,NTILT)
      CALL GRAMOV(0.0,XKLIMIT)
      CALL BROKEN(3)
      CALL LINCOL(1)
      CALL GRALIN(90.0,XKLIMIT)
      CALL CHASTR(' 95% limit')
      CALL MOVTO2(XMIN-3.0*CHAWID,YMIN + (YMAX-YMIN)/4.0)
      CALL CHAANG(90.0)
      CALL CHASTR('k-parameter')
      CALL CHAANG(0.0)
      CALL MOVTO2((XMAX-XMIN)/1.35,YMAX + 2.0*CHAHIG)
      CALL CHASTR('% UNFOLDING')
      CALL DEVEND
      CALL GINEND
      STOP
      END

      SUBROUTINE MEANS(XI1,D1,T1,DR1,N1,F1,XI2,D2,T2,DR2,N2,F2,R,DECM,
     *XINCM,A95,TEMP)
```

This subroutine calculates the mean direction and its alpha-95.

```
      DIMENSION XI1(N1),D1(N1),T1(N1),DR1(N1),XI2(N2),D2(N2),T2(N2),
     *DR2(N2)
      COMMON XIREF,BIREF
      REAL TEMP
      RAD = 180.0/3.141592654
      RX1 = 0.0
      RY1 = 0.0
      RZ1 = 0.0
      DO 1000,J = 1,N1
        RTILT = F1*T1(J)*0.01
        CALL ROTATE(CI,CD,DR1(J),RTILT,D1(J),XI1(J))
        X1 = COS(CI/RAD)*COS(CD/RAD)
        Y1 = COS(CI/RAD)*SIN(CD/RAD)
        Z1 = SIN(CI/RAD)
        RX1 = RX1 + X1
        RY1 = RY1 + Y1
        RZ1 = RZ1 + Z1
1000  CONTINUE
      RX2 = 0.0
      RY2 = 0.0
      RZ2 = 0.0
       DO 1001,J = 1,N2
        RTILT = F2*T2(J)*0.01
        CALL ROTATE(CI,CD,DR2(J),RTILT,D2(J),XI2(J))
        X2 = COS(CI/RAD)*COS(CD/RAD)
        Y2 = COS(CI/RAD)*SIN(CD/RAD)
        Z2 = SIN(CI/RAD)
        RX2 = RX2 + X2
        RY2 = RY2 + Y2
        RZ2 = RZ2 + Z2
1001  CONTINUE
      R = SQRT((RX1 + RX2)**2 + (RY1 + RY2)**2 + (RZ1 + RZ2)**2)
      XHAT = (RX1 + RX2)/R
      YHAT = (RY1 + RY2)/R
      ZHAT = (RZ1 + RZ2)/R
      DECM = ATAN2(YHAT,XHAT)*RAD
```

```
      IF(DECM.LT.0) DECM = DECM + 360.0
      XINCM = RAD*ASIN(ZHAT)
      A95T = (1.0/0.5)**(1.0/REAL((N1 + N2)-1))-1.0
      A95 = RAD*ACOS(1.0-((REAL(N1 + N2)-R)/R)*A95T)
      IF(ABS(XINCM-XIREF).LT.BIREF) THEN
      TEMP = 1.0
      ELSE
      TEMP = 0.0
      ENDIF
      RETURN
      END

      SUBROUTINE ROTATE(CDIP,CDEC,DIREC,TILT,DEC,DIP)
```

This subroutine was copied from the program TILT which is available in the Geophysics's program Library.

```
      IF (ABS(TILT) .LT. 0.01) THEN
        CDIP = DIP
        CDEC = DEC
        RETURN
      ENDIF
      RAD = 180.0/3.141592654
      COSTLT = COS(TILT/RAD)
      SINTLT = SIN(TILT/RAD)
      COSDIR = COS(DIREC/RAD)
      SINDIR = SIN(DIREC/RAD)
      COSDIP = COS(DIP/RAD)
      ZD = SIN(DIP/RAD)
      XD = COSDIP*COS(DEC/RAD)
      YD = COSDIP*SIN(DEC/RAD)
      U = XD*(COSDIR**2*(COSTLT-1.0)+1.0) +
     A   YD*SINDIR*COSDIR*(COSTLT-1.0) +
     B   ZD*SINTLT*COSDIR
      V = XD*SINDIR*COSDIR*(COSTLT-1.0) +
     A   YD*(SINDIR**2*(COSTLT-1.0)+1.0) +
     B   ZD*SINTLT*SINDIR
      W = ZD*COSTLT - XD*SINTLT*COSDIR - YD*SINTLT*SINDIR
      CDIP = ATAN(W/SQRT(U*U + V*V))*RAD
      CDEC = ATAN2(V, U)*RAD
      IF (CDEC .LT. 0.0) CDEC = CDEC + 360.0
      RETURN
      END
```

Table C-1 Results from the FOLDCONT program (DUMMY data).

DUMMY DATA

	DEC	INC	TILT	DIR
LIMB 1				
	198.0	-45.0	75.0	000.0
	195.0	-39.0	70.0	350.0
LIMB 2				
	178.0	02.0	25.0	180.0
	190.0	00.0	40.0	190.0

********** k MAXIMUM **********

LIMB 1 62.0 % UNFOLDED LIMB 2 0.0 % UNFOLDED
Mean Dec.= 187.5 Mean Inc.= 0.9 A95 = 2.9
Data = 4 R value = 3.980446 k max = 153.4

> > > > > > > > > EXPECTED(INC.= 0.0 +/- 3.0)< < < < < < < < <

MEAN DEC.= 187.5 MEAN INC.= 0.9
LIMB 1 62.0 % unfolded LIMB 2 0.0 % unfolded
A95 = 2.9 R value = 3.980446 k max = 153.4

********** USUAL FOLD TEST **********

LIMB 1 42.0 % UNFOLDED LIMB 2 42.0 % UNFOLDED
Mean Dec.= 187.6 Mean Inc.=-13.0 A95 = 3.3
Data = 4 R value = 3.974861 k max = 119.3

McELHINNY TEST (95% CONFIDENCE LIMIT)

Variance ratio (F) = 4.28
k1 (k-parameter for in situ) = 9.6
k2 (k-parameter at 95% limit; = k1 * F) = 41.1
k3 (k-parameter for fully unfolded) = 5.4

Table C-2 Results from the FOLDCONT program (REAL data).

STEARNS & VAN DER VOO's data

	DEC	INC	TILT	DIR
1-ST LIMB				
	230.0	29.0	58.0	169.0
	214.0	13.0	45.0	161.0
	221.0	28.0	55.0	159.0
2-ND LIMB				
	190.0	-01.0	36.0	095.0
	189.0	00.0	20.0	101.0
	174.0	06.0	41.0	098.0

PLUNGE CORRECTED : amount/dir = 40.0/ 121.0

1-ST LIMB				
	204.5	33.7	39.6	202.5
	204.8	11.8	27.1	216.0
	199.0	27.3	31.3	197.0
2-ND LIMB				
	195.2	-14.1	16.4	006.9
	193.8	-13.9	22.1	319.1
	177.5	-17.7	14.9	026.0

********** k MAXIMUM **********

1-ST LIMB 100.0 % UNFOLDED 2-ND LIMB 48.0 % UNFOLDED
Mean Dec.= 195.6 Mean Inc.= -8.5 A95 = 3.7
Data = 6 R value = 5.917854 k max = 60.9

> > > > > > > > > EXPECTED(INC.= -5.0 +/- 5.0)< < < < < < < < <

MEAN DEC.= 195.6 MEAN INC.= -8.5
1-ST LIMB 100.0 % unfolded 2-ND LIMB 48.0 % unfolded
A95 = 3.7 R value = 5.917854 k max = 60.9

********** USUAL FOLD TEST **********

1-ST LIMB 86.0 % UNFOLDED 2-ND LIMB 86.0 % UNFOLDED
Mean Dec.= 195.5 Mean Inc.= -3.4 A95 = 3.8
Data = 6 R value = 5.913939 k max = 58.1

McELHINNY TEST (95% CONFIDENCE LIMIT)

Variance ratio (F) = 2.97
k1 (k-parameter for in situ) = 10.8
k2 (k-parameter at 95% limit; = k1 * F) = 32.1
k3 (k-parameter for fully unfolded) = 52.8